



THE UNIVERSITY OF  
**WAIKATO**  
*Te Whare Wānanga o Waikato*

Research Commons

<http://researchcommons.waikato.ac.nz/>

## Research Commons at the University of Waikato

### Copyright Statement:

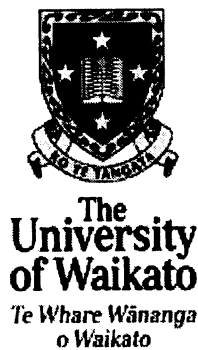
The digital copy of this thesis is protected by the Copyright Act 1994 (New Zealand).

The thesis may be consulted by you, provided you comply with the provisions of the Act and the following conditions of use:

- Any use you make of these documents or images must be for research or private study purposes only, and you may not make them available to any other person.
- Authors control the copyright of their thesis. You will recognise the author's right to be identified as the author of the thesis, and due acknowledgement will be made to the author where appropriate.
- You will obtain the author's permission before publishing any material from the thesis.

STUDIES OF THE FORMATION AND  
PROPERTIES OF UREA-FORMALDEHYDE  
RESIN ADHESIVES

A Thesis  
submitted in partial fulfilment  
of the requirements for the Degree  
of  
Doctor of Philosophy in Chemistry  
at the University of Waikato  
by  
HUIYANG ZENG



The University of Waikato

2001

# Studies of the Formation and Properties of Urea-Formaldehyde Resin Adhesives

## ABSTRACT

Urea-formaldehyde (UF) resin is used primarily as an adhesive for manufacturing wood panels (medium density fiberboard, particleboard and plywood). These are important New Zealand export products. A better understanding of the formation of UF resin will allow maximisation of its adhesive properties (high bonding strength) and minimisation of formaldehyde emissions (an adverse environmental effect). These improvements will enhance the competitive advantage of New Zealand resin products.

The research reported here has been directed primarily towards monitoring the UF reaction by Nuclear Magnetic Resonance spectroscopy (NMR), preparing UF resins, determining the performance of the resins produced and characterising the resins by high performance liquid chromatography (HPLC), gel permeation chromatography (GPC) and differential scanning calorimetry (DSC) methods.

The development of a dynamic (RAPID) NMR acquisition method has contributed to the identification of optimum conditions for UF resin manufacture. A series of NMR “snap-shots” of the UF reaction system over the entire reaction period has been obtained. A wide range of reaction conditions, eg formaldehyde to urea molar ratio, formaldehyde concentration, initial addition pH, condensation pH, addition reaction time and reaction temperature, have been investigated. From the species present and the changes in their relative concentrations during the reaction, optimum reaction conditions have been determined as:

Formaldehyde concentration:	35-46%
F/U molar ratio:	1.8-2.0
Temperature:	88°C
Addition reaction time:	25-30 min
Initial addition pH:	8.0-9.0

Condensation pH: 4.5-5.0

The dynamic (RAPID) NMR studies were complemented by HPLC characterisation of samples taken during the different reaction stages. The main low molecular weight species present in the UF reaction system have been identified. In general the HPLC results were consistent with those obtained by the dynamic (RAPID) NMR method.

Low molecular weight species were identified by electrospray mass spectrometry.

Molecular weight, molecular weight distribution and resin aging were investigated by the GPC method. The number average molecular weights of typical final UF resins were in the range of 600-800 Dalton. The weight average molecular weights of the same resins were in the range of 7000-10 000 Dalton.

A series of laboratory resins were prepared to test the appropriateness of the optimum reaction conditions predicted from the NMR and HPLC studies. Resin performance in wood panels was determined by measuring internal bond, formaldehyde emission and cold water swell. The effects of F/U molar ratio, resin loading and board thickness on the panel properties have also been determined. The results showed improvement in the internal bond and formaldehyde emissions.

Comparison of the experimental resin prepared under the optimum reactions with a commercial unmodified UF resin indicated that a 12% increase in internal bond. Formaldehyde emissions were similar.

It is clear from the results of this study that current manufacturing conditions for the production of unmodified UF resins are close to optimum. Future improvements are likely to be based upon structural and/or non-structural additives.

# ACKNOWLEDGEMENTS

The project would not have been possible without all the help and assistance by the following organisations and people.

I wish to thank my supervisors, Professor Alistair Wilkins and Associate Professor Alan Langdon for their encouragement and advice through this project.

I wish to thank my industry supervisors, Dr. Stewart Gumbley, Jeremy Kissock and Neil Walker of Orica NZ Ltd. for their assistance and advice during the experimentation and preparation work of this thesis.

I wish to thank Alex Bruce, Clyde Campbell, Noel Dunlop and Paul de Rijk for their technical suggestion, help and assistance regarding this project. Also, I wish to thank all the technical staff (John Wilson, Jane Woodcock, Neil Brown, Dale Bennington and Dave Highway *et al.*) and many other staff (Mandy Sloan, Steve Carroll, Paul Hastie and shift workers *et al.*) in the Adhesive & Resin, Orica NZ Ltd. for their ongoing encouragement and assistance.

I wish to thank Dr. Ralph Thomson, Ms Wendy Jackson and Ms Jannine Simes for their help and assistance in allowing me to obtain NMR, ESMS and GC-MS experiments. I also wish to thank many other staff in the Department of Chemistry, the University of Waikato for their providing ongoing support of this project.

I wish to thank Orica NZ Ltd. for providing funding and resources for this project, the Foundation for Research, Science and Technology for providing a GRIF (graduate research in industry fellowship) award and the Department of Chemistry, Unlink Office and other related offices of the University of Waikato for providing administration service.

Finally, I wish to thank my wife Fangying Lin for her support and encouragement during the past five years.

# TABLE OF CONTENTS

Abstract .....	ii
Acknowledgments .....	iv
Table of Contents .....	v
List of Figures .....	xi
List of Tables .....	xix
Abbreviations .....	xxiv
Symbols .....	xxvi

<b>1 CHAPTER ONE: GENERAL INTRODUCTION AND REVIEW .....</b>	<b>1</b>
1.1 GENERAL INTRODUCTION .....	2
1.2 CHEMISTRY OF UREA FORMALDEHYDE RESINS .....	3
1.2.1 Formaldehyde and Solvolysis of Formaldehyde.....	3
1.2.2 Reaction of Urea and Formaldehyde .....	4
1.2.3 Reaction Mechanisms and Kinetics of Urea Formaldehyde Resin Formation .....	8
1.2.4 Adhesion Mechanism of UF Resins.....	12
1.3 EFFECTS OF REACTION CONDITIONS .....	13
1.3.1 Formaldehyde to urea molar ratio .....	13
1.3.2 Effect of pH.....	16
1.3.3 Effect of Reaction Temperature and Time.....	18
1.3.4 Purity of Raw Materials .....	18
1.4 PREPARATION OF COMMERCIAL UF RESINS .....	20
1.5 APPLICATIONS OF UF RESINS IN BOARD MANUFACTURE.....	22
1.6 INSTRUMENTAL METHODS FOR UF RESIN CHARACTERISATION.....	23
1.6.1 Application of NMR Techniques.....	24
1.6.2 Chromatographic Analyses of UF Resins.....	30
1.6.3 Other Analytical Techniques .....	35
1.7 ENHANCING THE PROPERTIES OF UF RESINS.....	37
1.7.1 Enhancing the Water-Resistance and Durability .....	38

1.7.2	Reduction of the Free Formaldehyde and Formaldehyde Emission .....	40
1.7.3	Catalysts and Hardeners.....	43
1.8	SCOPE OF THE PRESENT INVESTIGATION .....	44
<b>2</b>	<b>CHAPTER TWO: METHODS AND MATERIALS .....</b>	<b>47</b>
2.1	NUCLEAR MAGNETIC RESONANCE (NMR) .....	48
2.1.1	General NMR Conditions .....	48
2.1.2	The STANDARD NMR Method .....	48
2.1.3	The RAPID <sup>13</sup> C NMR Method .....	49
2.1.4	The Dynamic (RAPID) NMR Procedure.....	50
2.1.5	<sup>13</sup> C Relaxation Time (T <sub>1</sub> ) Determination .....	51
2.2	HPLC MEASUREMENTS .....	52
2.3	GPC MEASUREMENTS .....	53
2.4	ESMS MEASUREMENTS.....	55
2.5	GC-MS MEASUREMENTS.....	55
2.6	DSC MEASUREMENTS .....	56
2.7	DETERMINATION OF THE FORMALDEHYDE CONTENT OF A FORMALDEHYDE SOLUTION.....	56
2.8	DETERMINATION OF FREE FORMALDEHYDE IN A UF RESIN .....	57
2.9	DETERMINATION OF FORMALDEHYDE EMISSION FROM A PANEL .....	58
2.10	DETERMINATION OF THE ACIDITY OF A FORMALDEHYDE SOLUTION .....	61
2.11	DETERMINATION OF THE METHANOL CONTENT OF A FORMALDEHYDE SOLUTION.....	61
2.12	PREPARATION OF UF RESINS .....	62
2.13	VISCOSITY .....	63
2.14	GEL TIME .....	63
2.15	PANEL MAKING.....	64
2.16	INTERNAL BOND DETERMINATION.....	65
2.17	COLD WATER SWELLING AND ABSORPTION.....	65

<b>3</b>	<b>CHAPTER THREE: DEVELOPMENT OF A DYNAMIC NMR METHOD</b>	<b>67</b>
3.1	INTRODUCTION	68
3.2	<sup>13</sup> C NMR SIGNAL ASSIGNMENTS	68
3.3	QUANTITATIVE NMR ANALYSES	75
3.4	EVALUATION OF THE INTEGRATION METHODOLOGY	78
3.5	FACTORS AFFECTING NMR SIGNAL INTENSITIES	80
3.5.1	Factors Which Affect NMR Signal Intensities	80
3.5.2	Evaluation of Experimental Cases	82
3.6	DETERMINATION OF UF RESIN T <sub>1</sub> VALUES	85
3.6.1	The Principle and Procedure of Measuring T <sub>1</sub>	86
3.6.2	Experimental Determination of T <sub>1</sub> Values for Three UF Resins	87
3.7	NOE MEASUREMENT	92
3.8	CROSS CALIBRATION OF THE STANDARD AND RAPID NMR SPECTRAL DATA	99
3.9	SUMMARY AND CONCLUSIONS	111
<b>4</b>	<b>CHAPTER FOUR: NMR INVESTIGATION OF THE UREA FORMALDEHYDE REACTION</b>	<b>113</b>
4.1	INTRODUCTION	114
4.2	PRELIMINARY INVESTIGATIONS USING THE DYNAMIC (RAPID) NMR EXPERIMENT	114
4.3	EFFECT OF REACTION CONDITIONS ON SPECIES KINETIC PROFILES	119
4.3.1	Effect of Reaction Temperature	119
4.3.2	Effect of Addition Reaction Time	126
4.3.3	Effect of Formaldehyde Concentration	133
4.3.4	Effect of F/U Molar Ratio	139
4.3.5	Effect of Initial Addition pH	144
4.3.6	Effect of Condensation Reaction pH	150
4.3.7	Optimum Conditions for the Urea Formaldehyde Production	153
4.4	KINETICS STUDIES OF THE UREA FORMALDEHYDE REACTION	154
4.4.1	Addition Reaction Stage	154

4.4.2	Absolute Molar Concentration.....	157
4.4.3	Rate Constants for Monomethylolurea Formation.....	160
4.4.4	Rate Constants for Dimethylolurea Formation .....	163
4.4.5	Condensation Stage Reactions .....	165
4.5	QUANTITATIVE DETERMINATION USING STANDARD NMR METHOD.....	168
4.5.1	Quantitative Measurement Principle.....	168
4.5.2	Quantitative NMR Investigation of UF Reaction Systems.....	169
4.5.3	Quantitative Determination of the Composition of Formaldehyde Solution .....	178
4.6	ORIGIN OF ETHER GROUPS .....	184
4.7	SUMMARY AND CONCLUSIONS.....	188
<b>5</b>	<b>CHAPTER FIVE: HPLC, ESMS AND GPC ANALYSES OF UF RESINS .....</b>	<b>190</b>
5.1	INTRODUCTION.....	191
5.2	EXPERIMENTAL CONDITIONS.....	193
5.2.1	Influence of Acetonitrile to Water Ratio.....	193
5.2.2	Influence of Mobile Phase Flowrate .....	195
5.2.3	HPLC Analysis of Model UF Resin Compounds .....	199
5.2.4	Refractive Index Detector Response Factors .....	202
5.3	GENERAL FEATURES OF THE UF RESIN REACTION SYSTEM AS ELUCIDATED BY HPLC.....	204
5.4	EFFECT OF REACTION CONDITIONS.....	209
5.4.1	Reaction Temperature .....	209
5.4.2	Addition Reaction Time ( $t_a$ ).....	211
5.4.3	Formaldehyde Concentration.....	213
5.4.4	Initial Addition pH.....	215
5.4.5	Condensation pH.....	216
5.4.6	pH Control Methods.....	218
5.4.7	Summary .....	219
5.5	IDENTIFICATION OF UF RESIN SPECIES BY ELECTROSPRAY MASS SPECTROMETRY.....	220
5.6	CHARACTERISATION OF UF RESINS BY GPC .....	224

5.6.1	Calibration of the Triple Detector GPC System .....	226
5.6.2	Effect of Reaction Time on the Molecular Weight and Molecular Weight Distribution.....	229
5.6.3	Effect of Storage Time (Aging) on the Molecular Weight and Molecular Weight Distribution .....	232
5.6.4	Summary and Conclusions.....	232
<b>6</b>	<b>CHAPTER SIX: RESIN DEVELOPMENT AND TESTING.....</b>	<b>234</b>
6.1	INTRODUCTION.....	235
6.2	EXPERIMENTAL .....	235
6.3	EFFECT OF REACTION CONDITIONS.....	236
6.3.1	Effect of Formaldehyde Concentration.....	236
6.3.2	Effect of F/U Molar Ratio.....	239
6.3.3	Effect of Reaction Temperature .....	239
6.3.4	Effect of Initial Addition pH.....	240
6.3.5	Effect of Condensation pH.....	241
6.3.6	Effect of Addition Stage Reaction Time.....	241
6.3.7	Effect of pH Control During the Addition Reaction Stage.....	241
6.3.8	Other Important Variables .....	244
6.4	COMPARISON OF EXPERIMENTAL RESINS WITH COMMERCIAL RESINS .....	246
6.4.1	Comparison with Literature Data.....	246
6.4.2	Comparison of Experimental Resins with a Commercial Resin.....	247
6.5	CONCLUSIONS.....	249
<b>7</b>	<b>CHAPTER SEVEN: GENERAL CONCLUSIONS AND OVERVIEW....</b>	<b>250</b>
7.1	DEVELOPMENT OF A DYNAMIC NMR METHOD .....	251
7.2	DYNAMIC NMR INVESTIGATION OF UF REACTION SYSTEMS .....	251
7.2.1	Standard NMR Monitoring of UF Reaction Systems .....	253
7.2.2	Kinetic Studies .....	253
7.3	HPLC, ESMS AND GPC INVESTIGATIONS.....	253
7.4	TRIALS USING LABORATORY RESINS.....	254
7.5	RECOMMENDATIONS FOR FUTURE RESEARCH.....	255

Appendix A	European and Japanese Standards for Formaldehyde Emission .....	257
Appendix B	Effects of Formaldehyde and Resin Aging on Resin and Resin Bonded Particleboard Properties .....	258
Appendix C	Effect of Wood Materials, Resin Loading and Panel Thickness on the Wood Panel Properties .....	263
Appendix D	Preliminary Investigation of UF Resins Using DSC .....	266
Appendix E	Conversion of Dynamic (RAPID) NMR Data to Absolute Concentrations .....	270
Appendix F	ESMS Spectra of Model Compounds and UF Resins .....	273
BIBLIOGRAPHY .....		283

# LIST OF FIGURES

Figure 1.1	Influence of pH on the addition and condensation reaction rates of urea and formaldehyde at 35°C .....	16
Figure 2.1	The STANDARD $^{13}\text{C}$ NMR pulse programme .....	48
Figure 2.2	The RAPID $^{13}\text{C}$ NMR pulse programme .....	50
Figure 2.3	The inversion-recovery pulse sequence.....	52
Figure 3.1	$^{13}\text{C}$ NMR spectrum of a typical UF resin acquired with $^1\text{H}$ decoupling .....	72
Figure 3.2	$^{13}\text{C}$ NMR spectrum of formaldehyde acquired with $^1\text{H}$ decoupling .....	72
Figure 3.3	$^{13}\text{C}$ NMR spectrum of an UF resin containing 0.50 mL DMSO-d6 .....	79
Figure 3.4	$^{13}\text{C}$ NMR spectrum of an UF resin containing 0.40 mL DMSO-d6 + 0.20 mL DMSO.....	79
Figure 3.5	Plot of the steady state magnetism ( $I_z$ ) versus $T_r/T_1$ for 4 pulse angles.....	83
Figure 3.6	Plot of the steady-state signal intensity ( $I_z$ ) for benzene as a function of the ratio $D_r/T_1$ .....	84
Figure 3.7	Plot of observed signal intensity vs $\tau$ for an UF resin signal .....	87
Figure 3.8	$^{13}\text{C}$ NMR spectra determined for UF resin sample S8-7 using the inversion-recovery method for determining $T_1$ s.....	88
Figure 3.9	Plot of calibration factor ( $f_c$ ) vs reaction time .....	103
Figure 4.1	A typical dynamic (RAPID) NMR spectrum of an UF reaction system determined during the addition reaction stage .....	115
Figure 4.2	A typical dynamic (RAPID) NMR spectrum of an UF reaction system determined during the condensation reaction stage .....	116
Figure 4.3	Dynamic (RAPID) NMR spectra determined for an UF reaction system during the addition stage. ....	117
Figure 4.4	Dynamic (RAPID) NMR spectra determined for an UF reaction system during the condensation stage. ....	118

Figure 4.5	Plots of the effect of reaction temperature on free urea levels vs reaction time during the addition stage. ....	120
Figure 4.6	Plots of the effect of reaction temperature on free formaldehyde levels vs reaction time during (a) the addition stage and (b) the entire reaction period. ....	121
Figure 4.7	Plots of the effect of reaction temperature on methylol group levels vs reaction time for (a) the addition stage and (b) the entire reaction period. ....	122
Figure 4.8	Plots of the effect of reaction temperature on methylene group levels vs reaction time during (a) the addition stage and (b) the entire reaction period. ....	122
Figure 4.9	Plots of the effect of reaction temperature on ether group levels vs reaction time during (a) the addition stage and (b) the entire reaction period. ....	123
Figure 4.10	Plots of the effect of reaction temperature on the methylene to ether (Me/E) group ratio vs reaction time. ....	124
Figure 4.11	Plots of the effect of reaction temperature on methylol group levels vs reaction time .....	125
Figure 4.12	Plots of the effect of reaction temperature on methylene group levels vs reaction time.....	125
Figure 4.13	Plots of the effect of reaction temperature on ether group levels vs reaction time .....	126
Figure 4.14	Plots of the effect of temperature on the Me/E group ratio vs reaction time.....	126
Figure 4.15	Plots of the effect of the addition reaction time ( $t_a$ ) on free urea levels vs reaction time for reactions performed at (a) 70°C and (b) 80°C. ....	127
Figure 4.16	Plots of the effect of addition reaction time ( $t_a$ ) on free formaldehyde levels vs reaction time during (a) the addition stage and (b) the condensation stage for a reaction performed at 70°C.....	128
Figure 4.17	Plots of the effect of the addition reaction time ( $t_a$ ) on free formaldehyde levels vs reaction time during: (a) the addition stage and (b) the condensation stage for a reaction performed at 80°C.....	128

Figure 4.18	Plots of the effect of addition reaction time ( $t_a$ ) on methylol group levels vs reaction time during (a) the addition stage and (b) the condensation stage for the reaction at 70°C.....	129
Figure 4.19	Plots of the effect of addition reaction time ( $t_a$ ) on methylol group levels vs reaction time during (a) the addition stage and (b) the condensation stage for the reaction at 80°C.....	130
Figure 4.20	Plots of the effect of addition reaction time ( $t_a$ ) on methylene group levels vs reaction time during (a) the addition stage and (b) the condensation stage for the reaction at 70°C.....	130
Figure 4.21	Plots of the effect of addition reaction time ( $t_a$ ) on methylene group levels vs reaction time during (a) the addition stage and (b) the condensation stage for the reaction at 80°C.....	131
Figure 4.22	Plots of the effect of addition reaction time ( $t_a$ ) on ether group levels vs reaction time during (a) the addition stage and (b) the condensation stage for the reaction at 70°C.....	132
Figure 4.23	Plots of the effect of addition reaction time ( $t_a$ ) on ether group levels vs reaction time during (a) the addition stage and (b) the condensation stage for the reaction at 80°C.....	132
Figure 4.24	The effect of formaldehyde concentration on methylol group levels during the addition stage. ....	134
Figure 4.25	The effect of formaldehyde concentration on linear methylol and branched methylol group levels during the addition stage. ....	135
Figure 4.26	The effect of formaldehyde concentration on methylol group levels during the entire reaction period. ....	136
Figure 4.27	The effect of formaldehyde concentration on methylene group levels vs reaction time during (a) the addition stage and (b) the entire reaction period.....	137
Figure 4.28	The effect of formaldehyde concentration on ether group levels vs reaction time during (a) the addition stage and (b) the entire reaction period. ....	138
Figure 4.29	The effect of formaldehyde concentration on the methylene to ether (Me/E) group ratio.....	139

Figure 4.30	The effect of F/U molar ratio on free formaldehyde levels vs reaction time during (a) the addition stage and (b) the entire reaction period. ....	140
Figure 4.31	The effect of F/U molar ratio on free urea levels during the addition stage. ....	141
Figure 4.32	The effect of F/U molar ratio on methylol group levels vs reaction time during (a) the addition stage and (b) the entire reaction period. ....	142
Figure 4.33	The effect of F/U molar ratio on methylene group levels vs reaction time during (a) the addition stage and (b) the entire reaction period. ....	142
Figure 4.34	The effect of F/U molar ratio on ether group levels vs reaction time during (a) the addition stage and (b) the entire reaction period .....	143
Figure 4.35	The effect of F/U molar ratio on the methylene to ether (Me/E) group ratio .....	144
Figure 4.36	The relationship of initial addition reaction pH and the pH during the addition reaction stage. ....	145
Figure 4.37	Plots of the effect of initial addition pH on free formaldehyde levels vs reaction time during the addition reaction stage. ....	146
Figure 4.38	Plots of the effect of initial addition pH on methylol group levels vs reaction time during (a) the addition stage and (b) the entire reaction period .....	147
Figure 4.39	Plots of the effect of initial addition pH on methylene group levels vs reaction time during (a) the addition stage and (b) the entire reaction period. ....	148
Figure 4.40	Plots of the effect of initial addition pH on ether group levels vs reaction time during (a) the addition stage and (b) the entire reaction period .....	148
Figure 4.41	Plots of the effect of initial addition pH on methylene to ether group (Me/E) ratio vs reaction time during (a) the addition stage and (b) the entire reaction period. ....	149
Figure 4.42	The effect of condensation (cond) pH on methylol group levels vs reaction time during the reaction period. ....	151

Figure 4.43	Plots of the effect of condensation pH on methylene group levels vs reaction time.....	152
Figure 4.44	Plots of the effect of condensation pH on ether group levels vs reaction time .....	152
Figure 4.45	Plots of the effect of condensation pH on the Me/E group ratio vs reaction time.....	153
Figure 4.46	Plots of UF <sub>1</sub> , UF <sub>2</sub> and UF <sub>3</sub> levels vs reaction time during the addition stage of a typical reaction at 80°C .....	155
Figure 4.47	Plot of the urea concentration vs reaction time during the addition stage of an urea formaldehyde reaction at 60°C .....	161
Figure 4.48	Plots of $r_2/[UF_1]$ vs $[F][U]/[UF_1]$ for reactions at 60°C to 97°C .....	162
Figure 4.49	Plots of (a) $\ln k'_{2f}$ vs 1/T and (b) $\ln k'_{1b}$ vs 1/T for the UF <sub>1</sub> formation reaction .....	163
Figure 4.50	Plots of $r_4/[UF_2]$ vs $[UF_1][F]/[UF_2]$ for reactions at 60°C to 97°C. ....	164
Figure 4.51	Plots of (a) $\ln k'_{2f}$ vs 1/T and (b) $\ln k'_{1b}$ vs 1/T for the UF <sub>2</sub> formation reaction .....	165
Figure 4.52	Plots of methylol group concentrations vs reaction time .....	177
Figure 4.53	Plots of methylene group concentrations vs reaction time .....	177
Figure 4.54	Plots of ether group concentrations vs reaction time.....	177
Figure 4.55	Plot of the methylene to ether (Me/E) molar ratio vs reaction time ....	177
Figure 4.56	<sup>13</sup> C NMR spectra of a typical UF resin sample before (upper spectrum) and after (lower spectrum) final urea addition. ....	178
Figure 4.57	A typical NMR spectrum of a formaldehyde solution (80-95 ppm region).....	182
Figure 4.58	Gas chromatogram of silylated polyoxymethylene glycol (formaldehyde solution) .....	183
Figure 5.1	The effect of the acetonitrile/water ratio in a mixed solvent on the HPLC separation of urea, MMU and DMU. ....	194
Figure 5.2	The effect of the flowrate on HPLC profiles determined using a 250 mm × 4.6 mm 5 μm PEI column and acetonitrile/water (92/8) (w/w) as the mobile phase. ....	195
Figure 5.3	Plots of the number of plates vs flowrate for urea and DMU. ....	197

Figure 5.4	HPLC profiles determined for (a) blank (air), (b) water and (c) water/methanol injections .....	199
Figure 5.5	HPLC traces of model UF resin compounds.....	200
Figure 5.6	HPLC traces of mixtures of model UF resin compounds.....	201
Figure 5.7	Calibration curves for urea, MMU and DMU .....	203
Figure 5.8	Calibration curve for MDU .....	203
Figure 5.9	HPLC traces of an UF reaction system during the addition stage.....	205
Figure 5.10	HPLC traces of an UF reaction system during the condensation stage.....	206
Figure 5.11	Plots of the $A_{xS}$ of free urea, MMU and DMU vs reaction time .....	207
Figure 5.12	Plots of the $A_{xS}$ of TMU and MDU vs reaction time .....	207
Figure 5.13	Plots of $A_{xS}$ of $P_0$ , $P_8$ and $P_{11}$ vs reaction time .....	208
Figure 5.14	Plots of $A_{xS}$ of $P_4$ , $P_6$ and $P_7$ vs reaction time .....	208
Figure 5.15	Typical HPLC traces of UF resins.....	209
Figure 5.16	Plot of HPLC determined free urea levels vs reaction time for reactions performed at 80, 88 and 97°C (common curve applied to all data). .....	210
Figure 5.17	Plots of MMU levels vs reaction time during (a) the addition stage and (b) the entire reaction period.....	210
Figure 5.18	Plots of DMU levels vs reaction time during (a) the addition stage and (b) the entire reaction period.....	211
Figure 5.19	Plots of free urea levels during the entire reaction period for reactions with differing addition stage reaction times.....	212
Figure 5.20	Plots of the effect of addition reaction time ( $t_a$ ) on MMU levels vs reaction time during (a) the addition stage and (b) the condensation stage.....	212
Figure 5.21	Plots of the effect of addition reaction time ( $t_a$ ) on DMU levels vs reaction time during (a) the addition stage and (b) the condensation stage.....	213
Figure 5.22	Plots of the effect of formaldehyde concentration (F conc) on free urea levels vs reaction time. ....	213

Figure 5.23	Plots of the effect of formaldehyde concentration (F conc) on the concentrations of MMUs vs reaction time during (a) the addition stage and (b) the entire reaction period. ....	214
Figure 5.24	Plots of the effect of formaldehyde concentration (F conc) on the concentrations of DMUs vs reaction time during (a) the addition stage and (b) the entire reaction period. ....	214
Figure 5.25	Plot of the effect of initial addition pH on free urea levels vs time.....	215
Figure 5.26	Plots of the effect of initial addition pH on the concentrations of MMUs vs reaction time during (a) the addition stage and (b) the entire reaction period. ....	216
Figure 5.27	Plots of the effect of initial addition pH on the concentrations of DMUs vs reaction time during (a) the addition stage and (b) the entire reaction period. ....	216
Figure 5.28	Plot of the effect of condensation pH on the free urea levels vs reaction time. ....	217
Figure 5.29	Plots of the effect of condensation pH on MMU levels vs reaction time.....	217
Figure 5.30	Plots of the effect of condensation pH on DMU levels vs reaction time.....	217
Figure 5.31.	Plot of the effect of addition pH control on free urea levels vs reaction time. ....	219
Figure 5.32	Plots of the effect of addition pH control on MMU levels vs reaction time.....	219
Figure 5.33	Plots of the effect of addition pH control on DMU levels vs reaction time.....	219
Figure 5.34	Triple-detector GPC traces of the PEG 4820, PEG 9230, PEG 11 250 and PEO 39 kDa standard samples. ....	227
Figure 5.35	The universal calibration curve determined using the PEG and PEO standards. ....	228
Figure 5.36	Triple detector GPC traces for a typical UF resin sample.....	228
Figure 5.37	Plot of $\log[\eta]$ vs $V_r$ for a typical UF resin .....	229
Figure 5.38	Plot of $\log M$ vs $V_r$ for a typical UF resin .....	229
Figure 5.39	The effect of the reaction time on the GPC traces (RI responses). ....	231

Figure 6.1	pH titration curve of a typical formaldehyde solution.....	240
Figure 6.2	pH profiles for (a) the pH adjusted reaction and (b) conventional reaction during the UF resin preparation along with their corresponding temperature profiles.....	242
Figure 6.3	Effect of the pH controlling method on the (a) internal bond and (b) formaldehyde emission of the wood panel. ....	243
Figure 6.4	Plot of log viscosity vs condensation reaction time for a typical UF reaction. ....	244

# LIST OF TABLES

Table 1.1	The relationship between F/U ratio, free formaldehyde (free F), formaldehyde emission (FE) and gel time of UF resins.....	15
Table 1.2	Comparison of particleboard prepared with UF resins of different F/U molar ratios .....	15
Table 1.3	Spin-lattice relaxation time ( $T_1$ ) of different species in UF resins. ....	26
Table 1.4	$^{15}\text{N}$ NMR signals assignments for UF resin species. ....	29
Table 1.5	Solid state CP/MAS $^{15}\text{N}$ NMR signal assignments of five model compounds.....	30
Table 1.6	Effect of reaction time and conditions on UF resin composition.....	34
Table 2.1	Typical NMR acquisition conditions, sample volumes and reference solvents. ....	49
Table 3.1	$^{13}\text{C}$ NMR signal assignments for UF resin species – carbonyl group carbon atoms and solvents.....	69
Table 3.2	$^{13}\text{C}$ NMR signal assignments for UF resins species – formaldehyde, its polymeric forms and derivatives. ....	70
Table 3.3	NMR integration signal ranges and symbols for UF resin species. ....	76
Table 3.4	Resin samples used for $T_1$ determination. ....	87
Table 3.5	Longitudinal relaxation times ( $T_1$ , sec) of UF resin species determined using the inversion-recovery sequence.....	90
Table 3.6	Calculated relative signal intensities obtained using the STANDARD and RAPID NMR methods.....	91
Table 3.7	Comparative signal intensity data. ....	92
Table 3.8	UF resin samples used for NOE determination. ....	95
Table 3.9	NOE factors for urea and formaldehyde analogues .....	95
Table 3.10	NOE factors for different species in UF resin S1-4. ....	96
Table 3.11	NOE factors for different species in UF resin S1-7. ....	97
Table 3.12	NOE factors for different species in UF resin S1-8. ....	97
Table 3.13	NOE factors for different species in UF resin S1-9. ....	98

Table 3.14	The relationship between NOE factors ( $\eta$ ) and reaction time.....	98
Table 3.15	Calculated signal intensities ( $I_{\text{calc}}$ ) for UF resin species in NMR spectra determined using the STANDARD and RAPID methods .....	100
Table 3.16	Formaldehyde solution and UF resin samples used for NMR cross calibration experiments .....	101
Table 3.17	Normalised signal intensities and cross calibration factors determined for aqueous formaldehyde solution. ....	102
Table 3.18	Signal intensities and cross calibration factors determined for resin sample S1-4 .....	102
Table 3.19	Signal intensities and cross calibration factors determined for resin sample S1-7 .....	103
Table 3.20	Signal intensities and cross calibration factors determined for resin sample S1-8. ....	104
Table 3.21	Signal intensities and cross calibration factors determined for resin sample S1-9. ....	104
Table 3.22	The relationships between cross correlation factors ( $f_c$ ) and reaction time. ....	105
Table 3.23	Observed DMSO/DMSO-d6 ( $I_n/I_D$ ) signal ratios in RAPID NMR spectra.....	107
Table 3.24	Observed DMSO/DMSO-d6 ( $I_n/I_D$ ) signal ratios in quantitative (STANDARD) NMR ( $D_1 = 25$ sec) spectra. ....	108
Table 3.25	Calculated and observed cross calibration factors for urea and its analogues in resin sample S1-9, determined relative to DMSO and DMSO-d6 .....	110
Table 4.1	The effect of reaction temperature on the time required for a maximum methylol group level ( $t_p$ ) to be achieved and the corresponding maximum ( $I_p$ ) .....	121
Table 4.2	Composition of UF mixtures used for dynamic NMR experiments....	135
Table 4.3	The effect of formaldehyde concentration (F conc) on the time ( $t_p$ ) required to achieve a maximum methylol group level. ....	135
Table 4.4	Effect of formaldehyde concentration on methylol group levels and the ratio of linear to branched methylol group levels. ....	136
Table 4.5	Composition of UF mixtures used for dynamic NMR experiments....	140

Table 4.6	Rate constants of the UF <sub>1</sub> formation reaction at different temperatures. ....	162
Table 4.7	Rate constants of the UF <sub>2</sub> formation reaction at different temperatures. ....	164
Table 4.8	Sample weights and STANDARD NMR data used to calculate $k_c$ .....	170
Table 4.9	Properties of UF1 resin sub-samples examined using the STANDARD NMR method.. ....	170
Table 4.10	Data determined for the UF1-02 resin sub-sample.....	171
Table 4.11	Data determined for the UF1-03 resin sub-sample.....	172
Table 4.12	Data determined for the UF1-04 resin sub-sample.....	173
Table 4.13	Data determined for the UF1-06 resin sub-sample.....	174
Table 4.14	Data determined for the UF1-07 resin sub-sample.....	175
Table 4.15	Data determined for the UF1-08 resin sub-sample.....	176
Table 4.16	Quantitative (STANDARD) NMR data for formaldehyde solutions (part 1).....	180
Table 4.17	Quantitative (STANDARD) NMR data for formaldehyde solutions (part 2).....	180
Table 4.18	Quantitative (STANDARD) NMR data for formaldehyde solutions (part 3).....	181
Table 4.19	Distribution of polyoxymethylene glycol species in a formaldehyde solution at 55°C. ....	183
Table 4.20	Distribution (relative molar %) of polyoxymethylene glycol species in formaldehyde solution (F soln) determined by GC-MS.....	184
Table 4.21	<sup>13</sup> C NMR signal assignments for species present in formaldehyde solutions.....	187
Table 4.22	Structural units which may be present in UF reaction systems and their chemical shifts.....	188
Table 5.1	The effect of the acetonitrile/water ratio on the resolution ( $R_s$ ) of urea and MMU peaks in HPLC analysis. ....	194
Table 5.2	The effects of flowrate on the HPLC retention time ( $t_r$ ), peaks areas, and % peak area contributions.....	196

Table 5.3	The effect of the flowrate ( $F_L$ ) on retention time ( $t_r$ ), peak width at base ( $w$ ) and the number of plates ( $N$ ) for urea and DMU. ....	198
Table 5.4	Retention times (min) of model UF resin compounds on a 5 $\mu$ m 250 mm $\times$ 4.6 mm PEI column. ....	201
Table 5.5	Retention times (min) of model UF resin compounds on a 5 $\mu$ m 300 mm $\times$ 2.1 mm PEI column. ....	202
Table 5.6	Proposed origin(s) of some background ESMS adduct ions observed when using acetonitrile/water (1:1) (v/v), or methanol, as the mobile phase (ES <sup>+</sup> mode). ....	221
Table 5.7	Selected ions observed in the ESMS of urea (ES <sup>+</sup> mode). ....	222
Table 5.8	Selected ions observed in the ESMS of MMU (ES <sup>+</sup> mode). ....	223
Table 5.9	Selected ions observed in the ESMS of DMU (ES <sup>+</sup> and ES <sup>-</sup> modes). ....	223
Table 5.10	Selected ions observed in the ESMS of biuret (ES <sup>+</sup> and ES <sup>-</sup> modes). ....	223
Table 5.11	Selected ions observed in the ESMS of UF resin samples (ES <sup>+</sup> mode).....	224
Table 5.12	The nominal molecular weight ( $M$ ), intrinsic viscosity [ $\eta$ ] and retention volume ( $V_r$ ) of the narrow molecular weight distribution PEG standard samples. ....	226
Table 5.13	The nominal molecular weight ( $M$ ), intrinsic viscosity [ $\eta$ ] and retention volume ( $V_r$ ) of the narrow molecular weight distribution PEO standard samples. ....	226
Table 5.14	Properties of UF4 resin sub-samples examined using the GPC methodology. ....	230
Table 5.15	Molecular weight characteristics determined for UF4 resin sub-samples. ....	231
Table 5.16	The effect of storage time on the molecular weight of an UF resin ....	232
Table 6.1	Resin preparation conditions. ....	237
Table 6.2	Resin properties. ....	238
Table 6.3	Effect of pH controlling methods during the addition reaction stage on the properties of resins and wood panels.....	243

Table 6.4	Effect of condensation reaction time (cond time) on resin performance. ....	245
Table 6.5	The relationship between final F/U molar ratio and resin properties. ....	246
Table 6.6	Effect of the final F/U molar ratio on the panel properties. ....	246
Table 6.7	Comparison of the experimental resin performance with literature data. ....	247
Table 6.8	Resin preparation conditions. ....	248
Table 6.9	Properties of resins and resins bonded particleboard. ....	248

## ABBREVIATIONS

au	Arbitrary unit
DMA	Dynamic mechanical analysis
DMU	Dimethylolurea
DMU-DME	Dimethylolurea dimethyl ether
DSC	Differential scanning calorimetry
DP	Differential pressure (the signal of the in-line viscometer)
DTA	Differential thermal analysis
ESMS	Electrospray mass spectroscopy
FE	Formaldehyde emission
GC	Gas chromatography
GPC	Gel permeation chromatography
IB	Internal bond
IR	Infrared spectrometry
LS	Light scattering, the response of the in-line laser light scattering detector
MMU	Monomethylolurea
MMU-ME	Monomethylolurea methyl ether
MDF	Medium density fibreboard
MDU	Methylene diurea
Me/E	Methylene to ether (ratio)
MF	Melamine-formaldehyde resin
MS	Mass spectrometry
MUF	Melamine-urea-formaldehyde resin
RI	Refractive index (differential refractive index detector)
NMR	Nuclear magnetic resonance
NOE	Nuclear Overhauser Effect
PEG	Polyethylene glycol
PEO	Polyethylene oxide
PUF	Phenol-urea-formaldehyde resins
SEC	Size exclusion chromatography
TMU	Trimethylolurea
TGA	Thermogravimetric analysis

TMA	Thermomechanical analysis
UF	Urea-formaldehyde (resin)
UF <sub>1</sub>	Monomethylolurea
UF <sub>2</sub>	Dimethylolurea
UF <sub>3</sub>	Trimethylolurea

## LIST OF SYMBOLS

$f_c$	cross calibration factor
$\eta$	nuclear Overhauser effect (NOE) factor
$[\eta]$	intrinsic viscosity (dL g <sup>-1</sup> )
$V_r$	retention volume (mL)
$t_r$	retention time (min)
$T_r$	repetition rate, $T_r = AQ + D_1$
$AQ$	acquisition time (sec)
$D_1$	repetition delay (sec)
$T_1$	longitudinal relaxation time or spin-lattice relaxation time (sec)
$\overline{M}_n$	number average molecular weight
$\overline{M}_w$	weight average molecular weight
R	correlation coefficient
R <sup>2</sup>	the square of correlation coefficient

## **CHAPTER ONE**

# **GENERAL INTRODUCTION AND REVIEW**

## 1.1 GENERAL INTRODUCTION

Urea-formaldehyde (UF) resins are formed when formaldehyde reacts with urea. Though invented over 70 years ago (John 1920) they remain important in the production of wood products and are currently used for wood bonding, laminating, treatment of paper and textiles, foundry sand binders, binders for glass-fiber insulation, varnishes and coatings (Vale and Taylor 1964, Tokarova and Juhas 1995).

The principal growth areas over recent years have been in the application of UF resins as wood adhesives (Christiansen *et al.* 1985). Between 1980 and 1995, the US demand for wood adhesives and binders grew at an average rate of 2 to 3% per year and achieved a rate of 4 to 5% growth between 1986-1989 (White 1990), increasing to 8.5% during 1994 (White 1995). In the US, the production of particleboard and medium density fibreboard (MDF) increased approximately 15 fold between 1959 and 1995 (Margosian 1995). The world production of plywood has also grown rapidly during the last three decades (Baldwin 1995).

In New Zealand the manufacture of UF resins has increased with the growth of wood panel (particleboard, MDF and plywood) exports from the early 1970s to the present time (Schäffler 1997, Coakley 1992, Sturgeon 1992, Maplesden and Horgan 1992). The only downturn was a slight decrease during the period of the Asian economic crisis (1997-1998). Resin production was up in 1999 and is expected to continue to increase over the next few years.

The main advantages of UF resins are their water solubility (which renders them suitable for bulk and relatively inexpensive production), hardness, self fire-extinguishing characteristics, good thermal properties, absence of colour in cured polymers, easy adaptability to a variety of curing conditions and low cost (Christiansen *et al.* 1985, Meyer 1979a).

Although UF resins have many advantages as wood adhesives, they have some drawbacks. Their main disadvantage is bond deterioration caused by water (Pizzi

1983). Water promotes hydrolysis and decomposition of the resin resulting in the release of formaldehyde.

While UF resins have been improved greatly in recent years, resin hydrolysis, lack of durability and formaldehyde emissions remain as continuing issues in their formulation and production (Osugi and Tone 2000, Lecka *et al.* 1999, Yossifov *et al.* 1999, Vargha 1998). Significant reductions in formaldehyde emission have been achieved by changing manufacturing conditions (molar ratio, pH and multi-stage reaction) and the use of formaldehyde scavengers (Osugi and Tone 2000).

In spite of these reductions, there is still a need to further enhance water resistance and weather durability (Doi *et al.* 1998, Roffael *et al.* 1995), and reduce the formaldehyde emission while maintaining desirable performance characteristics.

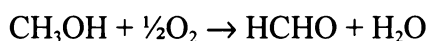
Research directed towards these improvements will continue to be the primary focus of UF resin development work for the foreseeable future (Christiansen *et al.* 1985) and is the major topic of this thesis.

## **1.2 CHEMISTRY OF UREA FORMALDEHYDE RESINS**

The reaction between formaldehyde and urea occurs over a wide range of pH and temperatures. Reaction is rapid and complex yielding many different species depending upon the reaction conditions (Vale and Taylor 1964, Walker 1967, Meyer 1979c).

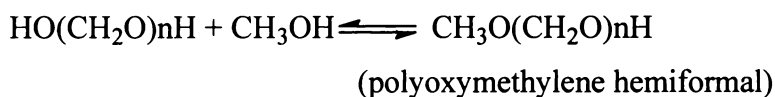
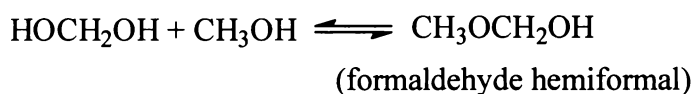
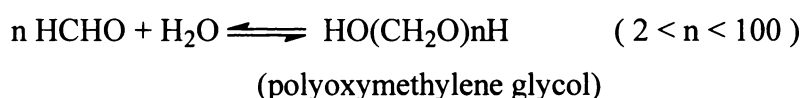
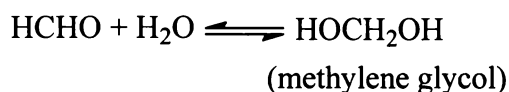
### **1.2.1 Formaldehyde and Solvolysis of Formaldehyde**

Although formaldehyde (HCHO) can be produced by the direct oxidation of hydrocarbon gases, industrial production is principally from the oxidation of methanol:



This gives formaldehyde containing some methanol and traces of formic acid. Pure monomeric formaldehyde is a colourless, pungent gas liquefying at  $-19^{\circ}\text{C}$ . Formaldehyde is very reactive. In pure form it readily polymerises. In aqueous or alcoholic solutions, it also undergoes solvolysis. Aqueous solutions contain less than 0.1 % of monomeric formaldehyde.

Formaldehyde is absorbed in water and hydrated to yield methylene glycol. Depending on the concentration, methylene glycol polymerises at room temperature forming polyoxymethylene glycol. Methylene glycol or polyoxymethylene glycol may also react with methanol to form formaldehyde hemiformal and polyoxymethylene hemiformal. A 50 wt % formaldehyde solution contains approximately 16% methylene glycol (Meyer 1979c). The main reactions between formaldehyde, water and methanol are as follows:



### 1.2.2 Reaction of Urea and Formaldehyde

The reactions between formaldehyde and urea are complex (Pizzi 1983). The combination of urea and formaldehyde can produce both linear and branched molecular structures. In polycondensation reactions, a reactant with functionality greater than two, eg urea and its derivatives, can undergo branching and crosslinking. The resultant three-dimensional network can grow indefinitely, becoming insoluble and infusible. Urea has four amino hydrogens, therefore it has a potential functionality of four and theoretically could, if the ratio of formaldehyde to urea is

high enough, form a tetramethylol derivative of urea. However tetramethylolurea has never been isolated or identified, the achievable functionality of urea is only three. The formation of one methylol group slows formation of further methylol groups, so that the rates at which the first, second, and third methylol groups are introduced bear the ratio of 1:1/3:1/9 (Skeist 1977, de Jong and de Jonge 1953, Pizzi 1983). This result shows that the reactivity of the amide group in different species is in the order: urea > monomethylolurea (MMU) > dimethylolurea (DMU) > trimethylolurea (TMU).

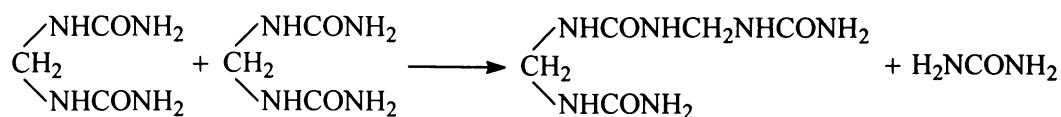
The main reasons for the decreased reactivity are statistical, the electron withdrawing nature of a methylol group (Nair and Francis 1983) and steric hindrance. The statistical factor results because the urea has four reactive positions, MMU has three, DMU has two and TMU only has one. The electron withdrawing feature of methylol may deactivate the methylols in electrophilic substitution. Methylol groups attached to an amino (urea) may block the accessibility of its amino hydrogen (steric hindrance) and thus deactivate the reactivity of the remaining amino hydrogen.

The types of reaction products derived from urea and formaldehyde under different reaction conditions have been summarised as follows (Pizzi 1983, Zigeuner 1954 and 1955):

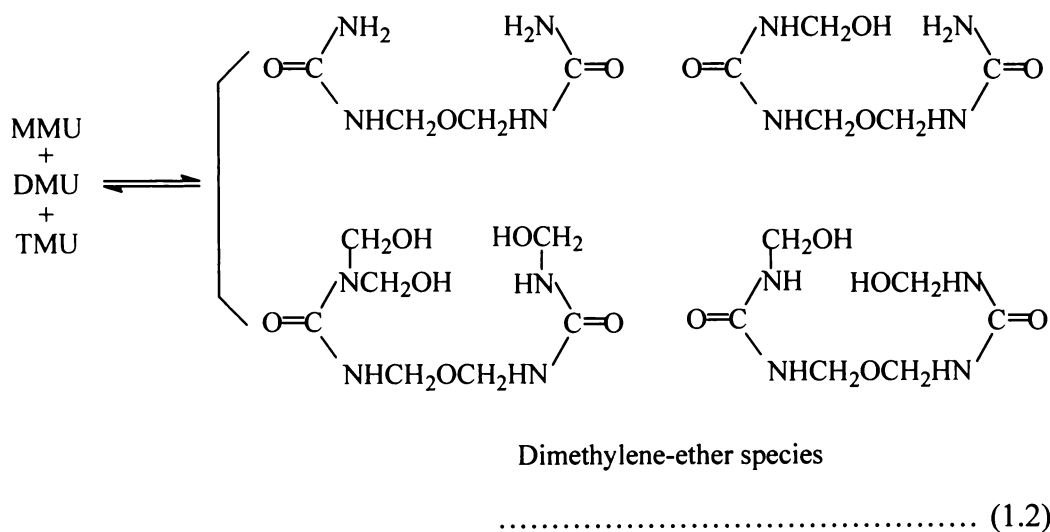
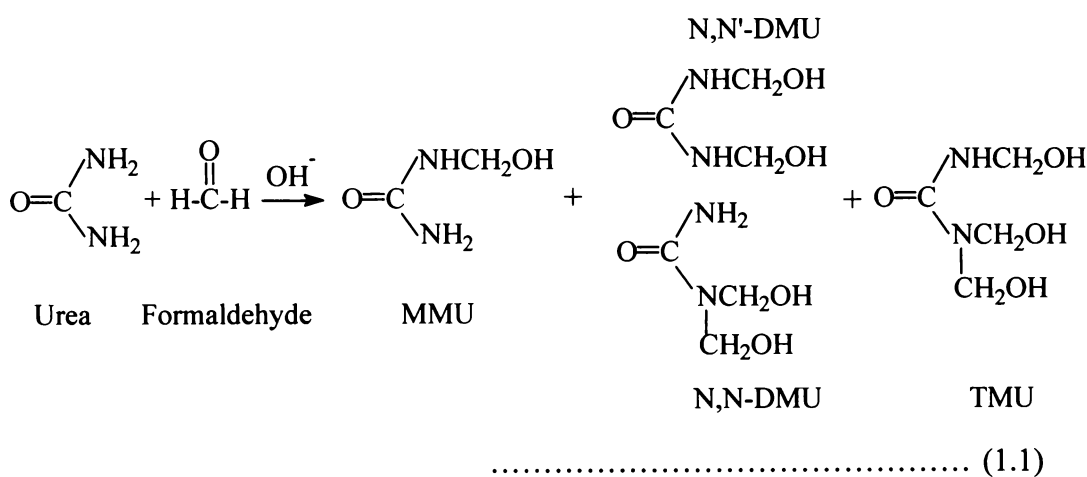
- In alkaline (pH 7-9) and weakly acid conditions (pH 4-7) urea and formaldehyde react to form mono-, di- and tri-methylolurea and dimethylene-ethers.
- In acid solution (pH  $\leq$  4), mainly methylene bridges are formed.
- Initially predominantly linear chain polymeric species are formed.
- The resinification may proceed by an intermolecular cracking of dimethylene-ether and methylene linkages forming higher molecular weight species.

The acid condensation of methylene-bisurea affords higher methylene ureas by a process of intermolecular cracking. In this process the methylene linkage of one

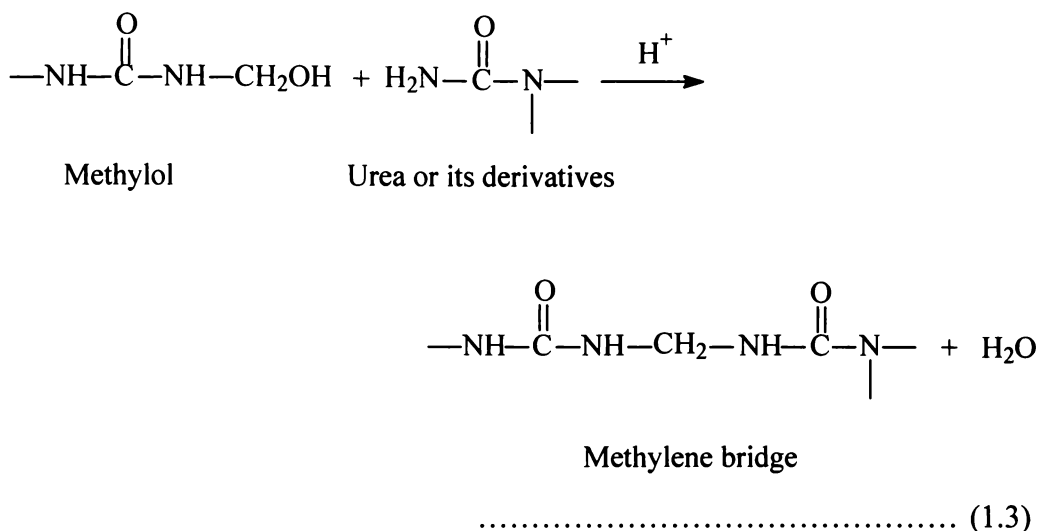
molecule is attacked by the amide group of another and forms a higher molecular species and an urea:



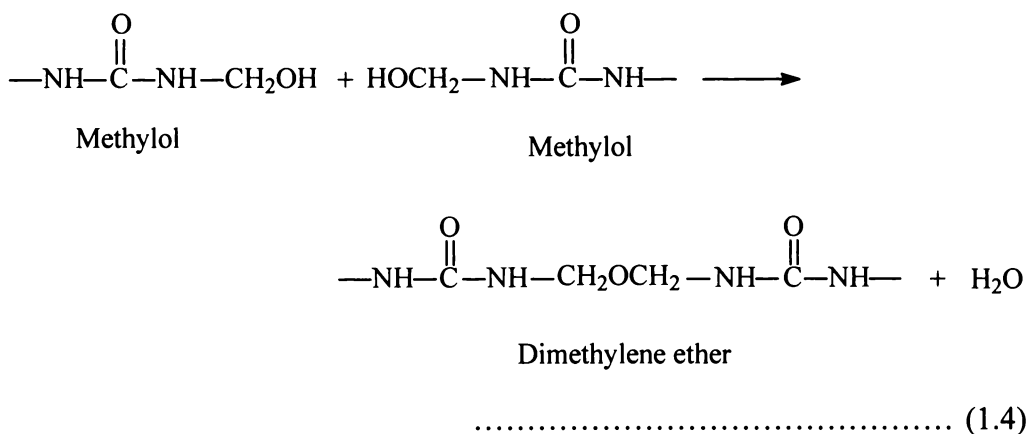
The formation of UF resins proceeds via two stages (Pizzi 1983). In the first stage, the methylation or addition stage, urea and formaldehyde react to form methylol derivatives including MMU, DMU (including N,N'-DMU and N,N-DMU) and TMU (Reaction 1.1) (Pizzi 1983, Huang *et al.* 1988, Meyer 1979b). The reaction is normally carried out at alkaline pH (typically pH 7-9). Some dimethylene ether species may also be formed during this stage (Reaction 1.2).



In the second or condensation stage, reaction occurs between methylol groups and amido hydrogen of urea, or its methylolurea derivatives (MMU, DMU and TMU), to form methylene bridges (Reaction 1.3).



The condensation reaction is normally carried out under acid conditions (pH 4-5). In this stage, the methylolurea derivatives can also condense with evolution of water, to form dimethylene-ether linkages (Reaction 1.4).

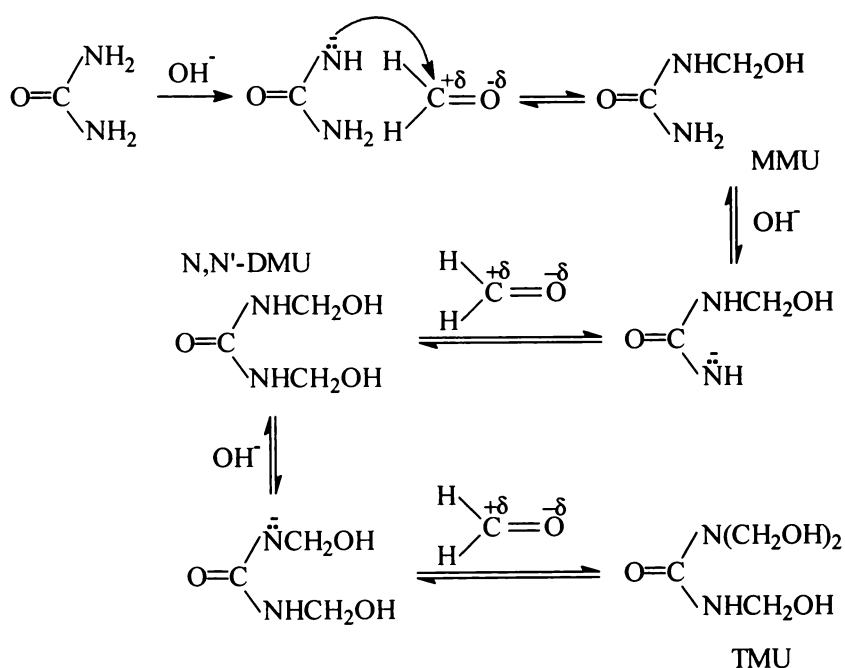


The reaction can also produce cyclic derivatives such as uron, monomethyloluron, and dimethyloluron:

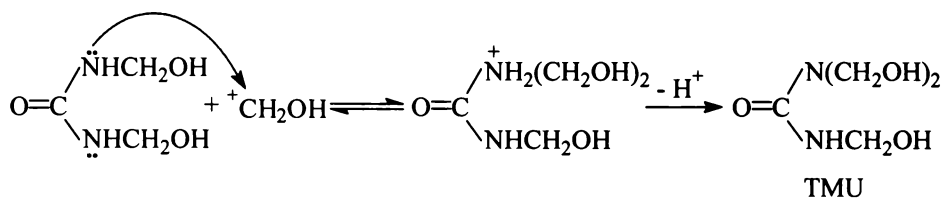
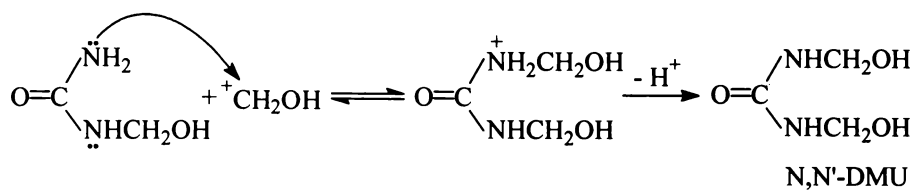
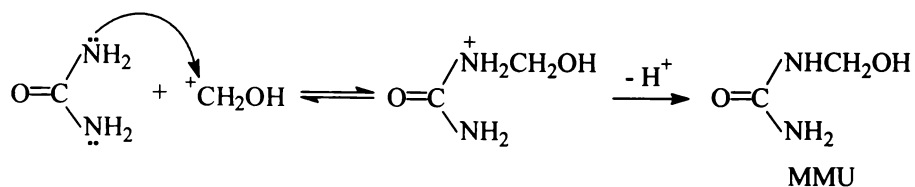
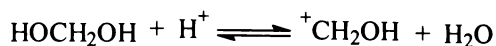
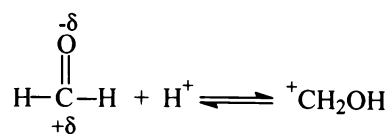


- i) the formation of an urea anion ( $\text{H}_2\text{NCONH}^-$ ) in alkaline condition (Pizzi 1983, Meyer 1979c, Crowe and Lynch 1948, Huang *et al.* 1988).
- ii) the dehydration of formaldehyde (present largely as methylene glycol) and the formation of carbenium cation ( $^+\text{CH}_2\text{OH}$ ) in acidic conditions.

In basic solution the base attacks the amine group and forms the urea anion, which, in turn, attacks formaldehyde and forms mono-, di- and tri-methylolurea. The reaction mechanism is shown in below:



In acidic solution the acid attacks the formaldehyde (or methylene glycol) and forms an intermediate carbenium ion. The carbenium ion then attaches to the nitrogen electron and expels an amine proton to form methylol groups:



In the condensation reaction, methylolurea polymerises via a carbenium cation to form high molecular weight polymethylene urea as shown in Reaction 1.5.

The polymerisation of methylolurea (Reaction 1.5) may continue and lead to the formation of highly branched and crosslinked network (cured resin).



The rate constants obtained by their method are overall functional group reaction rates, which were suitable for computer modeling but of less chemical significance.

#### **1.2.4 Adhesion Mechanism of UF Resins**

##### *Adhesion mechanism*

Ideally, a wood adhesive must be able to penetrate the wood material. Therefore, the UF resin must have a suitable molecular weight and molecular weight distribution, ie the resin viscosity is not too high and not too low.

Physical adhesion, which originates from the molecular attraction, is the main mechanism by which adhesives attach to wood. However, a chemical reaction between the adhesive and wood molecules to form chemical bonds will certainly enhance the bonding strength greatly. The adhesion mechanism of UF resins is generally considered to be both physical adhesion and chemical bonding.

##### *Bonding with cellulose*

Methylol groups react with cellulose in wood forming ether bridge structures (Pizzi 1983, Huang *et al.* 1988, Steele and Giddens 1956, Northeast Forestry College 1981). Bonds of this type are major contributors to the bonding strength of the UF resin bonded wood products (Huang *et al.* 1988, Pizzi 1983, Horioka *et al.* 1959, Sundin 1978).

Steele and Giddins (1956) have studied the reaction of UF resin with cellulose. They analysed the resins formed after treatment of paper sheets with solutions of methylolurea (the main species in an UF resin) and ammonium chloride. Their experiments showed that two to three urea units, on average, are linked by methylene group and joined to the celluloses by ether linkages. They gave the approximate formulation (Pizzi 1983):



### **1.3 EFFECTS OF REACTION CONDITIONS**

The adhesive properties (eg bonding strength and formaldehyde emission) of UF resins depend upon:

- molar ratio of formaldehyde to urea,
- pH of the reaction mixture,
- formaldehyde concentration,
- reaction temperature,
- reaction time.

These factors affect the progress of the urea-formaldehyde reaction (eg the formation of MMU, DMU, TMU, and their condensation products) and consequentially physical properties such as solubility, viscosity, water retention, shelf life, potlife, rate of curing and resin bonded wood properties such as bonding strength and formaldehyde emissions.

#### **1.3.1 Formaldehyde to Urea Molar Ratio**

UF resins are based on the condensation of methylolurea derivatives, therefore their concentrations in the resin are important. They are affected by the F/U molar ratio which is generally in the range from 1.3 to 2.0.

##### *Water resistance*

A comparison of two resins prepared under the same reaction conditions, one with F/U molar ratio 1.6 and the other with a F/U molar ratio 2.0, showed that the higher F/U molar ratio resin exhibited better water resistance (Nakarai and Watanabe 1962, Pizzi 1983).

The methylol group content of uncured UF resins depends on the molar ratio of formaldehyde to urea. The higher the molar ratio of formaldehyde to urea, the higher

content of methylol groups. The methylol groups affect water resistance and the bonding strength in competing ways. The higher the concentration of methylol groups, the greater the reactivity (adhesive bonding ability) and the stronger the bonds, but the poorer the water resistance. Increased hydrophilicity arising from residual free methylol groups reduces water resistance. Based on these contradictory effects, a compromise must be reached in selecting the optimum F/U molar ratio, such that the cured resin contains minimal methylol end groups, high levels of methylene groups and low levels of hydrolytically unstable dimethylene ether groups.

### *Reaction rate*

The formation of MMU in weak acid or alkaline aqueous solutions is characterised by an initial fast addition reaction, followed by a slow bimolecular condensation reaction (Pizzi 1983, Symthe 1947, Crowe and Lynch 1948). The rate of the addition reaction varies with F/U molar ratio and pH. (Pizzi 1983, Bettelheim and Cedwall 1948, Smets and Brozee 1952). For example, the F/U = 2.0 reaction proceeds more slowly than the F/U = 1.0 molar ratio reaction.

### *Formaldehyde emissions and bonding strength*

The effect of F/U molar ratio on the resin free formaldehyde level, formaldehyde emissions and resin gel time are shown in Table 1.1. A comparison of particleboard properties made with UF resins of different F/U molar ratios is given in Table 1.2.

It is apparent that the higher the F/U molar ratio, the shorter the resin gel time, the higher the internal bond and the lower the water swell of the resin bonded product. However, the higher the F/U molar ratio, the greater the concentration of free formaldehyde in the resins and the higher formaldehyde emission level from the resin-bonded product.

Table 1.1. The relationship between F/U ratio, free formaldehyde (free F), formaldehyde emission (FE) and gel time of UF resins (Huang *et al.* 1988).

F/U molar ratio	free F in resin <sup>a</sup> (%)	FE <sup>b</sup> (ppm)	gel time <sup>b</sup> (sec)
2.00			80-120
1.80	2.17	20-23	90-120
1.70	2.01		150-180
1.60	1.58	12-13	
1.40	1.00		
1.20	0.50	< 5	
1.05	0.10		

<sup>a</sup> Free formaldehyde in resins measuring method (Northeast Forestry College 1981, Meyer 1979a). <sup>b</sup> Formaldehyde emission and resin gel time (Northeast Forestry College 1981).

Table 1.2. Comparison of particleboard prepared with UF resins of different F/U molar ratios (Pizzi 1983).

F/U molar ratio	IB <sup>a</sup> (MPa)	water swell (%) <sup>b</sup>	FE <sup>c</sup> (mg/100 g wood)
1.40-1.50	0.70-0.80	4	80-100
1.30-1.35	0.60-0.70	4-5	40-50
1.20-1.25	0.45-0.55	5	25-35

<sup>a</sup> IB = internal bond; <sup>b</sup> Two hours cold water soak method (Meyer 1979a);

<sup>c</sup> Formaldehyde emission, perforator method (Meyer 1979a, Myers 1986).

Generally, the UF resins with higher F/U molar ratios are more durable and stable during storage than those with a lower F/U molar ratio (Northeast Forestry College 1981, Pizzi 1983).

### *Details of manufacture*

In the conventional manufacture of UF resin, urea is normally added in two portions (Pizzi 1983, Skeist 1965 and 1977). The first portion of urea is charged at the beginning of the reaction so that the initial F/U molar ratio is about 2.0. At the

completion of the condensation reaction, a second portion of urea is added to bring the F/U molar ratio down to about 1.1-1.4. The optimum second urea addition is normally about 20-30% of the total urea used. As the percentage of urea in the second urea addition is increased, the initial F/U molar ratio present during the resin synthesis is also increased. The time required for reaction increases and eventually a point is reached where insufficient urea is present to allow the condensation stage to continue. The resulting resins have low viscosity and a strong smell of free formaldehyde, which limits their usefulness as wood adhesives (Steiner 1973). The reverse trends are observed if lower percentages of the urea are added in the second addition. Low F/U molar ratios may lead to reaction rate increases, poor reaction control and likelihood of resin gelation.

### 1.3.2 Effect of pH

Reaction mechanism, reaction products, properties of the resins and properties of resin bonded wood products are critically dependent on reaction pH (Huang *et al.* 1988, Torrey 1978).

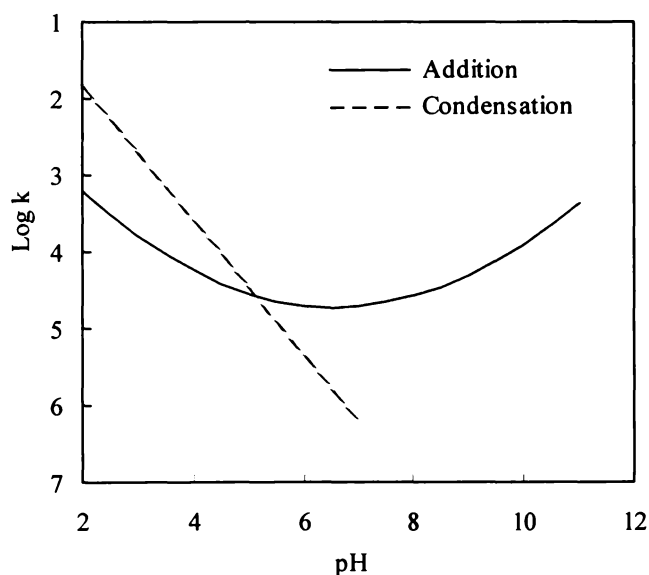


Figure 1.1. Influence of pH on the addition and condensation reaction rates of urea and formaldehyde at 35°C (Pizzi 1983).

The effect of pH on the rate of methylation has been studied by Crowe and Lynch (1948 and 1949). It was found that the rate increases rapidly from pH 8.7 to pH 12.7. The methylation reaction is catalysed by hydroxyl ions as well as by hydrogen ions (Figure 1.1). The reaction is reversible and the position of equilibrium is almost independent of pH (de Jong and de Jonge 1952 and 1953).

The condensation of urea and urea derivatives (MMU, DMU and TMU) is catalysed only by acid which favours the formation of methylene linkages (Smets and Borzee 1952). The rate of methylene bridge formation is proportional to the hydrogen ion concentration in the pH range of 3-7 (de Jong and de Jonge 1952 and 1953).

A comparison of the effect of pH on the addition and condensation reactions is given in Figure 1.1 (Pizzi 1983, Meyer 1979b). The rate of the addition reaction has a minimum in the pH range 5-7, whereas the rate of condensation increases linearly with decreasing pH. The effect of pH on the reaction mechanism has been given in Section 1.2.3.

Hse *et al.* (1994) studied the effects of reaction pH on the properties and performance of UF resin. They formulated the UF resin at three reaction pHs (1.0, 4.8 and 8.0) and four F/U molar ratios (2.5, 3.0, 3.5 and 4.0). The proportion of high molecular weight products and uron derivatives increased as reaction pH decreased. Panels bonded with resins prepared in strong acidic conditions resulted in lowest formaldehyde emission but had slightly lower internal bond. Based on the internal bond and formaldehyde emission data, weak acid catalysis seemed to provide the best compromise.

Generally, low pH ( $\text{pH} < 4$ ) causes rapid and uncontrollable condensation with overheating and formation of white compounds containing methylene bridges instead of methylol groups which solidify into useless masses (Pizzi 1983). Normally, the pH of additional stage is held at between 7.5 and 8.5, and at the condensation stage, the pH is lowered to 5.0.

### **1.3.3 Effect of Reaction Temperature and Time**

The reaction pH, temperature and time are three major interdependent factors controlling the UF reaction process. They determine the degrees of condensation. More condensed resins had higher molecular weights (and viscosities). In general, bond strength and bond durability increased with the degree of condensation (Inoue *et al.* 1956, Rice 1965).

The effects of pH and temperature vary with progress of reaction, eg pH and temperature have greater effect on reaction rate under acidic conditions than that under alkaline conditions and must be strictly and accurately controlled at each stage. Reaction temperature must be maintained at less than 100°C to avoid loss of control and resin gelation but should not be lower than 60°C to avoid low reaction rates and low degree of polymerisation.

If the reaction time is too long, the resin will have short storage life and low bonding strength due to excessive polymerisation. Inadequate reaction time will give low polymerisation and low bonding strength.

Normally, the reaction temperature is between 70 and 98°C, the reaction time is between 120 and 150 min (including an addition reaction time of 20-60 min and a condensation time of 40-100 min) (Huang *et al.* 1988, Northeast Forestry College 1981).

### **1.3.4 Purity of Raw Materials**

Both the formaldehyde solution and the urea may contain impurities and which affect preparation and properties of the UF resins.

#### *Effect of methanol*

Almost all commercial grade formaldehyde solutions contain some methanol either by the addition of methanol (7-12%) to stabilise the formaldehyde solution or

present as unoxidised methanol starting product. In addition, a small amount of methanol may be produced by the Cannizzaro reaction during the storage period. The level of methanol may vary from less than 3% up to 12% by weight.

Methanol retards the addition reaction and hinders the formation of methylene links in the condensation reactions (Pizzi 1983, Takahashi 1952). High water absorption results. Methanol-free formaldehyde (37-40% formaldehyde by weight), produces resins with good hot water resistance. Resin bonded wood panels have approximately 2% of water absorption. With formaldehyde containing 8-11% of methanol, the resin obtained was much less stable in water and had unusually high water absorption of 6-10% (Huang *et al.* 1988, Pizzi 1983).

High water absorption is due to the formation of methylated UF resins, which on curing give low crosslinking and poor resistance to hydrolysis. Thus either unstabilised formaldehyde (< 3% methanol maintained at about 60°C to avoid precipitation) or formaldehyde with the methanol removed by distillation should be used.

#### *Effect of formaldehyde acidity*

Because formaldehyde can be oxidised to formic acid by atmospheric oxygen and by the Cannizzaro reaction, there is always a small amount of formic acid in commercial formaldehyde solutions (0.05-0.10%). In concentration of more than 0.1%, formic acid may act as a catalyst and cause uncontrollable reaction (Huang *et al.* 1988 and Pizzi 1983). Overheating with the formation of a soft white gel which transforms into hard worthless resin, difficult to remove from the reactor, results. The formic acid must be neutralized before the urea is added.

#### *Effect of formaldehyde concentration*

Formaldehyde concentration has a major effect on the rate of reaction (Northeast Forestry College 1981). At a concentration of < 30%, the reaction rate is too slow to be useful, while at a concentration > 50%, the reaction rate is too fast to control

adequately. Normally, a formaldehyde concentration in the range of between 37 and 47% is used.

### *Effect of impurities*

Commercial urea may contain traces of impurities, such as sulphate salts and biuret ( $\text{H}_2\text{NCONHCONH}_2$ ). Even small amounts of sulphate salts ( $> 0.03\%$ ) in urea has an effect on the reaction rate and the performance of the UF resin bonded products (Huang *et al.* 1988, Northeast Forestry College 1981). When the sulphate salt content greater than 0.035-0.05%, reaction pH may fall during the initial stage causing the temperature to increase to the boiling point and producing a turbid solution. Sulphate salts in the resin products may shorten shelf life and cause deterioration of bonding strength.

Biuret in urea also has an effect on bonding strength and shelf life of final UF resins (Huang *et al.* 1988, Northeast Forestry College 1981). For example, the shelf life is about two months if the biuret content in urea is 1%. The shelf life is about one month if the biuret content is over 1.5%.

## **1.4 PREPARATION OF COMMERCIAL UF RESINS**

Most commercial UF resins are made in batch processes. Continuous production processes have also been described (Meyer 1979b, Vargiu *et al.* 1974).

The molecular weight of a commercial UF resin may vary from a few hundred Daltons to a few thousand Daltons, with a wide distribution of molecular size (Pizzi 1983, Katuscak 1981). The key characteristics of a commercial UF resin are normally its solubility, viscosity, pH and solids content. Commercial UF resins are available either in dry power form, or in aqueous solutions and as one-component or two-component systems.

The most common method of manufacturing commercial UF resins is the traditional two step method, which includes alkaline addition and acidic

condensation stages (Pizzi 1983, Williams 1984, Skeist 1965 and 1977). This method involves the reaction of urea with formaldehyde at a F/U molar ratio of more than 1.0. Generally, an initial F/U molar ratio of between 2.0 and 3.0 is used. A reaction temperature of up to the boiling point (98°C) of the reaction mixture is used to shorten the reaction time.

The pH of the formaldehyde solution is adjusted to between 7 and 9 in the reactor by addition of base and then the urea is charged into the reactor. The reaction mixture is then heated to the desired temperature for from 10 to 40 min. Methylolurea derivatives are formed. The reaction mixture is then cooled to between 70 and 80°C and the pH is lowered to between 4.8 and 5.0 to catalyse the condensation. The reaction is reheated to between 80 and 98°C and maintained in this temperature range until the desired viscosity is obtained. The condensation reaction is quenched by addition of base and the second charge of urea is added to bring down the F/U molar ratio to between 1.05 and 1.40 (Pizzi 1983).

Numerous other methods for the manufacture of UF resins have been reported (Vargiu *et al.* 1974, Spurlock 1983, Ho 1985). Most are modifications designed to lower the formaldehyde emissions while maintaining other properties unchanged (Huang *et al.* 1988, Skeist 1977, Pizzi 1983, Spurlock 1983, Bai 1981 and Ho 1985).

Ho (1985) modified the reaction method by using three or four additions of urea. The addition stage reaction was similar to the conventional method, but during the condensation stage, a second, a third or even a fourth urea addition stage was used to bring the F/U molar ratio down step by step from the original 2.0 to 1.8-1.9, then to 1.5 and finally to 1.0-1.15. The final resins had low free formaldehyde (< 0.15%). The particleboard made with these resins had internal bonds of between 0.51 and 0.55 MPa and gave formaldehyde emissions of between 8.7 and 9.2 mg HCHO per 100 g board.

A low pH one stage reaction has been reported (Eisele *et al.* 1977, Williams 1983a and 1983b). In this process, urea is slowly charged into acidic formaldehyde solution to maintain a temperature of between 50 and 70°C. No additional heat is required.

The pH is maintained between 0.5 and 2.5 (preferably 1.0) throughout the addition of urea. Urea is added to achieve a F/U molar ratio of between 2.9 and 3.1. After the desired viscosity has been obtained, the reaction mixture is neutralized by the addition of base. A final charge of urea is added to give a final F/U molar ratio of between 1.2 and 1.0. This resin can be cured without the addition of acidic hardeners. When cured, this resin contains substantially more methylene groups than methylene ether groups. As a result, the resin is more stable and emits less formaldehyde than the conventional UF resins. Other properties are comparable to those of conventional resins. But, this method suffers from the risk of losing control of the reaction (gelation) (Whiteside 1987) and some adverse effects on the internal bonds (Hse *et al.* 1994).

Another procedure with four stages has been patented by Williams (1984). Formaldehyde emissions of between 40 and 50% lower than the conventional resins and with twice as many as methylene groups as methylene-ether groups were claimed.

A continuous process had been described (Vargiu *et al.* 1974). The UF reaction mixture is passed through three reaction stages. An initial reaction stage is carried out at basic pH between 8.0 and 9.5 and with a F/U molar ratio of between 2.1 and 2.7. This is followed by a short intermediate stage (4-10 min) at pH of between 4.0 and 5.5. A final stage at pH between 6.6 and 7.0 and a F/U molar ratio of 1.4-1.65 is used.

## **1.5 APPLICATIONS OF UF RESINS IN BOARD MANUFACTURE**

Most UF resins are used as wood adhesives in the manufacture of particleboard, fiberboard, plywood and veneer. In a typical method (Skeist 1977) for producing particleboard or fiberboard 7-10 parts (by weight) of UF resin is sprayed into 100 parts of wood chips or fibres (moisture content 5-10%) and 2-3 MPa pressure is applied to the mat at 150-200°C for several minutes.

Control of the moisture content of the wood chips is important. Moisture content above 10% may result in blisters in the final product, whereas moisture content below 5% may cause excessive penetration of the resin and result in a weak bonding of the particles.

Sometimes, wax is incorporated to enhance water resistance, although it can result in a slight decrease in board strength.

The use of 1-2% pentachlorophenol as an additive has been reported to impart resistance to attack by fungi and insects (Skeist 1977, Huber 1958).

Conventional UF resin adhesive shrinks and crazes upon curing and aging. Addition of 5-50 parts of furfuryl alcohol to 100 parts of urea resin (solids) improves the craze resistance markedly (Skeist 1977, Simons 1950), or addition of dimethyl formamide in 31-38% by weight of dry UF resin produces a gap-filling, craze-resistant adhesive (Skeist 1977, Corwin 1959).

## **1.6 INSTRUMENTAL METHODS FOR UF RESIN CHARACTERISATION**

In the past, formulations for UF resins adhesives have been for the most part developed empirically (Hse 1974a). This situation has resulted from two principal factors: (a) the immediate requirements of industry have been satisfied with little fundamental research; (b) the complexity and instability of the resin system make complete chemical analysis extremely difficult.

Improved analytical instrumental techniques are providing new tools to investigate the UF reaction mechanism. The new instrumental methods have been used to observe the chemical reaction of urea with formaldehyde, to investigate and identify the species present in the UF resins and correlate them with the properties of the resins or resin bonded products.

One of the most useful analytical developments has been the application of NMR spectroscopy (especially  $^1\text{H}$ ,  $^{13}\text{C}$  and  $^{15}\text{N}$  NMR) to resin studies (Derome 1989, Ferg *et al.* 1993, Jada 1990, Chuang and Maciel 1992, Kim and Amos 1990, Sebenik *et al.* 1982, de Breet *et al.* 1977, Chuang *et al.* 1985, Ebdon *et al.* 1984, Taylor *et al.* 1982, Chiavarini *et al.* 1975, Schindlbauer and Schuster 1983, Hahmemstein *et al.* 1995, Meyer and Numlist 1981). Other methods include mass spectroscopy (MS) (Chang 1994) and electrospray mass spectroscopy (ESMS) (Gumbley 1995a), traditional column liquid chromatography (LC) and high performance liquid chromatography (HPLC) (Kumlin and Simonson 1978a, Chang 1994), gel permeation chromatography (GPC) (Braun and Bayersdorf 1980, Ludlam and King 1984, Hse *et al.* 1994), gas chromatography (GC) (Christensen 1980), infrared spectrometry (IR) (Camino *et al.* 1996, Pshenitsyna *et al.* 1980), Raman spectroscopy (Hill *et al.* 1984) and ultraviolet spectrometry (UV) (Camino *et al.* 1996), differential scanning calorimetry (DSC) (Sebenik *et al.* 1982, Camino *et al.* 1996, Hill *et al.* 1984) or differential thermal analysis (DTA) (Fomicheva and Semenenko 1991, Trub *et al.* 1989), thermogravimetric analysis (TGA) (Jada 1988, Myers 1981, Camino *et al.* 1996, Zeman and Tokarova 1992), thermomechanical analysis (TMA) (Yin *et al.* 1995), dynamic mechanical analysis (DMA) (Ludbrook and Whitwood 1992) and X-ray diffraction (Chow and Troughton 1975, Steiner 1974).

General reviews of the physical characterisation of UF resins may be found in the references (Tsuge 1981, Christensen 1980). The NMR and chromatography methods will be described in the following sections.

### **1.6.1 Application of NMR Techniques**

NMR, especially  $^{13}\text{C}$  Fourier transform NMR spectroscopy, has been used as a tool to qualitatively and quantitatively identify species present in UF resins (Valdez 1995, Tomita and Hatono 1978, Ferg *et al.* 1993).

The  $^{13}\text{C}$  NMR experiment is a relatively insensitive technique (ie it is characterised by a low signal to noise ratio signal) compared with other common analytical techniques. This is a consequence of the small population difference between the

levels of nuclei in the aligned and opposed nuclear spin states generated in an applied magnetic field and the low natural abundance of carbon-13 (c 1.1% of total carbon). To compensate for this, large amounts of sample (often several grams), are used and numerous scans (hundreds to thousands, or even tens of thousands) are acquired and averaged.

In order to obtain quantitative results, the time between two pulses (repetition of the NMR experiment) must be long enough (about 5 times of the spin-lattice relaxation time) to avoid saturation effects attributable to long spin-lattice relaxation times. Since the longest spin-lattice relaxation time of the species present in UF resins is typically of the order several seconds, it has been suggested that the time between two pulses (transient time or pulse repetition time) must be at least 20 seconds (Valdez 1995). A  $^{13}\text{C}$  NMR experiment can therefore require several tens of minutes, or hours, of data acquisition.

Ebdon and Heaton (1977), Tomita and Hatono (1978) and Slonim (1979) identified various functional groups and assigned chemical shifts by using model compounds. The chemical shift assignment of some of the key species in UF resins are:

- carbonyl carbons occur at around 160 ppm;
- methylene carbons occur at 47.7 ppm in  $-\text{NH}\underline{\text{C}}\text{H}_2\text{NH}-$ , 53.8 ppm in  $-\text{NH}(\text{CH}_2-)\underline{\text{C}}\text{H}_2\text{NH}-$  and 60.0 ppm in  $-\text{NH}(\text{CH}_2-)\underline{\text{C}}\text{H}_2\text{N}(\text{CH}_2)-$ ;
- methylol carbons occur at 65.1 ppm in  $-\text{NH}\underline{\text{C}}\text{H}_2\text{OH}$  and 71.7 ppm in  $-\text{N}(\text{CH}_2-)\underline{\text{C}}\text{H}_2\text{OH}$ ;
- dimethylene ethers occur at 69.4 ppm in  $-\text{NH}\underline{\text{C}}\text{H}_2\text{O}\underline{\text{C}}\text{H}_2\text{NH}-$  and  $-\text{NH}\underline{\text{C}}\text{H}_2\text{OCH}_2\text{OH}$ , 76.0 ppm in  $-\text{N}(\text{CH}_2-)\underline{\text{C}}\text{H}_2\text{OCH}_2\text{NH}-$  and  $-\text{N}(\text{CH}_2-)\underline{\text{C}}\text{H}_2\text{OCH}_2\text{OH}$ ;

- resin methoxy carbons occur at 55.6 ppm, while that of methanol occurs at 50 ppm;
- methylene glycol carbons occur at 83.1 ppm in (HOCH<sub>2</sub>OH), 86.6 ppm in (HOCH<sub>2</sub>OCH<sub>2</sub>OH), 90.7 ppm in (HOCH<sub>2</sub>OCH<sub>3</sub>) and 95.0 ppm in (H(OCH<sub>2</sub>)<sub>n</sub>OCH<sub>2</sub>OCH<sub>3</sub>).

Tomito and Hatono (1978) have measured the spin-lattice relaxation time ( $T_1$ ) by the inversion recovery method (Derome 1989, Akitt 1992, Field and Sternhell 1989). Their results are given in Table 1.3.

Table 1.3. Spin-lattice relaxation time ( $T_1$ ) of different species in UF resins.

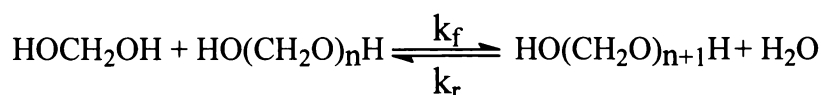
species	structure	$T_1$ (sec)
urea carbonyl carbon residue	>N <u>C</u> ON<	1.4
methyl carbon of methyl ethers	-NHCH <sub>2</sub> O <u>C</u> H <sub>3</sub> , -N(CH <sub>2</sub> -)CH <sub>2</sub> O <u>C</u> H <sub>3</sub>	1.8
methylene glycol species	HO <u>C</u> H <sub>2</sub> OH, HO <u>C</u> H <sub>2</sub> O-	1.5
hemiformals	-NHCH <sub>2</sub> O <u>C</u> H <sub>2</sub> OH, -NH(CH <sub>2</sub> -)CH <sub>2</sub> O <u>C</u> H <sub>2</sub> OH	0.21
combined formaldehydes and most of other carbons	- <u>C</u> H <sub>2</sub> -	0.04-0.07

Kim and Amos (1990) applied quantitative <sup>13</sup>C NMR to investigate the relationship between UF resin manufacturing conditions and the formaldehyde emission levels. They found that in methylation and methylene bond-forming reactions, substitution limits existed and led to free formaldehyde. When the initial F/U molar ratio was lowered to reduce free formaldehyde, the reaction rate was faster and the synthesis became difficult to control.

Chuang and Maciel (1994) used  $^{13}\text{C}$  cross-polarisation and magic angle spinning (CP/MAS) solid state NMR techniques to investigate the stability of UF resins toward hydrolytic treatments. With  $F/U = 1.0$ , the major components were linear methylene linkages, cross-linking methylene linkages and terminal methylols. The linear methylene linkages were more stable toward hydrolytic treatment than the cross-linking methylene linkages. The resin prepared with  $F/U = 2.0$  contained a wide variety of components, and some of those were susceptible to hydrolytic degradation, included dimethylene glycol ( $\text{HOCH}_2\text{OCH}_2\text{OH}$ ), poly(oxymethylene glycol) ( $\text{HO}(\text{CH}_2\text{O})_n\text{CH}_2\text{OH}$ ) and methylol attached to tertiary amides ( $-\text{CO}-\text{N}-\text{CH}_2\text{OH}$ ). These hydrolytically susceptible components were probably the main formaldehyde emitters in UF resin products. Linear methylene linkage and cross-linking methylene linkages were relatively stable toward hydrolytic treatments.

Hahnenstein *et al.* (1994) used  $^1\text{H}$  and  $^{13}\text{C}$  NMR to study the chemical equilibria in solutions of formaldehyde in water, deuterium oxide and methanol. They found that the equilibria involving poly(oxymethylene) glycol were independent of the use of water or deuterium oxide, with the equilibrium constants showing no concentration dependence.

In  $^1\text{H}$  NMR studies of aqueous formaldehyde it was indicated that the signals due to the methylene protons of methylene glycol species in acidic conditions were satisfactorily resolved, whereas in basic solutions these methylene peaks coalesced into a single broad peak (Tomita and Hirose 1976, Tomito and Hatono 1978). The broadening and coalescing of the peaks was attribute to a shortening of the average lifetime by increases in the reaction constants  $k_f$  and  $k_r$  (Tomito and Hatono 1978):



However, the  $^1\text{H}$  NMR spectrum of an UF resin does not provide enough information on the structure of the resin because the absorptions are broad and overlapping and the presence of water is still a problem.

NMR quantitative results were less dependable when UF resins were turbid and incompletely soluble in the NMR solvent or when they were highly substituted and cross-linked. Solid state CP/MAS NMR was more appropriate for the study of these systems and the species in the nonsoluble portion in UF resins or formed during the curing processes.

Quantitative solid-state NMR spectra of freeze-dried UF resins have fewer resonance peaks than solution NMR spectra. Peaks in the methylene region (0-100 ppm), essential for UF resin identification, are broad and overlapped. Another obvious difference between solid and solution NMR spectra of uncured UF resin is the lack of resonance peaks characteristic of methanol, methoxy and cyclic ethers. This means that the solid-state NMR technique utilising the freeze-dried samples may be not appropriate for by-products and other low molecular weight condensates present in low concentrations in uncured resin. However, the solid-state  $^{13}\text{C}$  NMR technique is sensitive to changes in the structure of uncured UF resins arising from pH change during synthesis.

Chuang and Maciel (1992) used  $^{13}\text{C}$  CP/MAS NMR to study the structure of UF resins formed under a variety of reaction conditions (F/U molar ratio, urea concentration and pH value). Jada *et al.* (1990) used CP/MAS  $^{13}\text{C}$  NMR to determine the proportion of various functional groups present in uncured UF resins and to compare the proportion of functional groups present in UF resins before and after curing. The resin prepared in acid medium showed more methylene units and less methylol moieties than the resin prepared in alkaline conditions.

Ebdon *et al.* (1984) used model compounds to assign the chemical shift in  $^{15}\text{N}$  NMR spectra of UF resins (see Table 1.4).  $^{15}\text{N}$  NMR can be used to distinguish between unsubstituted amino groups, secondary and tertiary amino groups carrying methylol substitutes, secondary and tertiary amino groups involved in methylene and methylene ether linkages. The information available from  $^{15}\text{N}$  NMR spectra supports that from  $^{13}\text{C}$  and  $^1\text{H}$  NMR spectra. Most of the information regarding the relative proportions of methylol groups, methylene linkages and methylene ether linkages can

be obtained more easily from  $^{13}\text{C}$  NMR, but  $^{15}\text{N}$  NMR spectroscopy is particularly useful for determining sequence lengths (Ebdon *et al.* 1984).

Table 1.4.  $^{15}\text{N}$  NMR signals assignments for UF resin species.

assignment	compound or resin species	chemical shift (ppm) <sup>a</sup>
$\underline{\text{N}}\text{H}_2\text{CON}\underline{\text{H}}_2$	urea	55.6
$\underline{\text{N}}\text{H}_2\text{CONHCH}_2\text{OH}$	monomethylolurea	55.3
$\underline{\text{N}}\text{H}_2\text{CONHCH}_2\text{NHCON}\underline{\text{H}}_2$ & $\underline{\text{N}}\text{H}_2\text{CONH-}$	methylenediurea and chain ends	54.2, 54.8
$\text{HOCH}_2\underline{\text{N}}\text{HCONH}_2$	monomethylolurea	80.4
$\text{HOCH}_2\underline{\text{N}}\text{HCON}\underline{\text{H}}\text{CH}_2\text{OH}$	N,N'- dimethylolurea	80.2
$\text{HOCH}_2\underline{\text{N}}\text{HCONH-}$	chain ends	79.2, 79.8
$(\text{HOCH}_2)_2\underline{\text{N}}\text{CONHCH}_2\text{OH}$	trimethylolurea	101.6
$\text{NH}_2\text{CON}\underline{\text{H}}\text{CH}_2\underline{\text{N}}\text{HCONH}_2$	methylenediurea and other dimers	73.2, 73.5
$-\underline{\text{N}}\text{HCH}_2\underline{\text{N}}\text{H-}$	within chains	73.0
$-\underline{\text{N}}\text{HCH}_2\text{OCH}_2\underline{\text{N}}\text{H-}$	ether linked dimers	72.6
$>\underline{\text{N}}\text{CH}_2(-\text{OCH}_2\text{-})$ or $-\underline{\text{N}}<$	branch points in chains	$\sim 93^{\text{b}}$

<sup>a</sup> relative to  $\text{NH}^+$ :  $\pm 0.1$  ppm, <sup>b</sup> predicted chemical shift.

Chuang *et al.* (1985) used solid state CP/MAS  $^{15}\text{N}$  NMR to investigate UF resins with and without  $^{15}\text{N}$  enrichment. They assigned chemical shifts of four model compounds (see Table 1.5). While a lower level of structural detail was obtained than that was provided by corresponding  $^{13}\text{C}$  CP/MAS NMR experiments,  $^{15}\text{N}$  data provided useful supplementary data for the elucidation of structure in cured UF resins.

Table 1.5. Solid state CP/MAS  $^{15}\text{N}$  NMR signal assignments of five model compounds.

assignment	model compound	chemical shift (ppm)
$\text{NH}_2\text{CONHCH}_2\text{NHCONH}_2$	methylenediurea	96.1
$\text{NH}_2\text{CONHCH}_2\text{NHCONH}_2$	methylenediurea	77.8
$\text{CH}_3\text{OCH}_2\text{NHCONHCH}_2\text{OCH}_3$	dimethylolurea dimethylether	93.7
$\text{HOCH}_2\text{NHCONHCH}_2\text{OH}$	dimethylolurea	101.6
$\text{NH}_2\text{CONH}_2$	$^{15}\text{N}$ -enriched urea	79.6

### 1.6.2 Chromatographic Analyses of UF Resins

Chromatography has been used in investigation of UF resins since the 1950s. Among the chromatographic methods applied, paper chromatography (Hamada 1955, Inoue and Kawai 1957, Lee 1972) and thin layer chromatography (Lee 1972 and Ludlam 1973) gave poor resolution of the components, and these methods are in general less suitable for quantitative determination. Gel permeation chromatography (GPC) (also known as size-exclusion chromatography, SEC) is useful for the characterisation of the molecular weight distribution (Armonas 1970, Hope *et al.* 1973, Tsuge *et al.* 1974, Tsuge 1976, Dankelman *et al.* 1976, Billiani *et al.* 1990, Hlaing *et al.* 1986, Ludlam and King 1984), but little or no information about the composition of the low molecular weight part is obtained. Traditional column liquid chromatography (Kumlin and Simonson 1978) and high performance liquid chromatography (HPLC) are useful for the determination of low molecular species present in UF resins. They are especially suitable for investigating the early stage of the UF reaction (Tsuge and Senba 1981).

#### *Paper and thin layer chromatography*

In the 1950s, Hamada (1955) and Inoue and Kawai (1957) studied urea-formaldehyde-methanol condensation products of low relative molecular mass by using one dimension paper chromatography. Poor separation of urea, MMU and

DMU severely limits the information that can be obtained by this technique. Ito (1959 & 1961) used two-dimensional paper chromatography to separate the low molecular weight species present in UF resins. The separation was much better than that of one-dimensional paper chromatography and a careful examination of the resins was undertaken.

Ludlam (1973) used thin layer chromatography to separate and identify the low relative molecular weight ( $< 200 \text{ g mol}^{-1}$ ) addition and condensation products of urea and formaldehyde and their methyl ether. Ludlam (1973) also synthesised model compounds, including MMU, DMU and methylenediurea (MDU) to assist in the identification of the species present in the UF resins and discussed the stability of the model compounds:

- MDU is stable in the solid state form. However it will hydrolyse in aqueous solution, the reaction being catalysed by hydrogen ions;
- The ethers are more stable, both in solution and as solids, than the methylol derivatives and can be stored for many months at room temperature without marked decomposition;
- The methylol compounds, show indication of decomposition after a few weeks, and in aqueous or alcoholic solution, will decompose in a few hours;
- The reactions of methylol compounds and, to a lesser extent, the ethers, are catalysed strongly by hydrogen ions. Therefore, if their solutions are directly applied to the acidic thin layer chromatography plates, decomposition will occur. This problem can be overcome by pre-treating the thin layer chromatography plates with ammonia vapour before application of the sample solution.

Nair and Francis (1983) used a quantitative thin layer chromatography technique to investigate the kinetics and mechanism of urea-formaldehyde reaction. Their results were:

- The rate constants for the formation of MMU pass through a minimum in the pH range 4.5-8.0, thereby proving catalysis by both  $H^+$  and  $OH^-$ ;
- The reaction under alkaline conditions leads to methylol formation, acidic conditions favour formation of methylene bridges;
- The higher homologues were formed through the methylation of methylene urea followed by its condensation with free urea and not by the reaction of methylene urea with methylol urea.

### *Liquid chromatography and high performance liquid chromatography*

Traditional column chromatography (including the classical open-column and non open-column liquid chromatography) and HPLC are all column liquid chromatography. Relative to the traditional column liquid chromatography, HPLC uses a smaller and shorter column with microparticle packing. The separation efficiency is much higher. The main advantages of HPLC are high speed, resolution, sensitivity and convenience for quantitative analysis.

Kumlin and Simonson (1978) studied UF resins by using a classical open-column liquid chromatography system. They used model compounds, including urea, formalin (42% formaldehyde aqueous solution), MMU, DMU, methylenediurea, monomethylolmethylenediurea, methyl- and ethyl ethers of mono- and dimethylolurea to determine their volume distribution coefficients in different column and mobile phase systems and correlated the distribution coefficients with their retention time. In another paper (Kumlin and Simonson 1978), the same authors used a classical preparative column to isolate N,N-DMU and TMU which were identified by high resolution  $^1H$  NMR. It was found that TMU was the dominant methylol compound at high F/U molar ratio ( $F/U \geq 4.0$ ), formation of tetramethylolurea was not observed and N,N-DMU was formed to a much lesser extent than N,N'-DMU.

In other papers, Kumlin and Simonson (1980 and 1981) described the formation of monourea methylol compounds and diurea compounds containing methylene and dimethylene ether bridges in different condition (pH and F/U molar ratio). It was pointed out that a pH value outside a narrow range could easily result in an uncontrolled condensation during the UF resin preparation (Kumlin and Simonson 1980 and 1981).

*Size-exclusion chromatography (gel permeation chromatography)*

During the past two decades, a substantial effort has been made to study the molecular weight and molecular weight distribution of UF resin using SEC (GPC) (Braun and Bayersdorf 1980, Katuscak *et al.* 1981, Kumlin and Simonson 1981, Armonas 1970, Hope *et al.* 1973, Tsuge *et al.* 1974, Dankelman *et al.* 1976, Matsuzaki *et al.* 1980, Taylor *et al.* 1980, Braun and Bayersdorf 1980, Dunky *et al.* 1981). Difficulties arise due to the poor solubility of high molecular weight species. Even the most effective solvent, dimethyl sulphoxide (DMSO), UF resin of high relative molecular mass does not dissolve completely (Ludlam and King 1984, Kumlin and Simonson 1981). UF resins are difficult to dissolve because there are strong intermolecular hydrogen bonds formed between the polar sites on the molecules and producing a super molecular structure.

Katuscak *et al.* (1981) studied the solubility of UF resins in water, tetrahydrofuran (THF), THF with 5, 10 and 20% water, dimethyl sulphoxide (DMSO), DMSO with 5, 10 and 20% water; dimethyl formamide (DMF), DMF with 5, 10 and 20% water; dioxane with 10, 20, 30, 40 and 50% water; formic acid (55%), carbon chloride, chloroform, benzene, methanol, ethanol, *n*-propanol, *isopropanol* and acetone. The most effective solvents were shown to be DMSO and dioxane with 40% and 50% water. Many UF resins were successfully dissolved in THF with 10% water, but cannot dissolve completely in DMF and water mixed solvent in the 1-10% concentration ranges.

UF resins even when condensed to a high degree can dissolve in DMF containing high concentration of LiCl ( $> 1 \text{ mol L}^{-1}$ ) and the solution can be infinitely diluted

with solvents such as DMF and DMSO (Ludlam and King 1984, Hlaing *et al.* 1986). The effect of the LiCl concentration in the mobile phase was examined by Nomayr *et al.* (1983). Their results showed that increasing the concentration of LiCl above 0.5% ( $c$  0.1 mol L<sup>-1</sup>) had little effect on the chromatogram obtained. Lithium chloride may eliminate the hydrogen bonds that are responsible for the association effect and ensure realistic values of molecular weight are obtained (Ludlam and King 1984). Besides lithium chloride, it was reported that lithium nitrate (LiNO<sub>3</sub>) may also eliminate the hydrogen bonds in UF resins (Gilbert and Booth 1986).

Gilbert and Booth (1986) used two SEC column systems with two solvents of N, N'-dimethylacetamide (DMA) and DMA + 0.1 mol L<sup>-1</sup> LiNO<sub>3</sub> to investigate an UF resin. They expressed the molecular weight distribution roughly as three parts, ie low molecular weight (low M), moderate molecular weight (moderate M) and aggregates (see Table 1.6).

Table 1.6. Effect of reaction time and conditions on UF resin composition.

sample	reaction time		weight % chains		weight %
	under reflux (hours)	at room temp (weeks)	low M	moderate M	aggregates
1	3.5	-	80	15	5
2	4.5	-	73	20	7
3	6.5	-	68	25	7
4	6.5	1	57	19	24
5	6.5	4	49	25	26

Katuscak *et al.* (1981) used SEC, combined with some other methods, to estimate the average molecular weights (number-average molecular weight  $\bar{M}_n$ , weight-average molecular weight  $\bar{M}_w$  and z-average molecular weight  $\bar{M}_z$ ), molecular weight distribution and polydispersity coefficient. A reaction with F/U = 2.0 at acidic medium of pH = 4.5-5.0 at 90°C was studied. Their conclusions were:

- After the reaction proceeded for 30-45 min, the viscosity of the reaction mixture reached 5-10 mPa.s. The average molecular weights were  $\bar{M}_n \approx 100 \text{ g mol}^{-1}$ ,  $\bar{M}_w \approx 200 \text{ g mol}^{-1}$  and more than 95% of the molecular weight was less than 200 g mol<sup>-1</sup>. The polydispersity coefficient ( $R = \bar{M}_w / \bar{M}_n$ ) was  $R < 1.5$ .
- At about 120 min, the low molecular weight oligomers with  $\bar{M} < 200 \text{ g mol}^{-1}$  decreased to about 10-20%. Viscosity reached 100 mPa.s. The average molecular weights of the resins were  $\bar{M}_n \leq 500 \text{ g mol}^{-1}$  and  $\bar{M}_w \leq 1500 \text{ g mol}^{-1}$ . The polydispersity coefficient was about 3.5. Commercial UF resins are usually produced in this stage.

The average molecular weights of commercial UF resins may vary greatly depend on the manufacturing conditions. Typical values were  $\bar{M}_n$  between 140 and 500 g mol<sup>-1</sup>,  $\bar{M}_w$  between 800 and 3000 g mol<sup>-1</sup>,  $\bar{M}_z$  between 3000 and 25 000 g mol<sup>-1</sup>, and polydispersity between 5 and 30 (Ludlam and King 1984).

### 1.6.3 Other Analytical Techniques

Other research techniques have been used to investigate UF resins including thermal analysis methods, eg differential scanning calorimetry (DSC), differential thermal analysis (DTA), thermogravimetric analysis (TGA) and thermomechanical analysis (TMA), dynamic mechanical analysis (DMA) and spectroscopic method, eg IR and Raman.

#### *Thermal analysis*

Thermal analysis involves measuring changes in a sample as its temperature is increased. Both DSC and DTA measure the same thermal effects (exothermic or endothermic) of the sample. The difference between DSC and DTA is mainly instrumental. DSC measures the differential power (heat input) necessary to keep a sample and a reference substance isothermal as temperature is changed (scanned, usually at 5-10°C min<sup>-1</sup>). DTA monitors the temperature difference between a sample and a reference substance as a function of temperature. Temperature is usually

scanned at a rate of from 5-10°C min<sup>-1</sup>. DSC and DTA can be used to study heats of reaction (eg crosslinking), thermal stability (decomposition and oxidation) and phase transitions (eg crystallising and melting) of UF resins.

TGA involves measuring the mass changes of a sample as its temperature is raised. It is useful in the study of curing reactions and thermal stability. Since the 1980s, TGA has been applied to the study of the thermolysis mechanism of UF resins (Trub *et al.* 1989, Zeman and Tokarova 1992).

TMA is the monitoring of the size (thickness) changes or flexion of a sample during an isothermal or temperature programmed analysis. TMA is suitable for the study of curing processes and mechanical properties of the cured resins and resin bonded products.

Szesztay *et al.* (1993) used DSC (in temperature programmed mode) to investigate the curing of UF resins. In spite of the very different origins of the adhesives (both commercial and laboratory made), several common features in their thermal behaviour were observed. The maximum curing reaction rate (exothermal maximum) was detected in the range of 80-85°C. Elimination of formaldehyde, ie the decomposition of the dimethylene ether linkage (-CH<sub>2</sub>OCH<sub>2</sub>-), was observed at 105-150°C (endothermic peak). At temperatures of about 170°C, thermal decomposition of methylene linkage took place which affected the mechanical properties of the adhesives. Temperatures over 200°C led to complete destruction of the resin accompanied by a series of exothermic and endothermic effects. They suggested an optimum curing temperature range of between 100 and 150°C. Their observation also showed that the areas under the endothermic peaks were proportional to the concentration of -CH<sub>2</sub>-O-CH<sub>2</sub>- linkages in the UF resins and could be used to estimate the formaldehyde emission levels.

Ebewele (1995) used DSC to study the thermal behaviour of amine modified and unmodified UF resins and to identify the physical and morphological factors responsible for improved performance. The modified resin exhibited a higher cure rate and greater cure exotherm than the unmodified resin.

Yin *et al.* (1995) used TMA to investigate the curing process directly in the wood joint. His results showed that the UF resin curing started at about 80°C (the elastic modulus started to increase) and completed at about 105°C (the elastic modulus reached a maximum). The maximum curing rate was at about 90°C.

Ebewele (1995) used TMA to study cured UF resins. By comparing the TMA thermal behaviour of amine modified and unmodified UF resins, he concluded that amine modified UF resins were inherently tougher and more durable than the unmodified UF resins.

### *Other methods*

Other methods for the physical characterisation of UF resins include dynamic mechanical analysis (DMA) (Lewis and Gillham 1962 & 1963, Gillham and Lewis 1963, Gillham 1974, Cook and Tod 1993, Steiner and Warren 1981, Ohyama *et al.* 1995) and infrared spectroscopy (IR) (Kozlova 1976 and Meyer 1979a, Myers 1981, Pshenitsyna *et al.* 1980) and Raman spectroscopy (Meyer 1979a, Paul and Hendra 1976, Meyer 1979d, Hill *et al.* 1984). DMA provides information about changes in mechanical properties during heating, whereas IR and Raman methods give information about functional groups. These methods were not used in this research.

## **1.7 ENHANCING THE PROPERTIES OF UF RESINS**

As outlined in Section 1.1, a disadvantage of UF resins is their poor water-resistance and high formaldehyde emission (Petrov *et al.* 1984, Word *et al.* 1984, Sedliacik *et al.* 1985) relative to other wood adhesives, eg phenol-formaldehyde resin. UF resins hydrolyse at elevated temperature (30-40°C) and high relative humidity (RH) (60-95%) (Huang *et al.* 1988, Dutkiewicz 1983, Meyers *et al.* 1985a and 1985b). The low durability of UF-bonded wood products under exposure to moisture or warm, humid conditions, limits the use of these products to interior, nonstructural applications (Tamura 1985). Extensive work has been done in order to overcome these problems.

### **1.7.1 Enhancing Water-Resistance and Durability**

UF products are sensitive to both hydrolysis (Myers 1985, Neusser and Schall 1970, Robitschek and Christensen 1976, Ginzl 1973, Troughton and Chow 1968, 1969a and 1969b, Higuchi and Sakata 1979, Freeman and Kreibich 1968) and stress scission (Dinwoodie 1977 and 1978, Bolton and Irle 1987, Irle and Bolton 1988). These sensitivities can be attributed to the following structural factors:

- Presence of bonds in the resin or between resin and wood that are susceptible to hydrolysis, eg free end methylol groups and ether groups;
- Inherent rotational stiffness of the urea structure, which creates a brittle cured resin that is unable to respond reversibly to stresses arising from cure shrinkage, wood swelling and shrinkage caused by moisture uptake and loss (cyclic moisture content).

#### *Modification of UF resins by melamine and phenol*

Modified commercial UF resins have been available to produce various degrees of moisture resistance in particleboard and MDF since the early 1970s. The development work was focused mainly on the use of melamine or phenol to produce melamine-urea-formaldehyde (MUF) resins and phenol-urea-formaldehyde (PUF) resins. The modification may be as simple as adding melamine powder into the finished UF resins or mixing UF resins with melamine formaldehyde (MF) resin, or as complicated as a multi-step copolymerisation process. For example, it was reported (Pizzi 1983b) that when a small amount of fine powdered melamine or 15-20% of MF resin was blended with an UF resin, the resin product obtained had increased resistance to boiling water. In another study (Shiau and Smith 1985), melamine (0.15-40%) was copolymerised with urea and formaldehyde to produce a melamine modified UF resin of low formaldehyde emission.

Hse and He (1990) used melamine (9.5-34.4 wt %) to modify UF resin in a two step reaction. Urea and formaldehyde were reacted under acidic conditions (pH = 1.0) at 60°C for 30 min. Then melamine was added and reacted under alkaline conditions (pH = 8.5) at 85°C for 70 min. It was claimed that the product with the optimum melamine content of 24 wt % exceeded the performance of phenol-formaldehyde (PF) resin and was 20% less expensive.

Similarly, addition of a small amount of phenol to the UF resin formulation produced copolymerised condensation products, which had the advantages of both UF and PF resins. The overall property of the modified resin was comparable with those of PF resin (Northeast Forestry College 1981, Pizzi 1983) and could be produced at lower cost.

Ohyama (1995) and Tomita and Hse (1992 and 1993) manufactured PUF co-condensed resin by alkaline treatment of the co-condensed resin once synthesised from UF-concentrate and phenol. They found that the resol-type co-condensed resin displayed almost the same curing behaviour and heat-resistance as a commercial resol. The optimum molar ratio of formaldehyde/urea/phenol was found to lie between 3:1:1 and 4:1:1.

#### *Modification of UF resins by non-structural additives*

Compounds such as multifunctional amines and synthetic emulsions (latexes), have been used as additives to modify UF resins:

- Urea-terminated di- and tri-functional aliphatic amines (hexamethylene-diamine, bishexa- methylenetriamine and triethylaminetriamine) were the most promising modifiers for UF resins (Ebewele *et al.* 1994). The resistance of wood joints to cyclic stress and moist-heat aging was superior to that of joints bonded with unmodified UF resins.
- Synthetic emulsions (Huang *et al.* 1988), for example butadiene-styrene latex (Zolochovski *et al.* 1983), styrene-butadiene latex (Doi 1994), carboxyl butadiene-

styrene latex (Jorshak *et al.* 1984), butadiene-acrylonitrile latex, butadiene-ethylene chloride latex, acrylate-acrylic acid copolymer latex (Glazkov *et al.* 1997, Huang *et al.* 1988) and polyvinylacetate latex (Doi 1994) were effective modifiers. Of these emulsions, butadiene-styrene and carboxyl butadiene-styrene latexes are the cheapest and best for this purpose.

- Polyethylene glycol phenyl ether may be used to chemically modify UF resins to enhance their water resistance. Some of the natural polymers, eg starch, starch carbonate, “black liquor” from paper industry, alkaline lignin, hydrolysis lignin, lignin sulphonate (ammonium or calcium salt) (Calve 1983) may also be used as modifiers. Such modification can enhance the water resistance of the resins bonded products.
- Blending a small portion of epoxy resin into UF resin can enhance both the water resistance and bonding strength.
- Inorganic salt or minerals,  $\text{Al}_2(\text{SO}_4)_3$  (Iosifov *et al.* 1985, Elbert 1984),  $\text{AlPO}_4$  (Iosifov *et al.* 1985) and NaBr may be used as fillers to enhance the water resistance.
- The durability of UF bonded wood products may be enhanced by flexible amines and hydrochloride amine salt curing agent. These additions alter the adhesive structure and produce a more flexible network (Ebewele *et al.* 1993).

### **1.7.2 Reduction of Free Formaldehyde and Formaldehyde Emission**

Formaldehyde release from UF resins and its bonded products is a major issue because formaldehyde is a toxic and irritating air pollutant (Walker 1967) and a suspected carcinogen (Meyer 1979e). Many countries have regulations regarding the formaldehyde emissions limits from the UF resin bonded wood products. The European and Japanese Standards of Formaldehyde Emission (see Appendix A) are widely used. The correlation between indoor air levels and the formaldehyde release rate from various UF-bonded products is not yet fully understood and has been the

subject of intensive research (Vargha 1998, Tohmura *et al.* 1998, Kelly *et al.* 1999, Groah *et al.* 1998, Mlynar 1997).

Originally, UF resins were prepared with a F/U molar ratio 2.0. This is the molar ratio required for crosslinking all the primary and most of the secondary amino groups. UF resin marketed as wood adhesive during the 1980s still contained a F/U molar ratio of 1.8 (Meyer and Hermanns 1986), even though it was recognised that lowering the overall molar ratio reduced the potential for post-manufacture formaldehyde release. The problem with low molar ratio resins was that they contained unreacted secondary and even primary amino groups that made the product hygroscopic and reduced internal bond.

During the last two decades, much progress has been made in formulating low molar ratio resins and in capping unreacted methylol groups (Mayer 1978). For example, modifying UF resins with melamine or phenol is an effective method for reducing formaldehyde emission level and enhancing the physical properties of the resin bonded products.

Szesztay *et al.* (1994) studied the pH control of the condensation reaction and its effect on the properties of UF resins with the aim of reducing formaldehyde emissions. They used a new buffer system containing ethylene glycol, boric acid, formic acid and sodium hydroxide in the preparation of UF resins and significantly improved the pH stability of the reaction mixture. The formaldehyde emissions of the resin prepared using this new buffer system were low and the ratio of methylene to methylene-ether linkages approached a maximum. In consequence of this new buffer system, the time of reaction became more definite. Also the variation of other values, such as viscosity and storage life, was minimised.

Most modern adhesive resins are manufactured in three or more steps. The original step still involves large formaldehyde excess, often  $F/U = 3-4$ . Modern resins are modified by second and third additions of urea that bring the over-all molar ratio down sufficiently to retain unreacted amino groups capable of acting as scavengers of formaldehyde that may remain unreacted or may be released by hydrolysis of

unreacted methylol functions (Meyer and Hermanns 1986, Roffael 1973). By multi-step manufacturing methods, the overall molar ratio of formaldehyde to urea may as low as 1.05 to 1.30. The free formaldehyde in the vicinity of a manufacturing site may be as low as 0.05 to 0.1% or less and formaldehyde concentration in air around the applying resin site may be less than 0.03-0.06 mg m<sup>-3</sup> (Spurlock 1983, Meyer 1984).

Addition of formaldehyde scavenger to the UF resins may reduce the free formaldehyde in the resins and reduce the formaldehyde emissions during curing. Generally speaking, substances which react with formaldehyde at room temperature can be used as formaldehyde scavengers, eg polymeric methylene diisocyanate (Tamura *et al.* 1998), polyacrylamide (Brzozowski *et al.* 1996, Elbert 1984), gelatin, ammonium lignin sulphonate (Calve *et al.* 1984), pea flour, thermoplastic PF resin powder, polyvinyl alcohol, melamine, urea (Meyer and Hermanns 1986, Mansson *et al.* 1984), resorcinol, *p*-tolueneamine sulphonate (Morze 1983) and azobisisobutyronitrile. The best is melamine (Shiau and Smith 1985).

The curing conditions are equally important for reducing formaldehyde emissions. In some processes additional urea is added separately to wood furnish before applying UF resin and curing (Meyer and Hermanns 1986, Mansson *et al.* 1984).

Treatment of the wood with inorganic salt solution that can react with formaldehyde can reduce emissions (Osugi and Tone 2000, Yossifov *et al.* 1999, Lecka *et al.* 1999, Higuchi 1998). Some of the inorganic salts include (NH<sub>4</sub>)<sub>3</sub>PO<sub>4</sub>, (NH<sub>4</sub>)<sub>2</sub>HPO<sub>4</sub>, (NH<sub>4</sub>)H<sub>2</sub>PO<sub>4</sub>, (NH<sub>4</sub>)<sub>2</sub>CO<sub>3</sub>, (NH<sub>4</sub>)HCO<sub>3</sub>, NH<sub>4</sub>Cl, (NH<sub>4</sub>)<sub>2</sub>(B<sub>2</sub>O<sub>4</sub>)·H<sub>2</sub>O, NaHSO<sub>3</sub> and Na<sub>2</sub>SO<sub>3</sub> (Torrey 1978, Huang *et al.* 1988). Treatment of the surface of the cured wood products with a solution of urea-NH<sub>4</sub>Cl can also lower formaldehyde emissions.

McGuire *et al.* (1985) disclosed a new method of applying formaldehyde scavenger. A mixture comprising urea or one of its analogs (melamine, guanidine), a readily decomposable ammonia liberating compound (ammonium carbonate, ammonium bicarbonate) and a resin catalyst (ammonium chloride, ammonium

sulphate and ammonium nitrate) was prepared in a finely granulated form. The mixture comprised 12-20 parts of the ammonia liberating compound, 65-88 parts of urea or its analog, and 0-15% of the catalyst. It was then added to the dried wood particles and blended, preferably prior to the addition of the adhesive binder resin. Using 6-22.5% by weight based on resin solids of this mixture and blending it with dried wood particles achieved a reduction of 45-80% of formaldehyde emission without adverse effect on physical properties or press time.

Dutkiewicz (1984) studied the effects of the amino or amido groups containing materials on reducing formaldehyde emission. He found that the addition of polyacrylamide, polymethacrylamide, biuret and casein might reduce the formaldehyde emissions. The most effective additives were polyacrylamide, biuret and casein. On the other hand, chitosan did not reduce the evolution of formaldehyde but, instead, slightly augmented it. It was concluded that not only the reactivity of a modifier, but also the stability of its possible combinations with formaldehyde had to be considered when selecting formaldehyde scavenger.

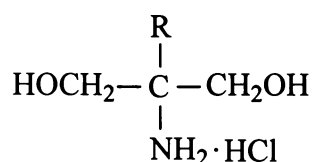
### **1.7.3 Catalysts and Hardeners**

The catalyst or hardener for UF adhesive systems is either acid or materials which liberate free acid upon addition to the UF resins. The most common catalysts are the ammonium salts of strong acids, eg ammonium chloride or ammonium sulphate. The usage is usually 1-5% by weight. Often, the catalysts are extended with wood flour and a buffer, such as tricalcium phosphate. Ammonium sulphate can be incorporated in single-package UF resin adhesives powder. It gives a reasonably stable mixture, and its catalytic effect does not come into play until the adhesive is mixed with water. The amount and types of catalyst added determines whether the adhesive bond is cured at room temperature or at elevated temperature. Curing time may vary from a few minutes at higher temperature to a few hours at room temperature.

The optimum curing speed depends on the application. For example, some large scale processes are slow and require a long potlife of the resin-hardener mixture.

Alternately some applications may require an accelerated curing speed in order to increase the production rate.

Often, retarders, such as urea, melamine, or hexamethylene-tetramine are incorporated with the catalyst to increase the potlife of the resin mixture. These retarders can also reduce the formaldehyde emission as described in Section 1.7.2. New catalyst or hardener systems have been developed, which produce acid only on heating, eg polyhydroxy amine hydrochloric acid salt (Torrey 1978):



Other hardener systems include the glycol-oxalic acid copolymer, acrylic acid-potato starch branching copolymer, acrylic acid-vinyl acetate branching copolymer, maleic acid starch ester (starch maleate), dimethyl oxalate or other easily hydrolysable esters, 0.1-0.2% of bromohydrocinnamic acid, dibromosuccinic acid (Pizzi 1983), 1,3-dichloro-2-propanol (Pizzi 1983), ammonium succinate, ammonium pentandioic acid and ammonium hexane diacid.

The curing speed may be accelerated by preparing highly reactive resins, or by using a high speed (high temperature) hardener. The high temperature hardeners include the ammonium salt of poly-isobutylene-maleic acid copolymer (100°C, 30 seconds curing),  $(\text{NH}_4)_2\text{S}_2\text{O}_8$  (1.5 times of the curing speed of  $\text{NH}_4\text{Cl}$ ),  $\text{NH}_2\text{SO}_3\text{H}$ , aniline hydrochloric acid salt, and  $\text{AlCl}_3$  (can achieve fast curing at high temperature). Concomitantly, the overall performance of the resin can also be enhanced.

## **1.8 SCOPE OF THE PRESENT INVESTIGATION**

UF resins have been used in industrial applications for at least 60 years. The manufacturing process is considered to be a mature technology. Reasons for continued interest in these "age-old" UF resins include:

- 1) UF resins occupy a dominant economic position within the wood adhesive resins group.
- 2) They have major applications in the areas of wood adhesives, textile and paper auxiliaries, coatings, castings and moulding compounds.
- 3) Complexity arises from the different synthetic routes utilised in the manufacture of commercial resins.
- 4) There is a need to understand and eliminate formaldehyde emissions from cured products.
- 5) Complexity arises due to the large number of species that may be present. The correlation between the reaction conditions, species and resin performances is not fully understood.

Fundamental questions remain unanswered. For example:

- 1) What transient species are formed during UF resin manufacture ?
- 2) What effect does formaldehyde solution age and degree of polymerisation have on final resin ?
- 3) What effects do the reaction conditions have on intermediates formed, the properties of the resins and resin bonded products and formaldehyde emissions ?

Reactions between urea and formaldehyde occur rapidly, especially under alkaline reaction conditions. In commercial processes, these reactions are typically complete in about two hours after the initial addition of urea and formaldehyde. In order to study the processes occurring, a methodology that allows the rapid analysis of the complex mixtures is required. The NMR technique provides a useful tool for this purpose. Some work has used NMR analysis of samples taken during the reaction. In

practice these experiments can obtain information about the final resin and only a limited number of stages of the reaction.

A major purpose of the present investigation was to develop a rapid, dynamic NMR technique whereby the UF polymerisation reaction could be monitored continuously in a NMR tube under manufacturing conditions. This technique offers the possibility of monitoring the transient species generated. Specific requirements of the dynamic NMR experiment are a short acquisition time (typically several minutes) and a reasonable signal to noise ratio. It was considered that the development of a dynamic NMR method would allow questions identified above to be addressed. Thus, the specific objectives of this thesis are to report the following:

- 1) The development of a high resolution  $^{13}\text{C}$  NMR method capable of identifying the species present and monitoring their concentration during the preparation of UF resins.
- 2) The use of the dynamic NMR method to monitor the UF reaction under a variety of conditions including F/U molar ratio, temperature, pH, reaction time and formaldehyde concentration.
- 3) The use of HPLC to complement the NMR work particularly in the identification and quantification of free urea, MMU, DMU and TMU present.
- 4) The use of GPC, ESMS and DSC to further identify species formed during the reaction.
- 5) The use of the results obtained in 1) to 4) above to predict optimum reactions conditions for the production of resins that in wood products have low formaldehyde emissions and high internal bond.
- 6) Preparation of a range of experimental resins designed to test the predictions based upon the NMR and HPLC results.

## **CHAPTER TWO**

# **METHODS AND MATERIALS**

## 2.1 NUCLEAR MAGNETIC RESONANCE (NMR)

### 2.1.1 General NMR Conditions

NMR spectra were acquired using a 10 mm multinuclear probehead installed in a Bruker AC300 spectrometer, operating at 300.13 MHz for proton, or 75.47 MHz for carbon-13. Unless otherwise stated NMR spectra were acquired at 55°C, and chemical shifts are reported relative to internal methanol (49.3 ppm) or DMSO-d<sub>6</sub> (38.7 ppm). Free induction decay (FID) signals were processed, either on-line using standard Bruker supplied software, or off-line using Felix NMR software for Windows (version 1.02, BIOSYM Technologies, San Diego, USA).

Two acquisition methods were utilised in this investigation to acquire <sup>13</sup>C NMR spectral data. These methods were (for convenience) designated as the STANDARD and RAPID methods (see Figure 2.1 and 2.2 respectively). NMR parameter settings and solvent volumes, etc, utilised in these NMR experiments are given in Table 2.1.

### 2.1.2 The STANDARD NMR Method

The STANDARD NMR pulse programme is depicted in Figure 2.1.

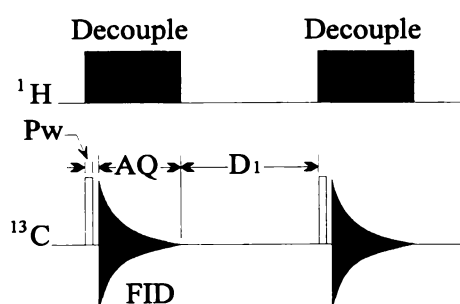


Figure 2.1. The STANDARD <sup>13</sup>C NMR pulse programme.

Table 2.1. Typical NMR acquisition conditions, sample volumes and reference solvents.

parameter	STANDARD method	RAPID method
pulse angle (radians)	$\pi/4$	$\pi/2$
number of FID points	16 K	16 K
repetition delay ( $D_1$ ) (sec)	4.0 or 25.0	0.50
acquisition time (AQ) (sec)	0.9175	0.9175
decoupling mode	inverse gated	continuous
includes NOE	no	yes
lock solvent	DMSO-d6 <sup>a</sup>	DMSO-d6 <sup>a</sup>
lock solvent volume (mL)	0.5-1.0	0.40
integration reference peak	DMSO-d6 <sup>a</sup>	DMSO-d6 <sup>a</sup> + DMSO <sup>b</sup>
volume DMSO added (mL)	none	0.20
resin volume (mL)	2.0	2.0
number of scans (NS)	400	100
typical S/N	200	100
typical acquisition time (min)	35 or 180	2.5
suitable for	quantitative analysis	dynamic experiments

<sup>a</sup> deuterated NMR grade, <sup>b</sup> analytical reagent grade.

Unless otherwise stated STANDARD NMR spectra were acquired using a  $\pi/4$  ( $45^\circ$ ) pulse and a repetition rate ( $T_r$ ) of 4.9 sec (ie  $T_r = AQ + D_1 = 4.9$  sec). Typical acquisition parameters are given in Table 2.1. Since proton decoupling is gated off during the interpulse delay period, STANDARD  $^{13}\text{C}$  NMR spectra were acquired without a Nuclear Overhauser Effect (NOE).

### 2.1.3 The RAPID $^{13}\text{C}$ NMR Method

The RAPID NMR pulse programme is depicted in Figure 2.2.

Unless otherwise stated RAPID NMR spectra were acquired using a  $\pi/2$  ( $90^\circ$ )

pulse and a repetition rate of 1.4 sec (ie  $T_r = A_Q + D_1 = 1.4$  sec). Typical acquisition parameters are given in Table 2.1. Since continuous proton decoupling is applied during the interpulse delay period, RAPID  $^{13}\text{C}$  NMR spectra were acquired with a Nuclear Overhauser Effect (NOE).

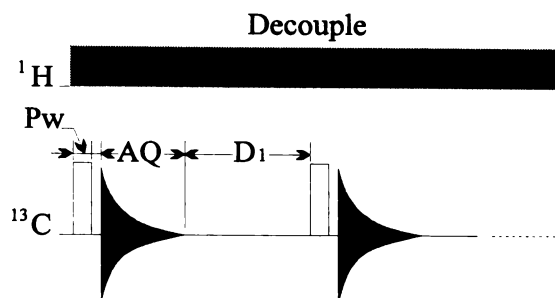


Figure 2.2. The RAPID  $^{13}\text{C}$  NMR pulse programme.

Peak areas were integrated relative to added DMSO (0.2 mL) and DMSO-d<sub>6</sub> (0.4 mL) unless otherwise stated, rather than DMSO-d<sub>6</sub> only, since the area of the DMSO-d<sub>6</sub> peak was too low for reliable integration (see Section 3.4).

RAPID  $^{13}\text{C}$  NMR spectra of adequate signal to noise ( $c$  100) for reliable peak area integration could be recorded in 2.5 min and 20-40 NMR spectral data sets could be acquired in 100 min, using the dynamic NMR procedure (Section 2.1.4)

#### 2.1.4 The Dynamic (RAPID) NMR Procedure

Dynamic (RAPID) NMR experiments were conducted using UF resin solutions prepared as described below:

Warm ( $55^\circ\text{C}$ ) formaldehyde solution (10.0 mL,  $c$  11.1 g,  $\text{pH} = 2.8\text{-}3.2$ ) was added to a 40 mL beaker and the  $\text{pH}$  of the solution was adjusted to the desired level (typically in the range  $\text{pH} 5.0\text{-}9.0$ ) using  $1.0 \text{ mol L}^{-1}$  sodium hydroxide solution. The beaker containing the  $\text{pH}$  adjusted formaldehyde solution was then placed in a water bath which was maintained at  $55^\circ\text{C}$ , and powdered urea (typically about 2.5-6.0 g depending on the required F/U molar ratio) was added. The reaction mixture was

stirred for 2 min, and then allowed to stand for 1 min, after which a portion of the UF resin mixture (2.0 mL) was transferred to a 10 mm NMR tube containing DMSO-d<sub>6</sub> (0.50-1.00 mL) or DMSO-d<sub>6</sub> (0.40 mL) + DMSO (0.20 mL).

Reaction time was recorded relative to the first addition of urea. The NMR tube was placed in the spectrometer after 5 min, and a series of NMR spectra acquired at 60-97°C using the RAPID NMR method described in Section 2.1.3. The time coordinate of each of the NMR spectra was recorded as the mid-point of each spectral data set (eg after 50 of 100 scans). NMR spectra were acquired during both (i) the initial addition stage, and (ii) the condensations stage.

After the desired addition stage reaction time (typically 20-60 min) the NMR tube was withdrawn from the spectrometer and the pH was measured (at 55°C) by using a PHM 93 Reference pH meter (Radiometer, Copenhagen, Denmark) and a long thin probe (6 × 300 mm). The pH of the UF resin mixture was lowered to the desired pH (typical 4.3-5.5) for the condensation stage reaction period by the addition of formic acid (1.0 mol L<sup>-1</sup>). The NMR tube was then re-inserted into the spectrometer, and NMR data acquisition continued (typically for a further 60-100 min).

The reaction process was continually monitored by the acquisition of a series of FID files (typically every 2.5 min) acquired during the entire reaction period. A major advantage of this technique is that a series of NMR spectra, corresponding to different reaction stages, can be acquired without disrupting the polymerisation process.

### **2.1.5 <sup>13</sup>C Relaxation Time (T<sub>1</sub>) Determination**

When placed in a magnetic field, the nuclear spins are aligned by B<sub>0</sub> (the magnetic field) and the spin population is distributed amongst the various states available according to a Boltzmann distribution equation. At equilibrium more nuclei are aligned in the direction of B<sub>0</sub> than against it, with the consequence that the sample is slightly magnetised in the direction of the magnetic field.

Absorption of RF (radio frequency) radiation at or near the Larmor frequency of the nuclei causes a redistribution of the nuclei spins, and gives rise to non-equilibrium populations. The population recovers to an equilibrium distribution by a first-order (exponential) process with a time constant  $T_1$ , defined as the longitudinal relaxation time (or the spin-lattice relaxation time).

The inversion-recovery method for  $T_1$  determination (Derome 1989, Akitt 1992, Levy and Craik 1984, Field and Sternhell 1989) uses the pulse sequence:  $\pi - \tau - \pi/2$  - acquire FID, depicted in Figure 2.3.

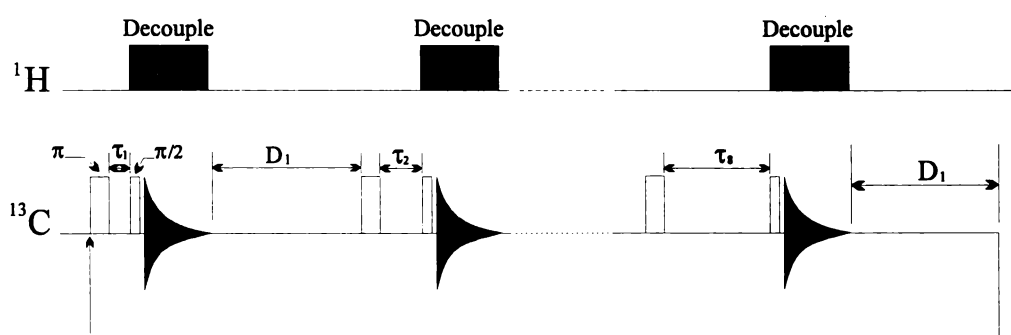


Figure 2.3. The inversion-recovery pulse sequence.

The following series of tau ( $\tau$ ) values were utilised in  $T_1$  determinations:

Series 1:  $\tau = 0.003, 0.01, 0.03, 0.1, 0.3, 1.0, 3.0$  and 10 sec.

Series 2:  $\tau = 0.005, 0.02, 0.1, 0.5, 2.0, 6.0, 10$  and 15 sec.

All other NMR conditions (solvents, temperature, chemical shift referencing, etc) were as described in Section 2.1.1.

## 2.2 HPLC MEASUREMENTS

HPLC analyses were performed using the following instrument and columns:

pump & controller:	Waters 600E multisolvent delivery system, including 600 controller and pump (direct injection)
injector:	Waters WISP 710B intelligent sample processor
detector:	Waters R401 differential refractometer
columns:	300 × 2.1 mm Alltech Spherisorb PEI (5 µm) 250 × 4.6 mm Alltech Spherisorb PEI (5 µm)
solvent:	acetonitrile (HPLC grade) / distilled water (92/8, wt/wt) acetonitrile and distilled water were filtered through 0.45 µm organic and aqueous HPLC filter respectively
flow rate:	0.2 mL min <sup>-1</sup> (300 × 2.1 mm column) or 0.8 mL min <sup>-1</sup> (250 × 4.6 mm column)
temperature:	25°C
injection volume:	10-50 µL (depending on sample concentration)
solvent sparge gas:	helium.
model compounds:	biuret was purchased from Sigma Chemical Co, USA. MMU, DMU and MDU (purity were > 95%) were supplied by Orica New Zealand, Ltd.

HPLC data was processed using GRAM/386™ for Chromatography software (Galactic Industries Corp., Salem, USA).

### *HPLC sample preparation*

Acetonitrile/water (92/8 wt/wt) mixed solvent (5.0 mL) was measured into a weighed sample bottle and the weight of the sample bottle plus solvent was recorded. Resin material (typically 20-40 mg) was added to the sample bottle, which was then re-weighed. Resin concentrations were typically in the range 4-10 mg mL<sup>-1</sup>. The resin solution was filtered through a 0.2 µm filter prior to its introduction onto the HPLC column.

## **2.3 GPC MEASUREMENTS**

GPC measurements were performed using the following instrument and columns:

pump & controller: Waters 600E multisolvent delivery system, including 600 controller and pump (direct injection)

injector: Waters WISP 710B intelligent sample processor

detectors: Waters R401 differential refractometer and Viscotek T-60 dual detector;

columns: three 250 × 10 mm columns in series (a, b, c):  
(a) Jordi-Gel DVB 100 Å (5 μm)  
(b) Alltech GPC Polar 500 Å (5 μm)  
(c) Alltech GPC Polar 1000 Å (5 μm)

solvent: dimethylformamide (DMF) (HPLC grade) + 0.1 mol L<sup>-1</sup> LiCl, was filtered through 0.45 μm Nylon HPLC filter

flow rate 1.0 mL min<sup>-1</sup>

temperature: 25°C

injection volume: 10-50 μL (depending on sample concentration)

solvent sparge gas helium

standard samples: polyethylene glycol (PEG) and polyethylene oxide (PEO)  
GPC standard kits were purchased from Toyo Soda Manufacturing Co. Ltd., Japan

GPC data was processed using GRAM/386™ for Chromatography software (Galactic Industries Corp., Salem, USA) and TriSEC GPC (version 3) software (Viscotek Corp., Houston, USA).

#### *GPC sample preparation*

N,N-Dimethylformamide with 0.1 mol L<sup>-1</sup> LiCl (5.0 mL) was measured into a weighed sample bottle and the weight of the sample bottle plus solvent was recorded. Resin material (typically 20-40 mg) was added to the sample bottle, which was then re-weighed. Resin concentrations were typically in the range 4-10 mg mL<sup>-1</sup>. The resin solution was filtered through a 0.2 μm filter prior to its introduction onto the GPC column.

## 2.4 ESMS MEASUREMENTS

ESMS was determined in positive, or negative ion mode using a VG-Platform instrument, and processed using MassLynx software. Typical acquisition conditions were:

cone voltage	+ (or -) 10-70 V
solvent	acetonitrile (HPLC grade) / distilled water (1/1) acetonitrile and distilled water were filtered through 0.45 $\mu\text{m}$ organic and aqueous HPLC filter respectively
flowrate	0.01 mL min <sup>-1</sup> .
cone temperature:	60°C
model compounds:	biuret was purchased from Sigma Chemical Co, USA MMU, DMU and MDU (purity were > 95%) were supplied by Orica New Zealand, Ltd.

Sample preparation: *c* 50 mg sample was dissolved in 1-2 mL of solvent to give a sample concentration of *c* 25-50 mg mL<sup>-1</sup>.

## 2.5 GC-MS MEASUREMENTS

GC-MS analyses were conducted using a HP 5090A gas chromatograph (GC) interfaced to a HP 5970B mass selective detector (MSD). Typical GC conditions were:

column	25 m $\times$ 0.22 mm HP-1, 0.2 $\mu\text{m}$ film thickness
injection volume	2 $\mu\text{L}$
injection mode	splitless
temperature program	60-135°C: 20°C min <sup>-1</sup> , 135-250°C: 8°C min <sup>-1</sup> and 250-290°C: 20°C min <sup>-1</sup> (15 min hold)
ionisation mode	electron impact (EI) at 70 eV

Formaldehyde samples were silylated prior to GC-MS analyses. Silylation was achieved by injecting silylation grade dimethylformamide (DMF) 5  $\mu\text{L}$ , silylation grade N,O-bis(trimethylsilyl)trifluoroacetamide (BSTFA) (25  $\mu\text{L}$ ) and formaldehyde

solution (3  $\mu\text{L}$ ) into a sealed screw top vial, which was then shaken to homogenise the solution. Silylated samples were analysed within 24 h of their preparation.

## **2.6 DSC MEASUREMENTS**

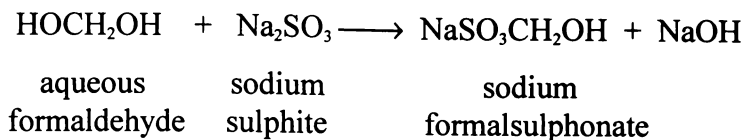
DSC measurements were performed using a Mettler (Switzerland) TA4000 Thermal Analysis System, consisting of a TC11 TA Processor (control and evaluation unit) and a DSC 25 cell (oven unit). Typically, a 3-10 mg sample (in a sealed sample cell) and a heating rate of  $5^{\circ}\text{C min}^{-1}$  were used. DSC data were processed using the build-in function (software). The “Spln” baseline function was used for the integration of peak area.

## **2.7 DETERMINATION OF THE FORMALDEHYDE CONTENT OF A FORMALDEHYDE SOLUTION**

Methods for determining the formaldehyde content of an aqueous formaldehyde solution include the alkaline peroxide method, the sodium sulphite method, the iodometric method, the ammonium chloride method, the mercurimetric method, the potassium cyanide method, the hydroxylamine hydrochloride method, and the methone or dimedon method (Meyer 1979a, Walker 1967). Because of its accuracy, simplicity, and rapidity, the sodium sulphite method is the most commonly used procedure, especially in industry.

The sulphite method is not, however, specific for formaldehyde, since sulphite reacts with any other aldehydes and ketones which may be present (as impurities) in the formaldehyde solution. Alcohols, organic and inorganic acids and their neutralised salts, excluding ammonia, do not react with sulphite.

The sodium sulphite method is based on the quantitative conversion of aqueous formaldehyde and sodium sulphite to sodium hydroxide and sodium formalsulphonate:



### *Analyses procedure*

The procedure utilised in this investigation was that described in the Orica test methods manual (de Rijk 1994). Sodium sulphite (60 mL of a 1 mol L<sup>-1</sup> solution) was measured into an autotitration beaker, and an accurately determined amount of aqueous formaldehyde solution (*c* 0.5 g) was added. The solution was titrated using an auto-titrator (Mettler DL25, Switzerland) and 1 mol L<sup>-1</sup> hydrochloric acid (HCl) solution. A blank value (in the absence of added formaldehyde) was also determined. Results were calculated using the following equation:

$$FC(\% w/w) = \frac{30.03 M_{\text{HCl}} (V_1 - V_0)}{1000 W_s} \times 100 = \frac{3.003 M_{\text{HCl}} (V_1 - V_0)}{W_s} \dots\dots (4.1)$$

Where  $FC(\% w/w)$  = formaldehyde content in weight %  
 30.03 daltons is the molar weight of formaldehyde  
 $M_{\text{HCl}}$  = concentration (mol L<sup>-1</sup>) of HCl  
 $V_1$  = volume (mL) of HCl required for titration  
 $V_0$  = volume (mL) of HCl required in the blank determination  
 $W_s$  = sample weight (g) of the formaldehyde solution  
 1000 = conversion factor of millilitre to litre  
 100 = percentage (%) conversion factor

## **2.8 DETERMINATION OF FREE FORMALDEHYDE IN A UF RESIN**

The most common methods for free formaldehyde determination are the acidimetric sulphite method, the hydroxylamine hydrochloride method, and the iodometric sulphite method (Meyer 1979a).

The sulphite method is based on de Jong and de Jonge's (1952 and 1953) observation that, at or below room temperature, methylolureas are only slowly

degraded (hydrolysed) to formaldehyde, at pH 7. Degradation proceeds more rapidly however at either alkaline, or acid, pHs. Judicious pH control therefore makes it possible, using a single sample, to initially determine free formaldehyde at pH 7 and then determine total (free + released) formaldehyde at pH greater than 9, or below 4 (Meyer 1979a).

In this work free formaldehyde (the unreacted formaldehyde) was determined as described below (Kearns 1990).

### *Free formaldehyde determination*

An accurately weighed amount of resin (*c* 10 g) was placed in a stoppered 250 mL conical flask containing 100 mL of cold water (< 20°C). The resulting resin solution was cooled to less than 2°C for 30 min in a freezer or an icebox. Chilled (*c* 2°C) sodium sulphite (25 mL of 1 mol L<sup>-1</sup> solution) was added and the solution was autotitrated using HCl (1 mol L<sup>-1</sup>). The free formaldehyde content was calculated using the expression:

$$\text{Free } F (\% \text{ w/w}) = 3.003 M_{\text{HCl}} (V_1 - V_0) / W_r \dots\dots\dots (4.2)$$

where *Free F* = free formaldehyde content in weight %

*V*<sub>1</sub> = volume of HCl (mL) used in the resin titration

*V*<sub>0</sub> = volume of HCl (mL) used in the blank titration

*M*<sub>HCl</sub> = HCl concentration (mol L<sup>-1</sup>)

*W*<sub>r</sub> = weight of resin (g)

## **2.9 DETERMINATION OF FORMALDEHYDE EMISSION FROM A PANEL**

Methods which can be used to determine the formaldehyde emission from the final products, such as particleboard and fibreboard, include the European perforator test (European Committee for Standardisation 1982, Meyer 1979a), the American 2 h

desiccator test (Meyer 1979a), the Japanese 24 h desiccator test (Meyer 1979a) and the ventilated or unvented air chamber (Meyer 1979a) methods.

Since the formaldehyde emission is greatly dependent on the testing method, the results can only be compared using the same test methods and conditions.

The perforator method (Myers 1986, Meyer 1979a), which uses liquid-liquid extraction to extract formaldehyde from sample blocks and then determines formaldehyde using the acetylacetone colouration method (Myers and Nagaoka 1981, European Committee for Standardisation 1982) was used in this investigation. In this method, acetylacetone (2,4-pentanedione) is reacted with formaldehyde to afford diacetyldihydrobutadiene which absorbs at 413.5 nm. The method is highly specific for formaldehyde. Acetaldehyde interference is less than 1% at 413.5 nm. The method is suitable for solutions containing up to 8 mg L<sup>-1</sup> of formaldehyde.

The analytical procedures used in this investigation are described in the Orica Test Methods Manual (Dalton 1994).

#### *Extraction of formaldehyde*

Accurately weighed sample blocks (*c* 100-105 g, typically 20 × 20 mm and stored at 25°C and 55% relative humidity for one week before tests) was placed in a 1 L flask containing AR toluene (600 mL) which was then fitted to the extractor and water (*c* 1.2 L) was added to the extractor. After 2 h at reflux temperature (*c* 111°C), the extractor was cooled. Water from the extractor was collected in a 2 L volumetric flask and made up to mark.

#### *Acetylacetone colour analyses*

2.5 mL of the extracted aqueous formaldehyde solution (from the 2 L volumetric flask) was pipetted into a graduated stoppered test tube containing 5.0 mL of acetylacetone solution, prepared by the addition of acetylacetone (2 mL), glacial acetic acid (3 mL) and ammonium acetate (150 g) to 1 L of water. The volume of the

test solution was made up to 10 mL with water (2.5 mL). The test tube was placed in a  $60 \pm 1^\circ\text{C}$  water bath for 10 min and then cooled for 5 min in a  $20^\circ\text{C}$  water bath. A portion of the sample solution was transferred to a 1 cm quartz sample cell and absorbance determined at 413.5 nm using an ultra violet-visible (UV-visible) spectrometer (Hitachi U-2000, Japan).

A calibration line was constructed using six standard solutions containing 0, 0.75, 1.5, 3.0, 7.5 and  $15.0 \mu\text{g mL}^{-1}$  formaldehyde. 5.0 mL of each of the standard solution was pipetted into a graduated stoppered test tube containing 5.0 mL of acetylacetone solution. The volume of the test standard solution was 10.0 mL. Since 2.5 mL of sample solutions and 5.0 mL of each standard solution were diluted to 10.0 mL, the relative dilution factor (RDF) of sample solutions compared to standard solutions is 2.

Formaldehyde emission expressed as mg formaldehyde per 100 g of oven dried wood panel sample (mg / 100 g wood panel) were calculated using the expression:

$$FE = \frac{RDF C_F V f_{MC}}{1000 W_d} \times 100 = \frac{2 \times C_F f_{MC} \times 2000}{1000 W_d} \times 100 = \frac{400 C_F f_{MC}}{W_d} \dots (4.3)$$

where  $FE$  = formaldehyde emission (mg formaldehyde/100g wood panel)

$C_F$  = formaldehyde concentration of test solution ( $\mu\text{g mL}^{-1}$ )  
determined from the acetylacetone colour analyses

$RDF$  = relative dilution factor of samples compared to standards (= 2)

$V$  = final volume (mL) of the extracted formaldehyde solution (= 2000 mL)

1000 = conversion factor (microgram to gram)

100 = conversion factor to afford a value of FE per 100 g of panel

$W_d$  = dry weight (g) of the wood panel, calculated as:

$$W_d = \frac{W_s}{1 + MC}$$

where  $W_s$  is measured wood panel weight (g), and  $MC$  is the % moisture content of the panel.

$f_{MC}$  = moisture content correction factor, calculated as:

$$\text{for } MC = 4\text{-}9\%: f_{MC} = -0.133 MC + 1.86$$

$$\text{for } MC < 4\% \text{ or } MC > 9\%: f_{MC} = 0.636 + 3.12 e^{-0.346MC}$$

Moisture content effects the perforator test results (FE value), since it promotes the hydrolysis of the UF resin during formaldehyde extraction period at high toluene refluxing temperature. The calculation (correction) is based on moisture content of 6.5%, ie  $f_{MC} = 1.0$  for  $MC = 6.5\%$ . Normally, the MC of the sample blocks is about 6-8%.

## 2.10 DETERMINATION OF THE ACIDITY OF A FORMALDEHYDE SOLUTION

Traces of formic acid are always present in a formaldehyde solution. The acidity of a formaldehyde solution is generally assumed to arise solely from formic acid and it can therefore be determined by acid-base titration.

Formic acid levels were determined using an automated autotitration method (Silcock 1990) which used 80 mL of formaldehyde solution and 0.1 mol L<sup>-1</sup> HCl standard solution.

## 2.11 DETERMINATION OF THE METHANOL CONTENT OF A FORMALDEHYDE SOLUTION

The methanol content of a resin is routinely determined using the relative density method. This method was based on relationship between the solution density, formaldehyde concentration and methanol content (Walker 1967, Meyer 1979a.).

Specific gravity can be measured to  $\pm 0.01\%$ . A level of 1% methanol in aqueous formaldehyde changes the specific gravity by about 0.20% (Meyer 1979a).

The calculation is based on the following equations (Silock 1996):

$$\text{CH}_3\text{OH} (\%) = 1.195 FC - 389.5 \cdot (SG - 1); \quad (\text{for methanol } 0\text{-}3.7\%)$$

$$\text{CH}_3\text{OH} (\%) = 1.160 FC - 377.0 \cdot (SG - 1); \quad (\text{for methanol } > 3.7 \%)$$

where,  $\text{CH}_3\text{OH} (\%) =$  methanol content in weight %,

$FC =$  formaldehyde concentration in weight %

$SG =$  specific gravity (units) of formaldehyde solution at 25°C, as determined by the relative density bottle method.

## 2.12 PREPARATION OF UF RESINS

The two-step preparation (addition and condensation stages) of a representative UF resin having an initial F/U molar ratio of 2.0 and a final F/U molar ratio of 1.10 is described below:

### *Addition stage*

Warm (45-55°C) formaldehyde (2700 g of 46% w/w solution, methanol content  $c$  2%, pH = 2.8 - 3.2) was added to a 5 necked 5 L glass reaction vessel fitted with an agitator, a temperature control probe (Honeywell, UK) and a long (300 mm  $\times$  10 mm) pH probe. Stirring was maintained throughout the polymerisation process. The pH of the solution was adjusted to the desired value by adding 10 mol L<sup>-1</sup> aqueous NaOH solution and the temperature of the mixture was maintained at 55°C. Urea (1242 g, first addition, time = 0 min) was added, where upon the temperature fell to 40-50°C, and then rose to 55°C after 5-8 min. After 8 min the reaction vessel was heated at a rate of 2.0°C min<sup>-1</sup> until the desired final temperature (typically in the range 70-97°C) was achieved and the temperature was maintained for a further period of time (typically 7-100 min depending on preparation conditions).

### *Condensation stage*

Heating was discontinued and the pH was lowered to 4.3-5.5 (depending on preparation conditions) using 10 mol L<sup>-1</sup> formic acid solution, after which heating

was continued until a viscosity of 0.3 Pa·s (ie 3.0 poises) was reached. Heating was then discontinued and the reaction was quenched by the addition of 10 mol L<sup>-1</sup> NaOH solution to afford a pH of 8.0-8.5. When the reaction mixture had cooled to 65°C, urea (1016.2 g, final addition) was added and the reaction was held at 65°C for 15 min, after which it was allowed to cool to below 40°C. The resin was transferred to a 4 L plastic container and was stored in an air conditioned room (20°C) for 24 h prior to determination of properties. A 24 h ageing period was used since it is known that there are small, but significant, changes in resin properties during the 24 h period immediately after final urea addition.

### **2.13 VISCOSITY**

The viscosities of resins prepared in this investigation were determined by using a cone and plate viscometer (sheer rate is 10 000 sec<sup>-1</sup>, motor speed is 750 rpm; Research Equipment, London). Viscosities in the range of 0.1-0.2 Pa·s (at 25°C) were typically obtained for UF resins prepared in this investigation.

### **2.14 GEL TIME**

Two methods, the 100°C glacial acetic acid method and the 100°C ammonium chloride method, were used in this investigation to determine the resin gel time.

#### *100°C glacial acetic acid method*

UF resin ( $19.0 \pm 0.10$  g) was weighed into a 150 × 24 mm test tube, glacial acetic acid (1.0 mL) was added and the contents of the test tube thoroughly mixed for  $60 \pm 5$  sec using a metal wire stirrer (Silcock 1994). The metal stirrer is a metal wire (shaft, as a handle) with a loop perpendicular to the wire. The test tube was then placed in a boiling water bath (time = 0) and the resin was stirred 2-3 times per sec with a gentle up and down motion until the resin gelled sufficiently to support the weight of the test tube and its contents (by holding onto the stirring wire). The gel time was recorded to the nearest sec. Typically gel times were in the range 50-200 sec.

*100°C ammonium chloride method*

UF resin ( $20 \pm 0.1$  g) was weighed into a disposable plastic cup and  $\text{NH}_4\text{Cl}$  (2 mL of an 8% solution, ie  $c 1.5 \text{ mol L}^{-1}$ ) was added (Kearns 1988). The contents of the cup were thoroughly mixed and quickly poured into a  $150 \times 24$  mm test tube, and the test tube was placed in a boiling water bath (time = 0). The resin was stirred 2-3 times per sec with a gentle up and down motion (using a metal wire with a perpendicular loop on the bottom end) until the resin gelled sufficiently to support the weight of the test tube and its contents (by holding onto the stirring wire). The gel time was recorded to the nearest sec. Typically gel times were in the range 50-200 sec.

**2.15 PANEL MAKING**

Typically, known amounts of wood particles, or fibres, UF resin, and hardeners, were mixed and placed in wooden frame and a hydraulic press was used to afford a mat. The mat was then placed in the hot press between two stainless sheet plates to afford a test panel. Representative quantities and conditions are listed below:

panel size (frame size):	$28.7 \times 38.1 \text{ cm}^2$
panel thickness (nominal):	3, 5, 8, 12 and 15 mm
typical particle or fibre weight	250, 400, 640, 960 and 1200 g
pressure (mat formation)	2.5-3.0 MPa ( $25.5\text{-}30.6 \text{ kg cm}^{-2}$ ) (at room temp, for several sec)
pressure (hot press):	2.8-3.1 MPa ( $28.7 - 31.6 \text{ kg cm}^{-2}$ )
temperature (hot press):	180°C
time (hot press):	60, 95, 150, 220 or 270 sec ( $c 18$ sec per mm panel thickness)
resin loading:	8.0% resin solids on dry wood particles or fibres
hardener:	2.0% (w/w) $\text{NH}_4\text{Cl}$ on resin solids for wood particles and none for wood fibres
mat moisture:	12% (w/w) on total ingredients

## 2.16 INTERNAL BOND DETERMINATION

Tensile strength perpendicular to the plane of the panel, commonly referred to as internal bond strength, was measured in accord with British Standard 5669(1). This procedure measures the force per unit area, applied at right angles to the plane of the panel, required to fracture the panel. The procedure described in the Orica Manual (Silcock 1995) was used in this investigation.

### *Internal bond procedure*

A hot melt adhesive was used to secure the test material (typically a 50 × 50 cm panel) between two aluminium blocks which were then positioned in the jaws of the internal bond tensile testing machine (Lloyd model LRX5K). The load (Newtons) required for rupture using a pull speed of 2.0 mm min<sup>-1</sup> was recorded. The internal bond strength was calculated using the expression:

$$IB = \frac{N}{a \times b} = \frac{N}{S}$$

where  $IB$  = internal bond, in MPa

$N$  = failing load in Newtons

$S$  = area of specimen, in mm<sup>2</sup> = a (length) × b (width)

## 2.17 COLD WATER SWELLING AND ABSORPTION

The cold water swelling and adsorption test methods described in the Orica Manual (Silcock 1991) were used in this investigation.

Typically, a 50 × 50 mm test panel block was soaked in a 20°C thermostat water bath at a depth of 25-30 mm (the top to the water surface, the block was stood upright with one edge faced up) for 24 h. The % swelling and % absorption were calculated as:

$$\text{Swell} = \frac{\text{wet thickness} - \text{dry thickness}}{\text{dry thickness}} \times 100\%$$

$$\text{Absorption} = \frac{\text{wet weight} - \text{dry weight}}{\text{dry weight}} \times 100\%$$

Typical swelling and absorption values were in the range 15-25% and 80-110% respectively.

## **CHAPTER THREE**

# **DEVELOPMENT OF A DYNAMIC (RAPID) NMR METHOD**

### 3.1 INTRODUCTION

In this research a dynamic (RAPID) NMR technique, whereby the UF reaction was performed and continuously monitored in a NMR tube, was developed to investigate different species (eg methylol, methylene and ether) and transient species generated and their concentration changes in UF reaction systems. Specific requirements of the dynamic NMR experiment were a short acquisition time (typically several min) and a reasonable signal to noise level. In this section, the development of the dynamic (RAPID) NMR method, including the different NMR pulse programmes, the evaluation and choice of the internal standard, is discussed, and the resulting spectral data are compared with those obtained using the conventional quantitative (STANDARD) NMR method. The NOE factors of different species in the actual UF resins system corresponding to different reaction stages have been estimated. The cross calibration factors for correlating the dynamic (RAPID) NMR data to the quantitative (STANDARD) NMR data have also been determined.

### 3.2 <sup>13</sup>C NMR SIGNAL ASSIGNMENTS

The <sup>13</sup>C NMR signal assignments of UF resin species are now well established (Ebdon and Heaton 1977, Tomito and Hatono 1978, Valdez 1995, Slonim *et al.* 1977, Rammon *et al.* 1986). Typically, the assignments presented in Tables 3.1 and 3.2 may differ by up to 1.0 ppm from source to source, depending on how chemical shifts were referenced, and on differences in experimental conditions (solvent, temperature, concentration, etc). In this work, chemical shifts are reported relative to internal methanol (49.3 ppm) irrespective of the concentration of methanol (typically less than 3%) and the temperature at which the spectrum was acquired.

Table 3.1.  $^{13}\text{C}$  NMR signal assignments for UF resin species – carbonyl group carbon atoms and solvents.

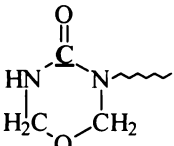
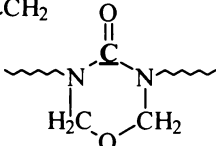
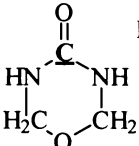
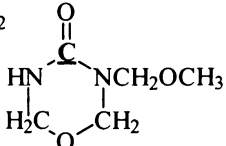
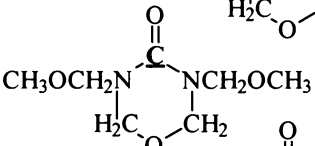
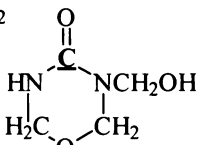
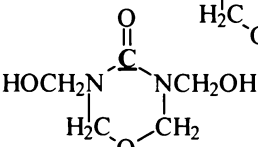
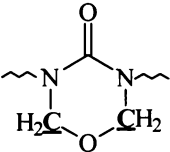
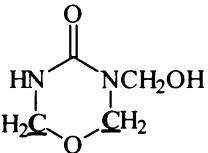
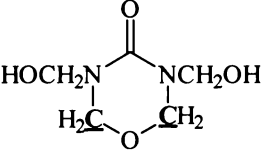
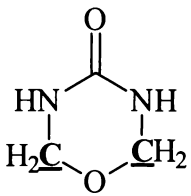
structural unit	species	chem shift (ppm)
$\text{H}\underline{\text{C}}\text{OO}^- \text{M}^+$	formate	170.7
$\text{H}_2\text{N}\underline{\text{C}}\text{ONH}_2$	urea	162.7
$\text{H}_2\text{N}\underline{\text{C}}\text{ONHCH}_2\text{NH}\underline{\text{C}}\text{ONH}_2$	methylene diurea	161.2
$\text{H}_2\text{N}\underline{\text{C}}\text{ONHCH}_2\text{OH}$	monomethylolurea	161.0
$\text{H}_2\text{N}\underline{\text{C}}\text{ONHCH}_2\text{OCH}_3$	monomethoxy methylene urea	160.5
$-\underline{\text{C}}\text{O}- - \underline{\text{C}}\text{O}-$	polymeric carbonyls	159.8
$-\underline{\text{C}}\text{O}- - \underline{\text{C}}\text{ONHCH}_2\text{OH}$	polymeric carbonyls	159.5
$\text{HOCH}_2\text{NH}\underline{\text{C}}\text{ONHCH}_2\text{OH}$	dimethylolurea	159.5
$-\underline{\text{C}}\text{O}- - \underline{\text{C}}\text{ON}(\text{CH}_2\text{OH})_2$	polymeric carbonyls	159.1
$\text{HOCH}_2\text{NH}\underline{\text{C}}\text{ON}(\text{CH}_2\text{OH})_2$	trimethylolurea	159.0
$\text{M}^{2+} \underline{\text{C}}\text{O}^{3-}$	carbonates	157.3
	bound urons	158.3
	bound urons	156.4
	uron	155.2
	monomethylol uron-hemiformal	155.1
	dimethylol uron - hemiformal	154.9
	monomethylol uron	154.7
	dimethylol uron	154.6
$\underline{\text{C}}\text{H}_3\text{OH}$	methanol	49.3
$(\underline{\text{C}}\text{H}_3)_2\text{S}=\text{O}$	dimethyl sulphoxide (DMSO)	39.6
$(\underline{\text{C}}\text{D}_3)_2\text{S}=\text{O}$ (centroid)	deuterated DMSO (DMSO-d6)	38.7

Table 3.2.  $^{13}\text{C}$  NMR signal assignments for UF resins species – formaldehyde, its polymeric forms and derivatives.

structural unit	species	shift (ppm)
$\text{H}(\text{OCH}_2)_n\text{O}\underline{\text{C}}\text{H}_2\text{OCH}_3$	methylenes of hemiformal glycols	94.0
$\text{HOCH}_2\text{OCH}_2\text{O}\underline{\text{C}}\text{H}_2\text{OCH}_3$	methylenes of hemiformal glycols	93.8
$\text{HOCH}_2\text{O}\underline{\text{C}}\text{H}_2\text{OCH}_3$	methylenes of hemiformal glycols	93.3
$--(\text{CH}_2\text{O})_n\underline{\text{C}}\text{H}_2\text{O}(\text{CH}_2\text{O})_n--$	central carbon of long chains	90.0
$\text{HO}\underline{\text{C}}\text{H}_2\text{OCH}_3$	formaldehyde hemiformal	89.9
$\text{HOCH}_2\text{OCH}_2\text{O}\underline{\text{C}}\text{H}_2\text{OCH}_2\text{OCH}_2\text{OH}$	central carbons-polymeric glycols	89.5
$\text{HOCH}_2\text{O}\underline{\text{C}}\text{H}_2\text{O}\underline{\text{C}}\text{H}_2\text{OCH}_2\text{OH}$	central carbon of glycols	89.3
$\text{HOCH}_2\text{O}\underline{\text{C}}\text{H}_2\text{OCH}_2\text{OH}$	central carbon of glycols	88.8
$\text{HO}\underline{\text{C}}\text{H}_2\text{OCH}_2\text{OCH}_2\text{O}\underline{\text{C}}\text{H}_2\text{OH}$	terminal carbon-polymeric glycols	86.5
$-\text{N}(\text{CH}_2-)\underline{\text{C}}\text{H}_2\text{O}\underline{\text{C}}\text{H}_2\text{OH}$	terminal carbon-glycol polymers	86.4
$-\text{NHCH}_2\text{O}\underline{\text{C}}\text{H}_2\text{OH}$	terminal carbon-glycol polymers	86.4
$\text{HO}\underline{\text{C}}\text{H}_2\text{OCH}_2\text{O}\underline{\text{C}}\text{H}_2\text{OH}$	terminal carbon of glycols	86.3
$\text{HO}\underline{\text{C}}\text{H}_2\text{O}\underline{\text{C}}\text{H}_2\text{OH}$	terminal carbon of glycols	85.7
$\text{HO}\underline{\text{C}}\text{H}_2\text{OH}$	monomeric glycol	82.4
$-\text{N}(\text{CH}_2-)\underline{\text{C}}\text{H}_2\text{OCH}_3$	methylene-hemiformal (branched)	79.0
	methylene in bound uron	79.0
	methylene in bound uron	78.6
	methylene in dimethylol uron	78.2
$-\text{N}(\text{CH}_2-)\underline{\text{C}}\text{H}_2\text{OCH}_2\text{OH}$	dimethylene ether (branched)	75.5
$-\text{N}(\text{CH}_2-)\underline{\text{C}}\text{H}_2\text{OCH}_2\text{NH}-$	dimethylene ether (branched)	75.1

(Table 3.2 continued)

	uron methylene carbon	74.6
-NH <u>CH</u> <sub>2</sub> OCH <sub>3</sub>	methylenes - hemiformal (linear)	72.6
-N(CH <sub>2</sub> -) <u>CH</u> <sub>2</sub> OH	methylols (branched)	71.3
HOCH <sub>2</sub> NHCON( <u>CH</u> <sub>2</sub> OH) <sub>2</sub>	trimethylolurea	71.0
-NH <u>CH</u> <sub>2</sub> OCH <sub>2</sub> OH	dimethylene ethers (linear)	69.1
-NH <u>CH</u> <sub>2</sub> O <u>CH</u> <sub>2</sub> NH-	dimethylene ethers (linear)	68.7
Uron- <u>CH</u> <sub>2</sub> OH	methylol uron	67.8
HO <u>CH</u> <sub>2</sub> NHCON(CH <sub>2</sub> OH) <sub>2</sub>	trimethylolurea	64.7
-NH <u>CH</u> <sub>2</sub> OH	methylol (linear)	64.4
HO <u>CH</u> <sub>2</sub> NHCONH <u>CH</u> <sub>2</sub> OH	dimethylolurea	64.3
-N(CH <sub>2</sub> -) <u>CH</u> <sub>2</sub> N(CH <sub>2</sub> -)-	branched methylene	59.3
-O <u>CH</u> <sub>3</sub>	long chain methoxy carbon	55.7
HOCH <sub>2</sub> OCH <sub>2</sub> O <u>CH</u> <sub>3</sub>	methoxy carbon	55.5
HOCH <sub>2</sub> O <u>CH</u> <sub>3</sub>	methoxy carbons - hemiformal	54.8
-NHOCH <sub>2</sub> O <u>CH</u> <sub>3</sub>	methoxy carbons	54.7
-N(CH <sub>2</sub> O-) <u>CH</u> <sub>2</sub> NH-	methylene carbons (branched)	53.3
-N(CH <sub>2</sub> N-) <u>CH</u> <sub>2</sub> NH-	methylene carbons (branched)	53.0
-NH <u>CH</u> <sub>2</sub> NH-	linear methylene carbons	47.4

The <sup>13</sup>C NMR spectra of aqueous formaldehyde and the UF resins prepared in this work (see Figures 3.1 and 3.2, respectively) exhibited a series of signals (peaks) which could be readily assigned by comparison with the chemical shift data presented in Tables 3.1 and 3.2.

Filename: ZHYER87A.001: UF resins prepared in lab., F/U=1.30; STANDARD method, 400 scans.

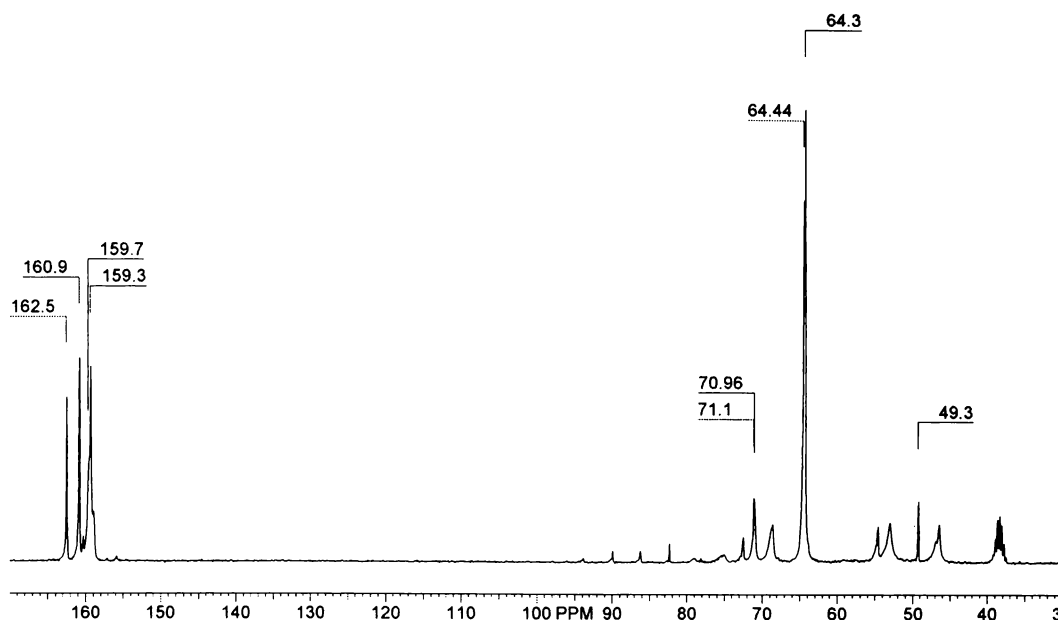


Figure 3.1.  $^{13}\text{C}$  NMR spectrum of a typical UF resin acquired with  $^1\text{H}$  decoupling.

Filename: HYZBFY01.001 47 % formaldehyde aqueous solution. Standard method, 400 scans, D1=4 seconds.

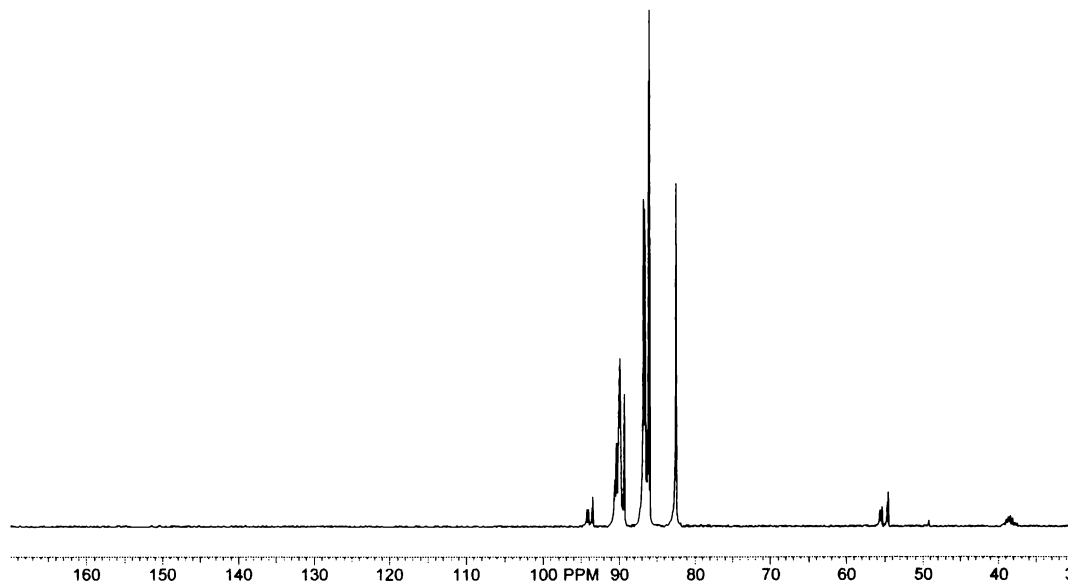


Figure 3.2.  $^{13}\text{C}$  NMR spectrum of formaldehyde acquired with  $^1\text{H}$  decoupling.

The  $^{13}\text{C}$  NMR resonances of UF resins occur predominantly in the regions between 155-165 ppm and 40-100 ppm, respectively, (see Figure 3.1). The resonances which occur between 155-165 ppm arise from the carbonyl carbons, while those which occur between 40-100 ppm arise from a variety of methylene

carbon environments. A more detail analysis of these chemical shift ranges is presented below:

#### *45-60 ppm region*

With some exceptions, signals in the 45-60 ppm “methylene carbon” region, arise predominantly from methylene carbons linked to two nitrogens: eg -NH- $\underline{\text{C}}\text{H}_2$ -NH-, -NH- $\underline{\text{C}}\text{H}_2$ -N< and >N- $\underline{\text{C}}\text{H}_2$ -N< type signals. Exceptions include signals between 49 and 56 ppm which originate from methanol:  $\underline{\text{C}}\text{H}_3\text{OH}$  (49.3 ppm), and from the reaction products of methanol with formaldehyde which afford methoxyl groups: eg  $\underline{\text{C}}\text{H}_3\text{OCH}_2\text{OH}$  and  $\underline{\text{C}}\text{H}_3\text{OCH}_2\text{O}$ - type signals (*c* 55.0 ppm). A small quantity of free (non-condensed) methanol is always present in the UF resins, since resins are generally manufactured from industrial grade formaldehyde which contains 1-3% of methanol, or it may arise from the decomposition of formaldehyde at higher pH by the Cannizzaro reaction, to give methanol and formic acid.

#### *68 and 76 ppm regions*

Signals in these regions arise mainly from dimethylene ether linkages (- $\underline{\text{C}}\text{H}_2\text{O}\underline{\text{C}}\text{H}_2$ -) (Valdez 1995). Signals which occur in the vicinity of 68 ppm (*c* 68-69 ppm) arise from linear dimethylene ether linkages carbons: eg -NH $\underline{\text{C}}\text{H}_2\text{OCH}_2\text{OH}$  and -NH $\underline{\text{C}}\text{H}_2\text{O}\underline{\text{C}}\text{H}_2\text{NH}$ - groups, while those occur in the vicinity of 76 ppm region (*c* 75-76 ppm) arise from branched chain dimethylene ether linkages: eg -N( $\text{CH}_2$ -) $\underline{\text{C}}\text{H}_2\text{OCH}_2\text{OH}$  and -N( $\text{CH}_2$ -) $\underline{\text{C}}\text{H}_2\text{OCH}_2\text{NH}$ - groups.

#### *64 and 71 ppm regions*

Signals in these region arise from the -N-methylol carbon signals (-NH $\underline{\text{C}}\text{H}_2\text{OH}$ ) (Valdez 1995). Signals which occur in the vicinity of 64 ppm (normally the region 64-65 ppm) arise from the linear -N-methylol carbons: eg  $\text{H}_2\text{NCONH}\underline{\text{C}}\text{H}_2\text{OH}$  (MMU),  $\text{HO}\underline{\text{C}}\text{H}_2\text{HNCONH}\underline{\text{C}}\text{H}_2\text{OH}$  (DMU),  $\text{HO}\underline{\text{C}}\text{H}_2\text{HNCON}(\text{CH}_2\text{OH})_2$  (TMU) and -N-methylol terminal carbon (-NH $\underline{\text{C}}\text{H}_2\text{OH}$ ) groups. Those which occur in the vicinity of 71 ppm (*c* 70.5-71.5 ppm) arise from branched chain -N-methylol carbons,

including those present in TMU ( $\text{HOCH}_2\text{HNCON}(\underline{\text{C}}\text{H}_2\text{OH})_2$ ) and the methanol terminal carbon:  $-\text{N}(\text{CH}_2-)\underline{\text{C}}\text{H}_2\text{OH}$  groups.

#### *82-94 ppm region*

This region includes four groups of peaks (Dankelman and Daemen 1976, Meyer *et al.* 1986): (i) methylene glycol carbons ( $\text{HO}\underline{\text{C}}\text{H}_2\text{OH}$ ); (ii) terminal methylene glycol carbon of polymerised methylene glycols ( $\text{HO}\underline{\text{C}}\text{H}_2\text{OCH}_2-$ ); (iii) central methylene carbons of polymerised methylene glycols ( $-\text{O}\underline{\text{C}}\text{H}_2\text{O}\underline{\text{C}}\text{H}_2\text{O}-$ ), and (iv) the methylene carbon of hemiformal glycols ( $-\underline{\text{C}}\text{H}_2\text{OCH}_3$ ).

Comparison of the UF resin spectrum (Figure 3.1) with the formaldehyde spectrum (Figure 3.2) clearly shows that signals in region arises mainly from the unreacted formaldehyde. Formaldehyde is predominantly present in polymeric forms (polyoxymethylene glycol type  $\text{HO}(\text{CH}_2\text{O})_n\text{OH}$  structures). The concentration of monomeric formaldehyde (HCHO) is too low ( $< 0.1\%$ , Walker 1967) to be detected in a NMR spectrum (see Figure 3.2). If the monomeric formaldehyde could be detected, the signal of the carbonyl carbon in HCHO would be expected to appear about 160 ppm. Though the concentration of monomeric form of formaldehyde is low, the equilibrium between monomeric formaldehyde and polymeric forms may readily be shifted. For example at elevated temperatures, polymeric forms will decompose quickly and give off gaseous formaldehyde. Since unreacted formaldehyde is the main contributor to formaldehyde emission during the panel making process and the early stage of the panel's working life, it is often denoted as free formaldehyde in UF resins.

#### *155-163 ppm region*

Signals which occur in this region arise from  $\text{H}_2\text{N}\underline{\text{C}}\text{ONH}_2$ ,  $-\text{NH}\underline{\text{C}}\text{ONH}_2$ ,  $-\text{NH}\underline{\text{C}}\text{ONH}-$ ,  $>\text{N}\underline{\text{C}}\text{ONH}-$  type carbonyl groups. In general this region is poorly resolved and it is difficult to use variations in  $^{13}\text{C}$  chemical shifts to deduce the number of proton atoms on adjacent nitrogen atoms (ie if the carbonyl is adjacent to a secondary or tertiary nitrogen center). For example, it is difficult to distinguish

methylene diurea ( $\text{H}_2\text{N}\underline{\text{C}}\text{ONHCH}_2\text{NH}\underline{\text{C}}\text{ONH}_2$ ) from monomethylolurea ( $\text{H}_2\text{N}\underline{\text{C}}\text{ONHCH}_2\text{OH}$ ), since the chemical shifts of the two carbonyl carbons are only 0.2 ppm apart (161.2 and 161.0 ppm respectively).

### 3.3 QUANTITATIVE NMR ANALYSES

Provided a NMR spectrum is acquired under quantitative conditions, the concentration (relative level) of each species will be proportional to the integrated area (integrals) of each cluster of signals in the NMR spectrum. The integration ranges used in this work are shown in Table 3.3.

Using these integration ranges and the symbol notations presented in Table 3.3, the total methylol, methylene and dimethylene group integrals can be expressed as:

$$A_{(\text{methylol})} = A_{64} + A_{71}$$

$$A_{(\text{methylene})} = A_{46} + A_{52} + A_{58}$$

$$A_{(\text{ether})} = A_{68} + A_{75}$$

Since the integrated peak areas are proportional to the molar concentration of that species, the following proportionalities apply:

#### *Methylol species*

linear methylol concentration ( $C_{(\text{L-methylol})}$ ):	$C_{(\text{L-methylol})} \propto A_{64}$
branched methylol concentration ( $C_{(\text{B-methylol})}$ ):	$C_{(\text{B-methylol})} \propto A_{71}$
total methylol concentration ( $C_{(\text{methylol})}$ ):	$C_{(\text{methylol})} \propto (A_{64} + A_{71})$

#### *Methylene linkages*

linear methylene concentration ( $C_{(\text{L-methylene})}$ ):	$C_{(\text{L-methylene})} \propto A_{46}$
branched methylene concentration ( $C_{(\text{B-methylene})}$ ):	$C_{(\text{B-methylene})} \propto (A_{52} + A_{58})$
total methylene concentration ( $C_{(\text{methylene})}$ ):	$C_{(\text{methylene})} \propto (A_{46} + A_{52} + A_{58})$

Table 3.3. NMR integration signal ranges and symbols for UF resin species.

no.	range (ppm)	species	symbol
0	37.0-41.0	DMSO (internal quantitative reference)	A <sub>39</sub>
1	45.2-48.2	linear methylene	A <sub>46</sub>
2	49.0-49.6	methanol (chemical shift reference, 49.3 ppm)	A <sub>49</sub>
3	51.5-54.5	branched methylene	A <sub>52</sub>
4	54.1-55.8	methoxy	A <sub>55</sub>
5	56.6-60.4	branched methylene	A <sub>58</sub>
6	63.6-65.7	linear methylol	A <sub>64</sub>
7	67.8-69.9	linear dimethylene ether	A <sub>68</sub>
8	70.0-71.9	branched methylol	A <sub>71</sub>
9	72.1-73.3	linear methylene - hemiformal	A <sub>72</sub>
10	74.3-76.3	branched dimethylene ether	A <sub>75</sub>
11	77.1-80.0	branched methylene - hemiformal	A <sub>79</sub>
12	81.4-83.8	methylene glycol	A <sub>82</sub>
13	85.0-87.9	terminal methylene - polymeric glycol	A <sub>86</sub>
14	88.6-91.3	central methylene - polymeric glycol	A <sub>89</sub>
15	92.0-95.0	methylene of hemiformal	A <sub>93</sub>
16	157.6-160.0	di- & tri- methylolurea (DMU + TMU)	A <sub>159</sub>
17	160.0-161.8	monomethylolurea (MMU)	A <sub>161</sub>
18	162.0-163.0	free urea	A <sub>162</sub>

A<sub>n</sub> = integrated area determined for peaks centered at n ppm.

### *Dimethylene ether*

For dimethylene ether  $-\underline{\text{CH}_2}\text{O}\underline{\text{CH}_2}-$  groups the concentration of oxygen atoms is half that of attached methylene ( $-\text{CH}_2-$ ) groups, hence it follows that:

$$C_{(\text{ether-oxygen})} = C_{(\text{ether})} / 2$$

where  $C_{(\text{ether-oxygen})}$  = the concentration of dimethylene ether oxygen and

$C_{(\text{ether})}$  = the concentration of dimethyl ether methylene carbons respectively.

The molar concentration of dimethylene ether methylene species is:

linear dimethylene ether ( $C_{(\text{L-ether})}$ ):  $C_{(\text{L-ether})} \propto A_{68}$

branched dimethylene ether ( $C_{(\text{B-ether})}$ ):  $C_{(\text{B-ether})} \propto A_{75}$

total dimethylene ether methylene carbons ( $C_{(\text{ether})}$ ):  $C_{(\text{ether})} \propto (A_{68} + A_{75})$

The molar concentration of dimethylene ether oxygen is:

total dimethylene ether-oxygen ( $C_{(\text{ether-oxygen})}$ ):  $C_{(\text{ether-oxygen})} \propto (A_{68} + A_{75}) / 2$

The concentration of free formaldehyde (ie unreacted forms of aqueous formaldehyde) in UF resins, as determined by  $^{13}\text{C}$  NMR analyses, is given by the expression:

$$C_{(\text{free-F})} \propto (A_{82} + A_{86} + A_{89} + A_{93}) = A_{(81-95)}$$

Total formaldehyde (ie all methylene (-CH<sub>2</sub>-) forms, including unreacted formaldehyde) in the resin, can be estimated by adding all of the signals in 45 to 95 ppm region, except methanol (A<sub>49</sub>) and methoxyl signals (A<sub>55</sub>), or by integration of that range as a whole and subtraction of methanol (A<sub>49</sub>) and methoxyl (A<sub>55</sub>) signal areas. Comparison of these two approaches afforded values which differed by less than 2-3%. Thus integration of the 45-95 ppm region (ie “total formaldehyde”) gives the total (aqueous) formaldehyde concentration in the resin:

$$C_{(\text{total-F})} \propto A_{(45-95)} - A_{49} - A_{55}$$

Similarly the integration of the 155-163 ppm region gives the total urea contribution (arising from feeding of urea during the reaction period):

$$C_{(\text{total urea})} \propto A_{(157-163)}$$

Free urea in the UF resin:  $C_{(\text{free-urea})} \propto A_{162}$

The formaldehyde to urea molar ratio (F/U ratio) can be obtained by dividing total formaldehyde by total urea:

$$F/U = C_{(\text{total-F})} / C_{(\text{total urea})} = (A_{(45-95)} - A_{49} - A_{55}) / A_{(157-163)}$$

### 3.4 EVALUATION OF THE INTEGRATION METHODOLOGY

A series of integration experiments were performed using the STANDARD and RAPID NMR data acquisition methods. Acquisition conditions are described in Section 2.1. Spectra were integrated using the shift ranges defined in Table 3.3.

Peak area contributions of species detected in  $^{13}\text{C}$  NMR spectra acquired using the STANDARD method were assessed relative to the integrated area of the DMSO-d6 peak.

Initially the same approach was employed in RAPID NMR experiments, in which the changes in integrated peak areas of target species during the course of a polymerisation reaction were assessed relative to the peak area of the constant level of DMSO-d6 in the polymerisation mixture. However, the intensity of the DMSO-d6 signal became very small due to the greater pulse angle and faster repetition rate partially saturating the DMSO-d6 peak, and the strong NOE factors of the protonated carbons (in methylene, methylol and dimethylene ether). The reduced size of the DMSO-d6 peak in the RAPID experiment rendered this approach unreliable due to the relatively large uncertainty in the area of the DMSO-d6 peak. This difficulty was addressed by adding 0.2 mL of non-deuterated DMSO to the UF resin mixture, and assessing target species peak areas relative to the area of the DMSO peaks. By this means, the varying levels of intermediate species present during polymerisation reactions could be reliably assessed relative to the constant DMSO peaks.

In RAPID NMR experiments, the intensity of the signal arising from 0.2 mL DMSO (a singlet centered at 39.6 ppm) was typically 1.5-1.9 times of that observed under the same conditions from 0.4 mL of DMSO-d<sub>6</sub> (a septet centered at 38.7 ppm). DMSO-d<sub>6</sub> was utilised in all NMR experiments as the lock solvent (signal).

Figures 3.3 and 3.4 depict the <sup>13</sup>C NMR spectra of an UF resin containing (i) 0.50 mL DMSO-d<sub>6</sub>, and (ii) 0.40 mL DMSO-d<sub>6</sub> + 0.20 mL DMSO, respectively, determined using the RAPID NMR method. In each case the total sample volume (resin and DMSO) was 2.5-2.6 mL.

Filename: HYZASS01.002 Dynamic experiment, F/U=2.0, T=80 C, addition stage, t=15 min

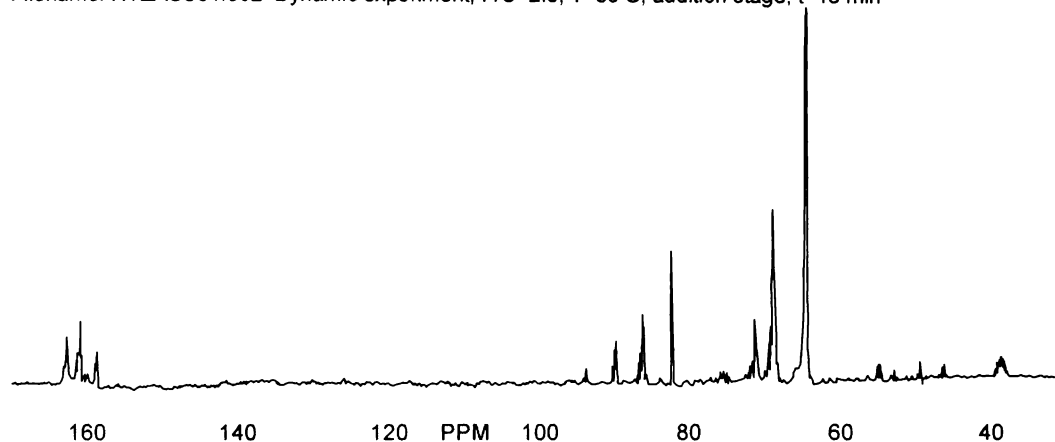


Figure 3.3. <sup>13</sup>C NMR spectrum of an UF resin containing 0.50 mL DMSO-d<sub>6</sub>.

Filename: HYZARS01.003 Dynamic experiment, F/U=2.0, T=80 C, addition stage, t=15 min

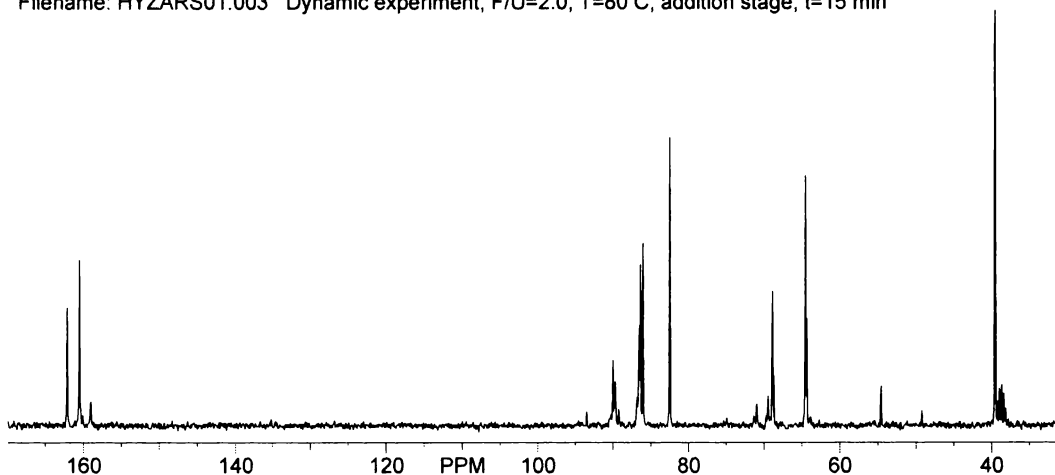


Figure 3.4. <sup>13</sup>C NMR spectrum of an UF resin containing 0.40 mL DMSO-d<sub>6</sub> + 0.20 mL DMSO.

The peak of DMSO-d6 in Figure 3.3 is very small. The DMSO-d6 integral may be as low as 0.2 units (the total integral of the whole spectrum is 10 units), ie only 2% of the total integral. Baseline noise levels can also limit the accuracy of the DMSO-d6 integral. Therefore, the normalised signal intensities of other species, relative to DMSO-d6, may be subject to significant error.

After addition of 0.20 mL DMSO, the integral of DMSO + DMSO-d6 increases to about 1.5 units (total 10 units), ie about 15% of the total. The signal to noise ratio of the internal standard DMSO peaks has been improved significantly (Figure 3.4). The normalised signal intensities of other species relative to DMSO + DMSO-d6 are much more reliable than those relative to DMSO-d6 only.

### 3.5 FACTORS AFFECTING NMR SIGNAL INTENSITIES

Factors which affect NMR signal intensities should be considered when performing quantitative NMR experiments and evaluated before experimental data are used (for example to derive mole ratio values).

#### 3.5.1 Factors Which Affect NMR Signal Intensities

The three major factors which affect NMR signal intensities are pulse angle, repetition rate and nuclear Overhauser effect (NOE).

##### (i) Pulse angle ( $\theta$ )

The power of a RF (radio frequency) pulse used to excite a nucleus in a NMR experiment is usually expressed in units of degrees or radians. In a pulsed NMR experiment, the intensity of the detected signals ( $I$ ) is a sinusoidal functional of the excitation pulse angle ( $\theta$ ) as shown in Equation 3.1.

$$I = I_0 \sin\theta \dots\dots\dots (3.1)$$

where,  $I_0$  is the intensity arising for a  $\pi/2$  pulse when nuclei are fully relaxed (ie the maximum signal intensity from the nuclei), and  $I$  is the signal intensity observed for a  $\theta$  pulse when nuclei are fully relaxed.

The steady state NMR signal intensity obtained from a sample following the application of a series of  $\pi/2$  pulses, is however constrained by the need to wait for several  $T_1$  periods ( $T_1$  = relaxation time) between pulse applications, to allow recovery of the equilibrium population of aligned and opposed spin states, before repeating the NMR experiment.

*(ii) Repetition rate*

Although, for some samples, a strong NMR signal may be obtained from just one pulse (or scan), this is rarely the case for resin samples. Consequently, it is necessary to apply many pulses and accumulate the time-averaged signal. The resulting spectrum has a S/N ratio improvement of  $(NS)^{1/2}$ , where NS = number of scans.

For repetitive data acquisition, the pulse repetition rate,  $T_r$ , is approximately equal to the sum of the signal acquisition time (AQ), plus the delay time ( $D_1$ ) between pulses (typically in the range 3-20 sec) (see Section 2.1.2).  $T_r$  has great effects on the NMR signal intensities, especially when  $T_r$  is less than 3-5  $T_1$ . This is discussed further in Section 3.5.2.

*(iii) Nuclear Overhauser effect (NOE)*

A NOE results in an intensity change (an increase or a decrease) in the NMR signal of a nucleus when the resonance of some other nearby nucleus in the molecule is saturated (irradiated). The intensity change depends on the gyromagnetic ratio of the interacting nuclei, their environment and the pathway for relaxation. In  $^{13}\text{C}$  NMR, broadband proton decoupling is normally applied during signal acquisition to simplify the detected spectrum, however this saturates proton transitions and may generate heteronuclear NOEs. For  $^{13}\text{C}$ , the maximum NOE from proton to  $^{13}\text{C}$  is 1.99 where  $\eta$ , the NOE factor, is expressed as the net enhancement, ie the detected

signal intensity may be up to 2.99 times greater than which would be observed without proton decoupling.

While protonated carbons often show strong NOEs in the presence of decoupling, quaternary (non-protonated) carbons show little, if any NOEs, under the same conditions. Considerable care must therefore be exercised in the interpretation of intensity ratio changes and peak area ratios determined from  $^1\text{H}$  decoupled  $^{13}\text{C}$  NMR spectra.

### 3.5.2 Evaluation of Experimental Cases

Three experimental cases should be considered:

(i)  $^{13}\text{C}$  NMR signal acquisition without  $^1\text{H}$  decoupling

If  $^1\text{H}$  decoupling is not applied during  $^{13}\text{C}$  NMR signal acquisition, no NOE will be present, and the steady state signal intensity ( $I_z$ ) will be:

$$I_z = I'_0 \frac{1 - e^{-T_r/T_1}}{1 - e^{-T_r/T_1} \cos\theta} = I_0 \sin\theta \frac{1 - e^{-T_r/T_1}}{1 - e^{-T_r/T_1} \cos\theta} \dots\dots\dots (3.2)$$

where  $I'_0 = I = I_0 \sin\theta$ , as given in Equation 3.1 for a pulse angle  $\theta$ .

A plot of  $I_z$  against  $T_r/T_1$ , calculated according to Equation 3.2, is shown in Figure 3.5. It is apparent that for  $\theta$  in the range  $0-\pi/2$ , the larger the pulse angle, the greater the steady state signal intensity ( $I_z$ ), and the greater the value of  $T_r/T_1$  needed to achieve maximum signal intensity, ie the slower the repetition rate required for maximum signal intensity.

In order to obtain 99% of the maximum signal intensity in a NMR experiment, which is normally the requirement of a good quantitative measurement, the repetition rate  $T_r$  must be equal to or longer than 2.7  $T_1$  for a  $\pi/6$  ( $30^\circ$ ) pulse, 3.4  $T_1$  for a  $\pi/4$  ( $45^\circ$ ) pulse, 3.9  $T_1$  for a  $\pi/3$  ( $60^\circ$ ) pulse or 4.7  $T_1$  for a  $\pi/2$  ( $90^\circ$ ) pulse. This is the

origin of the classic NMR statement that the repetition rate should typically be of the order  $5 T_1$  when using a  $\pi/2$  pulse.

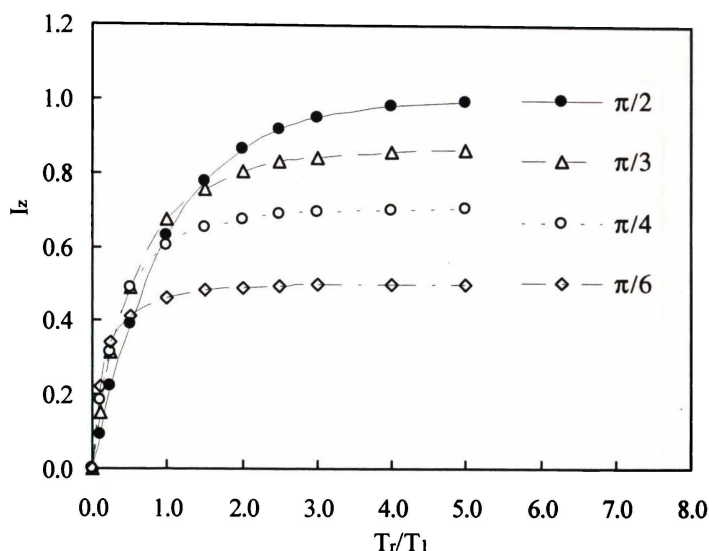


Figure 3.5. Plot of the steady state magnetism ( $I_z$ ) versus  $T_r/T_1$  for 4 pulse angles.

(ii)  $^{13}\text{C}$  acquisition with continuously applied  $^1\text{H}$  decoupling

If proton decoupling is continuously applied during the NMR experiment, protonated carbons (eg methyl, methylene and methine carbons) will experience strong NOEs, whereas non-protonated carbons (eg tertiary carbons and carbonyl carbons) will not. The signal intensity of some nuclei (exhibiting NOEs) will be up to 2.99 times greater than the  $I_z$  value given in Equation 3.2.

(iii)  $^{13}\text{C}$  NMR signals acquisition with inverse gated  $^1\text{H}$  decoupling

If a  $^{13}\text{C}$  NMR spectrum is acquired with inverse gated  $^1\text{H}$  decoupling, no NOEs should be observed, provided the repetition delay ( $T_r$ ) is of the order 3-5  $T_r/T_1$ , otherwise partial NOE build up will be observed (Field and Sternhell 1989, Gillet and Delpuech 1980). It has been shown, both theoretically and practically, that NOE build up can compensate for the effect of incomplete relaxation due to a faster than optimum pulse repetition rate. Field and Sternhell (1989) have shown that, under

some circumstances, NOE build-up effects can overcompensate for the loss of signal intensity, due to the generation of a non-equilibrium steady state population of excited nuclei (see Figure 3.6).

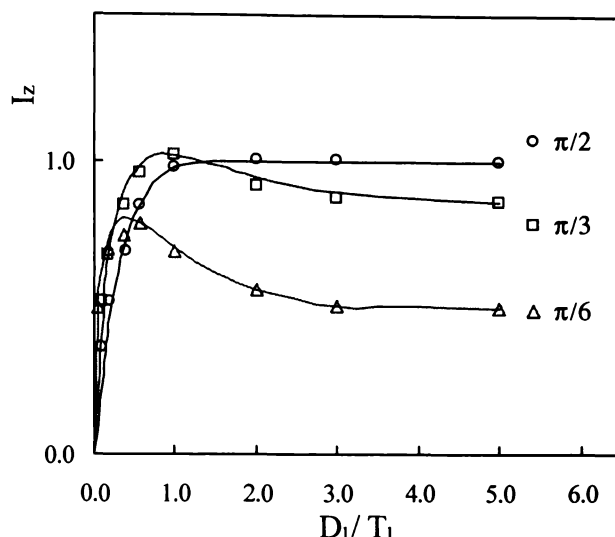


Figure 3.6. Plot of the steady-state signal intensity ( $I_z$ ) for benzene as a function of the ratio  $D_1/T_1$ .

Theoretical curves are represented by solid lines for pulse angle of  $\pi/2$ ,  $\pi/3$  and  $\pi/6$ , respectively, together with the corresponding experimental points (O,  $\square$  and  $\Delta$ , respectively). Acquisition time = 1.2 sec,  $D_1$  is the interpulse delay time and  $T_1$  is the longitudinal relaxation time of benzene (29.5 sec) (Field and Sternhell 1989).

Since NMR signal intensities can be greatly affected by  $T_r/T_1$  values, it is important that relaxation times ( $T_1$ s) be determined, and the reliability of quantitative data evaluated, before substantive data are derived from it.

NOE factor ( $\eta$ ) and  $T_1$  are two major factors affect the signal intensity under given NMR experimental conditions. In order to better understand the signal intensity relationship among different species in the UF resin system and help to determine optimum NMR experimental conditions, it is necessary to determine both  $\eta$  and  $T_1$  of all the major species present in the resins. Hence, experimental evaluations of the  $T_1$  values and NOE enhancement factors of some representative UF resins prepared in this investigation were performed and are reported in Sections 3.6 and 3.7 respectively.

### 3.6 DETERMINATION OF UF RESIN $T_1$ VALUES

The relaxation time  $T_1$  has a number of important experimental consequences, particular with respect to the observed signal intensity and optimum repetition rate (Derome 1989, Field and Sternhell 1989, Becker 1980).

The observable signal in a NMR experiment depends on the population difference between the states available to the nuclei. The maximum signal is observed when the nuclei in the sample are fully relaxed. The shorter the  $T_1$  is, the greater the number of scans that can be acquired in a particular time period and the higher the S/N ratio of the spectrum will be. In order to obtain good quantitative results, the time between transients must be adequate to allow complete longitudinal relaxation of the microscopic magnetic vector. This time is generally 5 times the longitudinal relaxation time ( $T_1$ ), when a  $\pi/2$  pulse is used (see Section 3.5.2)

The linewidth of a NMR signal is inversely related to  $T_1$ . The longer  $T_1$  is the sharper the NMR signal and vice versa.

$T_1$  values are particularly sensitive to molecular motion and can be used to derive information about the mobility and dynamics of whole molecules or segments of molecules. Generally, the smaller the molecule, the higher the molecular mobility, and the longer the longitudinal relaxation time.

$T_1$  is a valuable structural parameter. It is characteristic of the type of nucleus and its molecular environment, although it is often not as informative as chemical shift and coupling constant data.

The longest relaxing  $^{13}\text{C}$  nucleus becomes the carbon that establishes the rate of the acquisition. The underestimation of  $T_1$  (acquiring too rapidly) causes an error in the relative intensity of the species, and overestimation of  $T_1$  (ie acquiring more slowly than necessary) causes a loss of signal to noise ratio in a given time.

### 3.6.1 The Principle and Procedure for Measuring $T_1$

There are two common methods for determining  $T_1$  values (Abraham *et al.* 1988 Derome 1989, Becker 1980, Field and Sternhell 1989). These are the inversion recovery method and the progressive saturation method. The inversion-recovery method use a simple two-pulse sequence (see Section 2.1.5) and the intensity of the resulting NMR signal is given by the Equation:

$$I_\tau = I_0(1 - 2e^{-\tau/T_1}) \dots\dots\dots (3.3)$$

where  $I_0$  is the maximum signal intensity obtained, using a long delay time  $\tau$  (ie  $\tau > 5 T_1$ ) and  $I_\tau$  is the signal intensity for delay time  $\tau$ .

The first  $\pi$  pulse is used to align the equilibrium population of nuclear spins against the direction of the applied magnetic field. Following the  $\pi$  pulse, the spin population begins to recover towards its normal equilibrium position during the delay time  $\tau$ . The  $\pi/2$  pulse is used to convert the population difference between levels to a detectable NMR signal.

When  $\tau$  is very small (compared with  $T_1$ ) the sample effectively receives a  $3/2 \pi$  pulse (ie  $\pi + \pi/2$ ) and the observed signal is negative. When  $\tau$  is very long, the sample relaxes fully between the two pulses and it receives only a  $\pi/2$  pulse, so a maximum (positive) signal is observed. Between these two extremes, the observed signal increases exponentially with  $\tau$ .

The detected NMR signal passes through a null point ( $I_\tau = 0$ ) when  $\tau = \tau_{null} = (\ln 2) T_1$ .  $T_1$  values can therefore be calculated by:

$$T_1 = \tau_{null} / \ln 2 = 1.443 \tau_{null}$$

A typical plot of observed signal intensity  $I_\tau$  vs.  $\tau$  is shown in Figure 3.7.

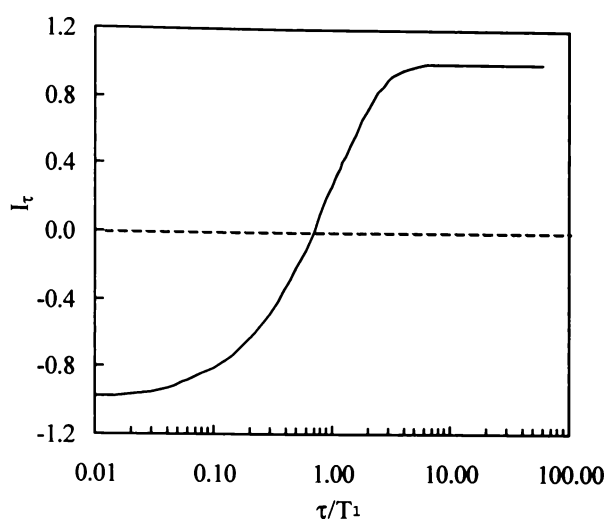


Figure 3.7. Plot of observed signal intensity vs  $\tau$  for an UF resin signal.

### 3.6.2 Experimental Determination of $T_1$ Values for Three UF Resins

Three UF resin samples have been used to perform the inversion recovery  $T_1$  measurement. The resin samples were taken from the same laboratory UF resin preparation at differing times. Resin sample details are given in Table 3.4.

Table 3.4. Resin samples used for  $T_1$  determination.

sample code	sample description	F/U ratio
S8-3	alkaline addition stage	2.0
S8-5	acidic condensation stage	2.0
S8-7	final resin	1.3

Figure 3.8 depicts the set of typical UF resin  $T_1$  spectra acquired by using the inversion-recovery sequence, with  $\tau$  values ranging from 0.003 to 15 sec. Long  $\tau_{null}$  values were observed for DMSO, and methanol, while the shortest  $\tau_{null}$  values were observed for higher molecular species, eg methylene, ether and methylol carbons.

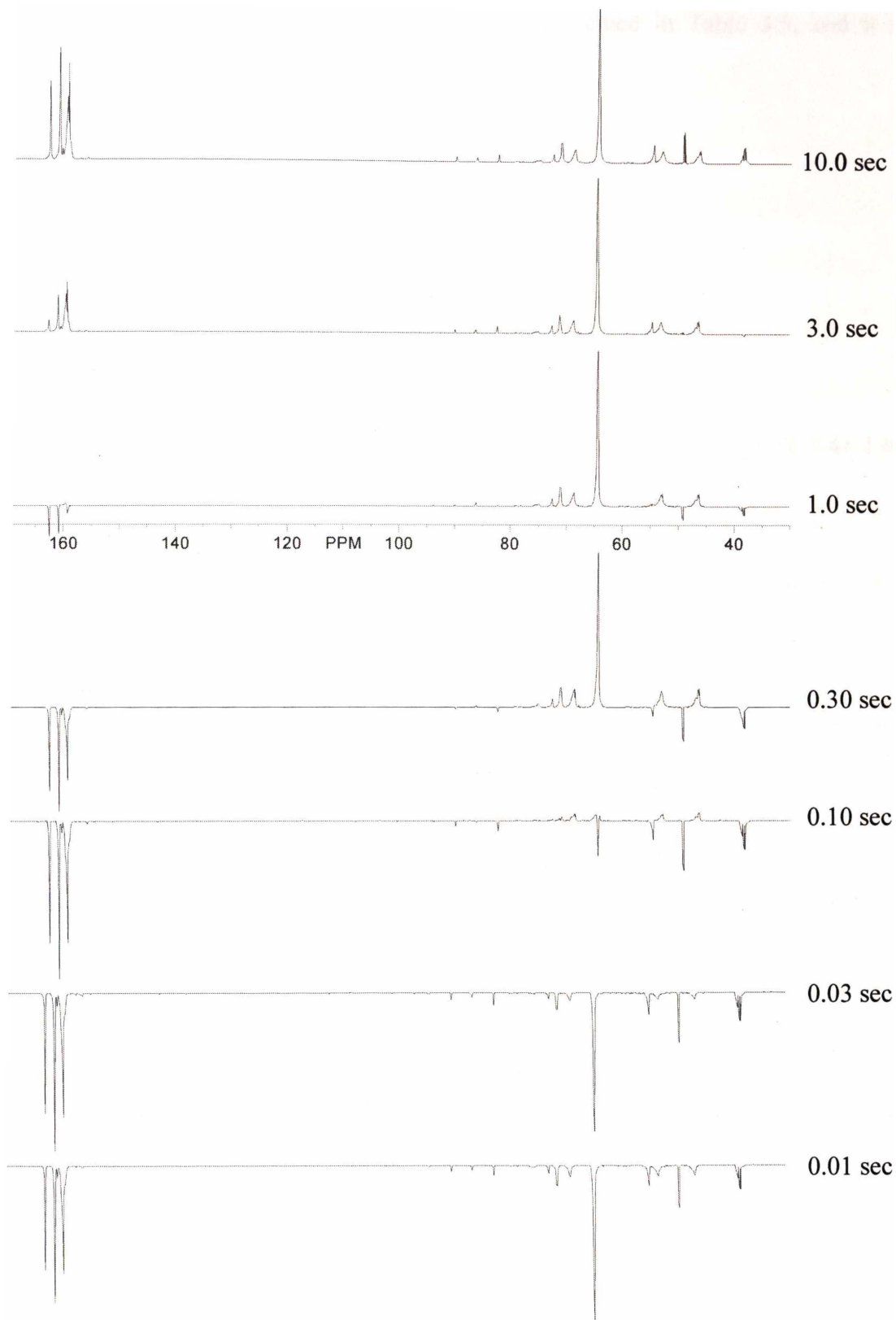


Figure 3.8.  $^{13}\text{C}$  NMR spectra determined for UF resin sample S8-7 using the inversion-recovery method for determining  $T_1$ s.

Delay time ( $\tau$ ) is shown alongside each spectrum.

$T_1$  results for three UF resin samples are represented in Table 3.5, and it is apparent that:

- the  $T_1$  of DMSO is about 6.0 sec;
- the  $T_1$  of methanol in the UF resin matrix is about 3.3 sec;
- the  $T_1$  of urea in the UF resin matrix is about 3.2 sec;
- the  $T_1$ s of carbonyl carbons in MMU, DMU and TMU are 1.77-2.02, 1.41-1.69 and 1.32-1.60 sec respectively;
- the  $T_1$  of methylo groups are about 0.11-0.22 sec.  $T_1$ s of methylene and ether groups are less than 0.1 sec.

Similar  $T_1$  values have been reported for UF resin species by Tomito and Hatono (1978).

The results presented in Table 3.5 also indicate that the repetition rate ( $T_r$ ) for quantitative UF resins spectra, acquired using a  $\pi/2$  pulse should be at least 18 sec, ie 5 times the longest  $T_1$  value (that of urea or methanol). This result in accord with the conclusions of other authors, who have suggested a repetition rate of at least 20 sec (Kim and Amos 1990, Valdez 1995).

If the proportional term  $k_z$  is assigned to the  $\sin\theta (1 - e^{-T_r/T_1}) / (1 - e^{-T_r/T_1} \cos\theta)$  term in Equation 3.2, the generalised form of the equation is:

$$I_z = k_z I_0 \dots\dots\dots (3.4)$$

The  $T_1$ s reported in Table 3.5 can be used to calculate expected relative signal intensities in UF resin NMR spectra. Results are given in Table 3.6.

Table 3.5. Longitudinal relaxation times ( $T_1$ , sec) of UF resin species determined using the inversion-recovery sequence.

shift (ppm)	species	sample code		
		S8-3	S8-5	S8-7
38.7	dimethyl sulphoxide (DMSO-d6)	5.70	6.35	5.94
46.7	linear methylene	0.073	0.072	0.069
49.3	methanol	3.03	3.35	3.46
52.8	branched methylene	0.080	0.075	0.073
55.0	methoxy	1.4	0.87	1.2
58.5	branched methylene	--	0.072	--
64.6	linear methylol	0.20	0.17	0.22
68.8	dimethylene ether	0.078	0.085	0.083
71.0	branched methylol	0.10	0.11	0.11
72.6	linear methylene connected to methoxy	0.10	0.11	0.12
75.5	branched dimethylene ether	0.075	0.080	0.096
79.0	branched methylene connected to methoxy	0.068	0.090	0.078
82.4	methylene glycol	0.98	1.12	1.02
86.4	polymeric methylene glycol	0.25	0.29	0.28
89.9	polymeric methylene glycol	0.77	0.70	0.63
93.8	methylene of hemiformal	0.28	0.30	0.25
159.3	trimethylol urea (TMU)	1.59	1.32	1.60
160.3	dimethylol urea (DMU)	1.69	1.41	1.66
160.9	monomethylol urea (MMU)	1.77	--	2.02
162.7	free urea	3.15	--	3.25

The STANDARD NMR method for determining the quantitative  $^{13}\text{C}$  NMR spectrum of an UF resin, as applied in this work, used inverse gated decoupling to simplify the spectrum and to suppress NOE. Since the RAPID method utilised continuously applied proton decoupling, NOE effects are expected for protonated carbons (eg DMSO, methanol, formaldehyde, methylol, methylene linkage and methylene ether carbons), but not for non protonated carbons (eg DMSO-d6, urea and other carbonyl signals). Substantial differences will therefore be observed in the

relative signal intensities for different UF resin carbon species in the STANDARD and RAPID NMR experiments.

For most species present in an UF resin, other than DMSO, DMSO-d<sub>6</sub>, methanol and urea, these conditions afford a maximum signal intensity of  $0.707 I_0$  (ie  $I_0 \sin\pi/4$ ). Therefore these species can be quantitatively determined using the STANDARD method.

Table 3.6. Calculated relative signal intensities obtained using the STANDARD and RAPID NMR methods.

species	$T_1$ (sec)	<u>STANDARD method</u>		<u>RAPID method</u>	
		<u>(<math>D_1 = 4.0</math> sec, <math>\pi/4</math> pulse)</u>		<u>(<math>D_1 = 0.5</math> sec, <math>\pi/2</math> pulse)</u>	
		$T_r / T_1$	$I_z (= k_z I_0)$	$T_r / T_1$	$I_z (= k_z I_0)$
DMSO-d <sub>6</sub>	6.0	0.82	$0.575 I_0$	0.236	$0.210 I_0$
DMSO	6.0	0.82	$0.575 I_0 + \text{NOE buildup}$	0.236	$0.210 I_0 + \text{NOE}^a$
methanol	3.3	1.49	$0.652 I_0 + \text{NOE buildup}$	0.430	$0.349 I_0 + \text{NOE}$
urea	3.2	1.54	$0.655 I_0$	0.443	$0.358 I_0$
MMU	1.9	2.59	$0.691 I_0$	0.746	$0.526 I_0$
DMU	1.6	3.07	$0.698 I_0$	0.886	$0.588 I_0$
TMU	1.5	3.28	$0.700 I_0$	0.945	$0.611 I_0$
<u>formaldehyde:</u>					
hemiformal	1.0	4.92	$0.706 I_0$	1.42	$0.76 I_0 + \text{NOE}$
methylene glycol	0.30	16.4	$0.707 I_0$	4.72	$0.99 I_0 + \text{NOE}$
methylene glycol	0.70	7.03	$0.707 I_0$	2.02	$0.87 I_0 + \text{NOE}$
methylene glycol	0.30	16.4	$0.707 I_0$	4.72	$0.99 I_0 + \text{NOE}$
methylol	0.16	30.7	$0.707 I_0$	8.86	$1.00 I_0 + \text{NOE}$
ether	0.09	54.6	$0.707 I_0$	15.7	$1.00 I_0 + \text{NOE}$
methylene	0.07	70.3	$0.707 I_0$	20.2	$1.00 I_0 + \text{NOE}$

<sup>a</sup> “+ NOE”, the NOE contribution, can be expressed as:  $\times (1 + \eta)$  ( $\eta$ , the NOE factor); eg the signal intensity for methylol is  $I_z = 1.00 I_0 + \text{NOE} = 1.00 I_0 (1 + \eta)$ .

Because the  $T_r/T_1$  values of DMSO-d<sub>6</sub> and urea are low for a 4 sec interpulse delay ( $D_1$ ) (0.82 and 1.54, respectively), these species are not fully relaxed using the

STANDARD method and signal intensities of about  $0.575 I_0$  and  $0.655 I_0$ , respectively are observed. These values represent 81.3% and 92.6% respectively of the theoretical maximum values of  $0.707 I_0$  for a  $\pi/4$  pulse.

For DMSO (non-deuterated DMSO) and methanol, both of which possess protonated carbons, incomplete relaxation of these molecules during the 4 sec interpulse delay period will afford reduced signals, which will be partially compensated by NOE buildup effects, hence their expected signal intensities are less predictable. Their signal intensities are about  $0.575 I_0 + \text{NOE buildup}$  and  $0.655 I_0 + \text{NOE buildup}$ , respectively.

### 3.7 NOE MEASUREMENT

The RAPID method utilises NOE to improve the S/N ratio of the spectrum. Considerable care must however have to be exercised when assessing apparent NOE enhancements determined using the RAPID mode since the rapid repetition can result in attenuation of signals due to  $T_1$  effects, thereby leading to a lower than expected NOE response. This complication can be suppressed by extending the interpulse delay period ( $D_1$ ) of the RAPID method to 25 sec (see Table 3.7).

Table 3.7. Comparative signal intensity data.

species	$T_1$ (sec)	<u>STANDARD method</u>		<u>RAPID method</u>	
		<u>(<math>D_1 = 25</math> sec, <math>\pi/4</math> pulse)</u>		<u>(<math>D_1 = 25</math> sec, <math>\pi/2</math> pulse)</u>	
		$T_r / T_1$	$I_z (= k_z I_0)$	$T_r / T_1$	$I_z (= k_z I_0)$
DMSO-d6	6.0	4.32	$0.704 I_0$	4.32	$0.987 I_0$
methanol	3.3	7.85	$0.707 I_0$	7.85	$1.000 I_0 + \text{NOE}^a$
urea	3.2	8.10	$0.707 I_0$	8.10	$1.000 I_0$
urea derivatives	1.8	14.4	$0.707 I_0$	14.4	$1.000 I_0$
formaldehyde	1.0	25.9	$0.707 I_0$	25.9	$1.000 I_0 + \text{NOE}$
other species	0.1	259	$0.707 I_0$	259	$1.000 I_0 + \text{NOE}$

<sup>a</sup> The term “+ NOE” indicates that an NOE enhancement of  $1 + \eta$  is expected, where  $\eta$  is the NOE factor (maximum  $\eta = 1.99$ ); eg the  $I_z$  of methanol in a continuous decoupling experiment is  $1.00 (1 + \eta)$ .

The NMR signal intensity is proportional to the carbon concentration in the sample. The general expression for the signal intensity ( $I_{zx}$ ) of species x, present at concentration level  $C_x$  (adapted from Equation 3.4, see Section 3.6.2) is:

$$I_{zx} = k_{zx} \cdot I_{0x} = k_{zx} \cdot k \cdot C_x \dots\dots\dots (3.5)$$

where  $I_{zx}$  is the signal intensity arising from a species x;

$k_{zx}$  is the proportional term  $k_z$  as in Equation 3.4 for a species x;

$k$  is a calibration constant. Ideally it should be same for all species in a sample and equal to unity (1.0);

$C_x$  is the concentration (carbon) of species x;

$I_{0x}$  the maximum signal obtainable using a  $\pi/2$  pulse for species x;

Since  $I_{0x}$  is proportional to  $C_x$ ,  $I_{0x}$  can be expressed as a function of  $C_x$ , ie  $I_{0x} = k C_x$ .

In continuously decoupled NMR spectra, signal intensity including NOE, is given by the expression:

$$(I_{zx})_E = k (k_{zx})_E C_x = k (1+\eta) C_x$$

In the absence of NOE (spectra acquired with inverse gated decoupling) signal intensity is given by the expression:

$$I_{zx} = k k_{zx} C_x$$

where the subscript "E" designate experiments with NOE

Signal intensities normalised relative to the DMSO-d6 signal will be:

$$(I_{zx})_{EN} = \frac{(I_{zx})_E}{(I_D)_E} = \frac{k(1+\eta)C_x}{(k_{zD})_E k C_D} = \frac{k(1+\eta)C_x}{0.987kC_D} \approx (1+\eta) \frac{C_x}{C_D}$$

$$(I_{zx})_N = \frac{I_x}{I_D} = \frac{k k_{zx} C_x}{k k_{zD} C_D} = \frac{0.707kC_x}{0.704kC_D} \approx \frac{C_x}{C_D}$$

where  $(I_{zx})_{EN}$  is the normalised signal intensity with NOE for species x;  
 $(I_{zx})_N$  is the normalised signal intensity without NOE for species x  
 $(I_D)_E$  is the DMSO-d6 signal intensity in the continuous decoupling experiment (RAPID method with  $D_1 = 25$  sec);  
 $I_D$  is the DMSO-d6 signal intensity in the inverse gated decoupling experiment (STANDARD method with  $D_1 = 25$  sec);  
 $C_x$  is the carbon concentration of species x;  
 $C_D$  is the carbon concentration of DMSO-d6.

Comparing  $(I_{zx})_{EN}$  and  $(I_{zx})_N$  leads to the expression:

$$\frac{(I_{zx})_{EN}}{(I_{zx})_N} = \frac{(1+\eta)C_x / C_D}{C_x / C_D} = 1 + \eta$$

Rearrangement of the above equation yields the expression:

$$\eta = \frac{(I_{zx})_{EN}}{(I_{zx})_N} - 1$$

Since all the signal intensity data are normalised to the internal standard DMSO-d6, the subscript “N” may be omitted for the simplicity of the expression. The subscript “x” designating species x can also be omitted. The simplified expression is:

$$\eta = \frac{I_{zE}}{I_z} - 1$$

NOEs calculated using this approach are presented in Tables 3.9 to 3.13. The samples used to perform NOE measurements were a urea aqueous solution, a commercial formaldehyde solution (47% w/w) and four UF resin samples. The four resin samples were taken from the same laboratory preparation. Resin sample details are given in Table 3.8.

It can be seen (Table 3.9) that, as expected, the NOE factor ( $\eta$ ) of urea is close to zero (0.03). The  $\eta$  values determined for clusters of peaks observed for an aqueous

formaldehyde solution are in the range 0.80-1.98 (see Table 3.9). Aqueous formaldehyde solution has average NOE factor ( $\eta$ ) of about 1.42.

Since carbonyl group signals which appear in the region of 155-163 ppm are poorly resolved (see Section 3.2), especially so for the late reaction stage UF resin samples, this region was integrated together as a whole. The  $\eta$  values of carbonyl group signals were typically in the range 0.24-0.33.

Table 3.8. UF resin samples used for NOE determination.

sample code	reaction time (min)	reaction stage	F/U ratio
S1-4	62	acidic condensation	2.00
S1-7	97	acidic condensation	2.00
S1-8	123	acidic condensation	2.00
S1-9	145	final resin	1.30

Table 3.9. NOE factors for urea and formaldehyde analogues.

signal range (ppm)	species	$I_z$	$I_{ZE}$	$\eta$
162.0-163.0	urea	0.93	0.96	0.03
81.0-96.0	<u>aqueous formaldehyde (overall):</u>	1.75	4.24	1.42
88.6-92.0	middle poly-methylene glycol methylene	0.45	1.34	1.98
85.0-87.9	terminal polymethylene glycol methylene	0.91	2.15	1.37
81.4-83.8	methylene glycol	0.34	0.61	0.80

Generally, the NOE factors ( $\eta$ ) of methylol, ether and methylene groups decrease in the order: methylol (0.83-0.97) > ether (0.38-0.42) > methylene (0.29-0.30). It is apparent that in linear chains these groups have slightly larger NOE factors than is the case for the corresponding branched chain analogues. Also,  $\eta$  of methylol species decreases with the reaction time. This effect is less obvious for methylene and ether

species. These results indicate that molecular size and the viscosity of the reaction system effect NOE factors: ie for a particular species  $\eta$  is not constant during the entire reaction period.

Table 3.10. NOE factors for different species in UF resin S1-4.

signal range (ppm)	species	$I_z$	$I_{zE}$	$\eta$
157.6-161.6	carbonyl groups	0.96	1.28	0.33
81.0-96.0	free formaldehyde (unreacted formaldehyde)	0.16	0.37	1.30
88.6-92.0	middle poly-methylene glycol methylene	0.024	0.045	0.86
85.0-87.9	terminal poly-methylene glycol methylene	0.067	0.16	1.39
81.4-83.8	methylene glycol	0.046	0.12	1.59
74.3-76.3	branched dimethylene ether	0.16	0.22	0.38
70.0-71.9	branched methylol	0.32	0.58	0.83
67.8-69.9	linear dimethylene ether	0.36	0.51	0.42
63.3-65.7	linear methylol	0.44	0.86	0.97
54.1-55.8	methoxy	0.059	0.15	1.56
51.5-54.1	branched methylene	0.40	0.52	0.30
45.2-48.2	linear methylene	0.24	0.31	0.29

Table 3.11. NOE factors for different species in UF resin S1-7.

signal range (ppm)	species	$I_z$	$I_{zE}$	$\eta$
157.6-161.6	carbonyl groups	1.06	1.36	0.28
81.0-96.0	free formaldehyde	0.20	0.53	1.65
88.6-92.0	middle methylene-poly-methylene glycol	--	--	--
85.0-87.9	terminal methylene-poly-methylene glycol	0.11	0.23	1.10
81.4-83.8	methylene glycol	0.11	0.22	1.00
74.3-76.3	branched dimethylene ether	0.10	0.16	0.60
72.1-73.4	methylene connected to methoxy	0.040	0.062	0.56
70.0-71.9	branched methylol	0.36	0.57	0.58
67.8-69.9	linear dimethylene ether	0.19	0.33	0.74
63.3-65.7	linear methylol	0.33	0.65	0.99
57.0-60.5	branched methylene	0.094	0.15	0.57
54.1-55.8	methoxy	0.095	0.18	0.88
51.5-54.1	branched methylene	0.50	0.66	0.32
45.2-48.2	linear methylene	0.22	0.33	0.48

Table 3.12. NOE factors for different species in UF resin S1-8.

signal range (ppm)	species	$I_z$	$I_{zE}$	$\eta$
157.6-161.6	carbonyl groups	1.00	1.24	0.24
74.3-76.3	branched dimethylene ether	0.13	0.16	0.24
70.0-71.9	branched methylol	0.36	0.57	0.57
67.8-69.9	linear dimethylene ether	0.22	0.33	0.51
63.3-65.7	linear methylol	0.31	0.51	0.65
51.5-54.1	branched methylene	0.50	0.70	0.40
45.2-48.2	linear methylene	0.18	0.24	0.35

Table 3.13. NOE factors for different species in UF resin S1-9.

signal range (ppm)	species	$I_z$	$I_{zE}$	$\eta$
157.6-161.6	carbonyl groups	1.21	1.53	0.26
74.3-76.3	branched dimethylene ether	0.14	0.17	0.21
70.0-71.9	branched methylol	0.33	0.54	0.63
67.8-69.9	linear dimethylene ether	0.24	0.33	0.40
63.3-65.7	linear methylol	0.35	0.60	0.71
51.5-54.1	branched methylene	0.50	0.65	0.30
45.2-48.2	linear methylene	0.28	0.37	0.33

Table 3.14. The relationship between NOE factors ( $\eta$ ) and reaction time.

species	<u>reaction time (mins)</u>			
	62	97	123	145
<u>methylol</u>				
linear	0.97	0.99	0.65	0.71
branched	0.83	0.58	0.57	0.63
overall	0.90	0.77	0.61	0.68
<u>methylene</u>				
linear	0.29	0.48	0.35	0.33
branched	0.30	0.32	0.40	0.30
overall	0.30	0.38	0.38	0.31
<u>ether</u>				
linear	0.42	0.74	0.51	0.40
branched	0.38	0.60	0.24	0.21
overall	0.40	0.69	0.40	0.32

### 3.8 CROSS CALIBRATION OF STANDARD AND RAPID NMR SPECTRAL DATA

The RAPID NMR method was used in dynamic ‘real time’ polymerisation experiments to acquire  $^{13}\text{C}$  NMR spectra using conditions (eg short interpulse delay, NOE for protonated carbons) which do not afford quantitative spectral data. The possibility that signal intensities observed in RAPID NMR experiments could be reliably cross calibrated to within 10-15% of those observed in STANDARD NMR experiments was therefore explored.

Since, due to changes in  $T_1$ , viscosity and molecular weight, the NOE factors ( $\eta$ ) of UF resin species vary as the polymerisation process proceeds, it was anticipated that (at least for some species) cross calibration factors would exhibit a time dependency, related to both the reaction stage and reaction time.

The expected intensities of signals in  $^{13}\text{C}$  NMR spectra determined using the STANDARD and RAPID methods, with interpulse delays of 25 sec and 0.5 sec, respectively, are given in Table 3.15. Calculated signal intensities ( $I_{\text{calc}}$ ), expressed as a function of the maximum signal obtainable using a  $\pi/2$  pulse ( $I_0$ ), were calculated using the following general expression:

$$(I_{\text{calc}})_x = I_{\text{zx}} = k_{\text{zx}} I_{0x} = k_x I_{0x}$$

where  $(I_{\text{calc}})_x$  is the calculated signal intensity for species-x, ie  $I_{\text{zx}}$

as in Equation 3.4, Section 3.6.2;

$k_{\text{zx}}$  is the term defined in Equation 3.4, Section 3.6.2;  $k_{\text{zx}}$  may

include a NOE contribution where appropriate;

$k_x$  is the simplified  $k_{\text{zx}}$  omitting the subscript “z”.

An analysis of the  $T_1$  and  $T_r/T_1$  values (see Section 3.6), and the calculated signal intensities presented in Table 3.15, shows that (as discussed in Section 3.6) the use of inverse gated coupling and a long interpulse delay ( $D_1 = 25$  sec) eliminates NOE and  $T_1$  effects from STANDARD NMR spectra. On the other hand, the use of continuous

proton decoupling and a short interpulse delay ( $D_1 = 0.5$  sec) in RAPID NMR experiments contribute to the  $T_1$  and NOE dependency of signal intensities for UF resin species such as hemiformal and methylene glycol groups.

Table 3.15. Calculated signal intensities ( $I_{\text{calc}}$ ) for UF resin species in NMR spectra determined using the STANDARD and RAPID methods.

species	chemical shift (ppm)	$T_1$ (sec)	STANDARD method		RAPID method	
			$(D_1 = 25 \text{ sec}, \pi/4 \text{ pulse})$		$(D_1 = 0.5 \text{ sec}, \pi/2 \text{ pulse})$	
			$T_r / T_1$	$I_{\text{calc}}^a$	$T_r / T_1$	$I_{\text{calc}}^a$
DMSO-d6	38.7	6.0	4.32	$0.704 I_0$	0.236	$0.210 I_0$
DMSO	39.1	6.0	4.32	$0.704 I_0$	0.236	$0.210 I_0 + \text{NOE}$
methanol	49.3	3.3	7.85	$0.707 I_0$	0.430	$0.349 I_0 + \text{NOE}$
urea	162.7	3.2	8.10	$0.707 I_0$	0.443	$0.358 I_0$
MMU	161.0	1.9	13.6	$0.707 I_0$	0.746	$0.526 I_0$
DMU	159.5	1.6	16.2	$0.707 I_0$	0.886	$0.588 I_0$
TMU	159.0	1.5	17.3	$0.707 I_0$	0.945	$0.611 I_0$
<u>formaldehyde</u> <sup>b</sup>	81-95	<1.0	>25.9	$0.707 I_0$	>1.42	$>0.76 I_0 + \text{NOE}$
-O <u>C</u> H <sub>2</sub> OCH <sub>3</sub> <sup>c</sup>	94.0	1.0	25.9	$0.707 I_0$	1.42	$0.76 I_0 + \text{NOE}$
-O <u>C</u> H <sub>2</sub> O <sup>c</sup>	90.0	0.30	86.4	$0.707 I_0$	4.73	$0.99 I_0 + \text{NOE}$
-O <u>C</u> H <sub>2</sub> OH <sup>c</sup>	85.5	0.70	37.0	$0.707 I_0$	2.02	$0.87 I_0 + \text{NOE}$
HO <u>C</u> H <sub>2</sub> OH <sup>c</sup>	82.4	0.30	86.4	$0.707 I_0$	4.73	$0.99 I_0 + \text{NOE}$
other species		<0.1	>259	$0.707 I_0$	>14.2	$1.00 I_0 + \text{NOE}$

<sup>a</sup> signal intensities calculated according to Equation 3.4, Section 3.6.2, plus (where appropriate) an NOE contribution; <sup>b</sup> integrated as a whole across the range 81.0-95.0 ppm; <sup>c</sup> integration of each clusters of peaks present in polymeric formaldehyde (see Table 3.2, Section 3.2).

The normalised intensities of signals appearing in the STANDARD and RAPID NMR spectra of a series of UF resin sub-samples, recovered at varying reaction times during the UF preparation (Table 3.16), were determined relative to DMSO-d6 + DMSO (see Tables 3.18 to 3.21). An aqueous formaldehyde solution also has been used in these experiments (see Tables 3.16 and 3.17).

Table 3.16. Formaldehyde solution and UF resin samples used for NMR cross calibration experiments.

sample code	time (min)	origin <sup>a</sup>	F/U ratio
formaldehyde (47%)	--	47% formaldehyde	--
S1-4	62	acidic condensation	2.00
S1-7	97	acidic condensation	2.00
S1-8	123	acidic condensation	2.00
S1-9	145	final resin	1.30

<sup>a</sup> initial addition stage: pH 8.7 for 42 min; condensation stage: pH 5.0, at 88°C.

<sup>b</sup> internal standard: DMSO-d<sub>6</sub> (0.4 mL) + DMSO (0.20 mL).

The cross calibration factor  $f_c$ , between the observed signal intensities in the STANDARD and RAPID NMR experiments can be defined as:

$$f_c = I_R / I_Q \dots\dots\dots (3.6)$$

where  $I_Q$  is the normalised signal intensity of species x relative to DMSO-d<sub>6</sub> + DMSO determined using the STANDARD NMR method;

$I_R$  is the normalised signal intensity of species x relative to DMSO-d<sub>6</sub> + DMSO determined using the RAPID NMR method.

Rearrangement of Equation 3.6 gives the expression:

$$I_Q = I_R / f_c$$

and it follows that division of the RAPID signal intensity ( $I_R$ ) by  $f_c$  (the cross calibration factor) gives the corresponding STANDARD (quantitative) signal intensity  $I_Q$ . Therefore, in order to use the dynamic (RAPID) NMR method for monitoring concentration changes, it is necessary to determine values of  $f_c$ s for appropriate resin samples.

The normalised signal intensities ( $I_Q$  and  $I_R$ ) and cross calibration factors determined for aqueous formaldehyde solution are shown in Table 3.17 and those for the resin samples (Table 3.16) are shown in Tables 3.18 to 3.21. The effects of the reaction time on the cross calibration factors are shown in Table 3.22 and Figure 3.9.

Table 3.17. Normalised signal intensities and cross calibration factors determined for aqueous formaldehyde solution.

shift range (ppm)	species	$I_Q$	$I_R$	$f_c$
81.0-96.0	aqueous formaldehyde (overall)	2.26	7.78	3.44
92.5-96.0	$\text{H}(\text{OCH}_2)_n\text{OCH}_2\text{OCH}_3$	0.038	0.16	4.20
88.6-92.0	$-(\text{CH}_2\text{O})_n\text{CH}_2\text{O}(\text{CH}_2\text{O})_m-$	0.56	2.37	4.23
85.0-87.9	$-(\text{OCH}_2)_n\text{OCH}_2\text{OH}$	1.22	4.16	3.40
81.4-83.8	$\text{HOCH}_2\text{OH}$ (methylene glycol)	0.44	1.12	2.55

Table 3.18. Signal intensities and cross calibration factors determined for resin sample S1-4.

signal range (ppm)	species	$I_Q$	$I_R$	$f_c$
158.0-63.0	carbonyl groups (overall)	0.80	1.30	1.63
81.0-96.0	polymeric formaldehyde analogues	0.17	0.38	2.24
85.0-87.9	$-(\text{OCH}_2)_n\text{OCH}_2\text{OH}$	0.061	0.22	3.60
81.4-83.8	$\text{HOCH}_2\text{OH}$ (methylene glycols)	0.057	0.12	2.05
74.3-76.3	branched dimethylene ethers	0.10	0.36	3.41
72.1-73.4	methylene connected to methoxyl	0.029	0.11	3.79
70.0-71.9	branched methylols	0.22	0.98	4.49
67.8-69.9	dimethylene ethers	0.20	0.80	4.06
63.3-65.7	linear methylols	0.30	1.39	4.57
54.1-55.8	methoxyls	0.041	0.13	3.12
51.5-54.1	branched methylenes	0.26	0.84	3.30
45.2-48.2	linear methylenes	0.13	0.42	3.17

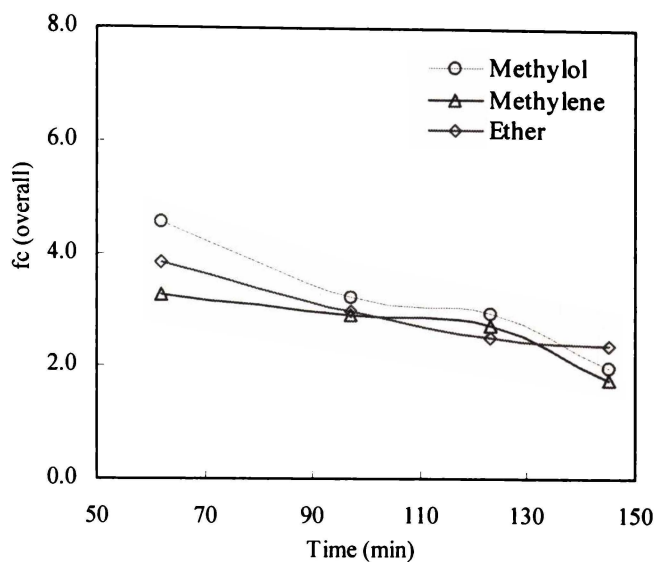
Figure 3.9. Plot of calibration factors ( $f_c$ ) vs reaction time.

Table 3.19. Signal intensities and cross calibration factors determined for resin sample S1-7.

signal range (ppm)	species	$I_Q$	$I_R$	$f_c$
157.6-163.0	carbonyl groups (mainly DMU + TMU)	0.66	0.87	1.31
81.0-96.0	polymeric formaldehyde analogues	0.060	0.16	2.70
85.0-87.9	$-(OCH_2)_nOCH_2OH$	0.051	0.20	3.92
81.4-83.8	HOCH <sub>2</sub> OH (methylene glycols )	0.040	0.10	2.50
74.3-76.3	branched dimethylene ethers	0.065	0.20	3.00
70.0-71.9	branched methylols	0.22	0.64	2.90
67.8-69.9	dimethylene ethers	0.11	0.32	2.96
63.3-65.7	linear methylols	0.18	0.66	3.60
54.1-55.8	methoxyls	0.069	0.16	2.32
51.5-54.1	branched methylenes	0.21	0.60	2.91
48.3-50.5	methanol	0.21	0.24	1.14
45.2-48.2	linear methylenes	0.084	0.24	2.86

Table 3.20. Signal intensities and cross calibration factors determined for resin sample S1-8.

signal range (ppm)	species	$I_Q$	$I_R$	$f_c$
157.6-163.0	total carbonyl groups (overall)	0.70	1.00	1.43
74.3-76.3	branched dimethylene ethers	0.056	0.15	2.68
70.0-71.9	branched methylols	0.21	0.57	2.71
67.8-69.9	dimethylene ethers	0.12	0.29	2.42
63.3-65.7	linear methylols	0.22	0.70	3.18
54.1-55.8	methoxyls	0.028	0.060	2.14
51.5-54.1	branched methylenes	0.10	0.28	2.80
45.2-48.2	linear methylenes	0.09	0.24	2.67

Table 3.21. Signal intensities and cross calibration factors determined for resin sample S1-9.

signal range (ppm)	species	$I_Q$	$I_R$	$f_c$
157.6-163.0	total carbonyl groups (overall)	0.75	0.98	1.31
162.0-163.0	urea	0.05	0.057	1.14
160.5-161.5	monomethylolurea (MMU)	0.14	0.17	1.21
157.5-161.5	di- & tri-methylolurea (DMU + TMU)	0.69	0.94	1.37
70.0-71.9	branched methylols	0.40	0.65	1.63
67.8-69.9	dimethylene ethers	0.12	0.29	2.36
63.3-65.7	linear methylols	0.33	0.78	2.36
54.1-55.8	methoxy	0.041	0.063	1.54
51.5-54.1	branched methylenes	0.15	0.26	1.74
45.2-48.2	linear methylenes	0.14	0.25	1.77

It can be seen (see Tables 3.17 to 3.22) that the  $f_c$ s differ from species to species and that they also vary with reaction time.

Table 3.22. The relationship between cross correlation factors ( $f_c$ ) and reaction time.

species	<u>reaction time (min)</u>			
	62	97	123	145
<u>methylol:</u>				
linear	4.57	3.60	3.18	2.36
branched	4.49	2.90	2.71	1.63
overall	4.54	3.22	2.95	1.96
<u>methylene:</u>				
linear	3.17	2.86	2.67	1.77
branched	3.30	2.91	2.80	1.74
overall	3.25	2.89	2.74	1.76
<u>ether:</u>				
linear	4.06	2.96	2.42	2.36
branched	3.41	3.00	2.68	
overall	3.84	2.98	2.50	2.36

It is also apparent (see Figure 3.9), that the  $f_c$  values of methylol, methylene and ether groups decrease with the reaction time and differences between the  $f_c$  values of methylol, methylene and ether groups decrease with reaction time. For reaction times greater than 97 min, the  $f_c$  values of these species differ by less than 10%.

In order to better understand and explain these data, some calculations of the  $f_c$ s are demonstrated below.

The signal intensity of the mixture of DMSO + DMSO-d<sub>6</sub>, used as internal integration standard in the RAPID NMR spectra is given in Equation 3.7:

$$\begin{aligned}
 (I_{\text{std}})_r &= (I_n)_r + (I_D)_r = (k_n)_r I_{0n} + (k_D)_r I_{0D} \\
 &= (k_n)_r k C_n + (k_D)_r k C_D = 0.21 (1+\eta_x) k C_n + 0.21 k C_D \dots\dots\dots (3.7)
 \end{aligned}$$

where the subscripts “r, n, or D” designate values determined using the RAPID method for non-deuterated DMSO and DMSO-d6 respectively and:

$I_n$  is the signal intensity of non-deuterated DMSO;

$I_D$  is the signal intensity of DMSO-d6;

$I_{0n}$  is the maximum signal intensities obtainable for DMSO;

$I_{0D}$  is the maximum signal intensities obtainable for DMSO-d6;

$k_x$  (or  $k_{zx}$ ) is the term defined in Equation 3.4 Section 3.6.2.

Typical values of  $k_x$  can be found in Table 3.15

The expression for  $(I_{std})_r$  (Equation 3.7) includes a NOE contribution for DMSO, ie  $k_n = 0.21(1+\eta_n)$ , but not for DMSO-d6 ( $k_D = 0.21$ ), and two coefficients ( $k_n$  and  $k_D$ ,  $\approx 0.21$ ) which are related to the  $T_1$  values (see Table 3.15) of both DMSO and DMSO-d6 in the particular resin system.

Equation 3.7 appears to indicate that the expected value of  $(I_{std})_r$  can only be calculated if the NOE factor for DMSO is known for the particular resin system.

If, however, the observation that the area ratios of the DMSO to DMSO-d6 signals appearing in RAPID NMR spectra are typically in the range 1.51 to 1.92 (average value 1.75, see Table 3.23) is utilised, it follows that, to with  $\pm 8\%$ ,  $I_n$  can be approximated to  $1.75 I_D$ . Equation 3.7 can therefore be re-written as:

$$\begin{aligned} (I_{std})_r &= (I_n)_r + (I_D)_r = 1.75 (I_D)_r + (I_D)_r \\ &= 2.75 (I_D)_r \\ &= 2.75 \times 0.21 k C_D \\ &= 0.578 k C_D \end{aligned}$$

The signal intensity of a species x may be expressed as (see Equations 3.5):

$$(I_x)_r = (k_x)_r I_{0x} = (k_x)_r k C_x$$

where: the subscript “x” designates the signal from species x and “r” designates the values determined using the RAPID NMR method;

$k$  is the constant in the expression:  $I_{ox} = k C_x$ ;

$k_x$  is constant term in equation:  $I_{calc} = k_x I_{ox}$  (see Table 3.15);

$C_x$  is the molar concentration of the carbon atoms of species  $x$ .

Table 3.23. Observed DMSO/DMSO-d6 ( $I_n/I_D$ ) signal ratios in RAPID NMR spectra.

sample <sup>a</sup>	R1-1	R1-2	R1-3	R1-4	R1-5	R1-6	R1-7	R1-10	R2-1	R2-3	F <sup>b</sup>
$I_n/I_D$	1.70	1.68	1.51	1.95	1.86	1.81	1.80	1.65	1.59	1.77	1.92
average:	1.75										
stdev <sup>c</sup>	0.14										
RSD <sup>d</sup>	0.08										

<sup>a</sup> Data from samples taken from two series (R1 and R2 series) of dynamic NMR experiments corresponding to different reaction times; <sup>b</sup> F = aqueous formaldehyde solution ; <sup>c</sup> stdev = standard deviation; <sup>d</sup> RSD = relative standard deviation.

The normalised signal intensity in RAPID NMR spectra will be:

$$I_x = \frac{(I_x)_r}{(I_{std})_r} = \frac{(k_x)_r k C_x}{0.578 k C_D} = 1.73 (k_x)_r \frac{C_x}{C_D} \dots\dots\dots (3.8)$$

The signal intensity of internal integration standard (DMSO + DMSO-d6) appearing in the quantitative (STANDARD) NMR spectra is:

$$(I_{std})_q = (I_n)_q + (I_D)_q = (k_n)_q k C_n + (k_D)_q k C_D \dots\dots\dots (3.9)$$

Since  $(k_n)_q$  and  $(k_D)_q \equiv 0.704$  ( $\approx 0.707$ , the maximum value expected in STANDARD spectra), Equation 3.9 simplifies to:

$$(I_{std})_q = 0.704 k (C_n + C_D)$$

The carbon molar ratio of  $C_n/C_D$  can be calculated from their volumes ( $V$ ) (DMSO = 0.20 mL, DMSO-d6 = 0.40 mL), molar mass ( $M$ ) and densities ( $d$ ):

$$(C_n/C_{d6})_{\text{calc}} = (2 V_n d_n/M_n)/(2 V_D d_D/M_D) = 0.503$$

where: the subscript “calc” designates a calculated value;

$V_n$ ,  $V_D$ ,  $d_n$ ,  $d_D$ ,  $M_n$  and  $M_D$  are the volume, density and molar mass of DMSO or DMSO-d6, respectively.

Since  $(I_{\text{calc}})_n/(I_{\text{calc}})_D = (C_n/C_{d6})_{\text{calc}}$ , it follows  $(I_{\text{calc}})_n/(I_{\text{calc}})_{d6} = 0.503$ . This value can be compared to observed values of  $I_n/I_D$  in the range 0.47 to 0.49 (average value 0.48) (see Table 3.24). Observed and calculated values agree to within 4.6%, so either value can be used in the calculation.

If the observed  $I_n/I_D$  value (0.48) is substituted into Equation 3.9, an expression for  $(I_{\text{std}})_q$  (the expected signal intensity in quantitative (STANDARD) NMR spectra) can be derived:

$$\begin{aligned} (I_{\text{std}})_q &= (I_n)_q + (I_D)_q = 0.48 (I_D)_q + (I_D)_q = 1.48 (I_D)_q \\ &= 1.48 \times 0.704 k C_D \\ &= 1.04 k C_D \dots\dots\dots (3.10) \end{aligned}$$

Table 3.24. Observed DMSO/DMSO-d6 ( $I_n/I_D$ ) signal ratios in quantitative (STANDARD) NMR ( $D_1 = 25$  sec) spectra.

samples	F <sup>a</sup>	F <sup>a</sup>	R1-1	R1-4	R2-1
$I_n/I_D$	0.472	0.482	0.482	0.490	0.475
average:	0.480				
stdev <sup>b</sup>	0.007				
RSD <sup>c</sup>	0.015				

<sup>a</sup> F = aqueous formaldehyde solution ; <sup>b</sup> stdev = standard deviation; <sup>c</sup> RSD = relative standard deviation.

The signal intensity of a species x in quantitative (STANDARD) NMR spectra may be expressed as:

$$(I_x)_q = (k_x)_q (I_{ox})_q = 0.707 k C_x \dots \dots \dots (3.11)$$

The normalised signal intensity of species x in the quantitative (STANDARD) NMR spectra is therefore (by division of Equation 3.11 by Equation 3.10):

$$I_q = \frac{(I_x)_q}{(I_{std})_q} = \frac{0.707kC_x}{1.04kC_D} = 0.68 \frac{C_x}{C_D} \dots \dots \dots (3.12)$$

Therefore, the cross calibration factor can be estimated by (division of Equation 3.8 by Equation 3.12)):

$$f_{calc} = \frac{I_r}{I_q} = \frac{1.73(k_x)rC_x / C_D}{0.68C_x / C_D} = 2.55(k_x)r \dots \dots \dots (3.13)$$

Equation 3.13 is the general expression for cross calibration factors ( $f_{calc}$ ) relative to DMSO + DMSO-d6.

Generally, calculated cross calibration factors are predominantly influenced by five variables, ie the  $T_1$  and  $\eta_x$  of the species, the  $T_1$  of both DMSO and DMSO-d6, and  $\eta$  of DMSO. Since in RAPID NMR experiments the repetition rate  $T_r$  is  $< 5 T_1$  for DMSO and DMSO-d6,  $k_n$  and  $k_D$  terms of Equation 3.7 also exhibit a  $T_1$  dependency.

Therefore, the  $f_{calc}$  may be expressed as a function of  $T_{1x}$ ,  $\eta_x$ ,  $T_{1n}$ ,  $\eta_n$ ,  $T_{1D}$ , ie:

$$f_{calc} = f(T_{1x}, \eta_x, T_{1n}, \eta_n, T_{1D}) \dots \dots \dots (3.14)$$

where:  $T_{1x}$ ,  $T_{1n}$  and  $T_{1D}$  are the  $T_1$ s for species x, DMSO and DMSO-d6 respectively;

$\eta_x$  and  $\eta_n$  are the NOE factor for species x and DMSO respectively.

The parameters which primarily influence  $f_c$  values and result in its variation with reaction time and stages, are  $T_{1x}$  and  $\eta_x$ . Since, during the reaction period, DMSO

and DMSO-d6 undergo no change, while changes in resin viscosity are likely to only slightly influence  $T_{1n}$ ,  $\eta_n$  and  $T_{1D}$ , it can be reasoned that changes in  $T_{1x}$  and  $\eta_x$  values are probably the major contributors to the observed  $f_c$  variations.

Thus, it is apparent that the cross calibration factor ( $f_{calc}$ ) of carbonyl species depends mainly on  $T_1$ , since there is no NOE enhancement and their  $T_1$  values (typically  $> 0.28$  sec) are such that the repetition rate  $T_r$  is  $< 5 T_1$ , their  $(k_x)_r$  is  $T_1$  dependency (see Table 3.15).

Calculated ( $f_{calc}$ ) and observed ( $f_c$ ) values for the carbonyl groups of urea, MMU, DMU and TMU, which have  $\eta_x = 0$  and  $(k_x)_r = 0.358, 0.526, 0.588$  and  $0.611$  (see Table 3.15), respectively, are given in Table 3.25. Observed values are about 11% smaller than the calculated values, except for urea. Since carbonyl signals are poorly resolved and the concentration (intensity) of free urea is very low the  $\approx 20\%$  difference between calculated and observed urea values is considered to be reasonable.

Table 3.25. Calculated and observed cross calibration factors for urea and its analogues in resin sample S1-9, determined relative to DMSO and DMSO-d6.

species	<u>calculated calibration factors</u>	<u>observed calibration factors</u>
	$f_{calc}$	$f_c$
urea	0.91	1.14
MMU	1.34	1.21
DMU	1.49	--
TMU	1.55	--
DMU + TMU	1.52 (mean) <sup>a</sup>	1.37 (overall) <sup>b</sup>
all carbonyls	1.46 (mean) <sup>a</sup>	1.32 (overall) <sup>b</sup>

<sup>a</sup> arithmetic average; <sup>b</sup> value obtained by integration the poorly resolved clusters of peak as a whole.

The calculated cross calibration factors ( $f_{calc}$ ) for methylol, methylene and ether species are given by the expression:

$$f_{\text{calc}} = 2.55 (k_x)_r = 2.55 \times 1.00 \times (1+\eta_x) = 2.55 (1+\eta_x)$$

ie the  $f_{\text{calc}}$ s of methylol, methylene and ether mainly depend on their NOE factors  $\eta_x$  and are not  $T_1$  dependent, since  $T_1 < 0.28$  sec (ie  $T_r > 5 T_1$ ).

The expected  $f_{\text{calc}}$  value is therefore at least 2.55 plus the NOE contribution. The observed  $f_c$  for methylol, methylene and ether species given in Tables 3.18 to 3.21 are generally greater than 2.55, except for the final resin sample S1-9.

The  $(k_x)_r$  values for the four clusters of polymeric aqueous formaldehyde species, in order of decreasing ppm value, are 0.76  $(1+\eta_x)$ , 0.99  $(1+\eta_x)$ , 0.87  $(1+\eta_x)$  and 0.99  $(1+\eta_x)$ , respectively. Hence, the calculated  $f_{\text{calc}}$  for these species are in the range:

$$f_{\text{calc}} = 2.55 (k_x)_r = (0.76 \sim 0.99) \times 2.55 \times (1+\eta_x) = (1.94 \sim 2.52) (1+\eta_x)$$

These values are expected to depend on both  $\eta_x$  and  $T_{1x}$  (typically in the range 0.76 ~ 0.99 sec, since  $T_{1x} > 0.28$  sec and  $T_r < 5 T_{1x}$ ).

### 3.9 SUMMARY AND CONCLUSIONS

The  $T_1$ s of different species present in the UF resin matrix were determined. The longest  $T_1$  was 3.2 sec for free urea, followed by 1.8-2.0 sec for MMU, 1.4-1.7 sec for DMU, 1.3 -1.6 sec for TMU, 0.11-0.22 sec for the methylene carbons in methylol groups and  $< 0.1$  sec for methylene carbons in methylene and ether groups.

A repetition rate ( $T_r$ ) of  $\geq 18$  sec is required for a quantitative NMR analysis of UF resins.

$T_1$ s and NOE values of species present in UF resins decrease slightly with reaction time.

The cross calibration factors determined for slowly relaxing, non-protonated, carbonyl groups were substantially smaller than those determined for rapidly relaxing methylol, methylene and ether groups.

Comparison of STANDARD and RAPID signal intensities showed that methylol, methylene and ether groups exhibited similar signal intensities in RAPID spectra. Provided reaction times are similar, signal intensities observed in RAPID and quantitative STANDRAD NMR experiments can be cross calibrated to within 15%. For more accurate work, measurement of the cross calibration factors is required.

## **CHAPTER FOUR**

# **NMR INVESTIGATION OF THE UREA FORMALDEHYDE REACTION**

## 4.1 INTRODUCTION

$^{13}\text{C}$  NMR has been used extensively to characterise final UF resins (eg commercial products), both qualitatively and quantitatively. However few reports have appeared concerning the use of the  $^{13}\text{C}$  NMR technique to monitor the UF reaction process. One of the main difficulties to be overcome in the application of the NMR technique to real time experiments is the low sensitivity of the NMR method (compared with other techniques such as infrared spectrometry). At the outset of this investigation, the conventional wisdom was that it would take 10-20 min to obtain a moderate signal to noise (S/N) ratio qualitative spectrum, and > 1-2 h to obtain a quantitative spectrum with complete relaxation between pulses.

In this research,  $^{13}\text{C}$  NMR technique was used to investigate the UF reaction process using the dynamic (RAPID) NMR data acquisition method described in Section 2.1.4 Chapter 2, and evaluated in Chapter 3. The integrals of each peak, or each cluster of peaks, were determined for the chemical shift ranges listed in Table 3.3 (Chapter 3). Integrals are expressed in arbitrary units (au) proportional to species concentration.

## 4.2 PRELIMINARY INVESTIGATIONS USING THE DYNAMIC (RAPID) NMR EXPERIMENT

In order to demonstrate the usefulness of the dynamic (RAPID) NMR experiment for monitoring changes in transient species during UF resin production, the method was applied to an experimental UF resin produced using the following set of typical synthesis conditions:

- formaldehyde concentration = 46%
- F/U molar = 2.0
- temperature = 70°C
- initial addition pH = 8.8
- condensation pH = 5.0
- addition reaction time = 37.5 min.

NMR spectra obtained for this reaction system are presented in Figures 4.1 and Figure 4.2, respectively.

Filename: HYZH0500.001 Dynamic NMR expt  
addition stage: t=14.5 min

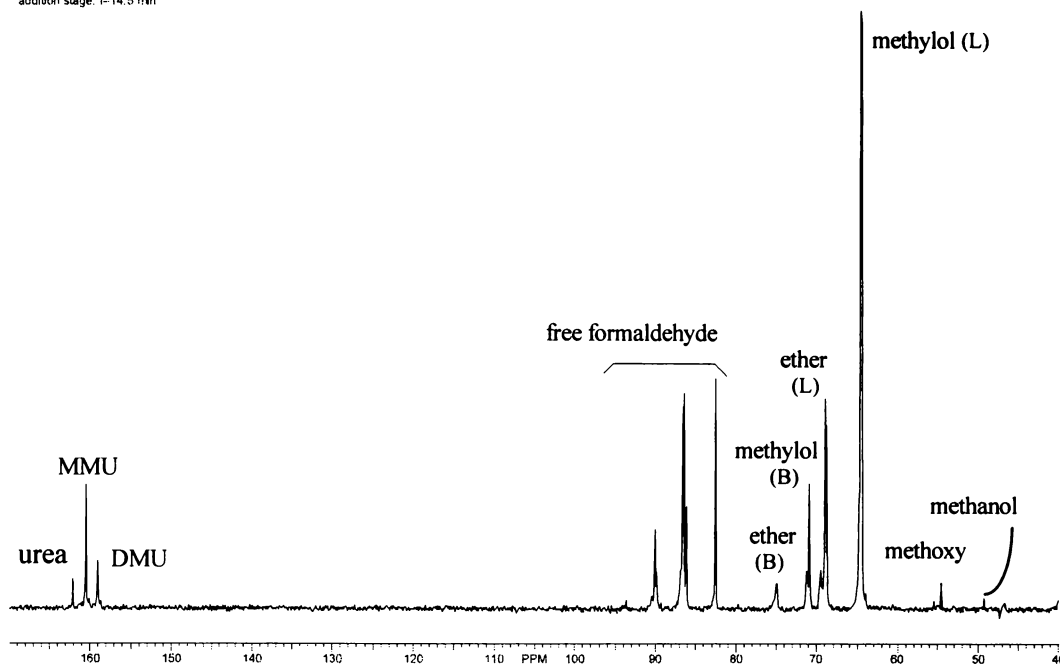


Figure 4.1. A typical dynamic (RAPID) NMR spectrum of an UF reaction system determined during the addition reaction stage.

L = linear species, B = branched species

Typically 13 to 14 clusters of peaks were observed in dynamic (RAPID) NMR spectra. Normally, methylol peaks were sharper, presumably due to their higher group mobility. Methylol groups, (-CH<sub>2</sub>OH) are located at the end of molecular chains, or as pendants within a molecular chain. Methylene and ether peaks were slightly broader than methylol peaks, presumably due to more restricted mobility, and to more varied minor positional differences within the molecular chain structures.

A more compressed set of spectra corresponding to different addition stage reaction times is presented in Figure 4.3. A set of spectra corresponding to different condensation times are presented in Figure 4.4.

## Chapter 4: NMR Investigation of the Urea Formaldehyde Reaction

Filename: HY240501.001 Dynamic NMR exp1  
condensation stage: tc = 8.7 min, t = 46.2 min

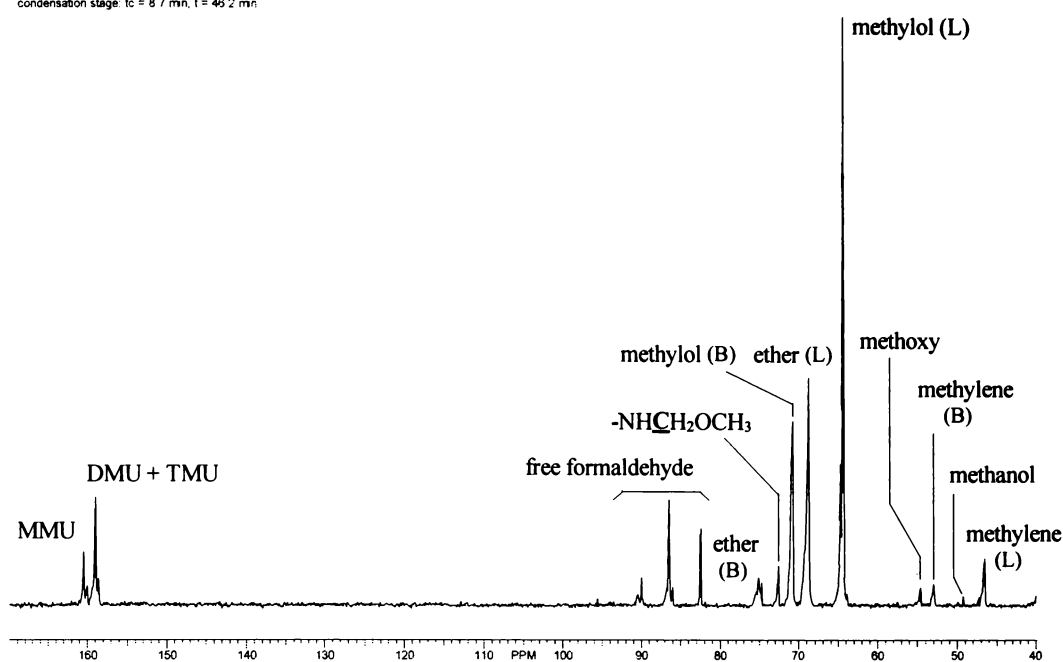


Figure 4.2. A typical dynamic (RAPID) NMR spectrum of an UF reaction system determined during the condensation reaction stage.

L = linear species, B = branched species

It is apparent from Figures 4.1 to 4.4 that the dynamic (RAPID) NMR technique can be used to identify key species present in the reaction system. In addition integration of the peak areas will allow changes in species levels to be monitored as reaction proceeds. Kinetic profiles of important species for different reaction conditions could thus be obtained.

## Chapter 4: NMR Investigation of the Urea Formaldehyde Reaction

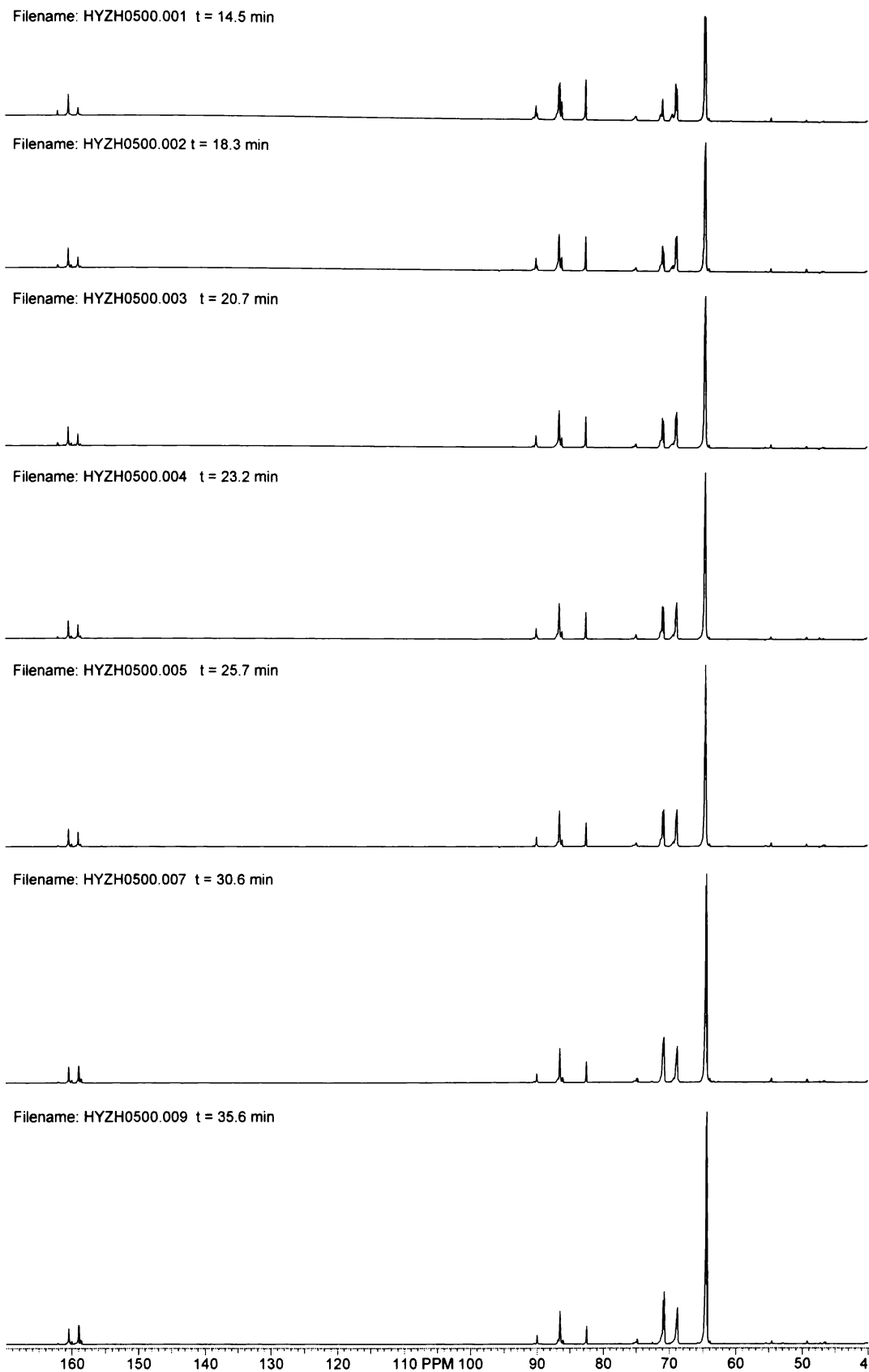
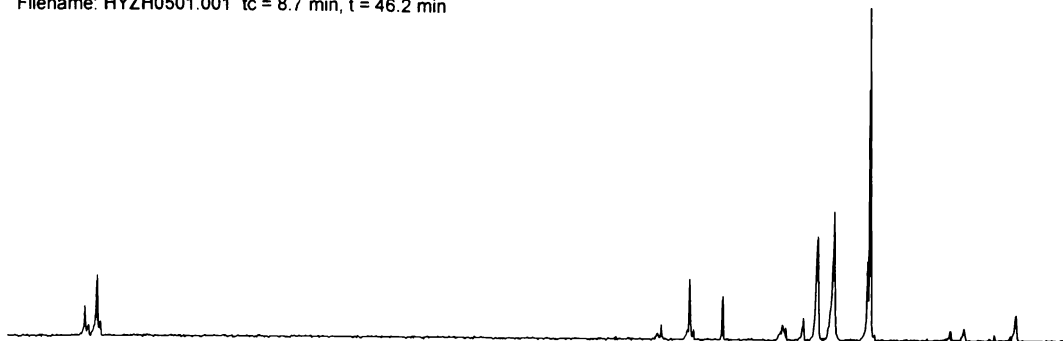


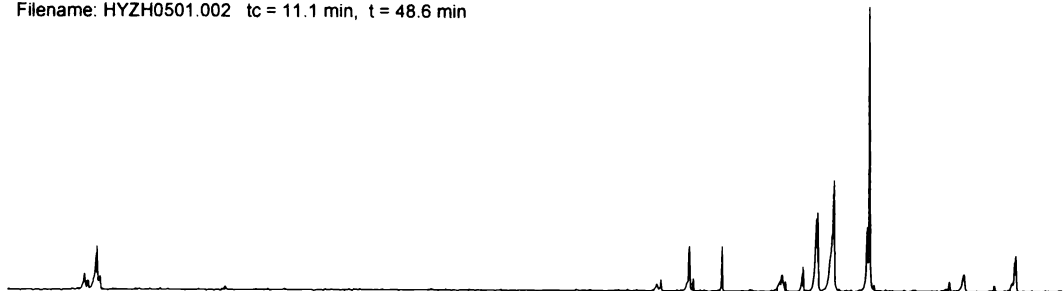
Figure 4.3. Dynamic (RAPID) NMR spectra determined for an UF reaction system during the addition stage.

## Chapter 4: NMR Investigation of the Urea Formaldehyde Reaction

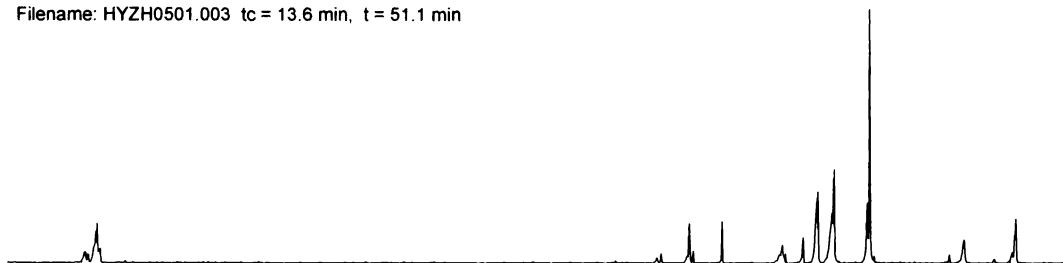
Filename: HYZH0501.001 tc = 8.7 min, t = 46.2 min



Filename: HYZH0501.002 tc = 11.1 min, t = 48.6 min



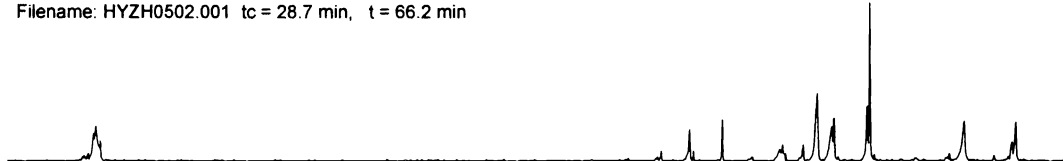
Filename: HYZH0501.003 tc = 13.6 min, t = 51.1 min



Filename: HYZH0501.007 tc = 18.6 min, t = 56.1 min



Filename: HYZH0502.001 tc = 28.7 min, t = 66.2 min



Filename: HYZH0502.004 tc = 46.2 min, t = 83.7 min



Filename: HYZH0502.013 tc = 98.5 min, t = 136.0 min

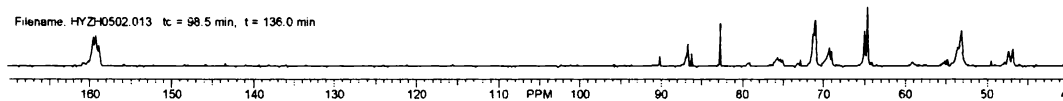


Figure 4.4. Dynamic (RAPID) NMR spectra determined for an UF reaction system during the condensation stage.

### **4.3 EFFECT OF REACTION CONDITIONS ON SPECIES KINETIC PROFILES**

The most important factors affecting the UF reaction process are formaldehyde concentration, F/U molar ratio, reaction temperature, reaction time (including both the addition reaction time and condensation reaction time (or total reaction time) and the initial addition stage and condensation stage pHs.

Methylene group formation contributes to the final cross-linked network, while ether groups are relatively unstable linkages in the resin system. Therefore, it is expected that a higher methylene group concentration and a lower ether concentration in the resin will yield better performance of the resin bonded wood products (ie high internal bond and low formaldehyde emission). The methylene to ether (Me/E) molar ratio has been correlated with the formaldehyde emission. It was found that the higher the Me/E molar ratio the lower the formaldehyde emissions (Szesztay *et al.* 1994).

These studies had the aim of determining reaction conditions for the urea formaldehyde reaction that would yield resins with minimal formaldehyde emissions, minimum water swell and maximum internal bond of wood products.

#### **4.3.1 Effect of Reaction Temperature**

The effect of reaction temperature on free urea, free formaldehyde, methylol, methylene and ether species is shown in Figures 4.5 to 4.14. The conditions common to all the experiments in this section are: formaldehyde concentration = 46%, F/U molar ratio = 2.0, initial addition pH = 8.7-8.8, condensation pH = 5.0.

##### *Free urea and formaldehyde*

It is apparent (see Figure 4.5) that the higher the reaction temperature, the more rapidly free urea diminishes. Normally free urea is not detectable during the condensation stage if the reaction temperature is 80°C, or higher.

It is also apparent (see Figure 4.6) that the higher the reaction temperature, the faster the reaction rate and disappearance of free formaldehyde. However, during the condensation stage, free formaldehyde remains approximately constant at a level of about 0.5 au, implying a steady state was reached. The reaction temperature has more effect on the reaction rate than on the free formaldehyde level. During the late condensation reaction stage, the free formaldehyde level may increase due to the formation of branching networks and release of formaldehyde. Gelation of the resin may occur if the reaction is not stopped.

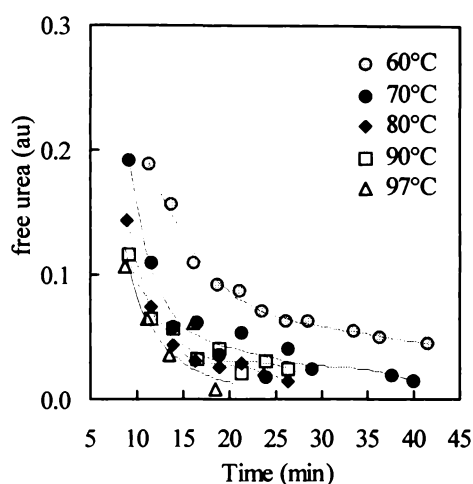


Figure 4.5. Plots of the effect of reaction temperature on free urea levels vs reaction time during the addition stage.

The 60°C reaction is especially slow (see Figure 4.5). Because of the slow reaction rate, the 60°C reaction had not progressed to completion. However at 97°C the reaction rate is excessively fast. Free formaldehyde starts to increase after about 30 min of the condensation reaction. This is indicative of impending gelation. The optimum reaction temperature for minimal free formaldehyde appears to be in the range 80-90°C.

### *Methylol groups*

It can be seen from Figure 4.7 that the reaction temperature has a large effect on the rate of reaction and the maximum level of methylol groups. For example, it takes

more than 40 min for methylol groups to reach a maximum level of about 4.6 au at 60°C whereas the maximum of 5.5 au is reached in only 13-15 min at 97°C. The methylol group level is greatest for the reactions carried out between 80 and 90°C (see Table 4.1).

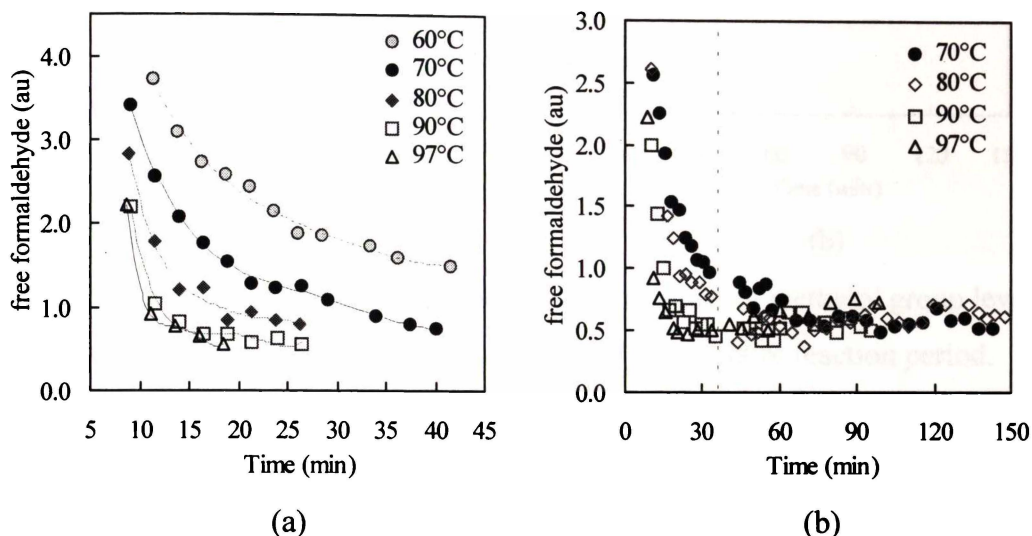


Figure 4.6. Plots of the effect of reaction temperature on free formaldehyde levels vs reaction time during (a) the addition stage and (b) the entire reaction period.

During the late condensation stage, the final methylol group level of the 70°C reaction is greater than those of observed for the 80, 90 and 97°C reactions indicating a lower conversion to methylene groups.

While there are significant differences in methylol group profiles during the addition stages of the 80, 90 and 97°C reactions, generally comparable levels of methylol groups are present during the condensation stage.

Table 4.1. The effect of reaction temperature on the time required for a maximum methylol group level ( $t_p$ ) to be achieved and the corresponding maximum ( $I_p$ ).

temperature (°C)	60	70	80	90	97
$I_p$ (au)	≈ 4.6	5.7	6.1	6.0	5.5
$t_p$ (min)	> 40	30-35	20-25	15-17	13-15

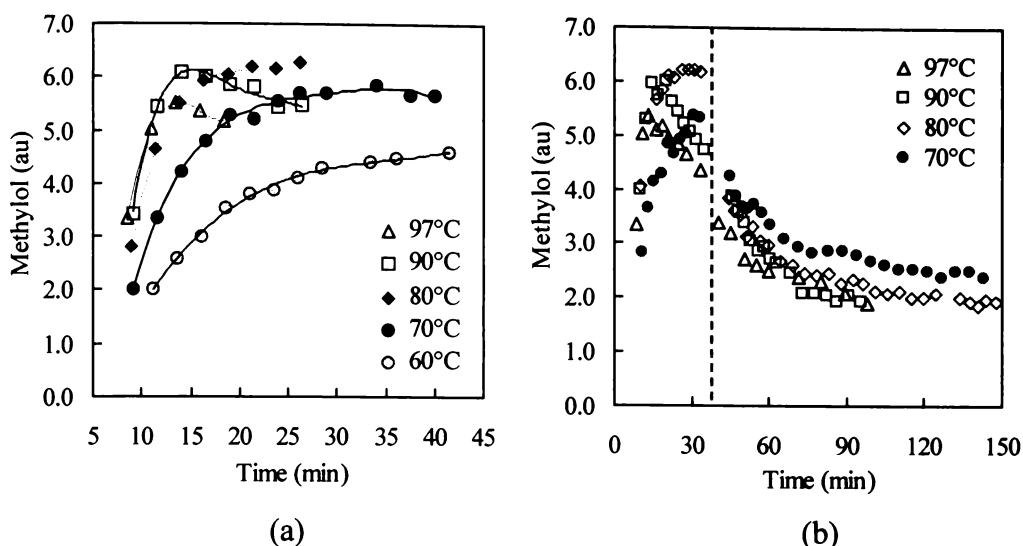


Figure 4.7. Plots of the effect of reaction temperature on methylol group levels vs reaction time for (a) the addition stage and (b) the entire reaction period.

### Methylene groups

The results presented in Figure 4.8 indicate that high reaction temperatures favour the formation of methylene groups. The rate of methylene group formation is very slow during the addition stage for reactions performed at 60 and 70°C.

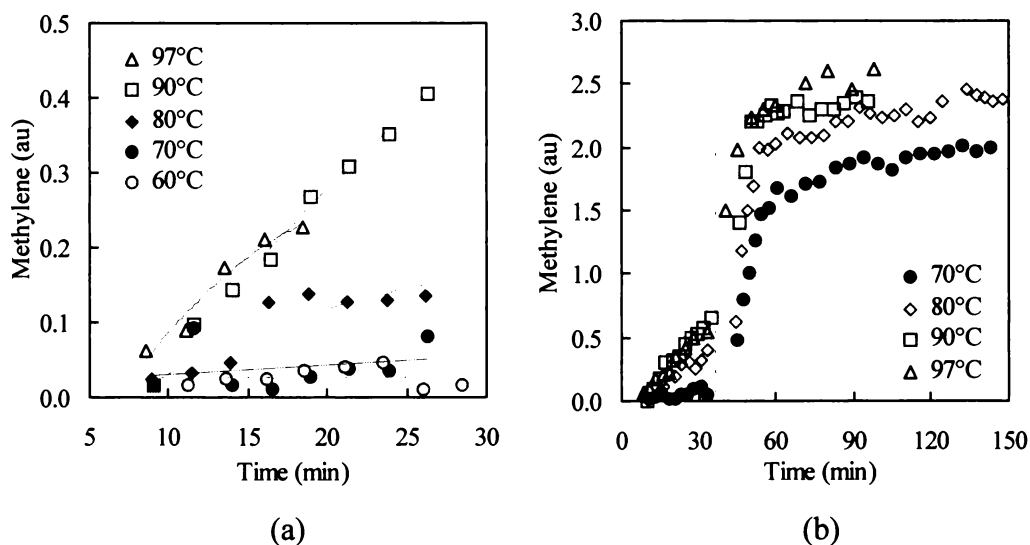


Figure 4.8. Plots of the effect of reaction temperature on methylene group levels vs reaction time during (a) the addition stage and (b) the entire reaction period.

The condensation reaction rate increases with temperature. The maximum methylene group level achieved in the 70°C reaction is lower than those for the 80, 90 and 97°C reactions. Maximum methylene group levels increase slightly with temperature in the order: 97°C > 90°C > 80°C.

### *Ether groups*

Reaction temperature has a dramatic effect on the level of ether species. At reaction temperatures greater than 80°C, ether group levels increase with time during the addition stage (Figure 4.9). At reaction temperatures below 80°C, little increase is observed after about 7 min of addition reaction.

Unfortunately, it is not possible to monitor ether group levels during the first 5-7 minutes of the polymerisation process by the NMR method. Several minutes are required to make the UF reaction mixture, set up the reaction system in a NMR tube, transfer it to the spectrometer, shim the sample and acquire the first FID data set. Hence early time points are not available.

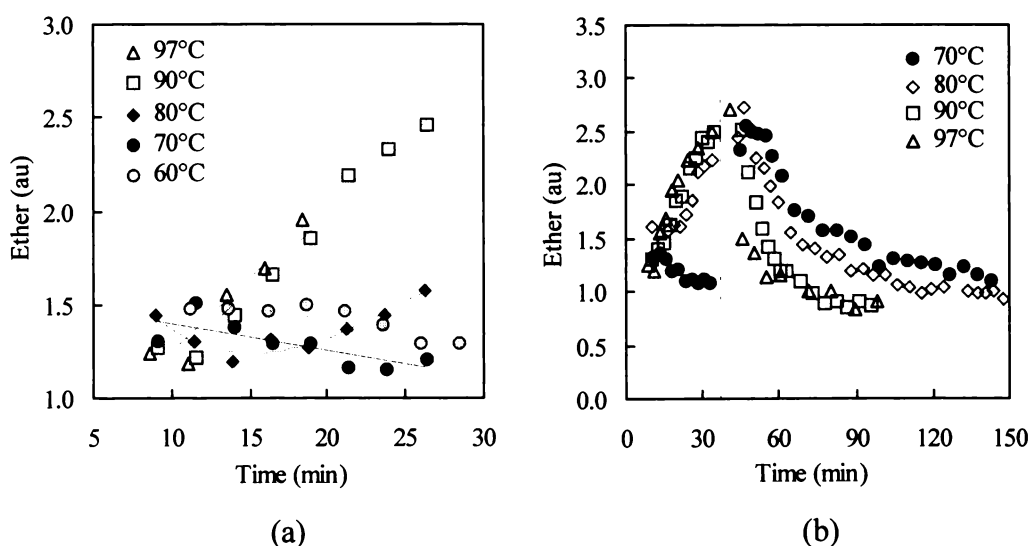


Figure 4.9. Plots of the effect of reaction temperature on ether group levels vs reaction time during (a) the addition stage and (b) the entire reaction period.

During the condensation stage, after reaching their maximum, ether group levels of higher temperature reactions diminish more rapidly than is the case for lower temperature reactions. That is, the higher the reaction temperature, the higher the ether group dissociation rate and the lower the final ether group level remaining in the late condensation stage.

The relationship between the methylene to ether (Me/E) group ratio, reaction temperature and reaction time is shown in Figure 4.10. The higher the reaction temperature, the greater the Me/E group ratio. Therefore, it can be anticipated that a resin prepared at a higher temperature (eg 90°C) will have lower formaldehyde emissions than a resin prepared at a lower temperature (eg 70°C).

Since many of the polymerisation reactions are reversible and competitive, equilibria exist among the reactions. Reaction temperature appears to affect both reaction rates and equilibria between species. The most favourable reaction temperature for resin production appears to be in the range 80-90°C, since the 60 and 70°C reactions proceed too slowly, while the 97°C reaction proceeds so rapidly that control may be difficult.

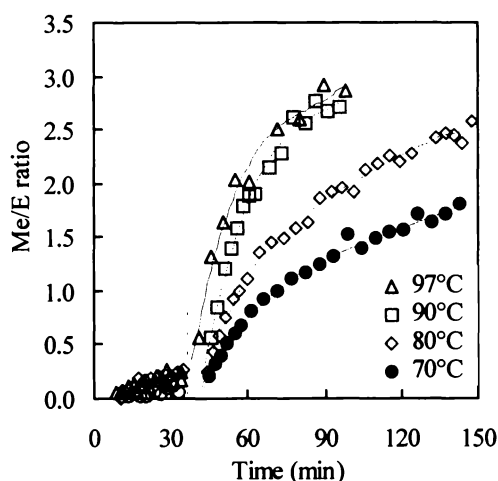


Figure 4.10. Plots of the effect of reaction temperature on the methylene to ether (Me/E) group ratio vs reaction time.

Further experiments at 82, 85 and 88°C were performed in order to gain a better understanding of variations in resin characteristics over this region.

No significant differences in free urea and free formaldehyde levels were observed for these reactions. Reaction profiles for methylol, methylene and ether groups at 82, 85 and 88°C are shown in Figures 4.11 to 4.13.

Reaction temperatures in the range 82-88°C had little effect on methylol group levels. However, some differences were apparent in methylene and ether group levels. High temperature (88°C) was found to favour the formation of both methylene and ether groups during the addition stage and the dissociation of ether groups during the condensation stage (Figure 4.12 and 4.13). Generally, the Me/E group ratio increases with temperature up to 88°C (Figure 4.14). Reaction temperatures higher than 88°C has little effect on the Me/E group ratio (see Figure 4.14).

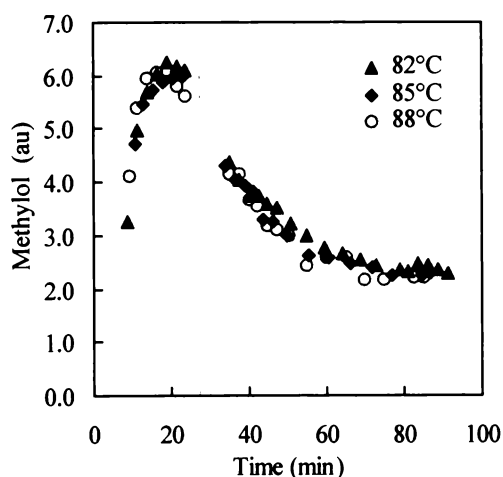


Figure 4.11. Plots of the effect of reaction temperature on methylol group levels vs reaction time.

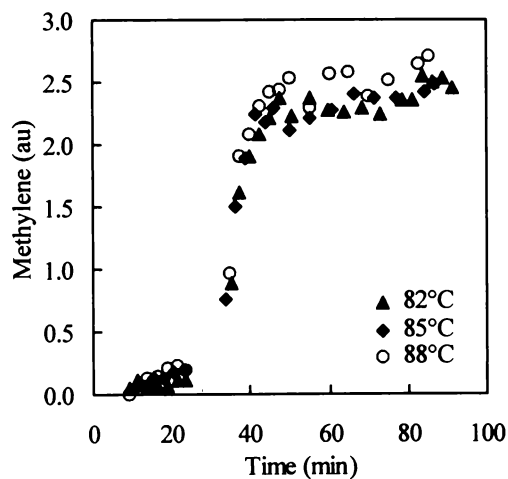


Figure 4.12. Plots of the effect of reaction temperature on methylene group levels vs reaction time.

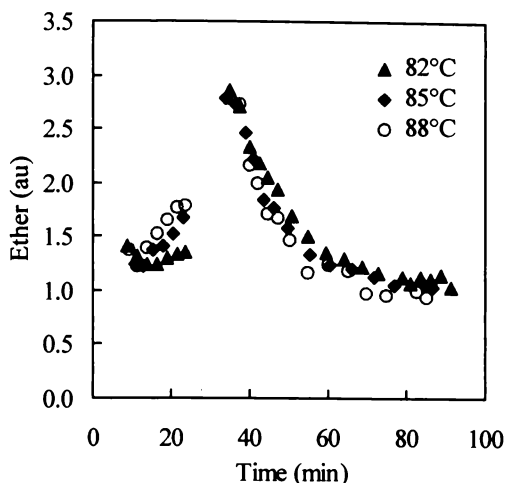


Figure 4.13. Plots of the effect of reaction temperature on ether group levels vs reaction time.

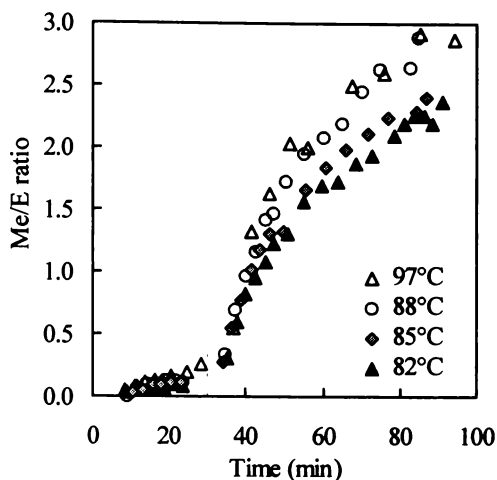


Figure 4.14. Plots of the effect of reaction temperature on the Me/E group ratio vs reaction time.

### Conclusions

Based upon the data obtained using the dynamic (RAPID) NMR technique, the optimum polymerisation temperature seems to be about 88°C. This is the minimum temperature at which high Me/E group ratio can be obtained under conditions where gelling (losing control of the reaction) is unlikely to be a problem (see Figure 4.14).

#### 4.3.2 Effect of Addition Reaction Time

The traditional method of UF resin production utilises a two stage process, ie an alkaline addition reaction stage followed by an acidic condensation reaction stage. During the alkaline addition stage, methylolurea species (eg MMU, DMU and TMU) are formed. These species react during the condensation stage to give methylene groups (the dominant linkage units in UF resins).

Conditions common to all of the experiments described in this section are: F/U molar ration = 2.0, formaldehyde concentration = 46%, initial addition pH = 8.7 and condensation pH = 5.0.

*Free urea and free formaldehyde*

The addition stage reaction was monitored for a range of addition reaction times ( $t_a$ ). All the data for free urea fitted the same curve as expected (see Figure 4.15). Free urea was generally undetectable after 30-40 min of addition reaction (see Figure 4.15).

The effect of  $t_a$  on free formaldehyde levels during the addition and condensation stage is shown in Figure 4.16. In this, and subsequent plots, the condensation stage time is measured from the time acid was added (pH = 5.0) to initiate the condensation stage reaction. Hence, the total reaction time ( $t$ ) is the sum of the addition stage ( $t_a$ ) and condensation stage ( $t_c$ ) reaction times: ie  $t = t_a + t_c$ .

Since free formaldehyde levels decrease with time during the addition stage, it follows that if  $t_a$  is too short, for the chosen reaction temperature, residual free formaldehyde will be present at the end of the addition stage and during the early condensation stage (Figure 4.16).

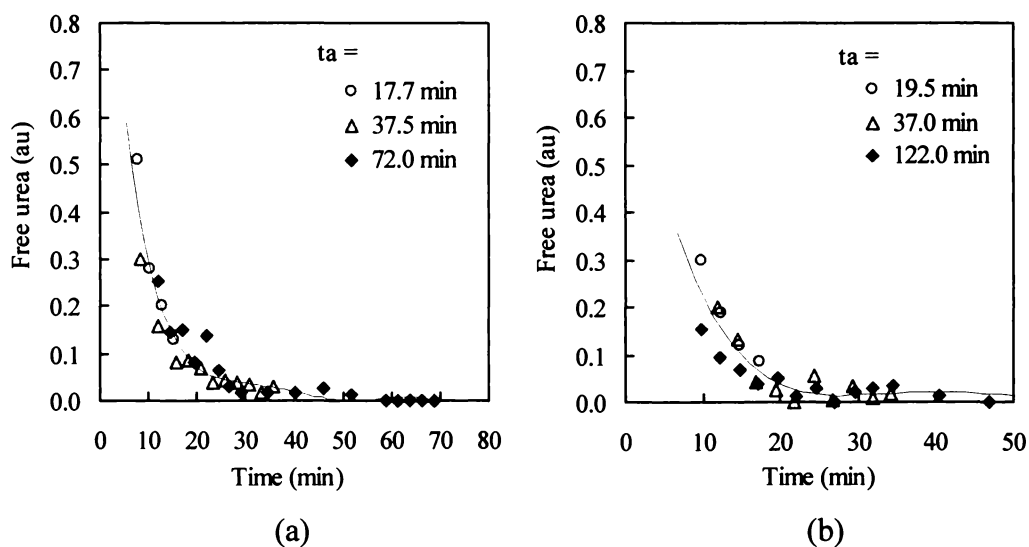


Figure 4.15. Plots of the effect of the addition reaction time ( $t_a$ ) on free urea levels vs reaction time for reactions performed at (a) 70°C and (b) 80°C.

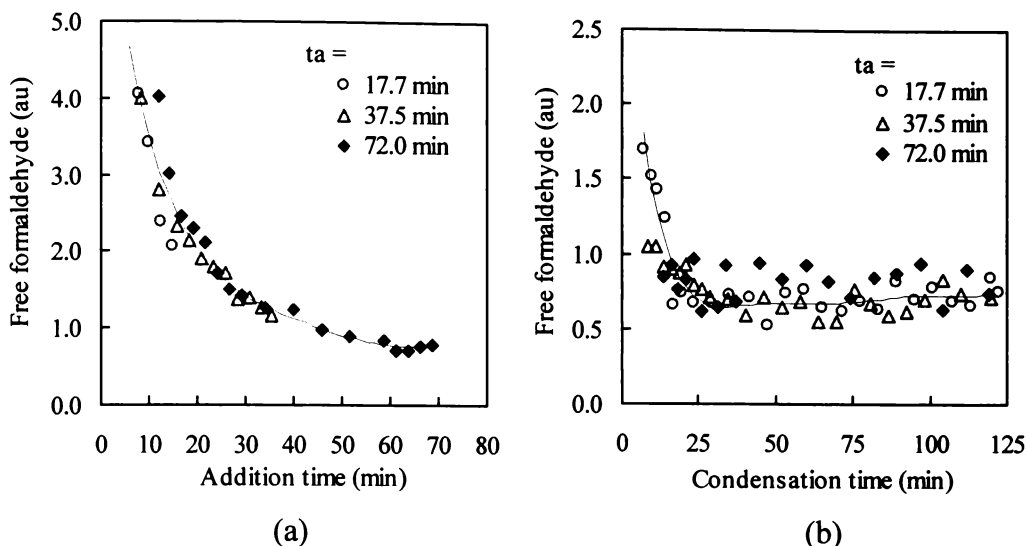


Figure 4.16. Plots of the effect of addition reaction time ( $t_a$ ) on free formaldehyde levels vs reaction time during (a) the addition stage and (b) the condensation stage for a reaction performed at 70°C.

If however a longer addition stage time  $t_a$  is employed, free formaldehyde decreases to a relatively constant level ( $c$  0.5-0.8 au) during the addition stage and does not change during the condensation stage (see Figures 4.16 and 4.17).

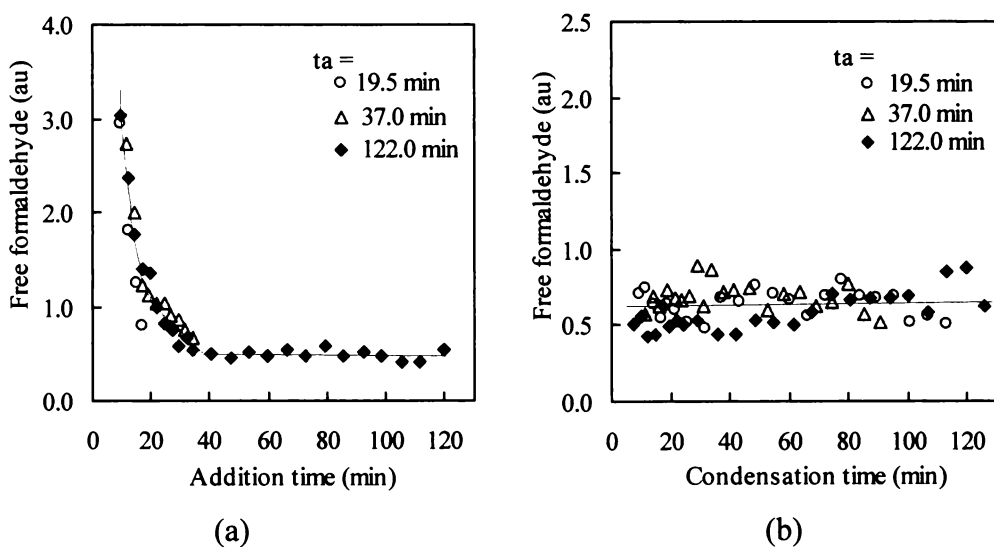


Figure 4.17. Plots of the effect of the addition reaction time ( $t_a$ ) on free formaldehyde levels vs reaction time during: (a) the addition stage and (b) the condensation stage for a reaction performed at 80°C.

*Methylol groups*

The effects of  $t_a$  on the methylol group profiles for 70°C and 80°C reactions are shown in Figures 4.18 and 4.19. The maximum methylol group level is achieved after an addition stage reaction time of 30-35 min for the 70°C reaction, and about 25 min for the 80°C reaction (see Table 4.1).

Values of  $t_a$ s greater than 30-35 min (for the 70°C reaction) or 25 min (for the 80°C reaction) have little effect on methylol group levels. Lower  $t_a$ s result in lower methylol group levels throughout the condensation stage.

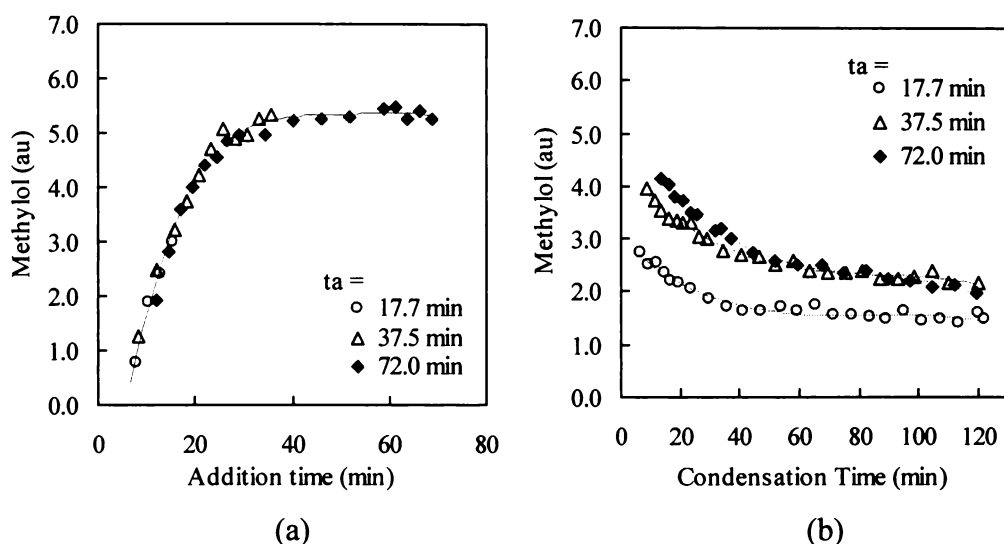


Figure 4.18. Plots of the effect of addition reaction time ( $t_a$ ) on methylol group levels vs reaction time during (a) the addition stage and (b) the condensation stage for the reaction at 70°C.

*Methylene groups*

The effects of  $t_a$  on the methylene group profiles are shown in Figures 4.20 and 4.21. Methylene group levels always increase with time during the addition stage. However, most of the methylene is formed in the condensation stage. Methylene groups formed during the addition stage have no significant effect on methylene group formation during the condensation stage.

The lower levels of methylol groups formed during the addition stage resulted in lower methylene group formation rates and levels during the condensation stage (see Figures 4.20 and 4.21).

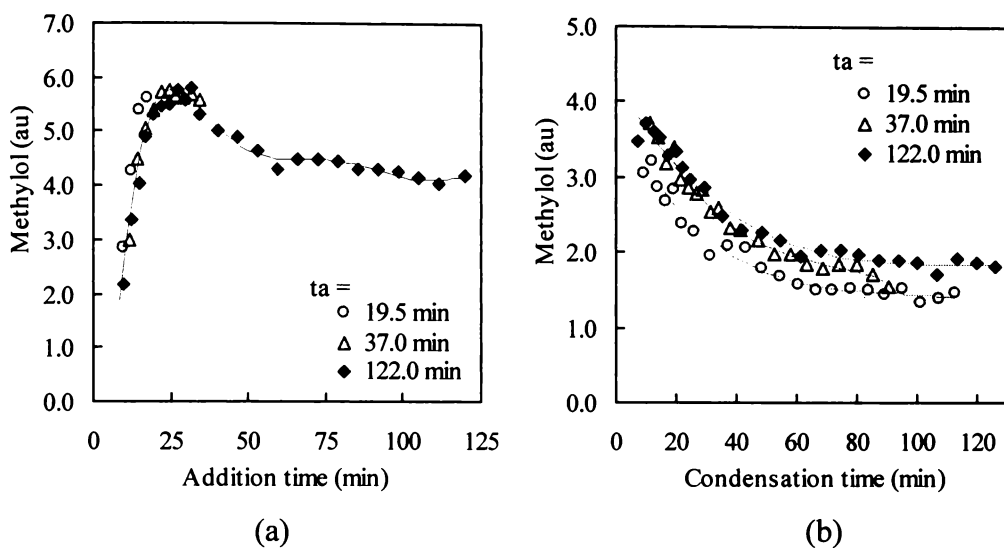


Figure 4.19. Plots of the effect of addition reaction time ( $t_a$ ) on methylol group levels vs reaction time during (a) the addition stage and (b) the condensation stage for the reaction at 80°C.

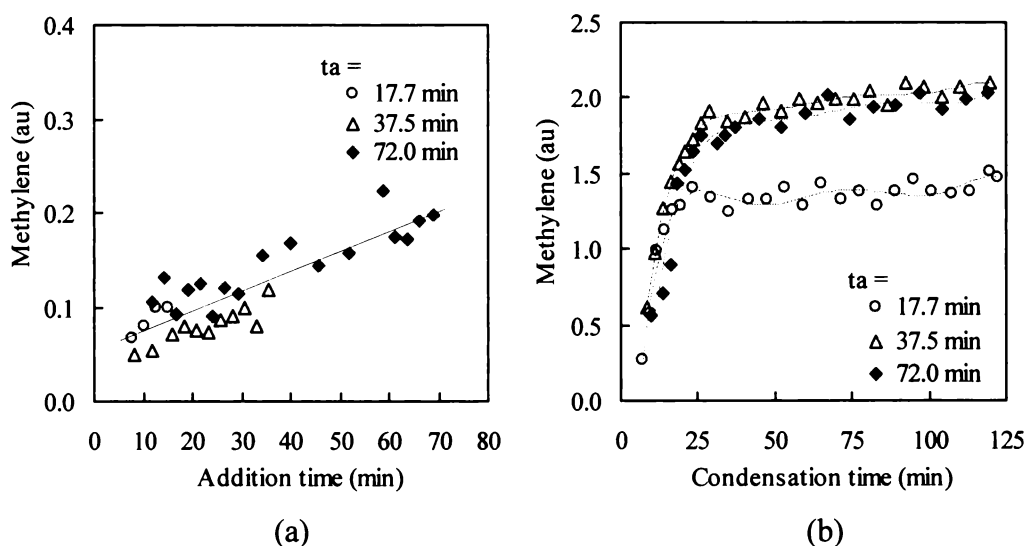


Figure 4.20. Plots of the effect of addition reaction time ( $t_a$ ) on methylene group levels vs reaction time during (a) the addition stage and (b) the condensation stage for the reaction at 70°C.

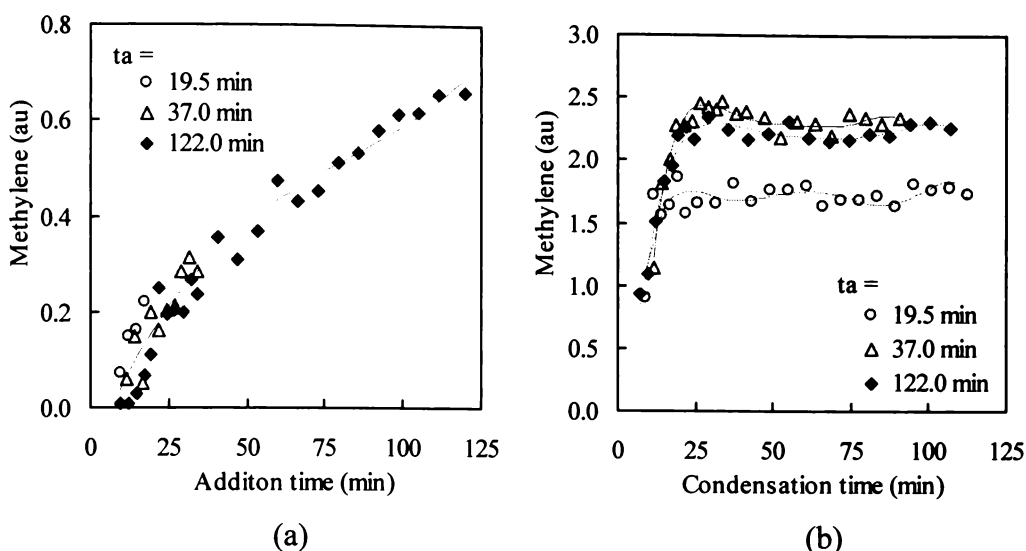


Figure 4.21. Plots of the effect of addition reaction time ( $t_a$ ) on methylene group levels vs reaction time during (a) the addition stage and (b) the condensation stage for the reaction at 80°C.

### *Ether groups*

The effects of  $t_a$  on ether group profiles are shown in Figures 4.22 and 4.23. It is apparent that  $t_a$  has little effect on ether group levels for  $t_a$ s greater than 25 min at 80°C or 30-35 min at 70°C. At shorter  $t_a$  times, ether group levels during the condensation stage were lower.

Since ether groups are formed from the condensation of two methylol molecules, the methylol group concentration would be expected to influence the rate at which ether groups are formed. The comparatively low level of ether groups present during the condensation stage of the reaction performed using a short addition stage (17.7 min) is a consequence of the low level of methylol groups formed during the addition stage.

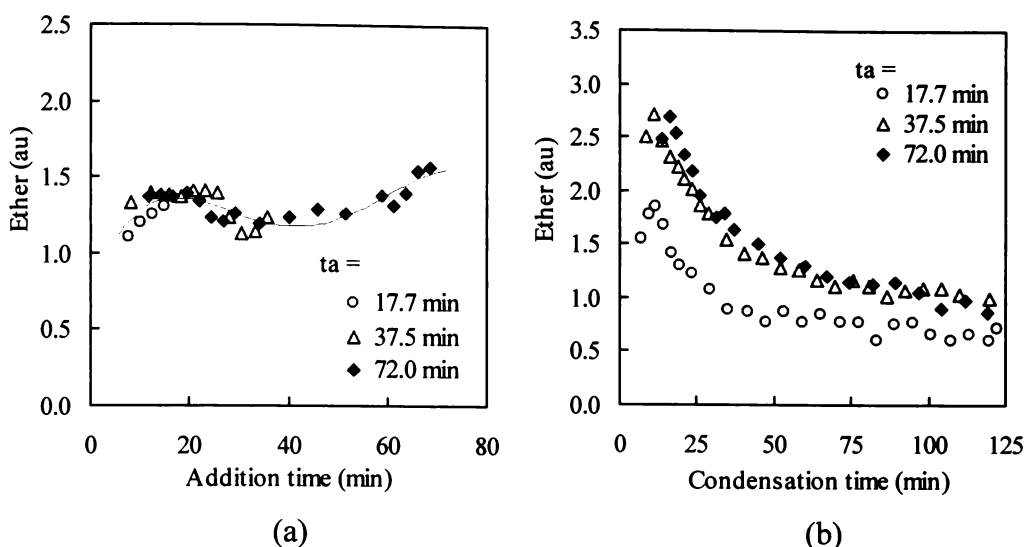


Figure 4.22. Plots of the effect of addition reaction time ( $t_a$ ) on ether group levels vs reaction time during (a) the addition stage and (b) the condensation stage for the reaction at 70°C.

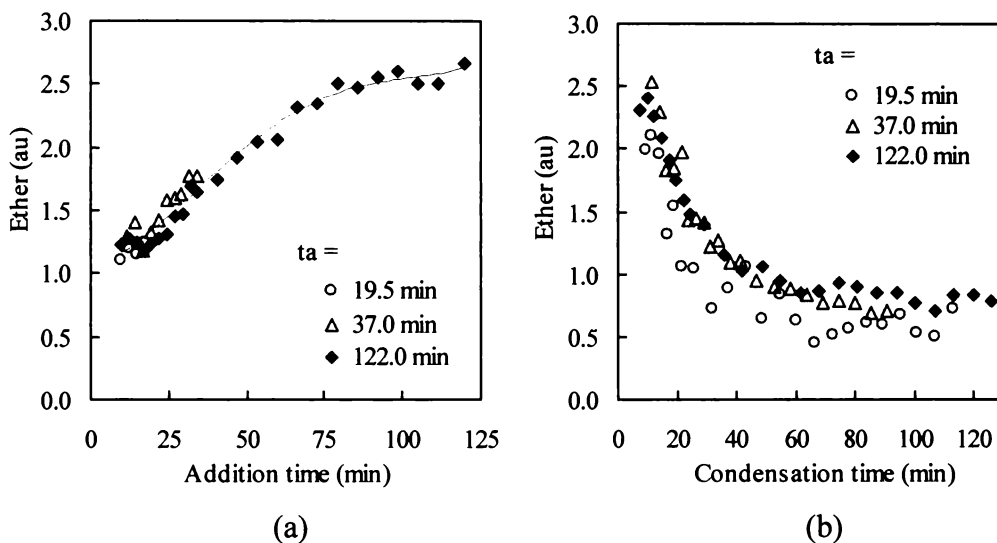


Figure 4.23. Plots of the effect of addition reaction time ( $t_a$ ) on ether group levels vs reaction time during (a) the addition stage and (b) the condensation stage for the reaction at 80°C.

### Summary and conclusions

Addition stage reaction time ( $t_a$ ) mainly affects the formation of methylol groups. If  $t_a$  is longer than the time necessary for methylol groups to reach their maximum

level for the chosen set of reaction conditions (eg reaction temperature), it has negligible effect on methylol, methylene and ether group levels during the condensation stage.

If  $t_a$  is shorter than the time required for methylol groups to reach their maximum level, lower concentrations of methylene groups are found during the condensation stage.

A  $t_a$  longer than the time necessary for methylol groups reach their maximum level for the chosen set of reaction conditions offers no advantage.

The optimum  $t_a$  period is the time required for methylol groups to reach the maximum level for the chosen reaction temperature. For the proposed optimum reaction temperature of 88°C, the optimum  $t_a$  period is predicted to be 25-30 min.

### **4.3.3 Effect of Formaldehyde Concentration**

Commercial formaldehyde is available as a 37-50% by weight aqueous formaldehyde solution. The influence of formaldehyde concentration on UF resin polymerisation reactions is reported below.

Conditions common to all of the experiments described in this section are: reaction temperature = 88°C, F/U molar ratio = 2.0, initial addition pH = 8.7 and condensation pH = 5.0.

#### *Methylol groups*

The effect of formaldehyde concentration (in the range 20 to 45%) on methylol group profiles during the addition stage is shown in Figures 4.24 and 4.25. It is clear that:

- 1) Methylol reaction profiles are similar in shape.

- 2) Methylol group levels in the reaction mixture vary with formaldehyde concentrations. A low initial formaldehyde concentration means less urea is added (to satisfy the condition  $F/U = 2.0$ ) and more water is present. Hence there is a reduction in the concentration of derived methylol groups (see Table 4.2).
- 3) The time required to achieve the maximum methylol group level ( $t_p$ ) increases as the formaldehyde concentration decreases (see Table 4.3).
- 4) Linear and branched methylol group profiles are similar to those observed for total methylol groups.
- 5) Initial formaldehyde concentration affects the linear to branched (L/B) methylol group ratio (see Table 4.4). It is apparent (see Table 4.4) that the L/B methylol group ratio increases as the initial formaldehyde concentration decreases. For example, the reaction performed using 45% formaldehyde solution gave a L/B methylol group ratio of 2.62, while at 20% formaldehyde solution the ratio was 3.05. Higher formaldehyde concentrations favour the formation of branched methylol species (lower L/B methylol group ratio).

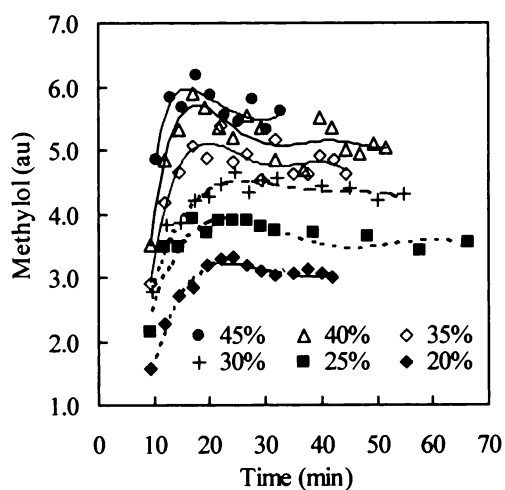


Figure 4.24. The effect of formaldehyde concentration on methylol group levels during the addition stage.

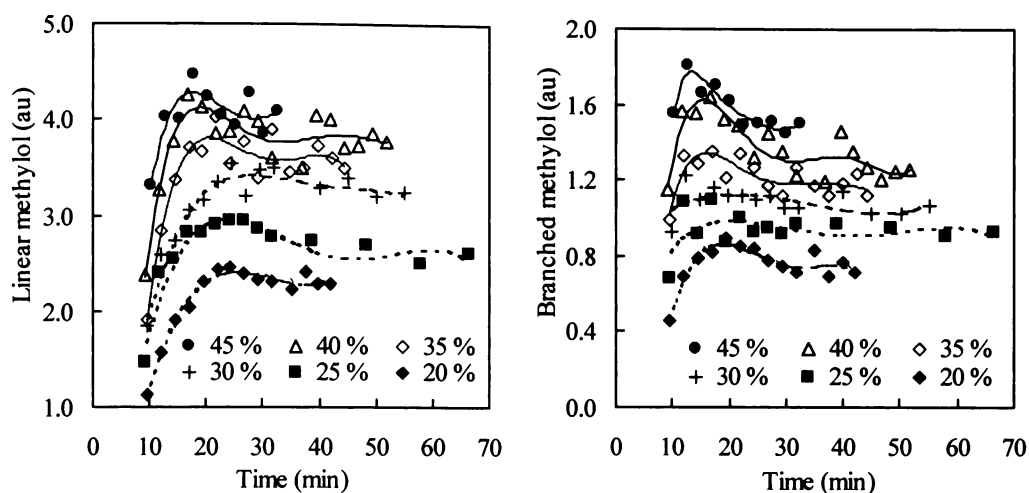


Figure 4.25. The effect of formaldehyde concentration on linear methylol and branched methylol group levels during the addition stage.

Table 4.2. Composition of UF mixtures used for dynamic NMR experiments.

F conc (%)	F wt (g)	total F		urea		UF mixture <sup>a</sup> (g)	F% <sup>b</sup>	water (g)
		(g)	(mole)	(g)	(mole)			
20	10.44	2.09	0.0695	2.09	0.0348	12.5	16.7	8.35
25	10.57	2.64	0.0880	2.64	0.0440	13.2	20.0	7.93
30	10.69	3.21	0.107	3.21	0.0534	13.9	23.1	7.48
35	10.91	3.82	0.127	3.82	0.0636	14.7	25.9	7.09
40	11.06	4.42	0.147	4.42	0.0736	15.5	28.9	6.63
45	11.10	5.00	0.166	5.00	0.0832	15.0	33.3	6.11

<sup>a</sup> UF mixture = weight of 10 mL of formaldehyde solution and the urea used in preparation the UF reaction mixture; <sup>b</sup> F% = percentage of formaldehyde in the UF reaction mixture.

Table 4.3. The effect of formaldehyde concentration (F conc) on the time ( $t_p$ ) required to achieve a maximum methylol group level.

F conc (% w/w)	45	40	35	30	25	20
$t_p$ (min)	15.5	17.0	18.2	24.5	24.1	24.5

The effect of initial formaldehyde concentration over the 25-45% range on methylol group profiles during the entire reaction period is shown in Figure 4.26.

It can be seen that while methylol group levels increase with formaldehyde concentration, the differences between methylol group levels are reduced during the condensation stage. This is because reactions with higher formaldehyde concentrations proceed at faster rates (to give methylene species) during the early condensation stage (*c* 10 min). After > 10 min condensation the methylol group levels are similar. More methylol groups react to form methylene groups in reaction systems with higher initial formaldehyde concentration reactions.

Table 4.4. Effect of formaldehyde concentration on methylol group levels and the ratio of linear to branched methylol group levels.

F conc. (% w/w)	45	40	35	30	25	20
Linear methylol (L)	4.33	4.20	3.90	3.44	2.93	2.44
Branched methylol (B)	1.65	1.58	1.30	1.11	0.95	0.80
L/B integral ratio	2.62	2.66	3.00	3.10	3.08	3.05

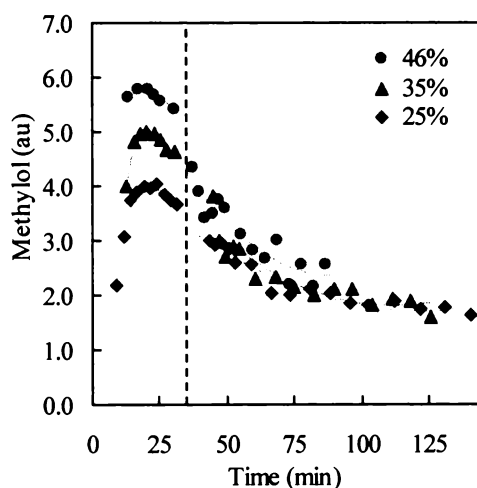


Figure 4.26. The effect of formaldehyde concentration on methylol group levels during the entire reaction period.

*Methylene groups*

The effect of formaldehyde concentration on methylene group profiles is shown in Figure 4.27. The higher the formaldehyde concentration, the greater the reaction rate and the higher the final methylene group level.

Since methylene groups are formed mainly during the condensation stage, methylene groups formed during the addition stage have little impact. Typically less than 15% of total methylene linkages are formed during the addition stage.

The results presented in Figure 4.27(b) show that the higher the formaldehyde concentration, the faster methylene groups are formed during the condensation stage (ie the curves shift towards the left with increasing formaldehyde concentration).

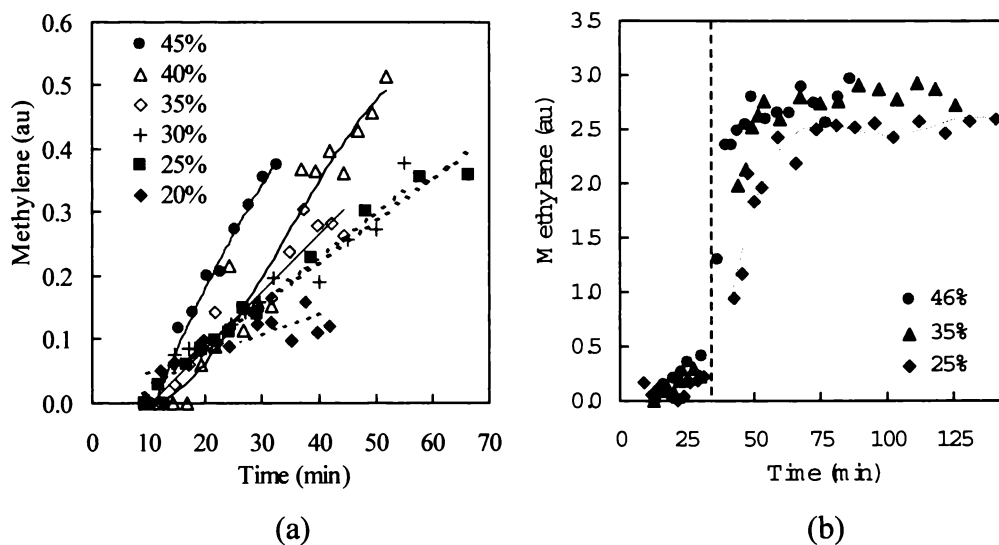


Figure 4.27. The effect of formaldehyde concentration on methylene group levels vs reaction time during (a) the addition stage and (b) the entire reaction period.

Also, the higher the formaldehyde concentration, the higher the final methylene group level. The differences in the reaction profiles for the 35% and 45% formaldehyde concentration reactions are not as great as those for the 35% and 25% formaldehyde concentration reactions. This finding indicates that a formaldehyde concentration of 35%, or greater, is desirable for the rapid production of maximum

levels of methylol groups during addition stage and methylene groups during condensation stage.

### *Ether groups*

The effect of formaldehyde concentration on ether group profiles is shown in Figure 4.28. As was the case for methylene groups, the higher the formaldehyde concentration, the higher the level of ether groups formed during the addition stage and the faster the rate at which ether groups are consumed during the early condensation stage.

The effect of formaldehyde concentration on the methylene to ether (M/E) group ratio is shown in Figure 4.29. The higher the formaldehyde concentration the lower the Me/E group ratio. This indicates that a high formaldehyde concentration will give a resin with more ether groups and may have higher formaldehyde emissions. However, lowering the formaldehyde concentration, lowers the overall reaction rate and the overall concentration of methylene groups, which is not desirable in a commercial environment.

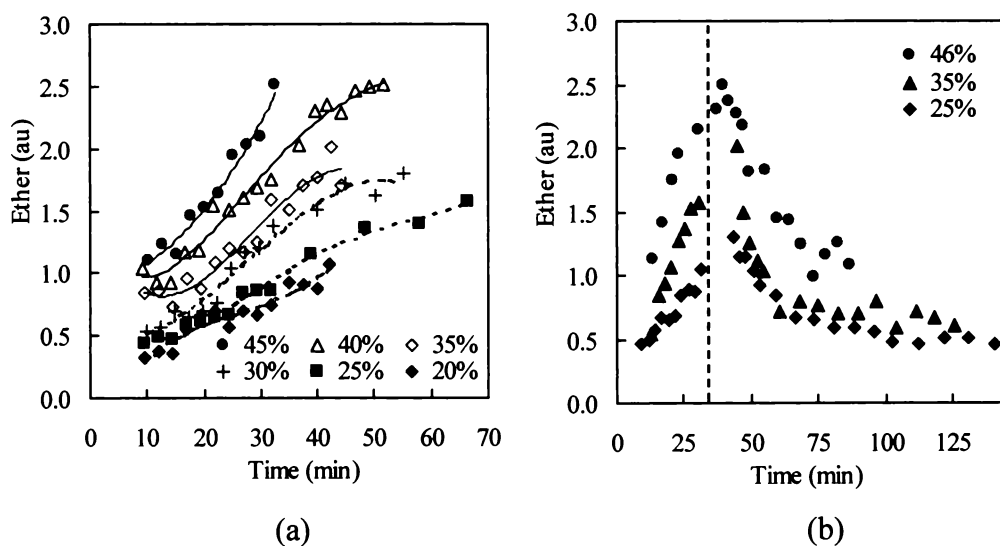


Figure 4.28. The effect of formaldehyde concentration on ether group levels vs reaction time during (a) the addition stage and (b) the entire reaction period.

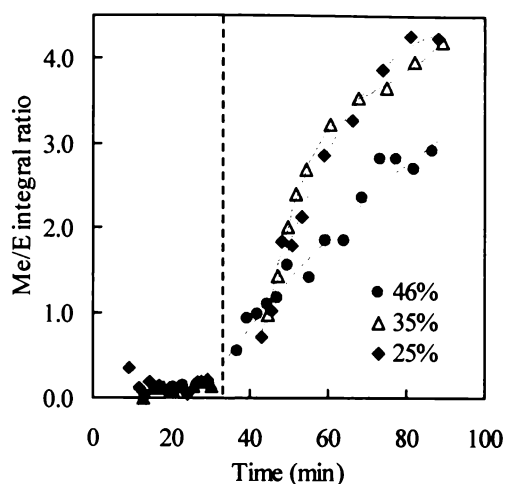


Figure 4.29. The effect of formaldehyde concentration on the methylene to ether (Me/E) group ratio.

### *Summary and conclusions*

A low formaldehyde concentration (25%) results in a higher Me/E group ratio and a slower reaction rate. A formaldehyde concentration of 35-46% is necessary to ensure an adequate reaction rate.

#### **4.3.4 Effect of F/U Molar Ratio**

The effect of variation in the F/U molar ratio over the range 1.6 to 2.4 was investigated. The conditions common to all the experiments in this section are: reaction temperature = 88°C, formaldehyde concentration = 45.2%, initial addition pH = 8.7 and condensation pH = 5.0. The preparation of the UF reaction samples and their ingredients are listed in Table 4.5.

#### *Free urea and free formaldehyde*

The effect of F/U molar ratio on the free formaldehyde level is shown in Figure 4.30. Reaction rate decreases and free formaldehyde increases with F/U molar ratio. Since the differences between the initial % formaldehyde content of the reaction mixtures are small (28.9% to 32.9%, see Table 4.5), the large differences in

formaldehyde levels (see Figure 4.30) cannot be attributed to variations in initial formaldehyde concentration. Rather, they must be a consequence of differing degrees of reaction of the formaldehyde species.

High F/U molar ratios lead to a low free urea level in the reaction system (see Figure 4.31).

Table 4.5. Composition of UF mixtures used for dynamic NMR experiments.

F/U ratio	F solu wt <sup>a</sup> (g)	total F		urea		UF mixture <sup>b</sup> (g)	F% <sup>c</sup> (w/w%)
		(g)	(mole)	(g)	(mole)		
1.6	11.14	5.04	0.168	6.30	0.105	17.44	28.9
1.8	11.14	5.04	0.168	5.60	0.093	16.74	30.1
2.0	11.14	5.04	0.168	5.04	0.084	16.18	31.2
2.2	11.14	5.04	0.168	4.58	0.076	15.72	32.1
2.4	11.14	5.04	0.168	4.20	0.070	15.34	32.9

<sup>a</sup> the weight of 10.0 mL of the formaldehyde solution (45.2%); <sup>b</sup> UF mixture is the weight of formaldehyde solution and urea; <sup>c</sup> F% is the percentage of the total formaldehyde in the UF mixture.

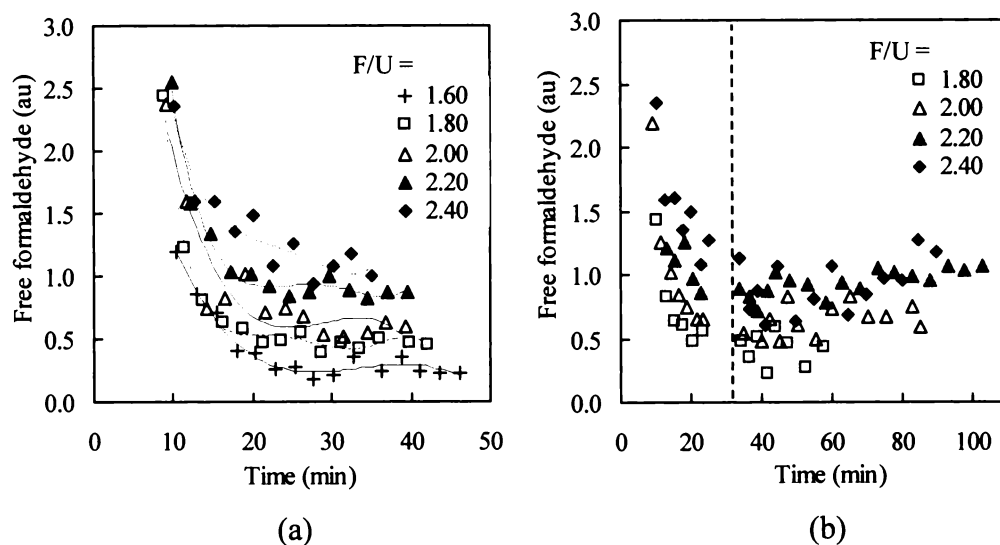


Figure 4.30. The effect of F/U molar ratio on free formaldehyde levels vs reaction time during (a) the addition stage and (b) the entire reaction period.

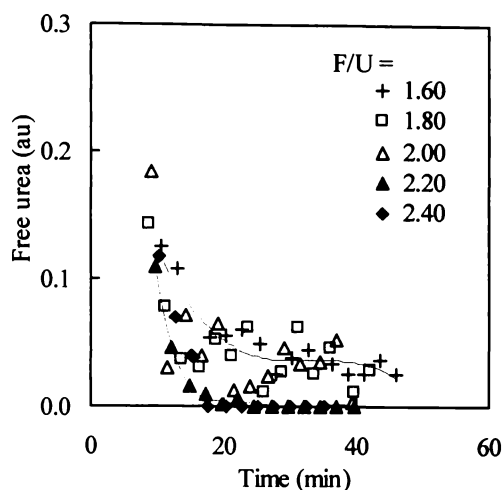


Figure 4.31. The effect of F/U molar ratio on free urea levels during the addition stage.

### *Methylol groups*

The effect of F/U molar ratio on the methylol group profiles is shown in Figure 4.32. Generally, the effect of the F/U molar ratio over the range 1.6 to 2.4 is not great.

From Figure 4.32 it can be seen that between F/U = 1.8 and 2.2, the F/U molar ratio has little effect on the methylol group level during both the addition stage and condensation stage. For reactions at both high and low F/U molar ratios, the methylol group levels are slightly lower than those determined for reactions with intermediate F/U ratios.

The maximum methylol group level appears earlier for the lower F/U molar ratio reactions and later for higher F/U molar ratio reactions. This suggests lower F/U molar ratios yield faster reaction rates.

### *Methylene groups*

The effect of F/U molar ratio on the methylene group profiles is shown in Figure 4.33. The lower the F/U molar ratio the higher the rate of methylene formation,

during both the addition stage and the condensation stage. It is clear that lower F/U molar ratios favour the formation of methylene species.

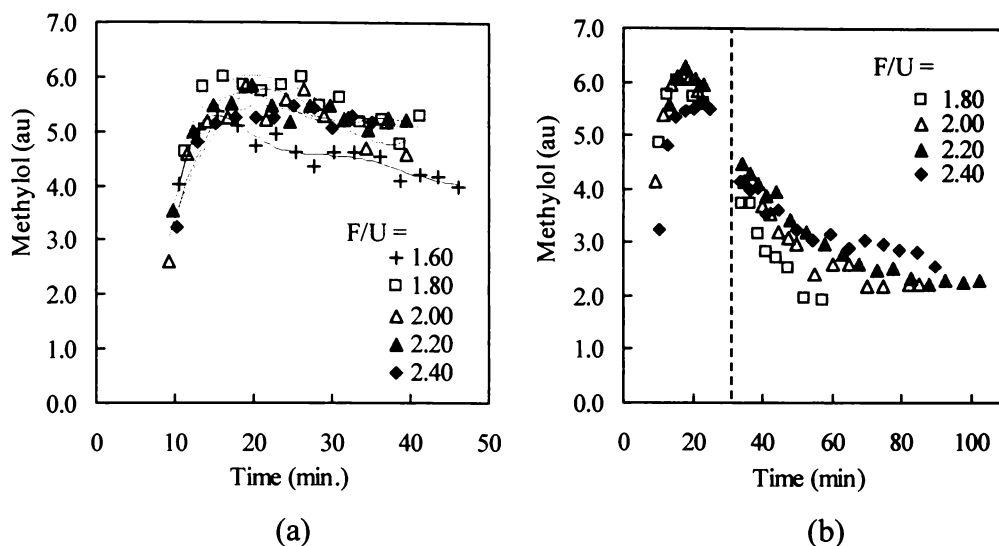


Figure 4.32. The effect of F/U molar ratio on methylool group levels vs reaction time during (a) the addition stage and (b) the entire reaction period.

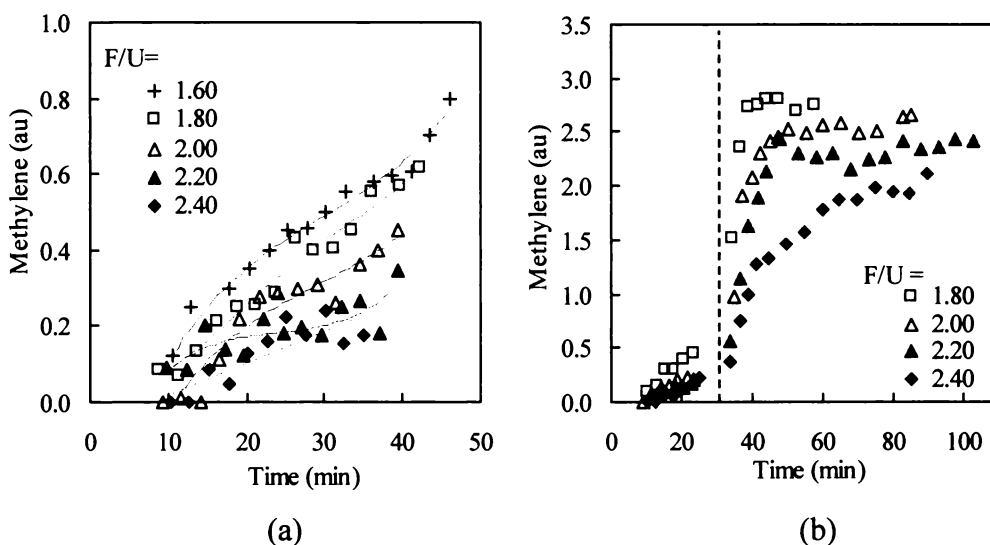


Figure 4.33. The effect of F/U molar ratio on methylene group levels vs reaction time during (a) the addition stage and (b) the entire reaction period.

*Ether groups*

The effect of F/U molar ratio on ether group profiles is shown in Figure 4.34. It is apparent that the F/U molar ratio has less effect on ether group formation during the addition stage (see Figure 4.34(a)) than is the case during the condensation stage (see Figure 4.34(b)). Ether group levels decrease more rapidly during the condensation stage for low F/U molar ratios. Lower F/U molar ratios favour ether linkage dissociation.

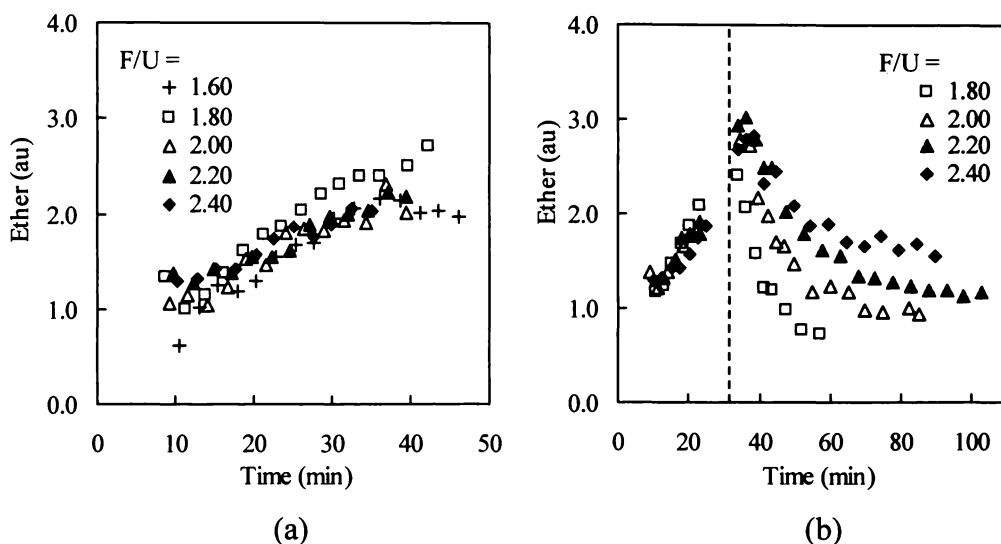


Figure 4.34. The effect of F/U molar ratio on ether group levels vs reaction time during (a) the addition stage and (b) the entire reaction period.

The effect of F/U molar ratios on the methylene to ether (Me/E) group ratio is shown in Figure 4.35. The Me/E group ratio increases with decreases in F/U molar ratio.

*Summary and conclusions*

Reactions with lower F/U molar ratio proceed at faster rates and afford resins with lower levels of methylol and ether species and higher levels of methylene species.

If F/U molar ratio is less than 1.60, the reaction may proceed at a rate that is

difficult to control. If F/U molar is higher than 2.4, the reaction rate is unacceptably slow and produces more ether groups and less methylene groups. The product is likely to have a higher formaldehyde emission level. The optimum F/U molar ratio range is between 1.80 and 2.20.

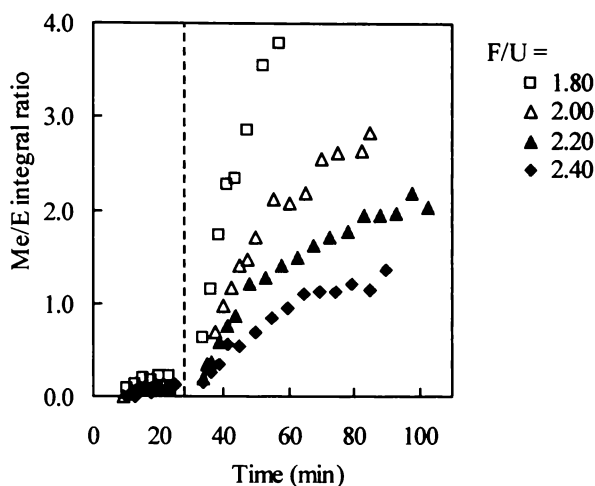


Figure 4.35. The effect of F/U molar ratio on the methylene to ether (Me/E) group ratio.

#### 4.3.5 Effect of Initial Addition pH

The UF reaction is catalysed by both acid and base. The addition stage reaction is often carried out at alkaline pH. In this section, the effect of initial addition stage pH on the UF reaction is described. Reaction conditions common to all of the experiments are: F/U molar ratio = 2.0, formaldehyde concentration = 46%, temperature = 88°C, condensation stage pH = 5.0.

The term “initial addition pH” refers to the pH at the commencement of the addition stage reaction. This pH is not maintained during the addition stage. Rather, the pH of the reaction system continuously changes during the reaction period. An understanding of the factors associated with pH variation and pH control during the reaction process is an important aspect of UF resin chemistry.

The pH of a commercial formaldehyde solution is normally about 3.0. After adjustment of the pH of the solution to a desired level (eg pH 8-9), the chosen pH is

maintained for only a very short time ( $< 1$  min at  $50^{\circ}\text{C}$  or above), before decreasing with time. For example, after a few minutes, the pH of a warm ( $50^{\circ}\text{C}$ ) formaldehyde solution, initially adjusted to pH 9.0, falls to pH 8.5-8.7. After the pH of the formaldehyde solution has been adjusted to the chosen value, the desired amount of urea is added immediately. The pH of the reaction mixture rises initially (see Figure 4.36) due to the presence of trace alkaline impurities ( $\text{NH}_2\text{COONH}_4$ ,  $c$  2%) in the added urea. However, the pH then falls due to the acidic products of Cannizzaro reaction and the reaction of the alkaline impurities with formaldehyde (de Jong and de Jonge 1952).

The pH profiles determined for some typical UF resin preparations at  $88^{\circ}\text{C}$  are shown in Figure 4.36. The ‘original pH’ of the formaldehyde solution used in these experiments was 3.1. Immediately prior to the addition of urea (at  $t = 0$ ) the pH of the formaldehyde solution was adjusted to a value in the range 5.0-8.7. A control experiment without pH adjustment (pH 3.1) was also performed.

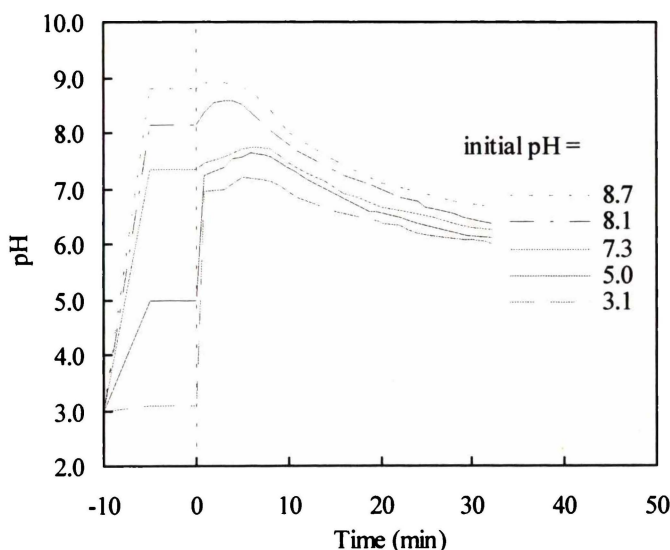


Figure 4.36. The relationship of initial addition reaction pH and the pH during the addition reaction stage.

$t = 0$  corresponds to the point where urea was added to the formaldehyde solution.

It can be seen from Figure 4.36 that even without adjustment of the pH, the pH of the original formaldehyde solution rises to about  $\text{pH} = 7.2$  upon the addition of urea. The use of higher initial pH formaldehyde solutions affords more strongly alkaline

pHs (see Figure 4.36). It is thus apparent that irrespective of the initial addition pH the addition reaction commences under alkaline conditions.

#### *Free urea and free formaldehyde*

Since the free urea level is very small ( $< 0.2$  au) during the entire reaction period, little information about the effect of the initial addition pH can be elucidated from it.

The effect of initial addition pH on the free formaldehyde levels is shown in Figure 4.37. There are no significant differences for the free formaldehyde profiles for different initial addition pH reactions.

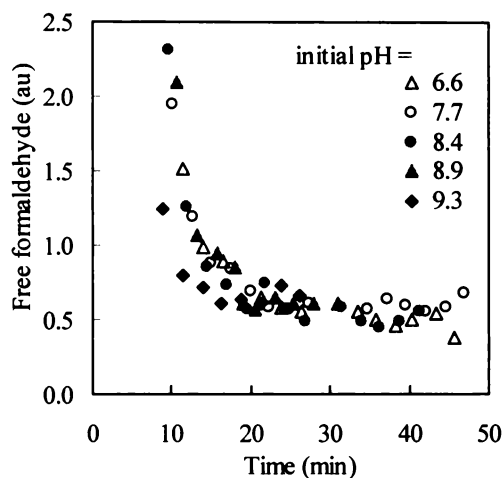


Figure 4.37. Plots of the effect of initial addition pH on free formaldehyde levels vs reaction time during the addition reaction stage.

#### *Methylol groups*

The effect of initial addition pH on methylol group profiles is shown in Figure 4.38. During the addition stage, the level of methylol groups rises to a maximum at times that decrease as the initial pH rises. This observation is consistent with the view that the higher the initial pH, the faster the base catalysed formation of methylols. There is however, little difference in methylol group levels during the condensation stage.

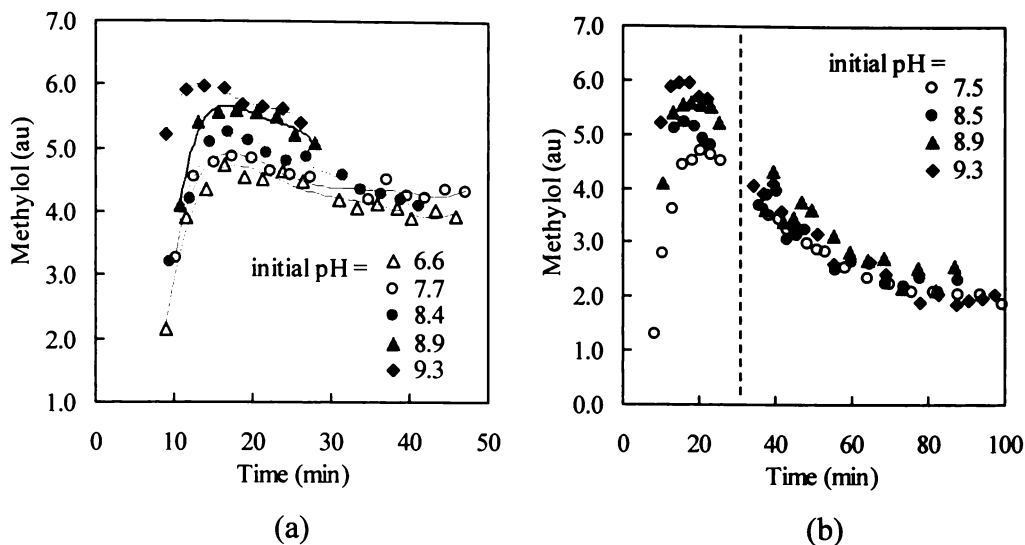


Figure 4.38. Plots of the effect of initial addition pH on methylol group levels vs reaction time during (a) the addition stage and (b) the entire reaction period.

### *Methylene groups*

The effect of initial addition pH on methylene profiles is shown in Figure 4.39. It can be seen that the higher the initial addition pH, the lower the level of methylene groups formed during the addition stage. This is consistent with the view that methylene group formation reaction is catalysed by acid.

During the condensation stage, methylene group formation rates and the amount of methylene groups formed are not significantly different for initial addition pHs of 8.5, 8.9 and 9.3. A slightly lower level of methylene groups was present during the condensation reaction performed with an initial addition pH of 7.5.

### *Ether groups*

The effect of initial addition pH on ether group profiles is shown in Figure 4.40. It is apparent that low initial pH favours the formation of ether groups during the addition stage. It has little effect on ether group levels during the condensation stage.

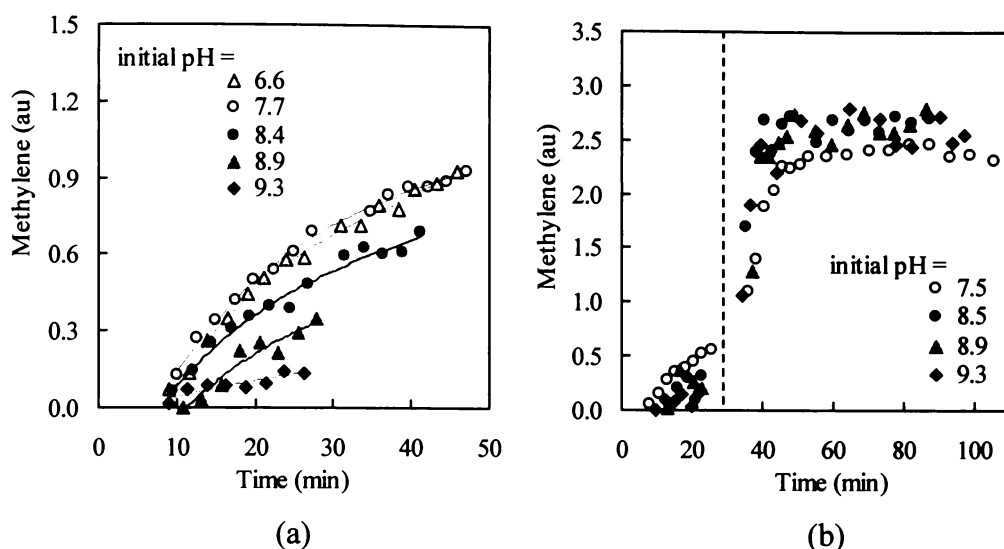


Figure 4.39. Plots of the effect of initial addition pH on methylene group levels vs reaction time during (a) the addition stage and (b) the entire reaction period.

The presence of more methylene and ether groups during the addition stage in the low initial addition pH (eg pH = 6.6-7.5) reaction mixtures, accounts for the corresponding lower level of methylol groups in these reaction mixtures.

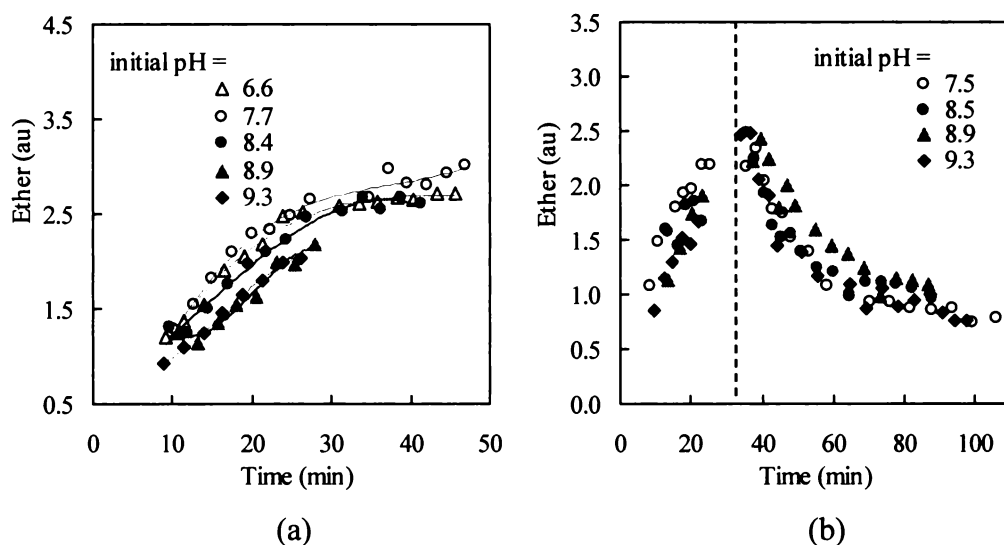


Figure 4.40. Plots of the effect of initial addition pH on ether group levels vs reaction time during (a) the addition stage and (b) the entire reaction period.

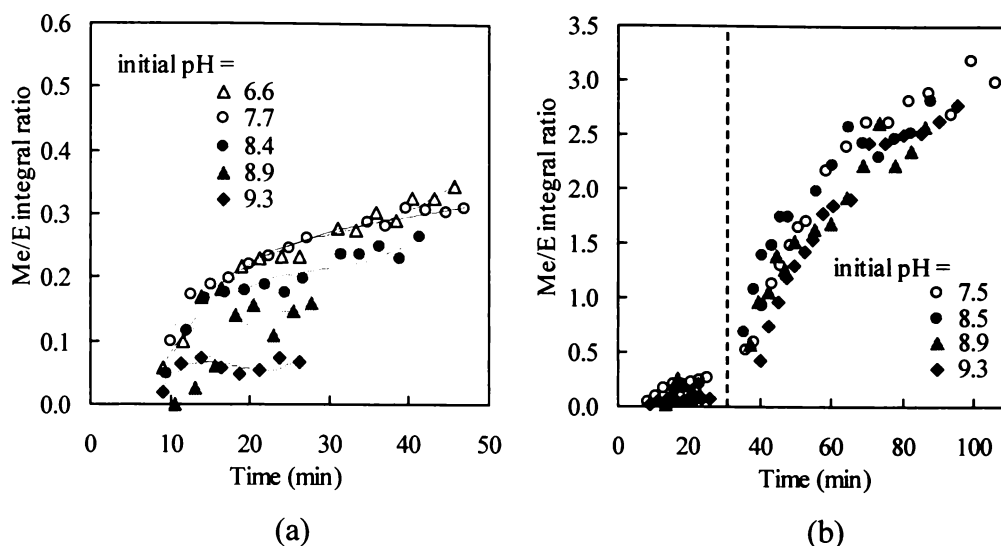


Figure 4.41. Plots of the effect of initial addition pH on methylene to ether group (Me/E) ratio vs reaction time during (a) the addition stage and (b) the entire reaction period.

The effect of initial addition pH on the Me/E group ratio is shown in Figure 4.41. Me/E group ratios increase with initial pH during the addition stage. However, initial addition pH has only a small effect on the Me/E group ratio during the condensation stage. The Me/E group ratio of low initial addition pH (7.5 and 8.5) reactions is marginally greater than that of high initial addition pH (8.9 and 9.3) reactions. This difference may be significant since higher Me/E group ratio resins generally have lower formaldehyde emissions.

### *Summary and conclusions*

The results indicate that:

- 1) Higher initial addition pHs favour higher levels and a faster formation rate of methylol groups while lower initial addition pHs favour the formation of methylene and ether groups during the addition stage.
- 2) Initial addition pH does not significantly influence methylol, methylene and ether group levels during the condensation stage.

- 3) Low initial addition pH reactions have slightly higher Me/E group ratios, which may result in lower formaldehyde emission from final resins.

There is no obvious optimum initial addition pH. For the purpose of further work, a pH of between 8.0 and 9.0 was chosen as representing a compromise between maximising Me/E group ratio and rate of methylol formation.

#### **4.3.6 Effect of Condensation Reaction pH**

Unlike the pH during the addition reaction stage, the pH during the condensation stage normally does not change significantly with time. After the addition stage, the pH at the start of the condensation stage is typically adjusted to pH 5.0 and normally this value does not vary by more than  $\pm 0.1$  pH unit during the entire condensation stage. Thus the pH during the initial and subsequent stages of the condensation reaction period is typically referred to simply as the “condensation pH”, rather than “initial condensation pH”.

The effects of condensation pH on methylol, methylene and ether group levels are discussed below. Free urea and free formaldehyde levels in the reaction systems were also assessed, however only low levels ( $< 0.3$  au for free urea and 0.5-0.7 au for free formaldehyde during the addition stages respectively) were detected and little variation in levels was observed.

Reactions conditions common to all the experiments in this section are: F/U molar ratio = 2.0, formaldehyde concentration 46%, temperature = 88°C, initial addition pH = 8.5, addition reaction time = 37 min.

##### *Methylol groups*

Since conditions during the addition stage were identical, the levels of methylol, methylene and ether groups present during the addition stage were expected to be similar (see Figures 4.42 to 4.44). The levels of these groups during the condensation

stage were strongly influenced by condensation pH. From Figure 4.42 it can be seen that the higher the condensation pH, the slower the decrease in methylol group levels. At the high condensation pH of 6.0, little reaction of methylol groups occurs.

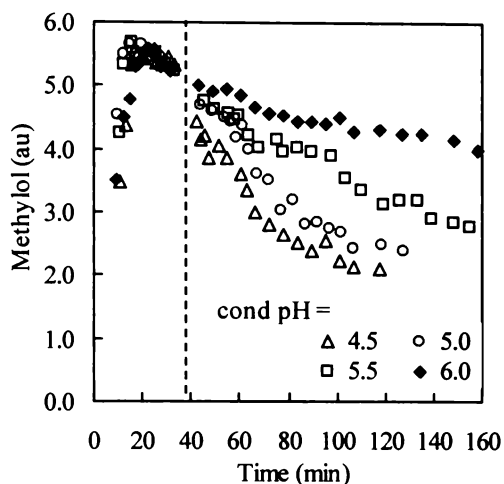


Figure 4.42. The effect of condensation (cond) pH on methylol group levels vs reaction time during the reaction period.

### *Methylene groups*

The results in Figure 4.43 show that the methylene group formation rates and final methylene group levels increase with decreasing condensation pH. Reaction is very slow at pH 6.0 (see Figure 4.43). On the other hand at pH 4.5, or less, methylene groups are formed very rapidly and it may be difficult to control the reaction in a commercial environment. The optimum condensation stage pH appears to be in the range 4.5-5.0.

### *Ether groups*

The results in Figure 4.44 also show that the higher the condensation pH, the slower the rate at which ether groups are consumed. The rate of decrease at pH 6.0 is especially slow. If a resin is prepared at a high condensation pH (eg 5.5-6.0), there will be an excess of ether groups remaining in the resin. High formaldehyde emissions are likely.

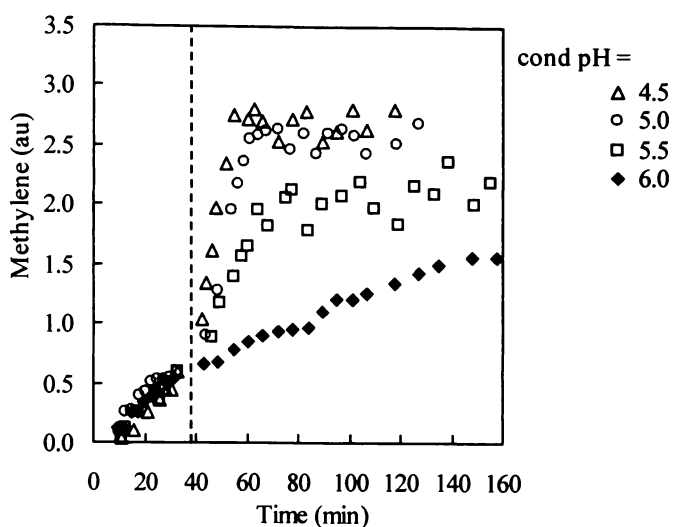


Figure 4.43. Plots of the effect of condensation pH on methylene group levels vs reaction time.

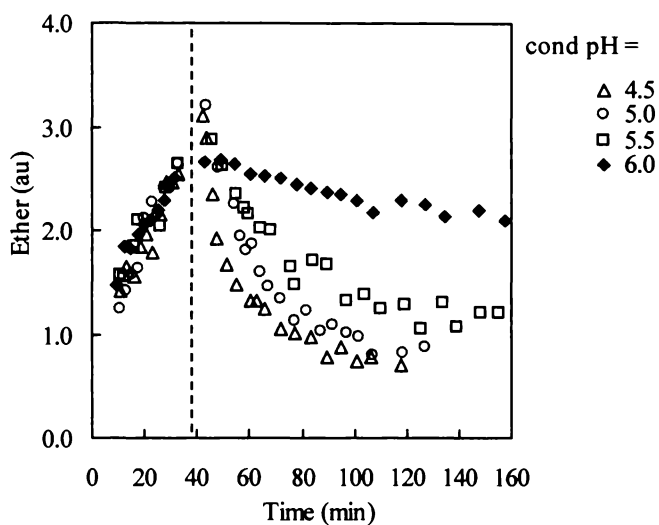


Figure 4.44. Plots of the effect of condensation pH on ether group levels vs reaction time.

The effect of condensation pH on the Me/E group ratio is shown in Figure 4.45. Me/E group ratios increase with decreasing condensation pH. It is likely that a resin prepared using a low condensation stage pH will have a lower formaldehyde emission. On this basis, it appears that the lower the condensation pH the better. However, commercial applications are constrained by the loss of control implicit in faster low pH reactions.

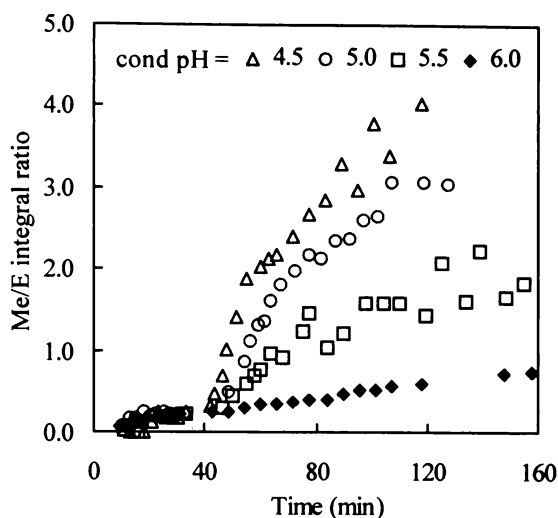


Figure 4.45. Plots of the effect of condensation pH on the Me/E group ratio vs reaction time.

### Summary and conclusions

The lower the condensation pH, the faster the rate at which methylene groups are formed and the ether groups are consumed, therefore, the higher the Me/E group ratio. It is anticipated that the formaldehyde emissions of the resin increase with the increasing condensation pH. The optimum condensation stage pH appears to be in the range 4.5 to 5.0.

### 4.3.7 Optimum Conditions for Urea Formaldehyde Resin Production

From the investigations reported above, the following reaction conditions have been chosen as an estimate of optimum conditions for the production of UF resins:

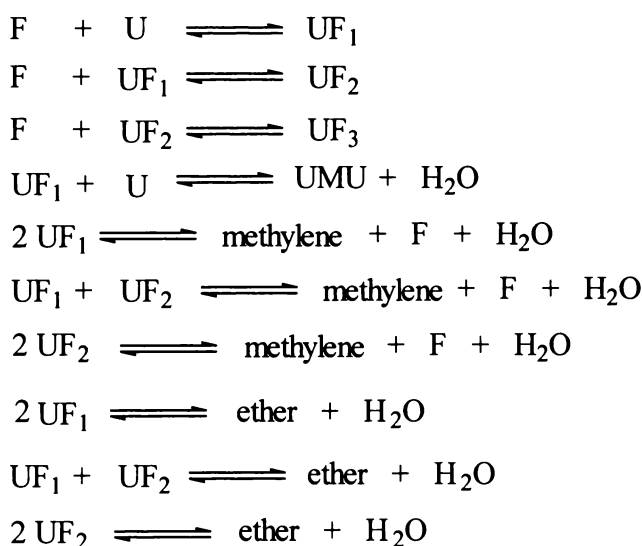
Formaldehyde concentration:	35-46%
F/U molar ratio:	1.8-2.2
Reaction temperature:	88°C
Addition reaction time:	25-30 min
Initial addition pH:	8.0-9.0
Condensation pH:	4.5-5.0

#### 4.4 KINETICS STUDIES OF THE UREA FORMALDEHYDE REACTION

The dynamic (RAPID) NMR data provide reaction profiles that may enable kinetic analysis and elucidation of reaction mechanism occurring during the addition stage and condensation stage reactions. As indicated in Section 1.2.3, no previous attempt has been made to elucidate the kinetics of the urea formaldehyde reaction system under conditions, close to commercial manufacturing conditions, that are achievable in the dynamic NMR experiment.

##### 4.4.1 Addition Stage Reactions

Possible reactions between urea, formaldehyde and methylol species are listed below:



where U = urea, F = formaldehyde,  $\text{UF}_1$  = monomethylolurea (ie MMU),  $\text{UF}_2$  = dimethylolurea (DMU),  $\text{UF}_3$  = trimethylolurea (TMU) and UMU = methylene diurea (MDU).

The urea formaldehyde reaction system is complex. It involves reversible, parallel and successive reactions. These ten reactions will have twenty reaction rate constants ( $k_f$ s and  $k_b$ s). Because many of the reaction products cannot be individually quantified, it is difficult to obtain the data required to determine all reaction rate constants in the urea formaldehyde reaction system under conditions close to a

commercial production. However, if appropriate assumptions are made, some general conclusions can be drawn.

For the purposes of kinetics analysis, data from the addition stage reaction at 60-97°C and other conditions as summarised in Section 4.3.1 were used. For these reactions methylene species produced during the addition stage (< 30 min) constitute less than 0.5 au (see Figure 4.8 in Section 4.3.1). Methylene species represent less than 10% of total methylol species (*c* 5.5-6.0 au) (see Figure 4.7). Therefore, methylene group formation processes can be ignored. Ether species remain relatively constant at approximately 1.5 au (see Figure 4.9), and therefore have little effect on the methylol group formation process.

The UF<sub>1</sub> and UF<sub>2</sub> data required for the analysis and available from the NMR experiments (see Section 4.3.1) are summarised in Figure 4.46. The UF<sub>3</sub> levels are small and can be ignored. However, it is clear that the UF<sub>2</sub> cannot be ignored.

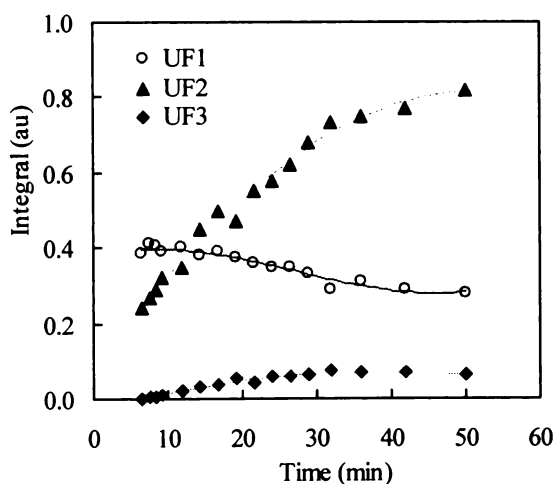
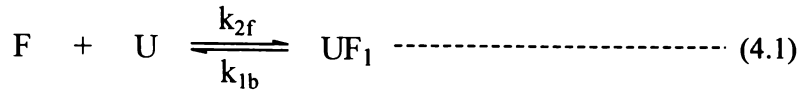


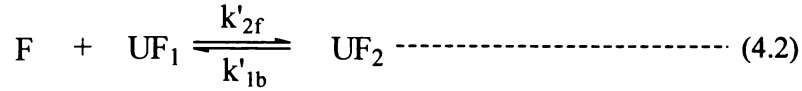
Figure 4.46. Plots of UF<sub>1</sub>, UF<sub>2</sub> and UF<sub>3</sub> levels vs reaction time during the addition stage of a typical reaction at 80°C.

From the reasons outlined above, the urea formaldehyde reaction system can be simplified as two reactions:



Boundary conditions:

	[F]	[U]	[UF <sub>1</sub> ]
at t = 0:	a	b	0
at t = t:	a-x-2y	b-x-y	x



Boundary conditions:

	[F]	[UF <sub>1</sub> ]	[UF <sub>2</sub> ]
at t = 0:	a	0	0
at t = t:	a-x-2y	x	y

Following the approach of de Jong and de Jonge (1952), the forward reactions of (4.1) and (4.2) are likely to be second order and their back reactions are likely to be first order. The following differential rate equations can be applied:

$r_1$ , the consumption rate of formaldehyde is:

$$r_1 = -\frac{d[F]}{dt} = k_{2f}[F][U] - k_{1b}[UF_1] + k'_{2f}[F][UF_1] - k'_{1b}[UF_2] \text{ .... (4.3)}$$

$$= k_{2f}(a - x - 2y)(b - x - y) - k_{1b}x + k'_{2f}(a - x - 2y)x - k'_{1b}y$$

$r_2$ , the consumption rate of urea is:

$$r_2 = -\frac{d[U]}{dt} = k_{2f}[F][U] - k_{1b}[UF_1] = k_{2f}(a - x - 2y)(b - x - y) - k_{1b}x \text{ ..... (4.4)}$$

$r_3$ , the formation rate of UF<sub>1</sub> is:

$$r_3 = \frac{d[UF_1]}{dt} = \frac{dx}{dt} = k_{2f}[F][U] - k_{1b}[UF_1] - k'_{2f}[F][UF_1] + k'_{1b}[UF_2] \text{ ..... (4.5)}$$

$$= k_{2f}(a - x - 2y)(b - x - y) - k_{1b}x - k'_{2f}(a - x - 2y)x + k'_{1b}y$$

$r_4$ , the formation rate of  $UF_2$  is:

$$r_4 = \frac{d[UF_2]}{dt} = \frac{dy}{dt} = k'_{2f}[F][UF_1] - k'_{1b}[UF_2] = k'_{2f}(a - x - 2y)x - k'_{1b}y \dots\dots (4.6)$$

Since these two reactions are reversible reactions, there are two equilibrium constants:

$$K_1 = \frac{k_{2f}}{k_{1b}} \dots\dots\dots (4.7)$$

$$K_2 = \frac{k'_{2f}}{k'_{1b}} \dots\dots\dots (4.8)$$

In principle, sufficient kinetic data would allow Equations 4.3 to 4.8 to be solved for  $k_{2f}$ ,  $k_{1b}$ ,  $k'_{2f}$ ,  $k'_{1b}$ ,  $K_1$  and  $K_2$  ideally using an appropriate computer modeling program.

Analysis of kinetic data is traditionally achieved using either an integrated form or the differential form of the rate equation. Both methods have their advantages and disadvantages (Fu and Chen 1981). In this research, the differential approach has been applied to estimate the kinetic parameters of the UF reaction system.

#### 4.4.2 Absolute Molar Concentrations

The dynamic (RAPID) NMR data are in arbitrary integration units. They have to be converted to the absolute mole concentrations before kinetic calculations can be made. According to the known formaldehyde concentration (46%), F/U molar ratio and the volume of the reaction mixture, the initial concentrations of formaldehyde and urea (ie before the reaction starts) can be calculated as  $[F]_0 = a = 12.8 \text{ mol L}^{-1}$  and  $[U]_0 = b = 6.4 \text{ mol L}^{-1}$ .

In order to determine the signal intensity expected for formaldehyde at  $t = 0$  ( $I_{F0}$ ), an appropriate amount of formaldehyde solution was analysed by itself and it was

determined as  $I_{F0} = 5.3$  au. The concentration of free formaldehyde during reactions was then determined from:

$$[F] = \frac{I_F}{I_{F0}} [F]_0 \dots\dots\dots (4.9)$$

where  $[F]$  = free formaldehyde concentration in the reaction system at time  $t$  in mol L<sup>-1</sup>;

$[F]_0 = 12.8$  mol L<sup>-1</sup>, initial formaldehyde concentration in the reaction system before the reaction started;

$I_F$  = signal intensity of free formaldehyde at any time  $t$  (au);

$I_{F0} = 5.3$  au, initial signal intensity of formaldehyde at time zero ( $t = 0$ ).

In the reaction system, the original urea converts into different species. The total urea can be expressed:

$$\begin{aligned} [U]_0 &= [U] + [U]_{UF1} + [U]_{UF2} + [U]_{\text{other}} \\ &= [U] + [UF_1] + [UF_2] + [U]_{\text{other}} \dots\dots\dots (4.10) \end{aligned}$$

where  $[U]_0 = 6.4$  mol L<sup>-1</sup>, the concentration of original urea;

$[U]$  = the molar concentration of free urea;

$[U]_{UF1} = [UF_1]$ , the molar concentration of urea (carbonyl group) present in  $UF_1$ ;

$[U]_{UF2} = [UF_2]$ , the molar concentration of urea (carbonyl group) present in  $UF_2$ ;

$[U]_{\text{other}}$  = the molar concentration of urea (carbonyl group) present in other species, eg  $UF_3$  and ether.

Experimental observations show that  $UF_3$  formation during the addition stage normally accounts for less than 2-3% of the original urea level if the reaction time is not more than 26 min for the reaction at 60-80°C and not more than 22 min for the reaction at 90-97°C. Ether group formation normally accounts for 18-22% of the total urea for a reaction time of not more than 26 min (at 60-97°C). Therefore, the urea

present as other species (ie UF<sub>3</sub> and ether group) is roughly equal to 22% of the total urea level. Thus, UF<sub>3</sub> and ether species should be subtracted from the original urea level:

$$[U]_0 - [U]_{\text{other}} \approx [U]_0 - 0.22 [U]_0 = 0.78 [U]_0$$

About 78% of the original urea is distributed as free urea, UF<sub>1</sub> and UF<sub>2</sub>:

$$0.78 [U]_0 = [U] + [UF_1] + [UF_2] \dots\dots\dots (4.11)$$

The Equation (4.11) can be expressed as:

$$0.78[U]_0 = k I = k I_U + k I_{UF_1} + k I_{UF_2}$$

where  $k$  = a proportionality constant used to convert the NMR signal intensity into absolute concentration;

$I_U, I_{UF_1}$  and  $I_{UF_2}$  = the quantitative (STANDARD) signal intensities of free urea, UF<sub>1</sub> and UF<sub>2</sub> respectively;

$I = I_U + I_{UF_1} + I_{UF_2}$ , the total quantitative (STANDARD) signal intensity of free urea, UF<sub>1</sub> and UF<sub>2</sub>.

The quantitative signal intensities can be obtained using the calibration factors determined in Section 3.8:

$$I_U = \frac{I_U'}{f_{cU}} = \frac{I_U'}{1.14}$$

$$I_{UF_1} = \frac{I_{UF_1}'}{f_{cUF_1}} = \frac{I_{UF_1}'}{1.21}$$

$$I_{UF_2} = \frac{I_{UF_2}'}{f_{cUF_2}} = \frac{I_{UF_2}'}{1.37}$$

where  $I_U$ ,  $I_{UF_1}$  and  $I_{UF_2}$  are the quantitative (STANDARD) signal intensities (au) for free urea,  $UF_1$  and  $UF_2$  respectively;

$I'_U$ ,  $I'_{UF_1}$  and  $I'_{UF_2}$  are the signal intensities (au) from the dynamic (RAPID) NMR spectra for free urea,  $UF_1$  and  $UF_2$  respectively;

$f_{cU}$ ,  $f_{cUF_1}$  and  $f_{cUF_2}$  are the calibration factors for urea,  $UF_1$  and  $UF_2$  respectively (see Table 3.21 and Table 3.25).

Therefore, the molar concentration of free urea, MMU and DMU can be obtained:

$$[U] = 0.78[U]_0 \frac{I_U}{I} \dots\dots\dots (4.12)$$

$$[UF_1] = 0.78[U]_0 \frac{I_{UF_1}}{I} \dots\dots\dots (4.13)$$

$$[UF_2] = 0.78[U]_0 \frac{I_{UF_2}}{I} \dots\dots\dots (4.14)$$

In this way (Equations 4.9, 4.12, 4.13 and 4.14), the dynamic (RAPID) NMR data can be converted to the corresponding absolute molar concentrations.

#### 4.4.3 Rate Constants for Monomethylolurea Formation

The consumption rate of urea can be expressed as (see Equation 4.4):

$$r_2 = -\frac{d[U]}{dt} = k_{2f}[F][U] - k_{1b}[UF_1]$$

therefore

$$\frac{r_2}{[UF_1]} = k_{2f} \frac{[F][U]}{[UF_1]} - k_{1b} \dots\dots\dots (4.15)$$

or 
$$\frac{r_2}{[F][U]} = k_{2f} - k_{1b} \frac{[UF_1]}{[F][U]} \dots\dots\dots (4.16)$$

This indicates that the plot of  $r_2/[UF_1]$  vs  $[F][U]/[UF_1]$  yields a straight line with a slope of  $k_{2f}$  and an intercept of  $-k_{1b}$ , or the plot of  $r_2/([F][U])$  vs  $[UF_1]/([F][U])$  yields a straight line with a slope of  $-k_{1b}$  and an intercept of  $k_{2f}$ .

The consumption rate of urea at any time  $t$  can be obtained from the  $[U]$  vs  $t$  curve, which can be obtained by either a graphical method or by a differential method. The graphical method uses the tangent to the plot of  $[U]$  vs  $t$  determined for different times. The slope of the tangent line is  $-d[U]/dt$ , ie the consumption rate of the urea at time  $t$ . If the  $[U]$  vs  $t$  curve can be regressed to fit a function,  $f(t)$ , the consumption rate of urea can be obtained in a more straight forward manner by differentiating  $f(t)$ , ie  $-d[U]/dt = -df(t)/dt$ . For example, the  $[U]$  vs  $t$  curve of the reaction at  $60^\circ\text{C}$  can be fitted to a function (see Figure 4.47):

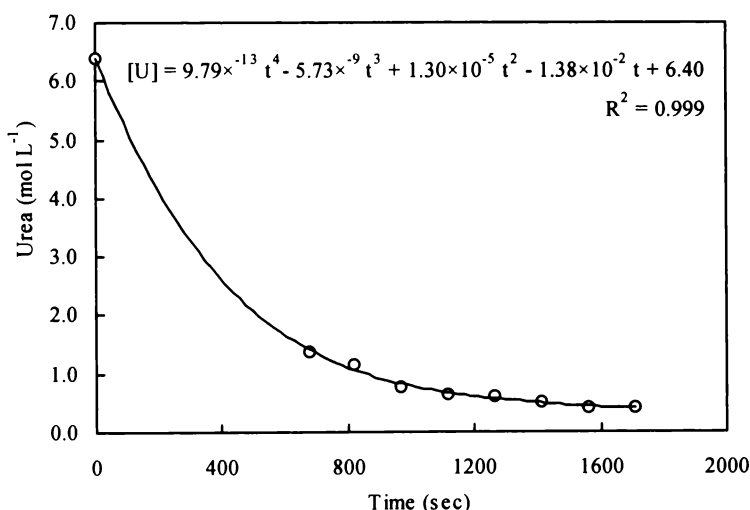


Figure 4.47. Plot of the urea concentration vs reaction time during the addition stage of an urea formaldehyde reaction at  $60^\circ\text{C}$ .

$$[U] = f(t) = 9.79 \times 10^{-13} t^4 - 5.73 \times 10^{-9} t^3 + 1.30 \times 10^{-5} t^2 - 1.38 \times 10^{-2} t + 6.40$$

Therefore, the consumption rate of urea is:

$$r_2 = -d[U]/dt = 3.92 \times 10^{-12} t^3 - 1.72 \times 10^{-8} t^2 + 2.60 \times 10^{-5} t - 1.38 \times 10^{-2} \dots\dots (4.17)$$

The rate constants ( $k_{2f}$  and  $k_{1b}$ ) obtained from the slopes and intercepts of the plots in Figure 4.48 are summarised in Table 4.6 along with the literature data for comparison.

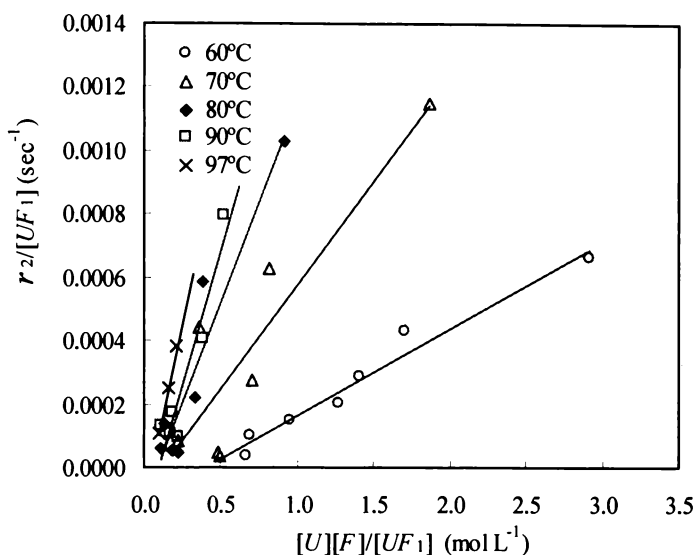


Figure 4.48. Plots of  $r_2/[UF_1]$  vs  $[F][U]/[UF_1]$  for reactions at 60°C to 97°C.

Table 4.6. Rate constants of the  $UF_1$  formation reaction at different temperatures.

temp (°C)	$k_{2f}$ (L mol <sup>-1</sup> sec <sup>-1</sup> )	$k_{1b}$ (sec <sup>-1</sup> )	$k_{2f}^a$ (L mol <sup>-1</sup> sec <sup>-1</sup> )	$k_{1b}^a$ (sec <sup>-1</sup> )
60	$2.7 \times 10^{-4}$	$7.5 \times 10^{-5}$	$5.92 \times 10^{-4}$	$3.38 \times 10^{-5}$
70	$6.5 \times 10^{-4}$	$8.1 \times 10^{-5}$	$1.06 \times 10^{-3}$	$7.78 \times 10^{-5}$
80	$1.3 \times 10^{-3}$	$1.5 \times 10^{-4}$	$1.83 \times 10^{-3}$	$1.71 \times 10^{-4}$
90	$1.7 \times 10^{-3}$	$1.8 \times 10^{-4}$	$3.07 \times 10^{-3}$	$3.59 \times 10^{-4}$
97	$2.9 \times 10^{-3}$	$2.6 \times 10^{-4}$	$4.33 \times 10^{-3}$	$5.89 \times 10^{-4}$

<sup>a</sup> Rate constants extrapolated from data reported by de Jong and de Jonge (1952).

Activation energies can be obtained by plotting the  $\ln k$  vs  $1/T$  (see Figure 4.49). Activation energies of the forward reaction,  $E_f = (62.6 \pm 5.4) \text{ kJ mol}^{-1} = (15.0 \pm 1.3) \text{ kcal mol}^{-1}$  and the back reaction,  $E_b = (35.5 \pm 5.0) \text{ kJ mol}^{-1} = (8.5 \pm 1.2) \text{ kcal mol}^{-1}$

were obtained. The activation energies of the monomethylolurea formation and decomposition reactions (forward and back reactions, respectively) have been reported to be 13 and 19 kcal mol<sup>-1</sup>, respectively (de Jong and de Jonge 1952).

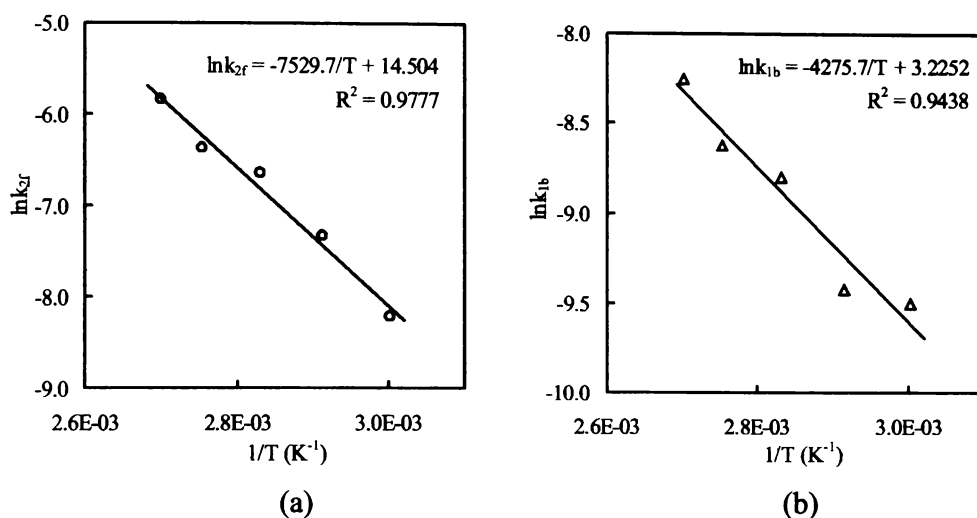


Figure 4.49. Plots of (a)  $\ln k_{2f}$  vs  $1/T$  and (b)  $\ln k_{1b}$  vs  $1/T$  for the UF<sub>1</sub> formation reaction.

It can be seen that the rate constants and activation energies of both the forward reaction and back reaction can be independently obtained by the differential method. The rate constants and activation energies determined in this investigation are similar to literature data. Given that the reaction conditions utilised in this research differ greatly from those used by de Jong and de Jonge (1952), and that reaction mechanisms may therefore not be identical, there is satisfactory agreement with literature data (de Jong and de Jonge 1952, Nair and Francis 1983).

#### 4.4.4 Rate Constants for Dimethylolurea Formation

Similarly, the formation rate of UF<sub>2</sub> can be expressed as (see Equation 4.6):

$$r_4 = \frac{d[UF_2]}{dt} = k'_{2f}[UF_1][F] - k'_{1b}[UF_2]$$

therefore:

$$\frac{r_4}{[UF_2]} = k'_{2f} \frac{[UF_1][F]}{[UF_2]} - k'_{1b} \dots\dots\dots (4.18)$$

$$\frac{r_4}{[UF_1][F]} = k'_{2f} - k'_{1b} \frac{[UF_2]}{[UF_1][F]} \dots\dots\dots (4.19)$$

A plot of  $r_4/[UF_2]$  vs  $[UF_1][F]/[UF_2]$  should yield a straight line with a slope of  $k'_{2f}$  and an intercept of  $-k'_{1b}$ , or a plot of  $r_4/([UF_1][F])$  vs  $[UF_2]/([UF_1][F])$  should yield a straight line with a slope of  $-k'_{1b}$  and an intercept of  $k'_{2f}$ .

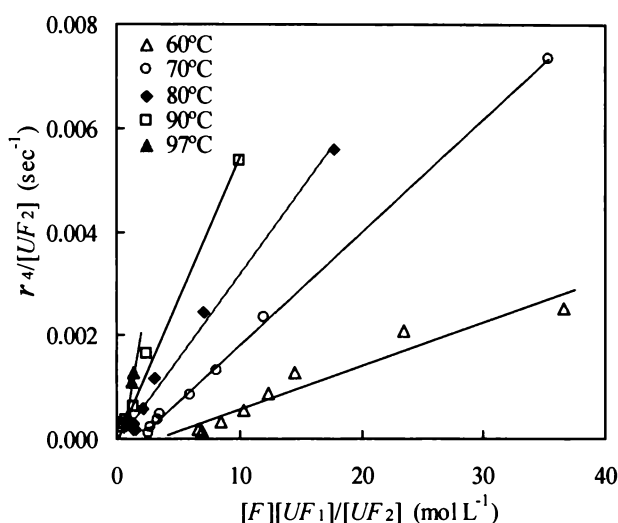


Figure 4.50. Plots of  $r_4/[UF_2]$  vs  $[UF_1][F]/[UF_2]$  for reactions at 60°C to 97°C.

Table 4.7. Rate constants of the  $UF_2$  formation reaction at different temperatures.

temp (°C)	$k'_{2f}$ (L mol <sup>-1</sup> sec <sup>-1</sup> )	$k'_{1b}$ (sec <sup>-1</sup> )	$k'_{2f}$ <sup>a</sup> (L mol <sup>-1</sup> sec <sup>-1</sup> )	$k'_{1b}$ <sup>a</sup> (sec <sup>-1</sup> )
60	$1.2 \times 10^{-4}$	$2.7 \times 10^{-4}$	$2.11 \times 10^{-4}$	$8.58 \times 10^{-5}$
70	$2.2 \times 10^{-4}$	$4.1 \times 10^{-4}$	$3.91 \times 10^{-4}$	$1.98 \times 10^{-4}$
80	$6.2 \times 10^{-4}$	$6.6 \times 10^{-4}$	$7.00 \times 10^{-4}$	$4.36 \times 10^{-4}$
90	$7.5 \times 10^{-4}$	$7.0 \times 10^{-4}$	$1.21 \times 10^{-3}$	$9.19 \times 10^{-4}$
97	$1.1 \times 10^{-3}$	$8.0 \times 10^{-4}$	$1.75 \times 10^{-3}$	$1.51 \times 10^{-3}$

<sup>a</sup> Rate constants extrapolated using literature data (de Jong and de Jonge 1953, Vale and Taylor 1964).

The rate constant ( $k'_{2f}$  and  $k'_{1b}$ ) obtained from the slopes and intercepts of the plots in Figure 4.50 are summarised in Table 4.7 along with the literature data.

The activation energies can be obtained by plotting the  $\ln k$  vs  $1/T$  (see Figure 4.51). Activation energies of the forward reaction,  $E_f = (62.3 \pm 7.1) \text{ kJ mol}^{-1} = (14.9 \pm 1.7) \text{ kcal mol}^{-1}$  and the back reaction,  $E_b = (30.1 \pm 4.6) \text{ kJ mol}^{-1} = (7.2 \pm 1.1) \text{ kcal mol}^{-1}$  were obtained. Given the differences in reaction condition noted earlier, and may be also reaction mechanisms, there is reasonable agreement with literature data (de Jong and de Jonge 1952 and 1953).

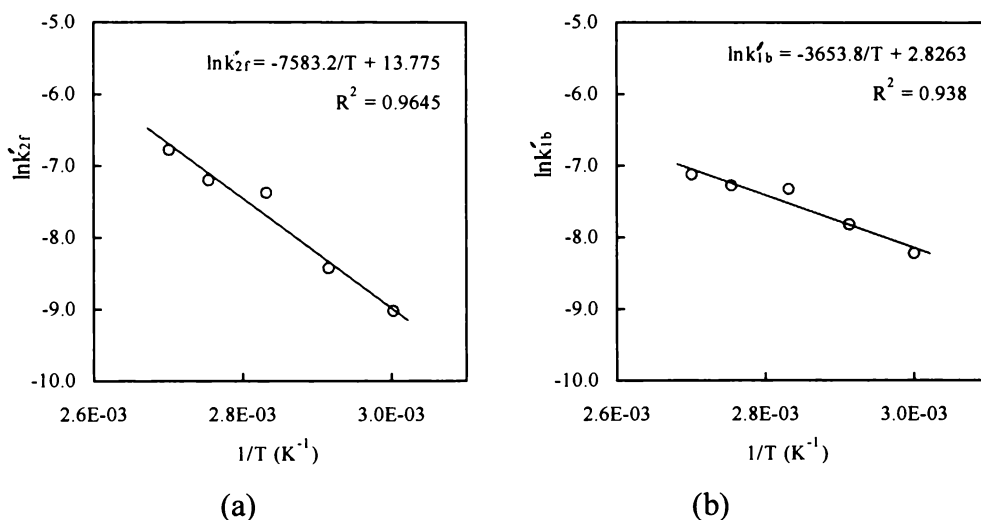
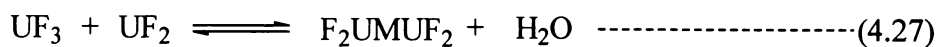
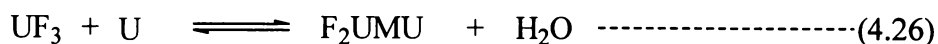
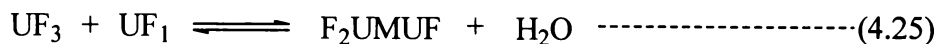
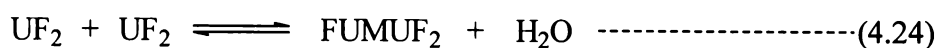
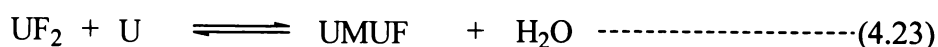
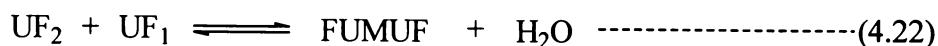
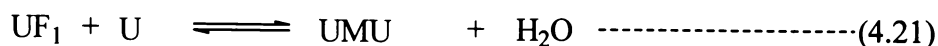
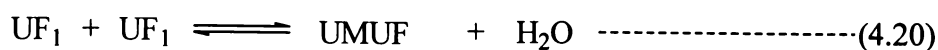


Figure 4.51. Plots of (a)  $\ln k'_{2f}$  vs  $1/T$  and (b)  $\ln k'_{1b}$  vs  $1/T$  for the  $\text{UF}_2$  formation reaction.

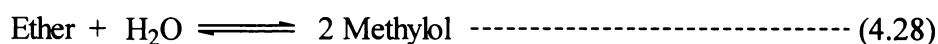
#### 4.4.5 Condensation Stage Reactions

Dynamic NMR experimental data show that methylol decreases, methylene increases, while ether increases through a maximum and then decreases with time (see Section 4.3) during the condensation stage. The following UF reactions can be postulated:

Methylene formation:



Ether formation and dissociation:



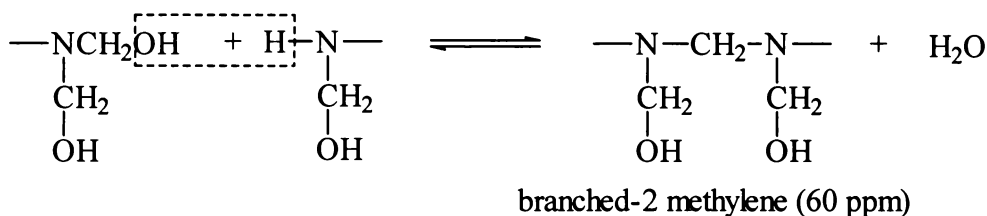
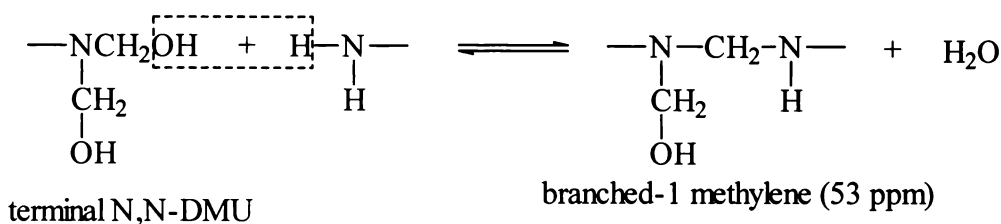
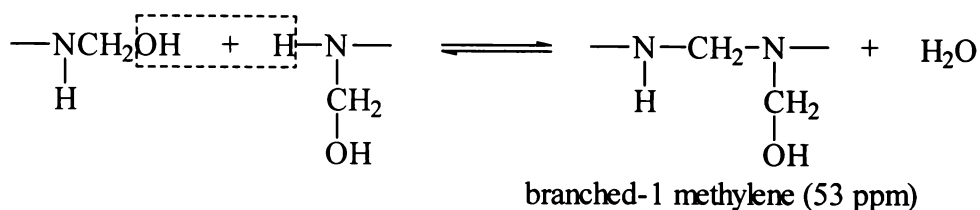
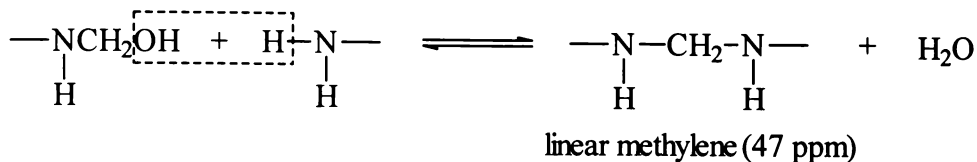
where  $UF_1 = MMU$ ,  $UF_2 = DMU$ ,  $UMU = MDU$ ,  $M = \text{methylene group}$ .

The reactions during the condensation stage are much more complex than the reactions during the addition stage. Methylene formation involves many different reactions forming different methylene structures (see Equations 4.20-4.27). Furthermore, during the late condensation stage (eg > 30 min of condensation), the further reaction of the methylol and methylene groups may lead to higher molecular weight chain methylene linkages. If an appropriate computer modeling program is used it should be possible to obtain all of the rate constants, provided the concentrations of species can be reliably measured. In practice this was not possible due to difficulties encountered in determining the concentrations of some of the species.

For example the  $^{13}\text{C}$  NMR experiment cannot distinguish the different methylene groups included in Equations 4.20 to 4.27. What it can distinguish are

“linear”, “branched-1” and “branched-2” methylene groups (see Figures 4.1 and 4.2).

The formation of these three types of methylene structures is illustrated below:



The methylene structures formed from the reactions of methylol groups (UF<sub>1</sub> and UF<sub>2</sub>) with urea can produce only linear methylene species (Equations 4.21 and 4.23). These appear as a cluster of peaks centered at 47 ppm. However, the reactions of a methylol group with another methylol group can form linear, branched-1 and branched-2 methylene species as indicated above.

Due to the difficulty of determining the concentrations of each individual methylene species by the <sup>13</sup>C NMR method, calculation of rate constants for methylene formation during the condensation was not attempted.

### Summary and conclusions

The dynamic (RAPID) NMR data can be used to estimate kinetic parameters of

the UF reaction system at near commercial production conditions (temperatures up to 97°C and at high concentration). The differential method used can independently obtain the rate constants and activation energies of both the forward and back reactions for the UF<sub>1</sub> and UF<sub>2</sub> species formation. Data obtained are in good agreement with literature data obtained at lower temperature and concentration.

#### 4.5 QUANTITATIVE DETERMINATION USING THE STANDARD NMR METHOD

The dynamic (RAPID) NMR method developed in this research has proven to be an effective tool for monitoring the UF reaction process (Sections 4.3). However, for the samples which do not involve reactions, or for reactions which proceed very slowly under the NMR conditions (eg formaldehyde solution, final resins, or resins samples taken during a resin preparation and commercial resin samples), it is better to use the quantitative (STANDARD) NMR method, since this method can provide better quantitative results (standard deviation < 5%). In this section, quantitative (STANDARD) NMR analysis of resin samples taken during a resin preparation and of formaldehyde solutions were performed to confirm results obtained from the dynamic (RAPID) NMR method and to investigate the formaldehyde aging process.

##### 4.5.1 Quantitative Measurement Principle

As discussed in Section 3.3 Chapter 3, the area of a NMR peak ( $A_x$ ) (ie signal intensity,  $I_x$ ) is proportional to the carbon atom concentration contributing to the NMR signal. Therefore, in the quantitative NMR analysis (ie the STANDARD method with  $D_1 = 25$  sec) the normalised signal intensity of a species x is:

$$I_{xN} = A_{xN} = \frac{I_x}{I_D} = \frac{A_x}{A_D} = \frac{k_{zx}kC_x}{k_{zx}kC_D} = \frac{0.707kC_x}{0.704kC_D} = \frac{C_x}{C_D} \dots\dots\dots (4.29)$$

- where,  $I_{xN}$  is the normalised (relative to DMSO-d6) signal intensity of species x;
- $A_{xN}$  is the normalised integral (peak area) of species x;
- $I_x$  and  $I_D$  are the signal intensities of species x and DMSO-d6;
- $A_x$  and  $A_D$  are the integrals (peak areas) of species x and DMSO-d6;

$k_{zx}$  is the proportionality term as in Equation 3.5 for a species x  
(see Section 3.7 and Table 3.7);

$k$  is a concentration calibration constant (ideally  $k = 1.0$ );

$C_x$  is the carbon atom molar concentration of species x;

$C_D$  is the carbon atom molar concentration of DMSO-d6. Since there are two carbon atoms in a DMSO-d6 molecule,  $C_D$  is twice the molar concentration of DMSO-d6:  $C_D = 2 (W_D/M_D)$  ( $W_D$  and  $M_D$  are weight and molecular mass of DMSO-d6 respectively).

Equation 4.29 indicates that the normalised signal intensity of a species x ( $I_{xN}$ ) is equal to the ratio of the carbon atom concentration of species x to that of DMSO-d6 ( $C_x/C_D$ ). In reality,  $I_{xN}$  might not exactly equal  $C_x/C_D$ , though  $I_{xN}$  should be proportional to  $C_x/C_D$ . The relationship between  $I_{xN}$  and  $C_x/C_D$  may be expressed according to Equation 4.30:

$$I_{xN} = k_c \frac{C_x}{C_D} \dots\dots\dots (4.30)$$

Several experiments were performed to determine the value of  $k_c$  using a urea solution and a formaldehyde solution. The results of these experiments are given in Table 4.8. The data in this table confirm the prediction that the  $k_c$  value is not exactly 1.0. However, the difference from unity is not great (*c* 8%) and the average  $k_c$  value was found to be 1.08. Hence, the concentration of a species x, determined by the STANDARD NMR method, can be formulated according to Equation 4.30 as:

$$C_x = \frac{I_{xN}}{k_c} C_D = \frac{I_{xN}}{1.08} C_D = 0.926 I_{xN} C_D \dots\dots\dots (4.31)$$

**4.5.2 Quantitative NMR Investigation of UF Reaction Systems**

The resin samples used for the NMR experiments were a series of sub-samples taken at varying reaction times during a typical UF resin preparation. Resin preparation conditions and reaction times are given in Table 4.9. These conditions are similar to the conditions used in Section 4.3, except that a final addition of urea was

made to lower the final F/U molar ratio. An interpulse delay ( $D_1$ ) of 25 sec was used in STANDARD NMR experiments.

Table 4.8. Sample weights and STANDARD NMR data used to calculate  $k_c$ .

samples	sample wt	DMSO-d6	DMSO	$C_x/C_D$	$I_{xN}$	$k_c$
	(g)	(g)	(g)			
urea	0.7337	0.5290	--	0.505	0.557	1.10
	1.2335	0.5290	--	0.301	0.328	1.09
formaldehyde (48.3%, 2.0 mL, 2.243 g)	1.0835	0.9679	--	1.569	1.726	1.10
	1.0835	0.9679	0.4483 <sup>a</sup>	1.045	1.130	1.08
formaldehyde (45.1%, 2.0mL, 2.236 g)	1.0084	0.4908	0.2279 <sup>a</sup>	1.919	1.930	1.01
mean						1.08
RSD <sup>b</sup>						0.03

<sup>a</sup> Since DMSO (non deuterated) and DMSO-d6 were used as internal standard,  $C_D$  is the sum of the carbon atom concentrations of both in DMSO-d6 and DMSO; <sup>b</sup> RSD = relative standard deviation.

Table 4.9. Properties of UF1 resin sub-samples examined using the STANDARD NMR method.

sub-sample	time (min)	origin <sup>a</sup>	F/U ratio	viscosity (Pa·s)
UF1-02	36	alkaline addition	2.00	0.015
UF1-03	48	alkaline addition	2.00	0.025
UF1-04	61	acidic condensation	2.00	0.035
UF1-06	96	acidic condensation	2.00	0.110
UF1-07	112	acidic condensation	2.00	0.205
UF1-08	136	final resin	1.30	0.165 <sup>b</sup>

<sup>a</sup> initial addition stage: pH 8.9 for 50 min; condensation stage: pH 5.0 at 88°C;

<sup>b</sup> prior to the addition of final urea, the viscosity was 0.30 Pa·s.

Species concentrations ( $C_x$ ), expressed as mol g<sup>-1</sup> resin (due to the unreliability of mol L<sup>-1</sup> measurements for 'sticky' resin samples), were calculated using Equation 4.31 (see Section 4.5.1). Quantitative NMR data for resin samples (UF1-02 to UF1-08) are given in Table 4.10 to 4.15.

Generally, F/U molar ratios determined using the quantitative (STANDARD) NMR method agreed with the actual (feed) F/U molar ratio to within 5%. For example, the feed F/U molar ratio of sample UF1-02 was 2.0 (see Table 4.9), while that determined by NMR was 1.9 (see Table 4.10).

Table 4.10. Data determined for the UF1-02 resin sub-sample.

shift (ppm)	species	$I_{\text{XN}}$ (au)	F dist <sup>b</sup> (%)	$C_x$ ( $\times 10^{-3}$ mol g <sup>-1</sup> )
45.2-48.2	linear methylene	0.017	1.9	0.18
51.5-54.0	branched methylene	0.007	0.7	0.07
63.2-65.6	linear methylol	0.500	55.6	5.40
67.8-69.8	dimethylene ether	0.150	16.7	1.62
70.2-71.4	branched methylol	0.136	15.1	1.47
71.8-73.4	methylene in hemiformal	0.005	0.6	0.054
73.4-76.4	branched dimethylene ether	0.032	3.5	0.34
81.0-94.6	free formaldehyde	0.054	6.0	0.58
	total formaldehyde	0.900	100	9.71
54.0-56.0	methoxy	0.022		0.24
49.0-49.6	methanol	0.005		0.054
162.0-163.0	free urea	0.012		0.13
157.0-163.0	total carbonyl groups	0.470		5.07

F/U mole ratio = 1.9, free formaldehyde = 1.7% (w/w);

methylene/ether group mole ratio = 0.13

<sup>a</sup> Resin sample weight ( $W_s$ ) = 2.4345 g; DMSO-d<sub>6</sub> (1.0 mL) weight = 1.1942 g;

<sup>b</sup> F dist = formaldehyde distribution.

During the addition stage, unreacted (free) formaldehyde species were found to be present at levels of 4.2-6% of that originally added (Table 4.10 and 4.11). These levels typically represented 1.2-1.7% of the total resin weight. During the condensation stage, free formaldehyde levels rose to 3.9% of total resin weight, corresponding to 14.6% of the originally added formaldehyde. This increase can be attributed to condensation stage reactions leading to the dissociation of ether groups to form methylol groups and free formaldehyde (Kim 1999). Also, during the condensation stage, methylol groups may be demethylolated to form free formaldehyde (Kim 1999).

Table 4.11. Data determined for the UF1-03 resin sub-sample.

shift (ppm)	species	$I_{\text{XN}}$ (au)	F dist <sup>b</sup> (%)	$C_x$ ( $\times 10^{-3}$ mol g <sup>-1</sup> )
45.2-48.2	linear methylene	0.031	3.6	0.35
51.5-54.0	branched methylene	0.033	3.8	0.37
63.2-65.6	linear methylol	0.350	40.8	3.92
67.8-69.8	dimethylene ether	0.173	20.1	1.93
70.2-71.4	branched methylol	0.174	20.2	1.94
71.8-73.4	methylene in hemiformal	0.022	2.5	0.24
73.4-76.4	branched dimethylene ether	0.040	4.7	0.45
81.0-94.6	free formaldehyde	0.036	4.2	0.40
	total formaldehyde	0.860	100.0	9.60
54.0-56.0	methoxy	0.019		0.21
49.0-49.6	methanol	0.005		0.050
162.0-163.0	free urea	0.007		0.080
157.0-163.0	total carbonyl group	0.448		5.00

F/U molar ratio = 1.9; free formaldehyde: 1.2% (w/w) in resin

methylene / ether molar ratio = 0.30

<sup>a</sup> Resin sample weight (Ws) = 2.365 g; DMSO-d<sub>6</sub> (1.0 mL) weight = 1.199 g;

<sup>b</sup> F dist = formaldehyde distribution.

Data determined for the UF1-02 sample (Table 4.10) show that during the addition stage 70.7% of the added formaldehyde has been converted to methylol groups (including linear and branched methylol groups) and that 20.2% of the formaldehyde has been converted to ether groups, while methylene groups accounted for only 2.6% of the original formaldehyde. These results are consistent with those obtained using the dynamic (RAPID) NMR method (see Section 4.3).

Table 4.12. Data determined for the UF1-04 resin sub-sample.

shift (ppm)	species	$I_{xN}$ (au)	F dist <sup>b</sup> (%)	$C_x$ ( $\times 10^{-3}$ mol g <sup>-1</sup> )
45.2-48.2	linear methylene	0.054	7.1	0.60
51.5-54.0	branched methylene	0.059	7.7	0.66
63.2-65.6	linear methylol	0.221	28.9	2.46
67.8-69.8	dimethylene ether	0.162	21.2	1.80
70.2-71.4	branched methylol	0.123	16.1	1.37
71.8-73.4	methylene in hemiformal	0.022	2.9	0.25
73.4-76.4	branched dimethylene ether	0.052	6.8	0.58
81.0-94.6	free formaldehyde	0.073	9.5	0.81
	total formaldehyde	0.766	100.0	8.53
54.0-56.0	methoxy	0.018		0.20
49.0-49.6	methanol	0.003		0.033
157.0-163.0	total carbonyl group	0.394		4.38

F / U molar ratio = 2.0; free formaldehyde = 2.4% (w/w) in resin

methylene/ether molar ratio = 0.53

<sup>a</sup> Resin sample weight (Ws) = 2.3909 g; DMSO-d<sub>6</sub> (1.0 mL) weight = 1.2086 g;

<sup>b</sup> F dist = formaldehyde distribution.

The reaction profiles of methylol, methylene, ether and the methylene to ether (Me/E) group molar ratio are shown in Figures 4.52 to 4.55. These plots correspond closely to those obtained using dynamic NMR method (see Section 4.3), other than for the last data point (which was affected by a final urea addition). This supports the use of the dynamic (RAPID) NMR as a suitable method for monitoring the reaction processes.

Table 4.13. Data determined for the UF1-06 resin sub-sample.

shift (ppm)	species	$I_{\text{XN}}$ (au)	F dist <sup>b</sup> (%)	$C_x$ ( $\times 10^{-3}$ mol g <sup>-1</sup> )
45.2-48.2	linear methylene	0.062	8.3	0.74
51.5-54.0	branched methylene	0.148	19.9	1.77
57.6-63.0	branched methylene	0.037	5.0	0.44
63.2-65.6	linear methylol	0.128	17.2	1.53
67.8-69.8	dimethylene ether	0.080	10.7	0.95
70.2-71.4	branched methylol	0.132	17.7	1.57
71.8-73.4	methylene in hemiformal	0.020	2.7	0.24
73.4-76.4	branched dimethylene ether	0.023	3.1	0.27
77.1-80.0	methylene in hemiformal	0.006	0.8	0.07
81.0-94.6	free formaldehyde	0.109	14.6	1.30
	total formaldehyde	0.745	100.0	8.89
54.0-56.0	methoxy	0.034		0.41
49.0-49.6	methanol	0.009		0.10
157.0-163.0	total carbonyl group	0.369		4.40

F / U molar ratio = 2.0;

free formaldehyde = 3.9% (w/w) in resin (3.5% by chemical analysis)

methylene/ether molar ratio = 2.4

<sup>a</sup> Resin sample weight (W<sub>s</sub>) = 2.2449 g; DMSO-d<sub>6</sub> (1.0 mL) weight = 1.2172 g;

<sup>b</sup> F dist = formaldehyde distribution.

The spectra of two typical UF resin samples prior to, and after, the addition of final urea are shown in Figure 4.56. NMR signal assignments correspond to those shown in Figures 4.1 and 4.2 (see Section 4.2).

Signals attributable to free urea and monomethylolurea appear in the carbonyl region at 162.7 and 161.0 ppm respectively. Before the final urea addition only a broad signal, due to unresolved contributions from DMU, TMU and related long chain derivatives appeared in this region.

Table 4.14. Data determined for the UF1-07 resin sub-sample.

shift (ppm)	species	$I_{\text{XN}}$ (au)	F dist <sup>b</sup> (%)	$C_x$ ( $\times 10^{-3}$ mol g <sup>-1</sup> )
45.2-48.2	linear methylene	0.064	8.5	0.72
51.5-54.0	branched methylene	0.166	22.1	1.87
57.6-63.0	branched methylene	0.047	6.3	0.53
63.2-65.6	linear methylol	0.121	16.0	1.36
67.8-69.8	dimethylene ether	0.078	10.4	0.88
70.2-71.4	branched methylol	0.131	17.3	1.47
71.8-73.4	methylene in hemiformal	0.018	2.4	0.20
73.4-76.4	branched dimethylene ether	0.018	2.4	0.20
77.1-80.0	methylene in hemiformal	0.009	1.2	0.10
81.0-94.6	free formaldehyde	0.102	13.6	1.15
	total formaldehyde	0.754	100.0	8.48
54.0-56.0	methoxy	0.036		0.40
49.0-49.6	methanol	0.009		0.10
157.0-163.0	total carbonyl group	0.369		4.13

F/U molar ratio = 2.1;

free formaldehyde = 3.5% (w/w) in resin (3.8% by chemical analysis)

methylene/ether molar ratio = 2.9

<sup>a</sup> Resin sample weight ( $W_s$ ) = 2.350 g; DMSO-d<sub>6</sub> (1.0 mL) weight = 1.200 g;

<sup>b</sup> F dist = formaldehyde distribution.

In the methylene group region (45-95 ppm), a substantial increase in intensity of the linear methylol group peak at 65.0 ppm was accompanied by decreases in intensity of the free formaldehyde peaks which occurred in the 82-95 ppm region (see Figure 4.56).

Table 4.15. Data determined for the UF1-08 resin sub-sample.

shift (ppm)	species	$I_{\text{XN}}$ (au)	F dist <sup>b</sup> (%)	$C_x$ ( $\times 10^{-3}$ mol g <sup>-1</sup> )
45.1-48.2	linear methylene	0.108	18.0	1.13
51.5-54.1	branched methylene	0.120	20.1	1.26
57.6-63.0	branched methylene	0.015	2.6	0.16
63.3-65.7	linear methylol	0.246	41.2	2.58
67.8-70.0	dimethylene ether	0.061	10.2	0.64
70.0-71.9	branched methylol	0.032	5.4	0.34
72.1-73.4	methylene of methoxy	0.006	1.0	0.063
74.3-76.3	branched dimethylene ether	0.007	1.2	0.073
81.0-92.3	free formaldehyde	0.002	0.3	0.021
	total formaldehyde	0.597	100.0	6.27
54.1-55.8	methoxy	0.025		0.26
49.0-49.6	free urea	0.006		0.06
157.3-162.5	total carbonyl groups	0.485		5.09

F/U molar ratio = 1.2; free formaldehyde = 0.06% (w/w) in resin

methylene/ether molar ratio = 3.6

<sup>a</sup> Resin sample weight ( $W_s$ ) = 2.5147 g; DMSO-d<sub>6</sub> (1.0 mL) weight = 1.1996 g;

<sup>b</sup> F dist = formaldehyde distribution.

It is apparent that the final urea addition mainly affects methylol, methylene, free urea and free formaldehyde group levels and that it has little effect on ether group levels. For example, in sample UF1-07 and UF1-08, free urea increases from nil (undetectable) to  $0.06 \times 10^{-3}$  mol g<sup>-1</sup> (0.36 w/w % total resin weight), while the free formaldehyde levels decrease from 3.5% to 0.06 w/w % total resin weight.

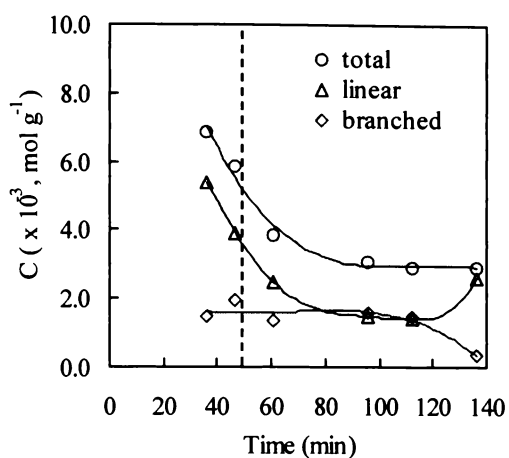


Figure 4.52. Plots of methylol group concentrations vs reaction time.

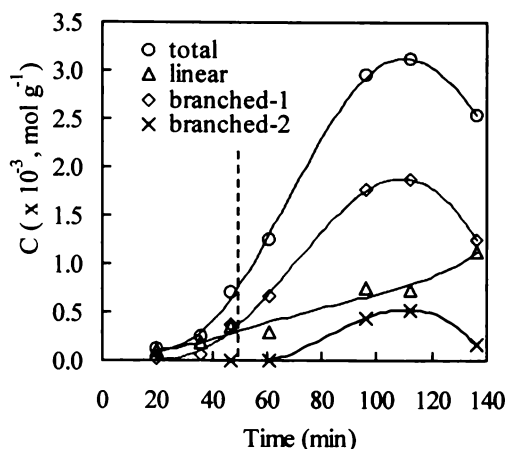


Figure 4.53. Plots of methylene group concentrations vs reaction time.

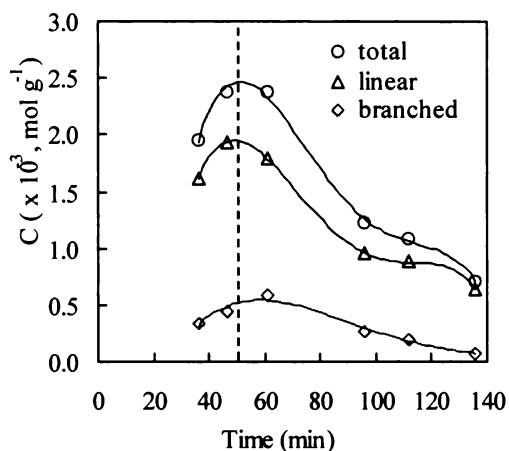


Figure 4.54. Plots of ether group concentrations vs reaction time.

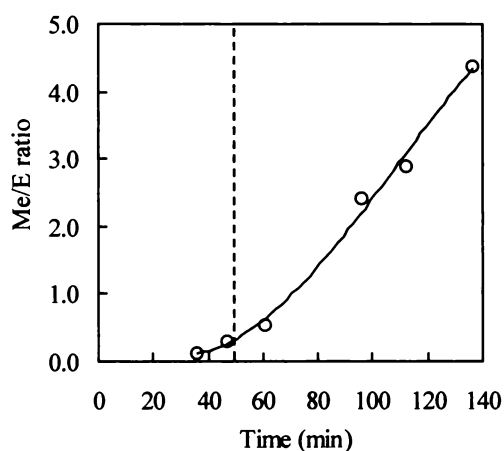
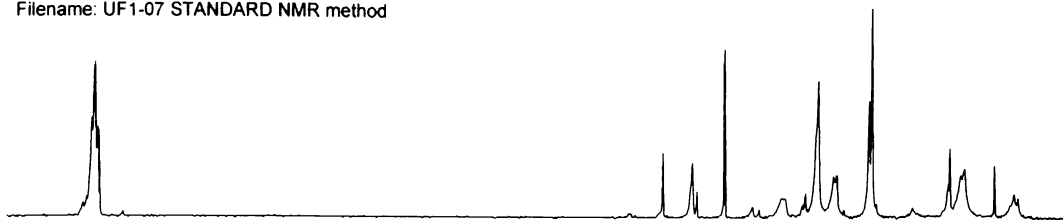


Figure 4.55. Plot of the methylene to ether (Me/E) molar ratio vs reaction time.

Since linear methylol and methylene groups increase following the final addition of urea, it appears that the additional urea mainly reacts with the free formaldehyde to form methylol groups (linear species) and methylene groups (linear species).

Filename: UF1-07 STANDARD NMR method



Filename: UF1-08 STANDARD NMR method

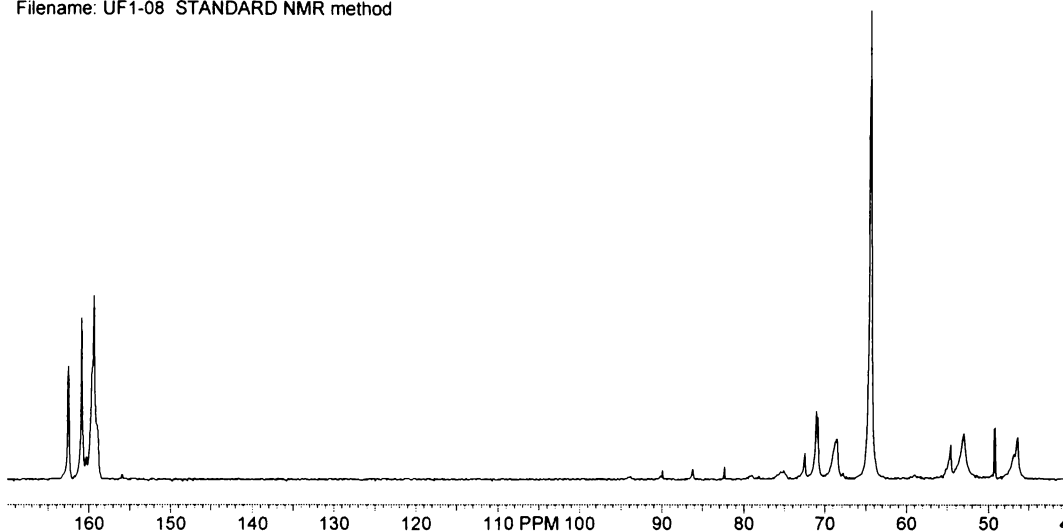


Figure 4.56.  $^{13}\text{C}$  NMR spectra of a typical UF resin sample before (upper spectrum) and after (lower spectrum) final urea addition.

Two factors may contribute to the decreases in branched methylol and branched methylene group levels. The first is the dilution effect, which is due to the addition of the final urea. The dilution effect may account for about 15% decrease in concentration (since the final urea addition accounts for about 15% of the total final resin weight). A second factor may be a change in the position of equilibrium brought about by additional urea. A substantial decrease in resin viscosity (typically from 0.30 Pa·s to 0.15 Pa·s) accompanied the final urea addition.

### 4.5.3 Quantitative Determination of the Composition of Formaldehyde Solution

The commercial formaldehyde solution used in this research normally contains 45-50% formaldehyde (weight % as HCHO) and < 3% methanol (weight % of the total methanol in the formaldehyde solution). The formaldehyde concentration (total

%), the percentage distribution of the four peak clusters (group-F1 to F4), the methoxy content (weight % calculated as methanol) and the free methanol content (weight %) can be determined using the quantitative (STANDARD) NMR method.

Results obtained for three formaldehyde solutions from different stocks have been given in Tables 4.16 to 4.18. Weight % of the formaldehyde solution is calculated as:

$$\text{Weight \%} = \frac{W_x}{W_F} \times 100 = 100 \times \frac{C_x M_x}{W_F}$$

where  $W_x$  and  $W_F$  are the weights (g) of species x and formaldehyde solution respectively;

$C_x$  is the molar concentration of species x determined according to Equation 4.31;

$M_x$  is the molar mass of species x.  $M_x = 30.03$  for formaldehyde species (F1 to F4) as HCHO, and  $M_x = 32.04$  for free methanol and 'methoxy' calculated as methanol (CH<sub>3</sub>OH);

100 is the conversion factor to %.

The data presented in Tables 4.16 to 4.18 show that the total formaldehyde concentrations determined using the NMR method agree well with those determined by chemical analysis. For example, the formaldehyde concentration determined by quantitative (STANDARD) NMR method is 47.4%, while chemical analysis gave a value of 46.5% (Table 4.16).

The formaldehyde distribution as F1 (ie methylene glycol) is from 15.9 to 20.3%, as F2 is from 51.4 to 52.8%, as F3 is from 25.6 to 29.7% and as F4 is from 1.35 to 2.98%. These results show that most of the formaldehyde is present as polymeric formaldehyde species and that batch to batch differences amongst F1 to F4 forms are not great (normally < 5%).

The total methanol (present as methoxy and free methanol) is about 1.7 to 3.3% whereas the free methanol content of formaldehyde solutions is only 0.11-0.27%. That is, most of the methanol (89.2-93.6%) present in a formaldehyde solution has

been converted to hemiformal (methoxyl) groups and only 6.4-10.8% of total methanol is present as free methanol.

Table 4.16. Quantitative (STANDARD) NMR data for formaldehyde solutions (part 1).

shift range (ppm)	species <sup>a</sup>	$I_{\text{XN}}$	F dist <sup>b</sup> (mol %)	weight % <sup>c</sup> (in the F solu.)
92.5-95.0	F4	0.120	2.98	1.42
88.6-92.0	F3	1.195	29.7	14.1
85.0-87.9	F2	2.068	51.4	24.4
81.4-83.8	F1	0.639	15.9	7.53
81.0-95.0	total	4.022	100.0	47.4
54.0-56.0	methoxy	0.127		1.60
49.0-49.6	methanol	0.008		0.11

<sup>a</sup> four clusters of formaldehyde species are designated as F1 to F4 (see Section 3.2); formaldehyde solution weight = 2.690 g (conc = 46.5%); DMSO-d<sub>6</sub> weight = 0.480 g; <sup>b</sup> F dist = formaldehyde distribution as % F1 to F4. <sup>c</sup> weight % as HCHO for formaldehyde species F1 to F4 and as CH<sub>3</sub>OH for methoxyl species.

Table 4.17. Quantitative (STANDARD) NMR data for formaldehyde solutions (part 2).

shift range (ppm)	species	$I_{\text{XN}}$	F dist (mol %)	weight % <sup>c</sup> (in the F solu)
92.5-95.0	F4	0.023	1.35	0.66
88.6-92.0	F3	0.437	25.6	12.5
85.0-87.9	F2	0.902	52.8	25.7
81.4-83.8	F1	0.348	20.3	9.92
81.0-95.0	total	1.710	100.0	48.8
54.0-56.0	methoxy	0.100		3.04
49.0-49.6	methanol	0.009		0.27

Note: formaldehyde: 2.2433g (conc = 48.30%); DMSO-d<sub>6</sub>: 0.9679 g;

Table 4.18. Quantitative (STANDARD) NMR data for formaldehyde solutions (part 3).

shift range (ppm)	species	$I_{\text{XN}}$	F dist (mol %)	weight % (in the F solu)
92.5-95.0	F4	0.043	2.22	1.00
88.6-92.0	F3	0.555	28.7	12.9
85.0-87.9	F2	1.022	52.8	23.8
81.4-83.8	F1	0.314	16.2	7.31
81.0-95.0	total	1.934	100.0	45.0
54.0-56.0	methoxy	0.092		2.14
49.0-49.6	methanol	0.011		0.26

Note: formaldehyde: 2.050 g (conc = 45.6%); DMSO-d<sub>6</sub>: 0.40 mL (0.480 g) + DMSO: 0.20 mL (0.225 g).

The quantitative (STANDARD) NMR method also can be used to determine the formaldehyde distribution as methylene glycol (HOCH<sub>2</sub>OH), bis(oxymethylene) glycol (HOCH<sub>2</sub>OCH<sub>2</sub>OH) and tris(oxymethylene) glycol (HOCH<sub>2</sub>OCH<sub>2</sub>OCH<sub>2</sub>OH) (see Figure 4.57). The NMR spectrum of a typical formaldehyde solution in the region from 80.0 to 95.0 ppm is shown in Figure 4.57. It is possible to determine the concentration of formaldehyde solution, present as polymeric forms of the type (HO(CH<sub>2</sub>O)<sub>n</sub>H) for n = 1-3. For n = 4 or higher, it is not possible to reliably determine individual concentrations due to peak overlap.

From Figure 4.57, it is apparent that the signal intensity of methylene glycol species ( $I_{\text{MG1}}$ ) is:

$$I_{\text{MG1}} = A_{82.5}$$

where “A” is the peak area of the chemical shift (ppm) designated by the subscript.

The signal intensity of bis(oxymethylene) glycol species ( $I_{\text{MG2}}$ ) is:

$$I_{\text{MG2}} = A_{85.8}$$

The signal intensity of tris(oxymethylene) glycol species ( $I_{MG3}$ ) is:

$$I_{MG3} = A_{86.4} + A_{89.0}$$

The formaldehyde distributions as methylene glycol, bis(oxymethylene) glycol and tris(oxymethylene) glycol species are given in Table 4.19.

NMR cannot reliably distinguish the higher polymeric forms of polyoxymethylene glycol ( $n > 3$ ) in a formaldehyde solution, however gas chromatography (GC) can. Therefore, the formaldehyde solutions were also analysed by gas chromatography-mass spectrometry (GC-MS). Since formaldehyde solutions are thermally unstable and depolymerise readily when separation is attempted by GC, it is standard practice to silylate hydroxyl groups present in the polymeric formaldehyde species using N,O-bis-(trimethylsilyl) trifluoroacetamide (BSTFA). Meyer (1978c) has reported that this reaction does not significantly disturb equilibrium levels of formaldehyde species. Replacement of the hydroxyl protons by trimethylsilyl ( $(\text{CH}_3)_3\text{Si}$ ) groups stabilises the formaldehyde polymers and prevent their decomposition on the GC column (Utterback *et al.* 1984).

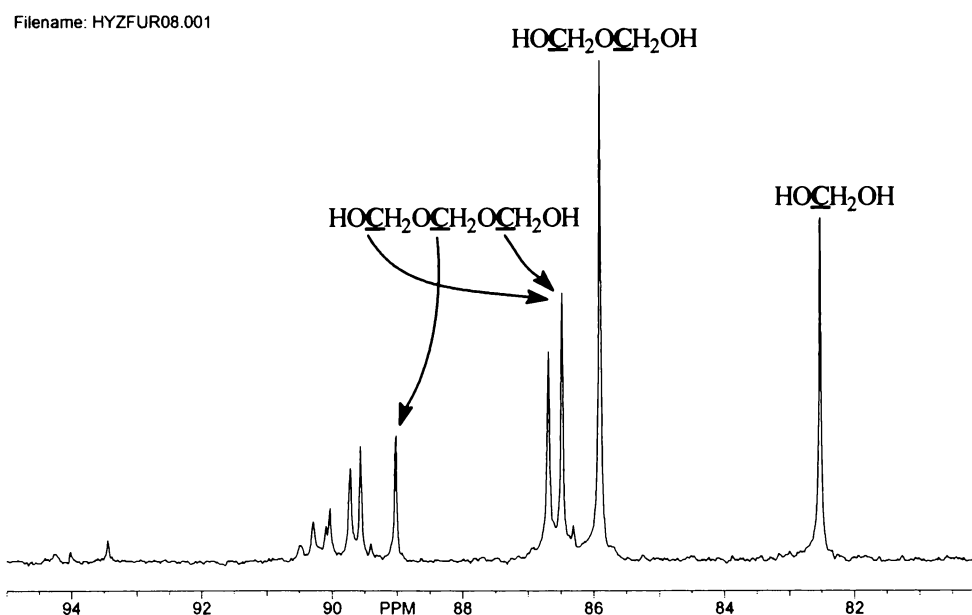


Figure 4.57. A typical NMR spectrum of a formaldehyde solution (80-95 ppm region).

Table 4.19. Distribution of polyoxymethylene glycol species in a formaldehyde solution at 55°C.

formaldehyde samples <sup>a</sup>	HO(CH <sub>2</sub> O) <sub>n</sub> H, %		
	n = 1	n = 2	n = 3
F solu (1) (46.5%)	15.8	21.8	17.8
F solu (2) (48.3%)	20.3	25.6	17.6
F solu (3) (45.6%)	16.2	24.9	18.8

<sup>a</sup> Formaldehyde solutions (F solu) are the same as those in Table 4.16 to 4.18.

A typical GC trace of a silylated formaldehyde solution is shown in Figure 4.58. The peaks attributable to different polymers of polyoxymethylene glycol were identified using a combination of retention time and MS data. Results are summarised in Table 4.20.

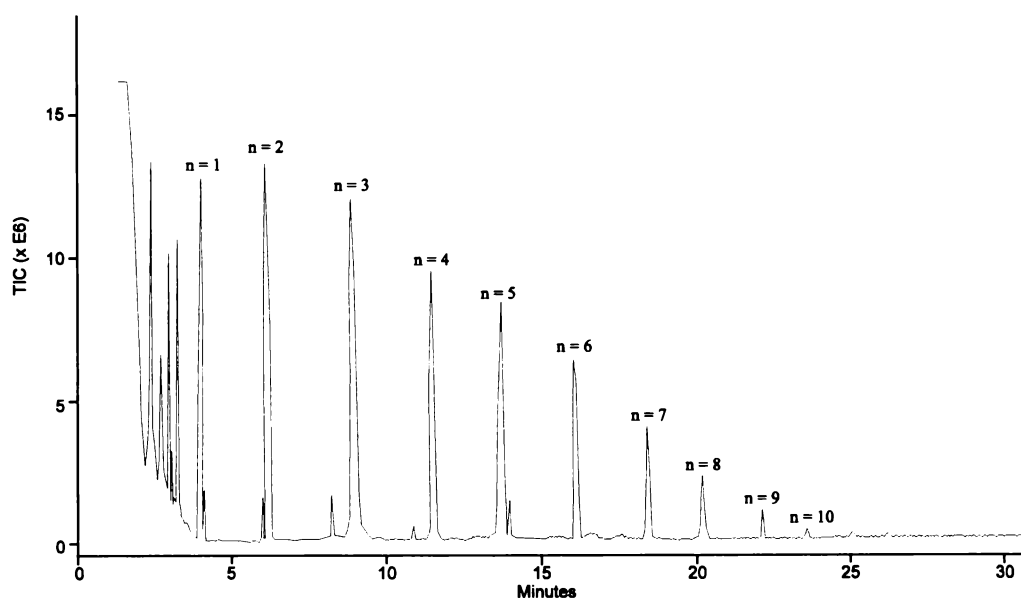


Figure 4.58. Gas chromatogram of silylated polyoxymethylene glycol (formaldehyde solution).

Table 4.20. Distribution (relative molar %) of polyoxymethylene glycol species in formaldehyde solution (F soln) determined by GC-MS.

n =	HO(CH <sub>2</sub> O) <sub>n</sub> OH								
	1	2	3	4	5	6	7	8	9
F solu (2)	21.5	24.8	19.9	14.7	8.9	6.2	2.9	1.0	0.1
F solu (3)	16.8	23.9	21.2	14.7	9.9	7.2	4.3	1.7	0.3

A comparison of NMR (Table 4.19) and GC-MS (Table 4.20) results shows that the distribution of methylene glycol (n = 1), bis(oxymethylene) glycol (n = 2) and tris(oxymethylene) glycol (n = 3) species agree to within 10-12%. This agreement is reasonable given that the data were obtained from two different instrumental methods and that the NMR peaks corresponding to bis- and tris(oxymethylene) glycols overlap slightly with other peaks (see Figure 4.57).

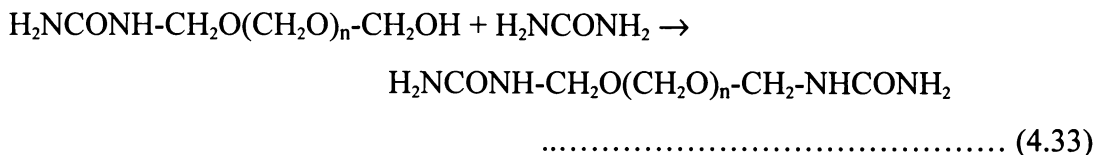
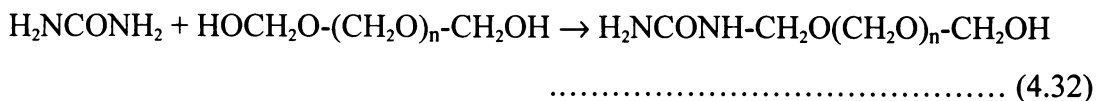
The data of Tables 4.16 to 4.18 also show that the distribution of F1-F4 formaldehyde species as determined by NMR differ for different batches of formaldehyde solution.

Formation of polymethylene glycols is influenced by many factors, including total concentration of the formaldehyde solution, temperature, additives (eg methanol) and aging (Meyer 1979c). It is therefore to be expected that the compositions of different batches will vary. Some preliminary investigations of the aging process are included in Appendix B. Generally, aging of formaldehyde raw materials has little effect on properties of the resins and resin bonded wood panels.

#### 4.6 ORIGIN OF ETHER GROUPS

The ether groups of UF resins may contain polyoxymethylene structures. The hydrolysis and dissociation of these linkages can be expected to adversely affect resin performance in terms of formaldehyde emissions and reduced durability. It was therefore of interest to use the dynamic (RAPID) NMR method to identify whether such polyoxymethylene groups were formed during UF preparation.

Aqueous formaldehyde is present mainly as polymeric analogues of (HOCH<sub>2</sub>-(OCH<sub>2</sub>)<sub>n</sub>-OCH<sub>2</sub>OH) where n is typically 1-9. These species may react directly with urea or amide groups as follows:



If these reactions occur, it can be anticipated that polyoxymethylene containing sub-units (eg -NHCH<sub>2</sub>O(CH<sub>2</sub>O)<sub>n</sub>CH<sub>2</sub>OH or -NH-CH<sub>2</sub>O(CH<sub>2</sub>O)<sub>n</sub>CH<sub>2</sub>-NH-) will be present during some phases of the polymerisation process. The possibility that these species might be identified by NMR analyses was therefore explored.

The NMR chemical shifts of species present in formaldehyde solutions are well established (Meyer *et al.* 1986, Dankelman *et al.* 1976, Dankelman and Daemen 1976). Typical species and chemical shifts are summarised in Tables 4.21 and 4.22.

It can be seen that the four characteristic clusters of signals observed for formaldehyde solutions arise from:

- Cluster-1 (F1): 82.5 ppm, methylene glycol units only;
- Cluster-2 (F2): 85.7 to 87.0 ppm, terminal methylol methylene carbon atoms (including dimethylene glycol (HOCH<sub>2</sub>OCH<sub>2</sub>OH));
- Cluster-3 (F3): 88.8 to 90.0 ppm, non-terminal methylene carbon atoms and the methylene carbon of formaldehyde hemiformal (see below);
- Cluster-4 (F4): from 93.3 to 94.0 ppm, methylene carbon atoms directly bonded to methoxy groups in polyoxymethylene hemiformals (CH<sub>3</sub>OCH<sub>2</sub>-(OCH<sub>2</sub>)-OH),

other than the methylene carbon atom of formaldehyde hemiformal ( $\text{CH}_3\text{O}\underline{\text{C}}\text{H}_2\text{OH}$ ) which is 89.9 ppm in the F3 chemical shift region.

Other polyoxymethylene hemiformal carbon resonances occur at 54.8-55.7 ppm (methoxyl carbons), 86.4-86.6 ppm (terminal methylene carbons) and 89.5-90.0 ppm (central methylene carbons).

A comparison of the structures and chemical shifts presented in Table 4.21 and Table 4.22 indicates that:

- 1) If reaction 4.32 occurs leading to the presence of  $-\text{NHCH}_2\text{OCH}_2\text{O}\dots\text{CH}_2\text{OH}$  groups in the reaction system, signals (which will not be concealed by signals from other more dominant resins species) should appear at *c* 69.1 ppm (linear ether region), 75.5 ppm (branched ether region), 86.4 ppm (terminal methylo groups in polyoxymethylene glycols) and possibly 89.3-90.0 ppm (central methylene groups of polymethylene glycols). The latter two chemical shift windows overlap parts of F2 and F3 signal regions of free formaldehyde.
- 2) If reaction 4.33 occurs leading to the presence of  $-\text{NH}-\text{CH}_2\text{OCH}_2\text{O}\dots\text{CH}_2-\text{NH}-$  groups in the reaction system, signals (which will not be concealed by signals from other more dominant resins species) should appear at 68.7 ppm (linear ether groups), 75.1 ppm (branched ether groups) and 90.0 ppm (central methylene carbons in polyoxymethylene glycols). The 90.0 ppm signals will overlap a part of F3 signal region of free formaldehyde.

Thus the presence of either, or both of reaction 4.32 and reaction 4.33 products will affect signal intensities appearing in either or both of the F2 and F3 chemical shift regions. There was no evidence of this, and in all the cases the free formaldehyde levels decreased with time, with no increases in F2 and F3 regions (see Figures 4.1 to 4.4 in Section 4.1 and Figure 4.56 in Section 4.4). These results indicate that the reactions 4.32 and 4.33 either occur very slowly, or not at all. Therefore, it can be concluded that the dimethylene ether groups present in UF resins are predominantly present as  $-\text{NH}\underline{\text{C}}\text{H}_2\text{O}\underline{\text{C}}\text{H}_2\text{NH}-$  and  $-\text{N}(-\text{CH}_2-)\text{CH}_2\text{OCH}_2\text{NH}-$  groups

(ie only one ether linkage). This is consistent with the reaction mechanism set out in Section 1.2.3.

Table 4.21.  $^{13}\text{C}$  NMR signal assignments for species present in formaldehyde solutions.

compound	n	structure and chemical shift (ppm)
HO-(CH <sub>2</sub> O) <sub>n</sub> OH	1	HOCH <sub>2</sub> OH ↑ 82.4
	2	HOCH <sub>2</sub> OCH <sub>2</sub> OH ↑     ↑ 85.7 85.7
	3	HOCH <sub>2</sub> OCH <sub>2</sub> OCH <sub>2</sub> OH ↑     ↑ 86.3 88.8
	4	HOCH <sub>2</sub> OCH <sub>2</sub> OCH <sub>2</sub> OCH <sub>2</sub> OH ↑     ↑ 86.5 89.3
	5	HOCH <sub>2</sub> OCH <sub>2</sub> OCH <sub>2</sub> OCH <sub>2</sub> OCH <sub>2</sub> OH ↑     ↑     ↑ 86.6 89.3 89.5
	6	HOCH <sub>2</sub> OCH <sub>2</sub> OCH <sub>2</sub> OCH <sub>2</sub> OCH <sub>2</sub> OCH <sub>2</sub> OH ↑     ↑     ↑ 86.7 89.5 89.7
	7	HOCH <sub>2</sub> OCH <sub>2</sub> OCH <sub>2</sub> OCH <sub>2</sub> OCH <sub>2</sub> OCH <sub>2</sub> OCH <sub>2</sub> OH ↑     ↑     ↑     ↑ 86.8 89.5 89.7 89.9
	> 7	HOCH <sub>2</sub> O-----OCH <sub>2</sub> O-----OCH <sub>2</sub> OH ↑                     ↑ 87.0                     90.0
CH <sub>3</sub> O(CH <sub>2</sub> O) <sub>n</sub> OH	1	CH <sub>3</sub> OCH <sub>2</sub> OH ↑     ↑ 54.8 89.9
	2	CH <sub>3</sub> OCH <sub>2</sub> OCH <sub>2</sub> OH ↑     ↑     ↑ 55.5 93.3 86.4
	3	CH <sub>3</sub> OCH <sub>2</sub> OCH <sub>2</sub> OCH <sub>2</sub> OH ↑     ↑     ↑     ↑ 55.6 93.8 89.5 86.5
	> 4	CH <sub>3</sub> OCH <sub>2</sub> O --- OCH <sub>2</sub> O --- OCH <sub>2</sub> OH ↑     ↑                     ↑                     ↑ 55.7 94.0                     90.0                     86.6

Table 4.22. Structural units which may be present in UF reaction systems and their chemical shifts.

terminal methylol containing structures	polyoxymethylene ether containing structures
$\begin{array}{c} \text{-NHCH}_2\text{OCH}_2\text{OH} \\ \uparrow \quad \uparrow \\ 69.1 \quad 86.4 \end{array}$	$\begin{array}{c} \text{-NHCH}_2\text{O---CH}_2\text{O---CH}_2\text{NH-} \\ \uparrow \quad \uparrow \\ 68.7 \quad 90.0 \end{array}$
$\begin{array}{c} \text{-NHCH}_2\text{OCH}_2\text{OCH}_2\text{OH} \\ \uparrow \quad \uparrow \quad \uparrow \\ 69.1 \quad 89.3 \quad 86.4 \end{array}$	$\begin{array}{c} \text{-N---CH}_2\text{O---CH}_2\text{O---CH}_2\text{NH-} \\   \quad \uparrow \quad \uparrow \quad \uparrow \\ \text{CH}_2 \quad 75.1 \quad 90.0 \quad 68.7 \\   \end{array}$
$\begin{array}{c} \text{-NHCH}_2\text{O---CH}_2\text{O---CH}_2\text{OH} \\ \uparrow \quad \uparrow \quad \uparrow \\ 69.1 \quad 90.0 \quad 86.4 \end{array}$	
$\begin{array}{c} \text{-N---CH}_2\text{OCH}_2\text{OH} \\   \quad \uparrow \quad \uparrow \\ \text{CH}_2 \quad 75.5 \quad 86.4 \\   \end{array}$	
$\begin{array}{c} \text{-N---CH}_2\text{O---CH}_2\text{O---CH}_2\text{OH} \\   \quad \uparrow \quad \uparrow \quad \uparrow \\ \text{CH}_2 \quad 75.5 \quad 90.0 \quad 86.4 \\   \end{array}$	

#### 4.7 SUMMARY AND CONCLUSIONS

The dynamic NMR method developed in this research proved to be an effective way of monitoring the reaction profiles of species formed during UF reactions. Optimum reaction conditions for the production of UF resins have been predicted using data from this method.

The kinetics of the formation of monomethylolurea and dimethylolurea have been determined and rate constants and activation energies obtained for near industrial conditions. The results are in satisfactory agreement with de Jong and de Jonge's (1952) data obtained at much lower concentrations and temperatures.

Quantitative (STANDARD) NMR experiments produced similar reaction profiles for the three key species in the UF reaction system. The results confirmed the validity of the dynamic NMR method.

The formaldehyde species in formaldehyde solution can include species of the form  $\text{HO}(\text{CH}_2\text{O})_n\text{H}$ . Quantitative (STANDARD) NMR provide information about species for  $n = 1$  to 3. GC-MS determines species with  $n = 1$  to 9.

Both dynamic (RAPID) and quantitative (STANDARD) NMR showed that the ether groups in the UF resins were present as the basic ether form:  $-\text{CH}_2\text{OCH}_2-$ . No polyoxymethylene glycol type ether groups were present.

## **CHAPTER FIVE**

# **HPLC, ESMS AND GPC ANALYSES OF UF RESINS**

## 5.1 INTRODUCTION

HPLC is an important technique for the separation and analysis of organic molecules. Kumim and Simonson (1980) have also used HPLC to obtain kinetic data from UF resin reaction systems. In this research, UF reactions carried out using different reaction conditions were investigated using HPLC methodology. The performance of the HPLC system was optimised using low molecular weight model UF resin species.

### *Principle of HPLC*

When a sample comprising of an analyte and an inert solvent is injected onto a HPLC column, the solvent is assumed not to interact with the stationary phase and to transverse the column with the mobile phase and emerges from the column after time  $t_0$  (the retention time of an unretained solute), while the analyte species emerges from the column at time  $t_r$  (analyte retention time). Subtraction of  $t_0$  from  $t_r$  affords the corrected retention time of the analyte.

$$\text{ie } t_r' = t_r - t_0 \quad \text{or} \quad t_r = t_r' + t_0$$

Ideally, a HPLC peak can be considered to be a Gaussian peak and to have a normal distribution of the analyte concentration in the column effluent given by expression (Heftmann 1983):

$$C = \frac{1}{F_L} \frac{Q}{\sigma_t \sqrt{2\pi}} e^{-\frac{(t-t_r)^2}{2\sigma_t^2}}$$

where  $C$  is the analyte concentration in the column effluent,

$F_L$  is the flowrate ( $\text{mL min}^{-1}$ ),

$Q$  is the mass of analyte injected into the column,

$\sigma_t$  is the standard deviation measured in time units (sec).

A Gaussian peak has the following properties:

$$w = 4 \sigma_t,$$

$$w_h = 2.354 \sigma_t$$

$$A = 2.507 C_{\max} \sigma_t$$

where  $w$  = peak width at base (base intercept);

$w_h$  = peak width at half-height;

$A$  = peak area;

$C_{\max}$  = the maximum concentration, ie the peak height.

### *Evaluation of column efficiency and resolution*

The efficiency of the HPLC column is typically expressed in terms of the number of (theoretical) plates ( $N$ ), or as the height equivalent of a theoretical plate (HETP). These two column efficiency parameters are given by the expressions:

$$N = 4 \left( \frac{t_r}{w_i} \right)^2 = 5.54 \left( \frac{t_r}{w_h} \right)^2 = 16 \left( \frac{t_r}{w} \right)^2$$

$$H = \frac{L}{N}$$

where  $w_i$  = peak width at inflection points

$H$  = height equivalent of a theoretical plate (ie HETP)

$L$  = column length.

The smaller the value of  $H$ , the smaller is the magnitude of band spreading per unit column length and the larger  $N$ . The larger  $N$  is, the greater the efficiency of the chromatographic system.

The resolution ( $R_s$ ) of a pair of peaks is given by the expression:

$$R_s = \frac{\Delta t_r}{\bar{w}} = \frac{2(t_{r1} - t_{r2})}{w_1 + w_2}$$

where  $\Delta t_r = t_2 - t_1$  = separation time difference between peaks 1 and 2;

$\bar{w} = (w_1 + w_2) / 2$  = mean width of peaks 1 and 2 at their bases.

Normally, if  $R_s \geq 1.5$ , the peaks are considered to be fully resolved (ie they are > 98% resolved at their bases).

## 5.2 EXPERIMENTAL CONDITIONS

HPLC analyses were performed using 300 mm  $\times$  2.1 mm, or 250 mm  $\times$  4.6 mm, Alltech Spherisorb 5  $\mu$ m polyethyleneimine (PEI) columns. General HPLC conditions are given in Section 2.2. Column performance was evaluated for flowrates in the range 0.10-0.40 mL min<sup>-1</sup> (300 mm  $\times$  2.1 mm column) and 0.60-2.0 mL min<sup>-1</sup> (250 mm  $\times$  4.6 mm column).

### 5.2.1 Influence of Acetonitrile to Water Ratio

Because of the polar nature of UF resins, acetonitrile/distilled water mixtures were chosen as the mobile phase. The influence of acetonitrile/water mixtures over the range 86/14 to 95/5 (w/w) on retention time and resolution characteristics were evaluated using urea, monomethylolurea (MMU) and dimethylolurea (DMU) as model analytes. HPLC traces are shown in Figure 5.1. Resolution data ( $R_s$ ) for urea and MMU are given in Table 5.1.

It is apparent (see Figure 5.1 and Table 5.1) that the greater the acetonitrile proportion, the greater the resolution of the urea and MMU peaks. Acetonitrile is, however, a poor solvent for higher molecular weight UF resin species. Increasing the water proportion of the solvent system improves the solubility of the UF resins, but lowers the resolution of low molecular weight resin components such as urea and

MMU. A further consideration is that a higher water contribution may result in higher molecular weight species being retained on the HPLC column. Therefore an acetonitrile/water ratio of 92/8 (w/w) was chosen as the 'routine' UF resin solvent system.

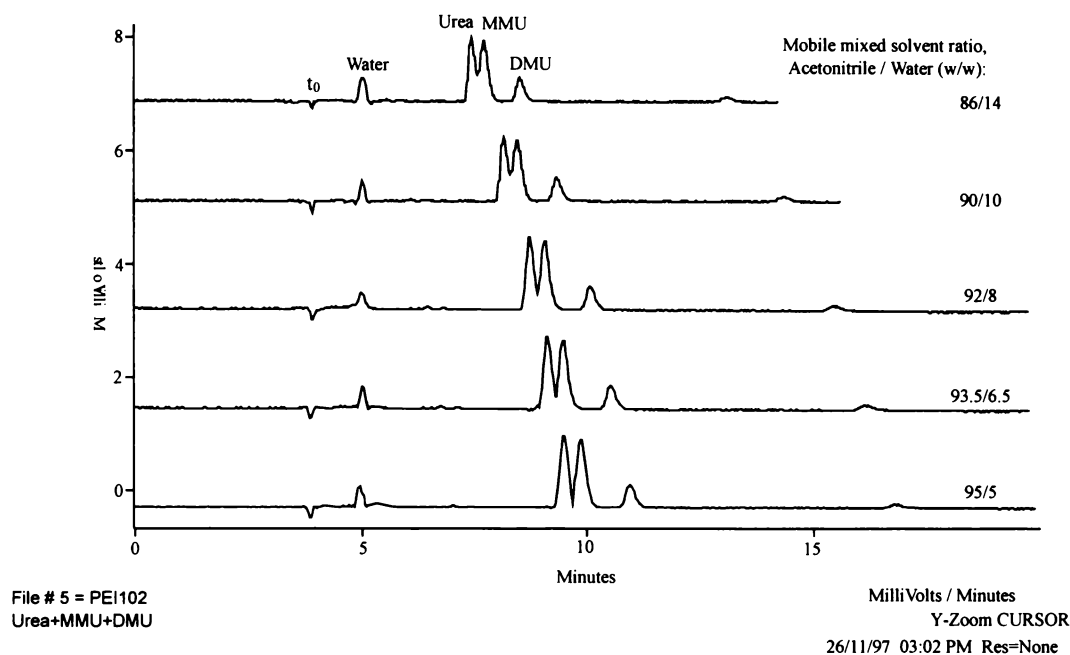


Figure 5.1. The effect of the acetonitrile/water ratio in a mixed solvent on the HPLC separation of urea, MMU and DMU.

Table 5.1. The effect of the acetonitrile/water ratio on the resolution ( $R_s$ ) of urea and MMU peaks in HPLC analysis.

acetonitrile/water ratio	86/14	90/10	92/8	93.5/6.5	95/5
resolution ( $R_s$ )	0.92	0.98	1.06	1.10	1.12

A major limitation of the HPLC technique for the investigation of UF resin systems, at least when using acetonitrile/water mixtures as solvent, is that samples have an enriched level of lower molecular weight species (< 500 Dalton) and a lower level of higher molecular weight species (> 500 Dalton), since acetonitrile/water mixtures do not dissolve higher molecular weight UF resin components. Thus while HPLC affords useful information in respect of the relative levels of low molecular weight species, it is less useful for higher molecular weight species.

## 5.2.2 Influence of Mobile Phase Flowrate

The flowrate of the mobile phase affects retention time and resolution characteristics. Results obtained for a 2/1 (w/w) mixture of urea and dimethylolurea (DMU) for flowrates of 0.20 to 2.0 mL min<sup>-1</sup> using the 250 mm × 4.6 mm 5 μm PEI column are given in Tables 5.2. HPLC profiles determined using the 250 mm × 4.6 mm 5 μm PEI column are shown in Figure 5.2.

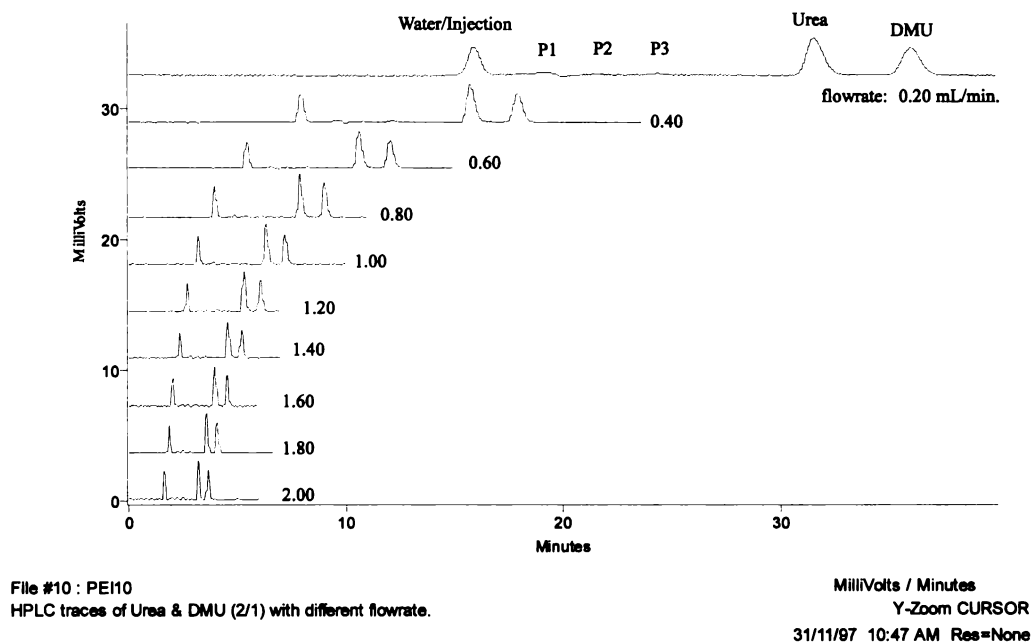


Figure 5.2. The effect of the flowrate on HPLC profiles determined using a 250 mm × 4.6 mm 5 μm PEI column and acetonitrile/water (92/8) (w/w) as the mobile phase.

Six peaks appeared in the HPLC profile of the reference urea and DMU sample (Figure 5.2). The peak with the smallest retention time arises from the presence of water in the solvent used to dissolve the reference sample. The next three weak peaks (P<sub>1</sub>, P<sub>2</sub> and P<sub>3</sub>) are attributable to trace impurities (eg biuret: H<sub>2</sub>NCO-NH-CONH<sub>2</sub>) in the reference urea and DMU samples. The 5<sup>th</sup> and 6<sup>th</sup> peaks arise from urea and DMU respectively.

Table 5.2. The effects of flowrate on the HPLC retention time ( $t_r$ ), peaks areas, and % peak area contributions.

Flowrate (mL min <sup>-1</sup> )	total area	P <sub>1</sub>			P <sub>2</sub>			P <sub>3</sub>			urea			DMU		
		$t_r$ (min)	area	area%	$t_r$ (min)	area	area%	$t_r$ (min)	area	area%	$t_r$ (min)	area	area%	$t_r$ (min)	area	area%
0.20	6.00	20.2	0.348	5.80	22.9	0.076	1.27	26.0	0.093	1.55	34.0	3.042	50.7	39.5	2.44	40.7
0.40	3.03	10.2	0.097	3.19	11.5	0.034	1.12	12.8	0.048	1.57	17.1	1.567	51.7	19.8	1.28	42.4
0.60	2.00	6.80	0.060	3.00	7.65	0.036	1.80	8.70	0.033	1.65	11.3	1.031	51.6	13.2	0.84	42.1
0.80	1.53	5.10	0.045	2.91	5.73	0.032	2.12	6.50	0.025	1.64	8.53	0.777	50.7	9.88	0.65	42.7
1.00	1.25	4.10	0.039	3.13	4.60	0.025	2.00	5.18	0.023	1.86	6.78	0.635	50.6	7.91	0.53	42.4
1.20	1.10	3.40	0.036	3.24	3.82	0.026	2.39	4.33	0.022	2.01	5.60	0.533	48.4	6.59	0.48	44.0
1.40	0.91	2.92	0.021	2.36	3.26	0.023	2.53	3.72	0.018	1.98	4.56	0.457	50.4	5.64	0.39	42.8
1.60	0.82	2.55	0.025	3.04	2.87	0.024	2.09	3.29	0.017	2.09	4.05	0.411	49.9	4.94	0.35	42.1
1.80	0.71	2.29	0.015	2.17	2.58	0.021	2.90	2.90	0.012	1.71	3.80	0.358	50.6	4.40	0.30	42.7
2.00	0.64	2.06	0.015	2.32	2.32	0.015	2.40	2.65	0.012	1.92	3.50	0.325	50.6	3.97	0.28	42.8
mean (n = 10) <sup>a</sup>				3.1			2.1			1.8			50.5			42.5
stdev				1.0			0.55			0.20			0.92			0.82
RSD				0.34			0.27			0.11			0.018			0.019
mean (n = 6) <sup>b</sup>				2.9			2.2			1.87			50.3			42.7
stdev				0.30			0.27			0.19			1.1			0.71
RSD				0.11			0.12			0.10			0.021			0.017

Column: 5  $\mu$ m 250 mm  $\times$  4.6 mm PEI, mobile phase acetonitrile/water 92/8 (w/w); RSD = relative standard deviation.; stdev = standard deviation;

<sup>a</sup> calculated for all data; n = number of data points; <sup>b</sup> calculated for flowrates of 0.6-1.6 ml min<sup>-1</sup>.

The integrated areas and % area contributions of the P<sub>1</sub>, P<sub>2</sub>, P<sub>3</sub>, urea and DMU peaks are listed in Table 5.2. The mean, standard deviation and relative standard deviation of the peak areas at flowrates of 0.6-1.6 mL min<sup>-1</sup> are also given in Table 5.2. The effects of mobile phase flowrate on t<sub>r</sub>, base peak width and the number of plates, for urea and DMU are given in Table 5.3. The plots of flowrate vs number of plates for urea and DMU are shown in Figure 5.3.

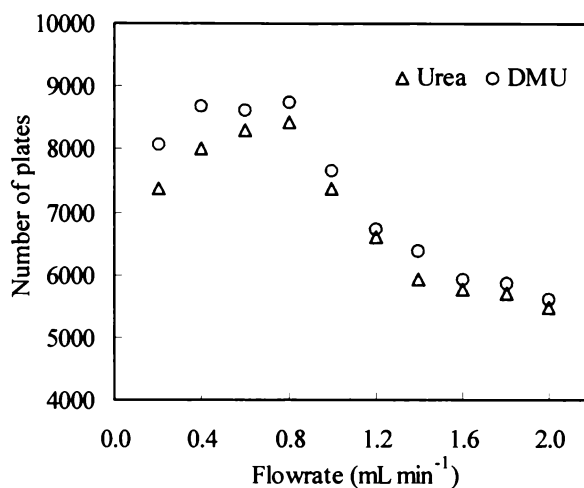


Figure 5.3. Plots of the number of plates vs flowrate for urea and DMU.

It is apparent (see Figure 5.2 and Table 5.2) that the lower the flowrate, the greater the retention times of the urea and DMU peaks and the greater the separation (min) between these peaks. Flowrate had only a minor effect on the % area contributions of the urea and DMU peaks. However, the RSD corresponding to typical practical flowrates (0.6-1.6 mL min<sup>-1</sup>) gives better RSDs. For example, the RSDs of the major urea and DMU peaks were 0.018 and 0.019 respectively for all data (flowrates of 0.2 to 2.0 mL min<sup>-1</sup>), or 0.021 and 0.017 respectively for ‘practical’ flow rates in the range 0.6-1.6 mL min<sup>-1</sup>. The RSDs of the three weak peaks (P<sub>1</sub>, P<sub>2</sub> and P<sub>3</sub>) were higher (between 0.11 and 0.34 for all data, or between 0.10 and 0.12 for flowrates in the range 0.6-1.6 mL min<sup>-1</sup>).

The area of each peak and also the total peak area decreased as the flowrate was increased. This is consistent with the well established inverse flowrate response of a differential refractive index (RI) detector (Viscotek 1996).

Table 5.3. The effect of the flowrate ( $F_L$ ) on retention time ( $t_r$ ), peak width at base ( $w$ ) and the number of plates ( $N$ ) for urea and DMU.

flowrate (mL min <sup>-1</sup> )	$t_0$ (min)	<u>urea</u>			<u>DMU</u>		
		$t_r$ (min)	$w$ (min)	$N$	$t_r$ (min)	$w$ (min)	$N$
0.20	15.60	34.0	1.59	7360	39.50	1.76	8060
0.40	7.85	17.1	0.76	8020	19.80	0.85	8690
0.60	5.37	11.3	0.50	8290	13.20	0.56	8620
0.80	3.96	8.53	0.37	8420	9.88	0.42	8750
1.00	3.20	6.78	0.32	7370	7.91	0.36	7660
1.20	2.67	5.60	0.28	6610	6.59	0.32	6730
1.40	2.28	4.60	0.24	5930	5.64	0.28	6380
1.60	2.03	4.05	0.21	5760	4.94	0.27	5930
1.80	1.81	3.80	0.20	5702	4.40	0.23	5870
2.00	1.63	3.50	0.19	5480	3.97	0.21	5590

The relationship between flowrate and number of plates ( $N$ ) for urea and DMU using the 5  $\mu\text{m}$  250 mm  $\times$  4.6 mm PEI column is depicted in Figure 5.3. The greatest number of plates for urea and DMU were *c* 8420 and 8750 respectively, at a flowrate of 0.8 mL min<sup>-1</sup>. When the flowrate was greater than 1.0 mL min<sup>-1</sup> the number of plates dropped sharply. Analyses using the 5  $\mu\text{m}$ , 250 mm  $\times$  4.6 mm, PEI column were therefore routinely performed using a mobile phase flowrate of 0.80 mL min<sup>-1</sup>.

Experiments performed using the 5  $\mu\text{m}$ , 300 mm  $\times$  2.1 mm PEI column, with flowrates of 0.10, 0.20 and 0.30 mL min<sup>-1</sup> gave results similar to those obtained using the 250 mm  $\times$  4.6 mm column. The number of plates for urea and DUM were highest (*c* 7000 and 7500 respectively) when the flowrate was 0.20 mL min<sup>-1</sup>. Analyses were therefore routinely performed on this column using a mobile phase flowrate of 0.20 mL min<sup>-1</sup>.

### 5.2.3 HPLC Analysis of Model UF Resin Compounds

The PEI HPLC columns separate species mainly according to their polarity. Higher polarity species are more strongly retained on the columns and elute later (ie  $t_r$  is greater). The polarity of urea, MMU, DMU and TMU increases in the order: urea, MMU, DMU and TMU, therefore urea elutes first, followed by MMU, DMU and TMU (see Figure 5.5).

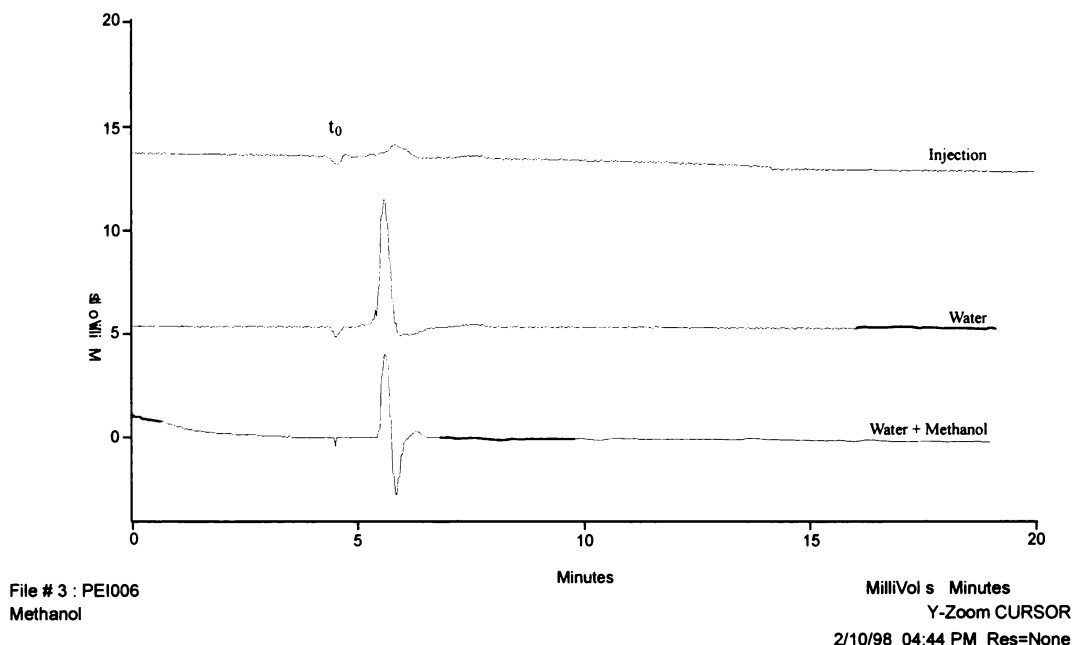


Figure 5.4. HPLC profiles determined for (a) blank (air), (b) water and (c) water/methanol injections.

HPLC conditions: 5  $\mu$ m 300 mm  $\times$  2.1 mm PEI column;  
solvent: acetonitrile/water = 92/8 (w/w), flowrate = 0.20 mL min<sup>-1</sup>.

In most cases the first baseline disturbance (retention time  $t_0$ ) observed in HPLC traces (see Figure 5.4) corresponds to low levels of air introduced during the injection process, and/or to solvent peak(s) eluting with the column void volume ( $V_0$ ) (Snyder and Kirkland 1974). When using a refractive index detector these peaks may appear as positive or negative peaks. A typical UF resin contains about 40% water. Injection of a sample containing a greater level of water increased the size of the positive component of the solvent peak which appeared shortly after the initial air (injection peak) (see Figure 5.4), while injection of an increased level of methanol enhanced the negative peak which eluted immediately after the water peak.

The relationship between  $t_0$  and  $V_0$  is given by the expression  $V_0 = t_0 F_L$  where  $F_L$  is the flowrate of the mobile phase solvent. The void volume of the  $5\ \mu\text{m}$   $250\ \text{mm} \times 4.6\ \text{mm}$  PEI column was  $3.15\ \text{mL}$ , for  $t_0 = 3.94\ \text{min}$  and  $F_L = 0.80\ \text{mL min}^{-1}$ , while the void volume of the  $5\ \mu\text{m}$   $300\ \text{mm} \times 2.1\ \text{mm}$  PEI column was  $0.90\ \text{mL}$ , for  $t_0 = 4.50\ \text{min}$  and  $F_L = 0.20\ \text{mL min}^{-1}$ .

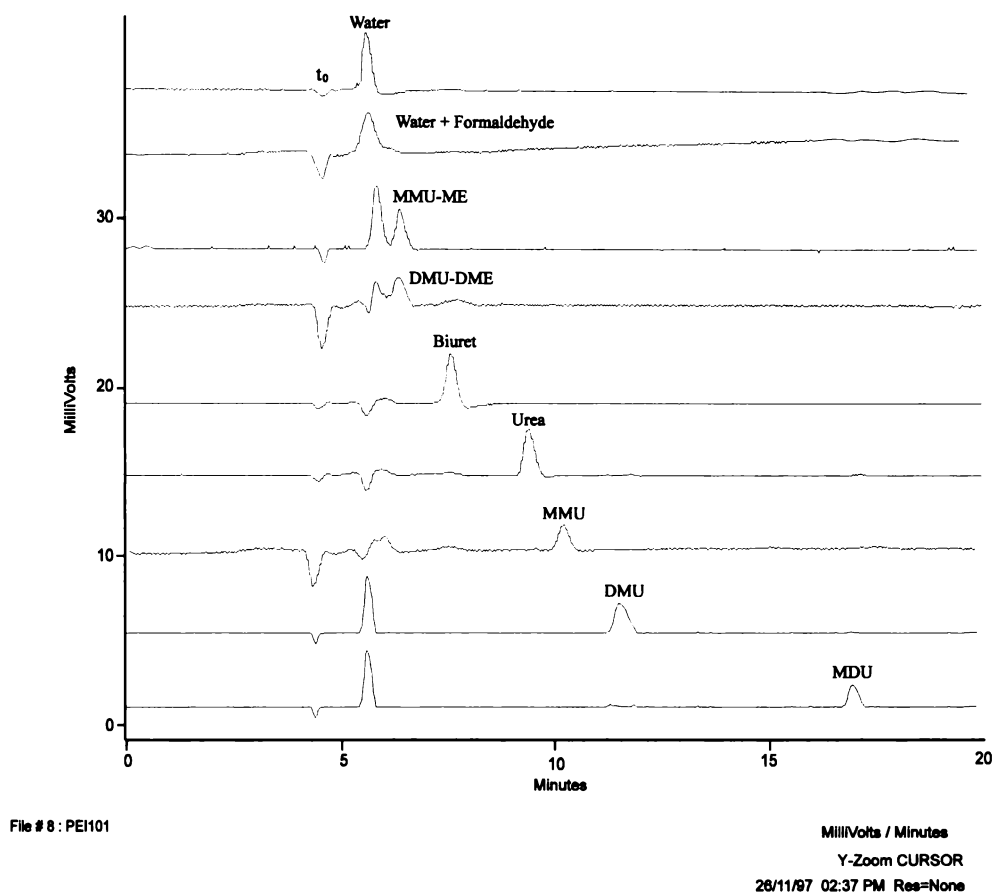


Figure 5.5. HPLC traces of model UF resin compounds.

HPLC conditions:  $5\ \mu\text{m}$   $300\ \text{mm} \times 2.1\ \text{mm}$  PEI;  
solvent: acetonitrile/water 92/8 (w/w), flowrate  $0.20\ \text{mL min}^{-1}$ .

The HPLC traces of model UF resin compounds are shown in Figure 5.5 and those of mixtures of model UF resin compounds are shown in Figure 5.6. The retention times of urea, biuret, MMU, DMU, monomethylolurea methyl ether (MMU-ME), dimethylolurea dimethyl ether (DMU-DME) and methylene diurea (MDU) which were utilised as model UF resin compounds, were found to be consistent to within  $\pm 2\text{-}3\%$  when using the same batch of mobile phase solvent, and to within  $c 5\%$  when a

different batch of mobile phase solvent was used. For example, the retention time of urea varied between 9.30 and 9.70 min using 5  $\mu\text{m}$  300  $\times$  2.1 mm PEI column.

Aqueous formaldehyde did not afford a distinct HPLC peak. It was also apparent (see Figure 5.6) that there were traces of biuret ( $t_r \approx 6.8$  min) and MDU ( $t_r \approx 15.2$  min) in commercial urea samples.

The assignment of the model UF resin compounds for the 250 mm  $\times$  4.6 mm and 300 mm  $\times$  2.1 mm columns were determined and are given in Tables 5.4 and 5.5 respectively.

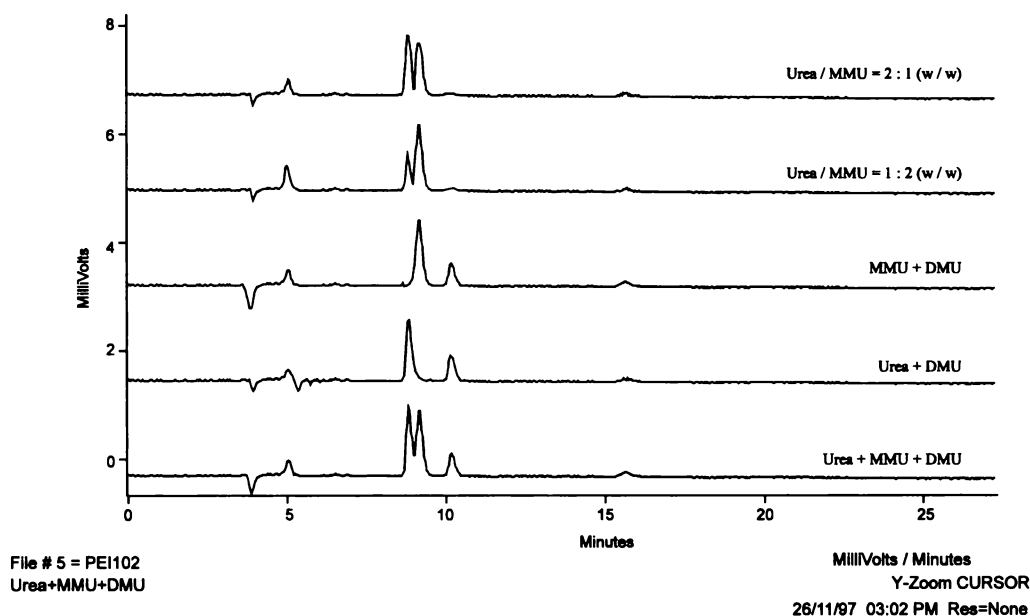


Figure 5.6. HPLC traces of mixtures of model UF resin compounds.

HPLC conditions: 5  $\mu\text{m}$  250 mm  $\times$  4.6 mm PEI;  
solvent: acetonitrile/water 92/8 (w/w), flowrate: 0.80 mL min<sup>-1</sup>.

Table 5.4. Retention times (min) of model UF resin compounds on a 5  $\mu\text{m}$  250 mm  $\times$  4.6 mm PEI column<sup>a</sup>.

species	water	MMU-ME	DMU-DME	biuret	urea	MMU	DMU	TMU	MDU
$t_r^b$ (min)	5.00	5.50	5.50	6.82	8.50	9.00	9.90	10.5	15.2

<sup>a</sup> mobile phase: 0.80 mL min<sup>-1</sup> acetonitrile/water (92/8) (w/w); <sup>b</sup> average of 5 injections.

Table 5.5. Retention times (min) of model UF resin compounds on a 5  $\mu\text{m}$  300 mm  $\times$  2.1 mm PEI column<sup>a</sup>.

species	water	MMU-ME	DMU-DME	biuret	urea	MMU	DMU	TMU	MDU
$t_r^b$ (min)	5.60	6.10-6.20	6.10-6.20	7.58	9.50	10.1	11.5	12.7	17.2

<sup>a</sup> mobile phase : 0.20 mL min<sup>-1</sup> acetonitrile/water (92/8) (w/w); <sup>b</sup> average of 5 injections.

#### 5.2.4 Refractive Index Detector Response Factors

The deflection type RI detector used for HPLC analyses detects differences in the RI of mobile phase and analyte containing mobile phase. Detector response is proportional to the concentration (ie mass) of analyte in the mobile phase (Waters Manual 1976, Viscotek Manual 1996). Detector response may be expressed as:

$$A \propto C V / F_L \propto M_s / F_L$$

where  $A$  is the peak area of the analyte species;

$C$  is the concentration of the sample solution;

$V$  is the injection volume;

$M_s = C V$ , is the mass injected into the column;

$F_L$  is the flowrate of the mobile phase.

At constant flowrate this expression simplifies to:

$$A \propto M_s = k_c M_s$$

where  $k_c$  is the response factor of the analyte species.

$k_c$  is proportional to the ratio  $dn/dc$  (ie the change in RI of the analyte relative to the change in concentration of the analyte). Since  $dn/dc$  ratios vary from solute to solute, the response factors are different for different species. It is necessary to determine an analyte RI response factor using an authentic specimen of the analyte.

Calibration curves for urea, MMU, DMU and MDU, determined using the 300 mm  $\times$  2.1 mm PEI column are presented in Figures 5.7 and 5.8. The corresponding

area ( $A$ ) vs mass ( $Q$ ) equations were:

for urea:

$$A = -0.003Q^2 + 0.442Q + 0.058 \quad (\text{for } Q \text{ up to } 60 \mu\text{g}, R = 0.999)$$

for MMU:

$$A = -0.001Q^2 + 0.229Q - 0.009 \quad (\text{for } Q \leq 30 \mu\text{g}, R = 0.998)$$

for DMU:

$$A = -0.001Q + 0.279Q + 0.023 \quad (\text{for } Q \leq 50 \mu\text{g}, R = 0.998)$$

for MDU:

$$A = -0.0003Q^2 + 0.197Q + 0.058 \quad (\text{for } Q \leq 3 \mu\text{g}, R = 0.996)$$

where  $A$  = HPLC peak area (mV min);

$Q$  = mass of the target (solute) species ( $\mu\text{g}$ );

$R$  = correlation coefficient.

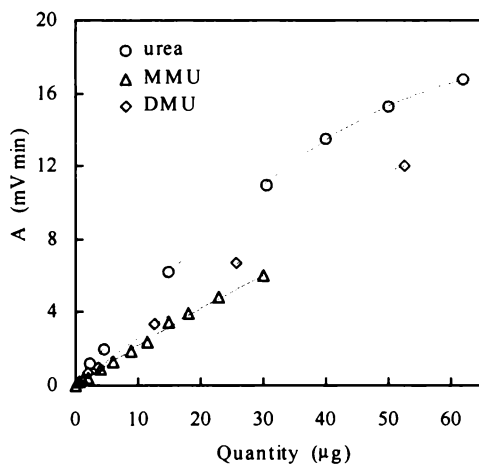


Figure 5.7. Calibration curves for urea, MMU and DMU.

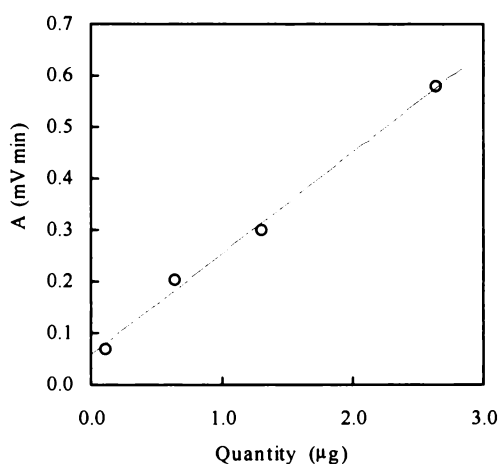


Figure 5.8. Calibration curve for MDU.

For all species, calibration curves were almost linear for the quantities less than 30  $\mu\text{g}$  (urea, MMU and DMU), or 3  $\mu\text{g}$  (MDU). The linearity range extended up to 50

$\mu\text{g}$  for DMU. Urea had the greatest response factor (for  $Q \leq 30 \mu\text{g}$ ), while MDU had the lowest response factor.

Since not all the peaks in a typical HPLC trace of an UF resin have been identified, the response factors of some resin species cannot be determined using authentic standards. In these circumstances concentrations were determined using peak areas normalised relative to the injected sample quantity ( $Q_s$ ), where the normalised peak area is the peak area ( $A$ , in  $\text{mV}\cdot\text{min}$ ) divided by the quantity ( $Q_s$ ) of the injected analyte (sample):

$$A_N = A/Q_s = A/(C \times V)$$

where  $A_N$  is the normalised peak area in  $\text{mV}\cdot\text{min mg}^{-1}$ ;

$A$  is the target compounds peak area in  $\text{mV}\cdot\text{min}$ ;

$Q_s (= C \times V)$  is the quantity (mass) of the sample compound

(concentration  $C \text{ mg } \mu\text{L}^{-1}$  and volume  $V \mu\text{L}$ ) injected into the HPLC column.

Provided that all the HPLC experimental conditions, eg RI detector's attenuator setting and mobile phase flowrate, are identical, the normalised peak areas are comparable.

### 5.3 GENERAL FEATURES OF THE UF RESIN REACTION SYSTEM AS ELUCIDATED BY HPLC

A typical HPLC trace of an UF resin has 10-20 peaks depending on the reaction stage of the resin. The HPLC traces of an UF reaction system during the addition stage and condensation stage are shown in Figures 5.9 and 5.10 respectively.

It can be seen that during the addition stage mainly three species, urea, MMU and DMU, present in the resin. Free urea decreases with time, while MMU and DMU increase with time at first and then decrease with time.

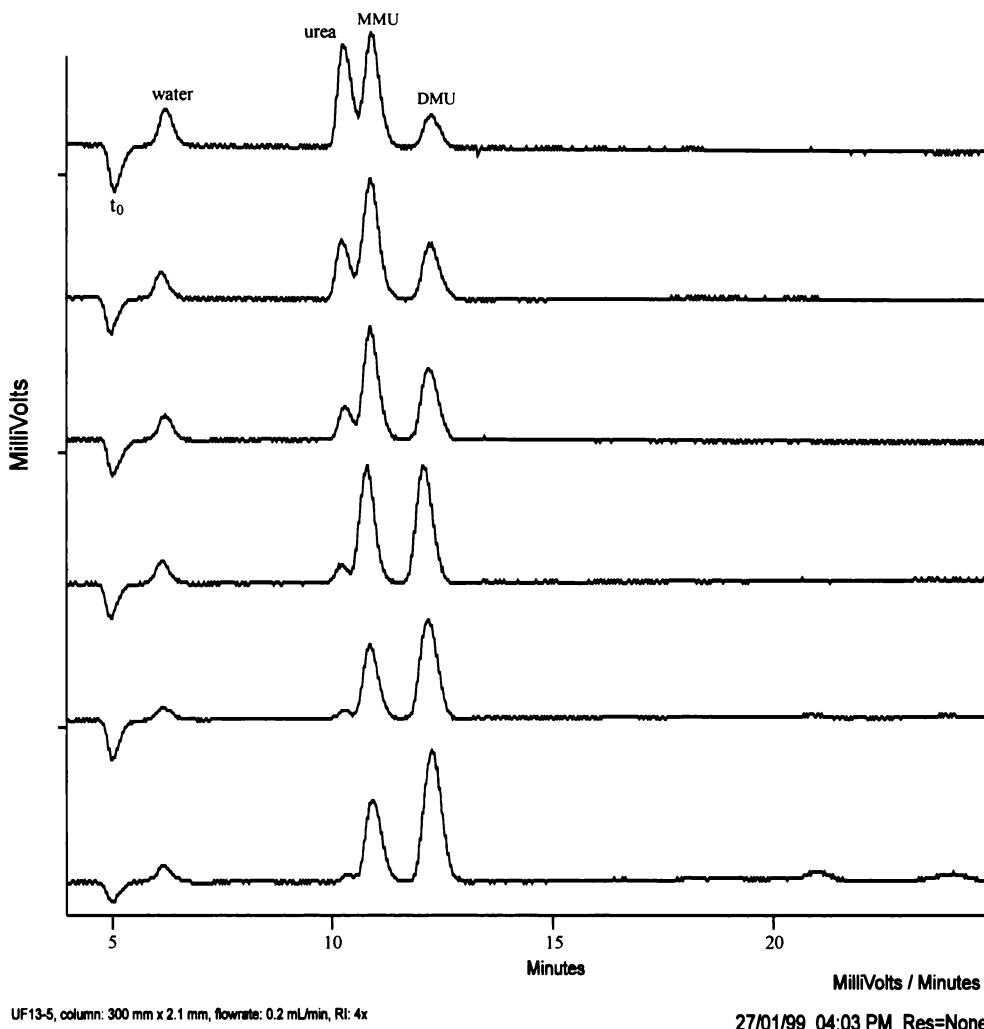


Figure 5.9. HPLC traces of an UF reaction system during the addition stage.

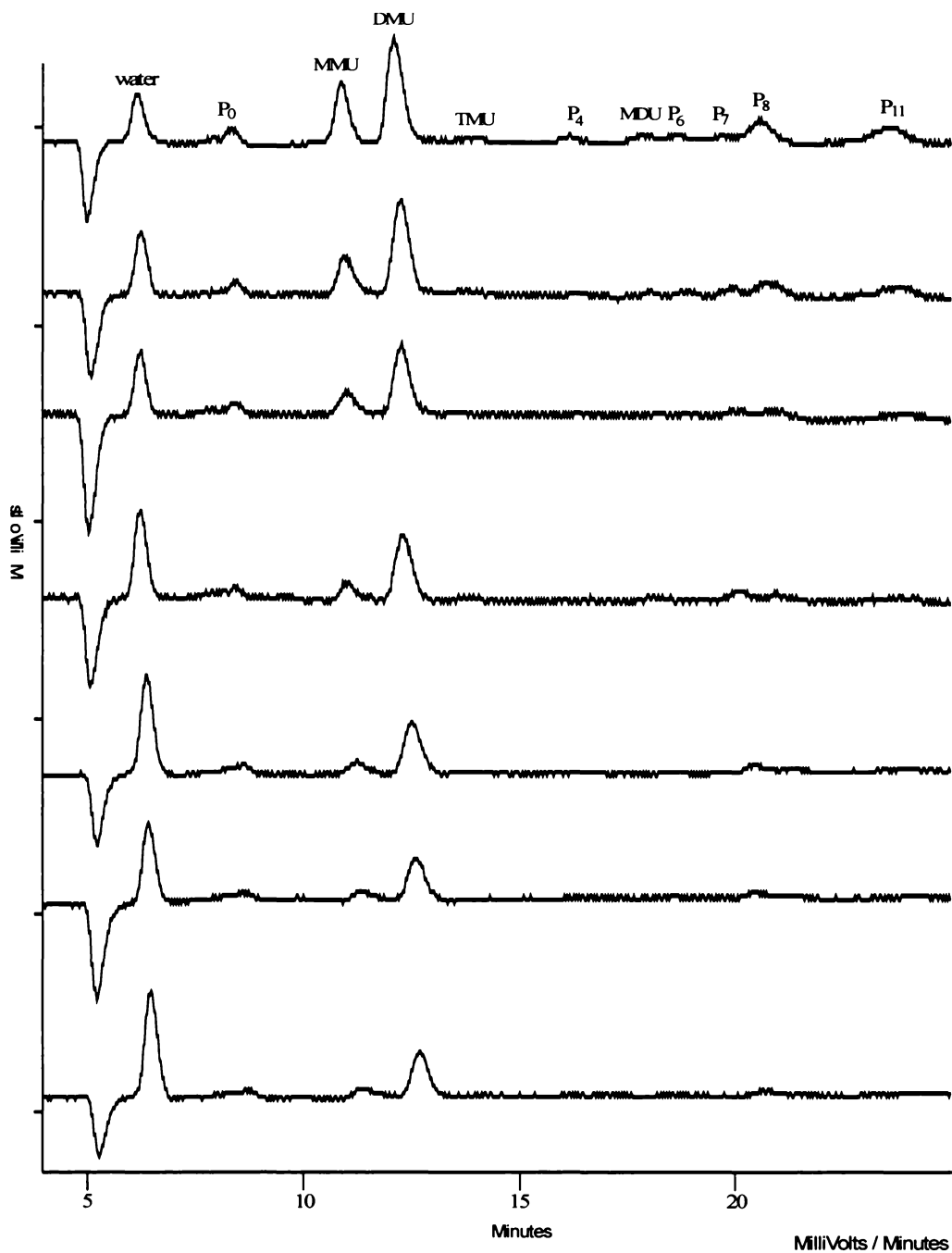
Reaction conditions: temp = 88°C, F/U ratio = 2.0, formaldehyde conc = 46.0%, initial addition pH = 8.7, reaction time corresponding to the traces from top to bottom are: 6.5, 10.6, 19.6, 24.7, 31.2 and 36.5 min respectively. HPLC conditions: column 300 mm × 2.1 mm, flowrate = 0.20 mL min<sup>-1</sup>, temp = 25°C.

#### *Free urea, MMU, DMU, TMU and MDU*

The plots of the normalised integrals ( $A_x$ ) of free urea, MMU and DMU vs times are shown in Figure 5.11. Those of TMU and MDU are shown in Figure 5.12.

From Figures 5.11 and 5.12, it can be seen that  $A_x$  of free urea decreases rapidly with time. Normally, after 40-60 min, free urea is undetectable. The  $A_x$ s of MMU and DMU increase rapidly with time during the early addition stage (15-17 min), reach a maximum, and then decrease throughout the rest of the addition stage and

condensation stage. The maximum  $A_x$  of MMU appears a few minutes earlier than that of DMU, however, its  $A_x$  is lower than that of DMU.



UF13, inj.=15uL, 300x2.1col., 0.2mL/min, RI: 4X

28/01/99 12:03 PM Res=None

Figure 5.10. HPLC traces of an UF reaction system during the condensation stage.

Reaction conditions: temp = 88°C, F/U ratio = 2.0, formaldehyde conc = 46.0%, initial addition pH = 8.7, condensation pH = 5.0, addition time = 32 min, reaction time corresponding to the traces from top to bottom are: 38.6, 50, 65.5, 111, 160, 182 and 199 min respectively. HPLC conditions: column 300 mm × 2.1 mm, flowrate = 0.20 mL min<sup>-1</sup>, temp = 25°C.

The plot of the of TMU vs time is similar with those determined for MMU and DMU, however its  $A_x$  is much lower than those of MMU and DMU (< 2% of MMU or DMU) (see Figure 5.12).

The plots of  $A_x$ s of urea and MMU vs reaction time are very similar to those obtained using dynamic NMR experiments (see Section 4.3). Comparison of the HPLC results with those obtained using dynamic (RAPID) NMR data, shows that HPLC is more suitable for determination of MMU, DMU and TMU levels, since during the condensation stage, MMU, DMU and TMU cannot be distinguished by NMR due to overlapping (poorly resolved) carbonyl carbon signals.

The  $A_x$  of MDU, ie the basic methylene species, increases with time during the addition stage. It increases with time during the early condensation stage, reaches a maximum and decreases with time for the rest of condensation. The decrease during the late condensation stage is due to its conversion to higher molecular weight methylene species.

Generally, the HPLC determined free urea, MMU, and TMU results are consistent with those obtained using dynamic NMR data (see Section 4.3).

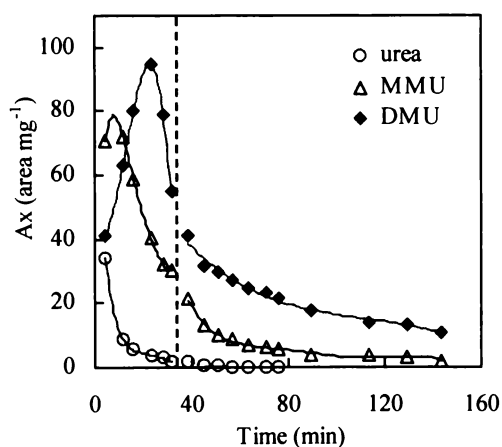


Figure 5.11. Plots of the  $A_x$ s of free urea, MMU and DMU vs reaction time.

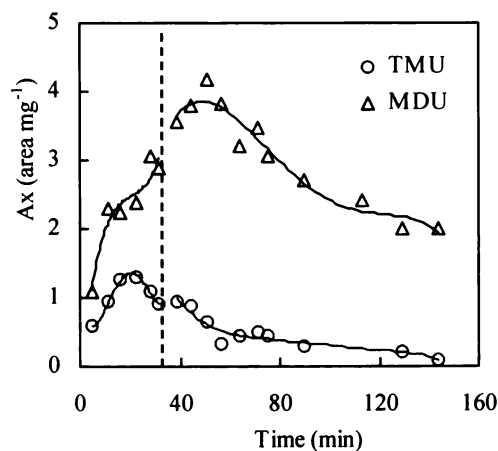


Figure 5.12. Plots of the  $A_x$ s of TMU and MDU vs reaction time.

*Other species*

The plots of  $A_{xS}$  of other species, including  $P_0$ ,  $P_4$ ,  $P_6$ ,  $P_7$ ,  $P_8$  and  $P_{11}$  are shown in Figures 5.13 and 5.14. The peaks of  $P_1$ ,  $P_2$  and  $P_3$  are too weak to give reliable information and they are excluded from the discussion.

Generally, the  $A_{xS}$  of  $P_0$ ,  $P_4$ ,  $P_6$ ,  $P_7$ ,  $P_8$  and  $P_{11}$  (see Figures 5.13 and 5.14) increase with time during the addition stage, and decrease with time, during the condensation stage.

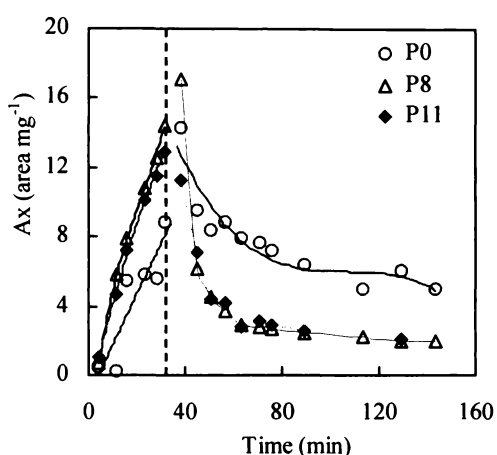


Figure 5.13. Plots of  $A_{xS}$  of  $P_0$ ,  $P_8$  and  $P_{11}$  vs reaction time.

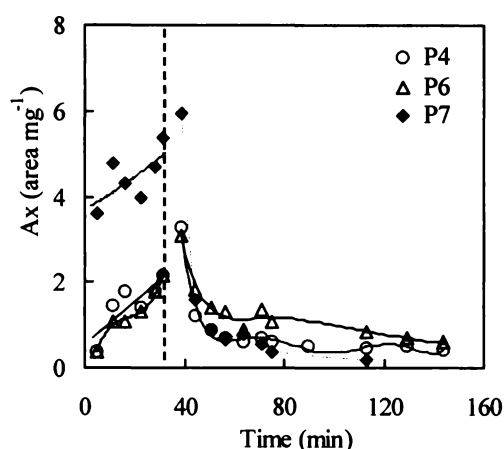


Figure 5.14. Plots of  $A_{xS}$  of  $P_4$ ,  $P_6$  and  $P_7$  vs reaction time.

*Effect of the addition of final urea*

The HPLC traces of a typical UF resin before and after the addition of the final urea are shown in Figure 5.15. A comparison of these traces shows that after the addition of final urea, the concentrations of free urea and MMU increase and that of DMU decreases. The increased MMU concentration arises from the reaction of urea with free formaldehyde forming new MMU. The decrease of other species is due to the addition of final urea (dilution effect). This result is consistent with the quantitative NMR experimental data (see Section 4.5.2).

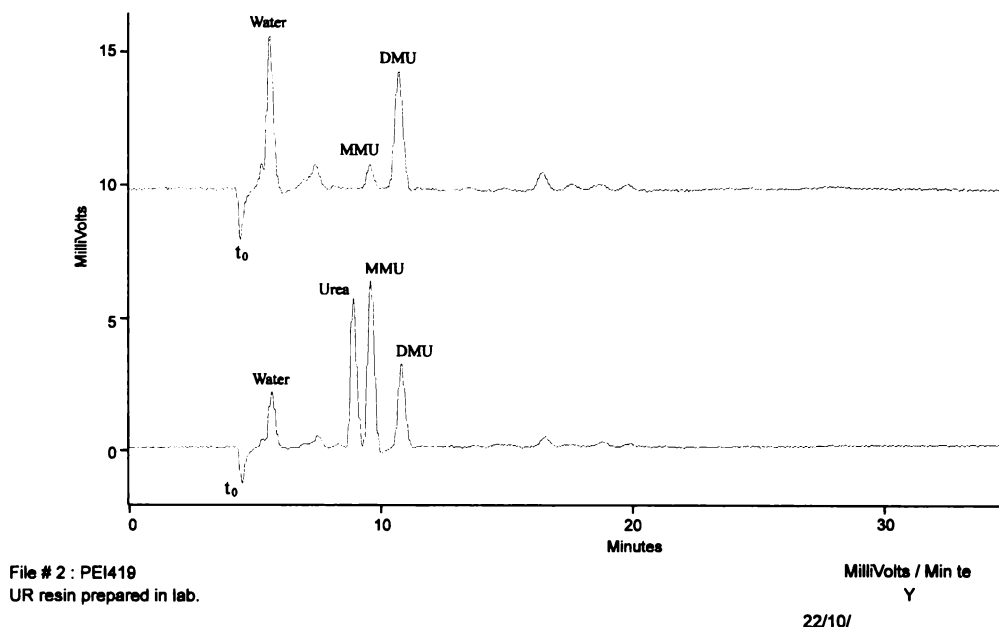


Figure 5.15. Typical HPLC traces of UF resins

Upper trace: UF resin at condensation stage, F/U ratio = 2.0;  
 lower trace: final UF resin, F/U ratio = 1.3; column: 300 mm × 2.1 mm ;  
 flowrate: 0.20 mL min<sup>-1</sup>; solvent: acetonitrile/water = 92/8 (w/w).

## 5.4 EFFECT OF REACTION CONDITIONS

The effect of reaction conditions on the levels of low molecular weight species detectable by HPLC methods (predominantly urea, MMU and DMU), are described in Sections 5.4.1 to 5.4.6.

### 5.4.1 Reaction Temperature

Common conditions for the reaction systems investigated in this sub-section were: F/U molar ratio = 2.0, formaldehyde concentration = 46%, initial addition pH = 8.7, condensation pH = 5.0 and addition time = 32 min.

The effect of reaction temperature on the free urea, MMU and DMU levels, (where  $A_x$  is the normalised peak area) vs reaction time, are shown in Figures 5.16, 5.17 and 5.18.

Similar free urea levels were observed for reactions performed at 80, 88 and 97°C

(see Figure 5.16). Using HPLC methodology, free urea could not be detected after 40 min.

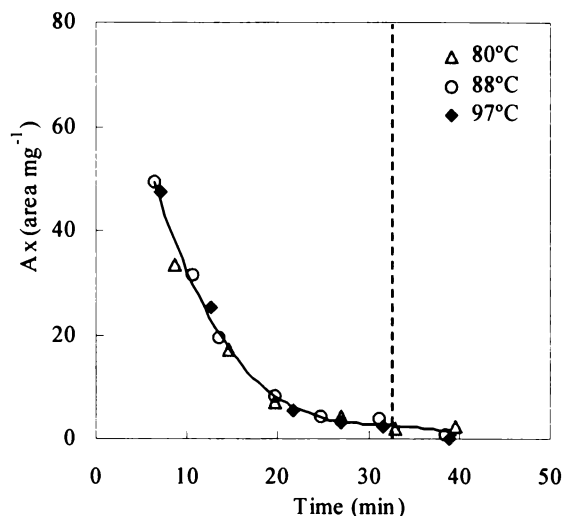


Figure 5.16. Plot of HPLC determined free urea levels vs reaction time for reactions performed at 80, 88 and 97°C (common curve applied to all data).

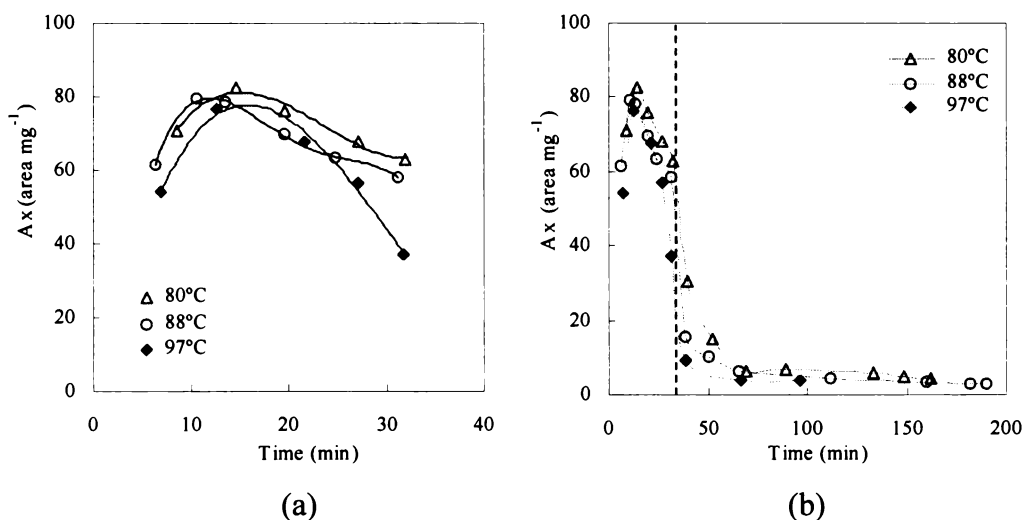


Figure 5.17. Plots of MMU levels vs reaction time during (a) the addition stage and (b) the entire reaction period.

The effect of reaction temperature (80, 88 and 97°C) on the MMU and DMU levels are shown in Figures 5.17 and 5.18. Reaction temperature has little effect on the level of MMU, which reaches a maximum after 15-18 min of the addition stage reaction. The higher the reaction temperature the earlier the maximum level of DMU

is observed. The MMU level of the 97°C reaction decreases more rapidly than is the case for the 80 and 88°C reactions.

During the late condensation stage there were no significant differences in the levels of DMU, or MMU, in the three reaction systems investigated (see Figures 5.17(b) and 5.18(b)).

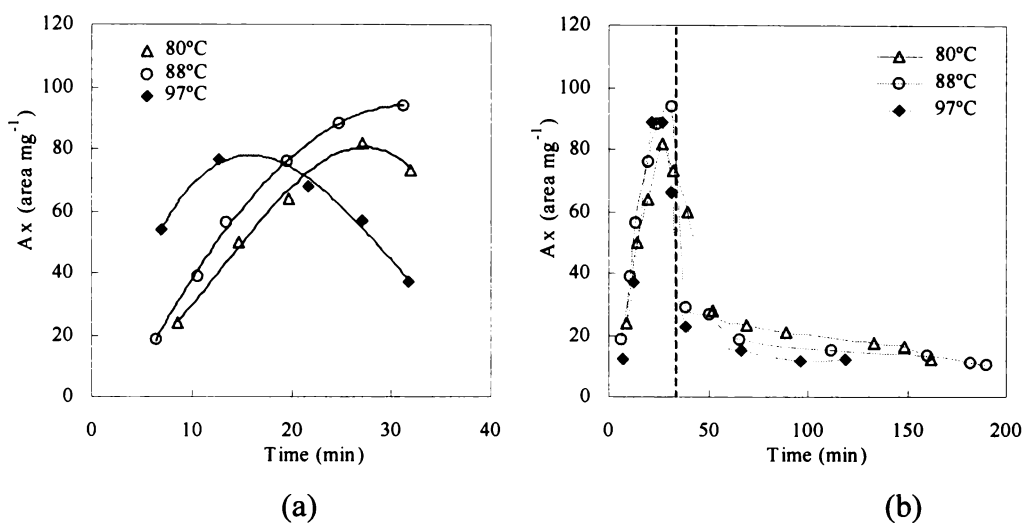


Figure 5.18. Plots of DMU levels vs reaction time during (a) the addition stage and (b) the entire reaction period.

#### 5.4.2 Addition Reaction Time ( $t_a$ )

Reaction conditions common to all the reactions in this sub-section are: F/U molar ratio = 2.0, formaldehyde concentration = 46%, reaction temperature = 88°C, initial addition pH = 8.7 and condensation pH = 5.0.

Since reaction conditions were identical other than for the addition stage reaction times ( $t_a$ ), it was expected that similar free urea, MMU and DMU would be observed. While this was the case for MMU and DMU, some scatter was observed however for free urea levels (see Figure 5.19). In all cases there was a rapid decline in free urea levels

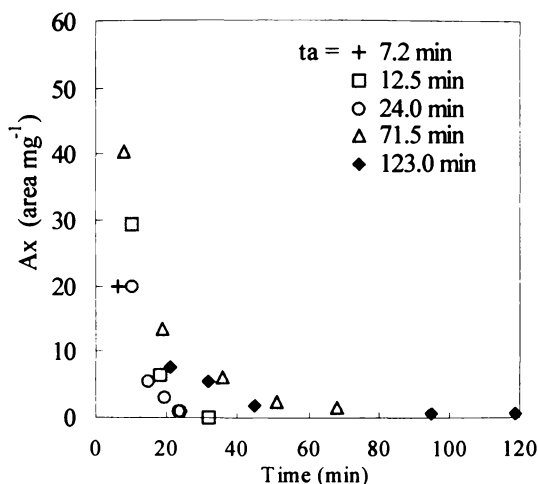


Figure 5.19. Plots of free urea levels during the entire reaction period for reactions with differing addition stage reaction times.

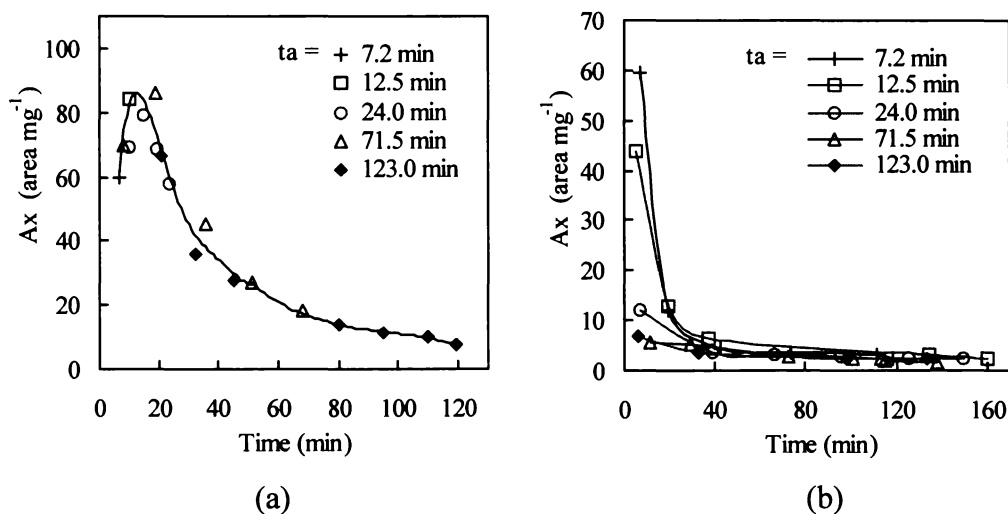


Figure 5.20. Plots of the effect of addition reaction time ( $t_a$ ) on MMU levels vs reaction time during (a) the addition stage and (b) the condensation stage.

Varying the addition stage reaction time mainly influences MMU and DMU levels during the early condensation stage (*c* 25 min) (see Figures 5.20 and 5.21). The shorter the addition reaction time, the higher the levels of MMU and DMU during the early condensation stage. After reaching their maximum values, MMU and DMU levels fall to similar levels, irrespective of the addition stage reaction time. This result is consistent with that determined using NMR data (see Section 4.3.2).

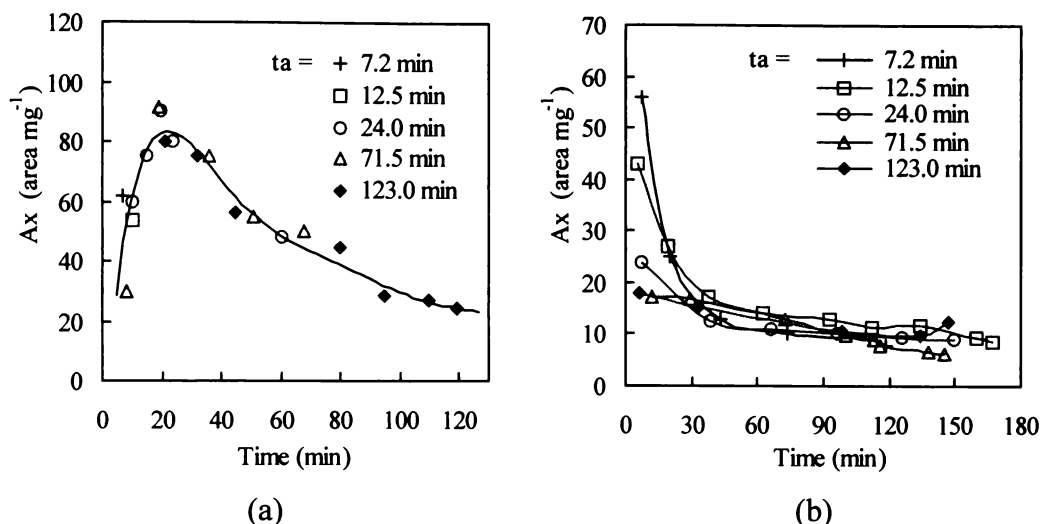


Figure 5.21. Plots of the effect of addition reaction time ( $t_a$ ) on DMU levels vs reaction time during (a) the addition stage and (b) the condensation stage.

#### 5.4.3 Formaldehyde Concentration

Conditions common for all the reactions in this sub-section are: F/U molar ratio = 2.0, initial addition pH = 8.7, condensation pH = 5.0, addition time = 32 min and reaction temperature = 88°C.

Similar free urea levels were observed for the reactions performed using 37% and 46% formaldehyde solutions (see Figure 5.22).

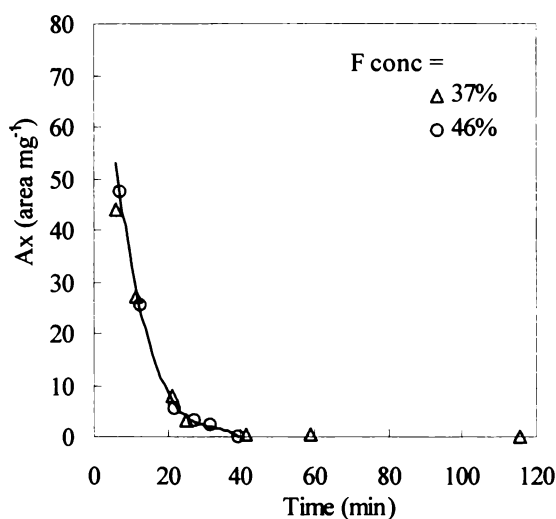


Figure 5.22. Plots of the effect of formaldehyde concentration (F conc) on free urea levels vs reaction time.

The effect of formaldehyde concentration on MMU and DMU levels are shown in Figures 5.23 and 5.24. The reaction with 46% formaldehyde afforded a higher addition stage DMU level, a lower condensation stage DMU level and a lower MMU level during the entire reaction period, than was the case for the reaction with 37% formaldehyde. These observations are consistent with dynamic (RAPID) NMR data (see Section 4.3.3).

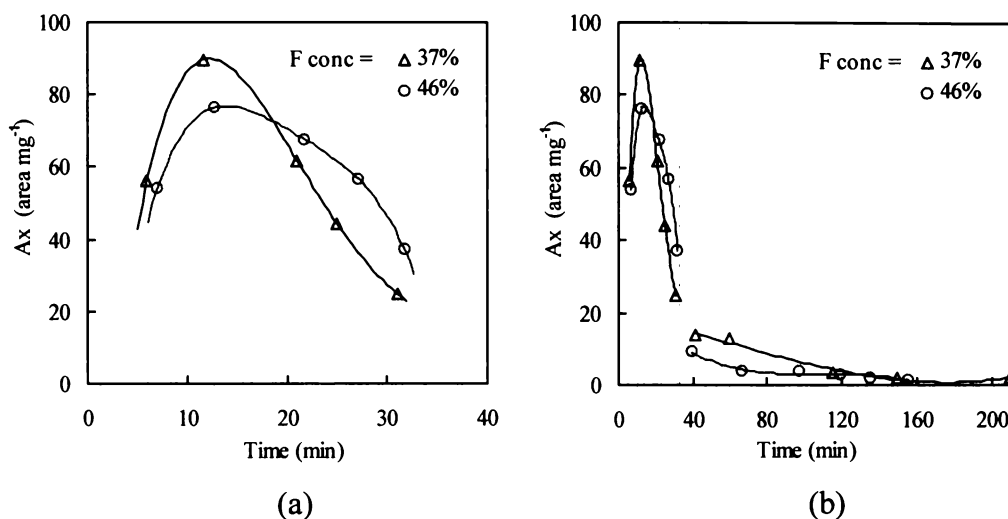


Figure 5.23. Plots of the effect of formaldehyde concentration (F conc) on the concentrations of MMUs vs reaction time during (a) the addition stage and (b) the entire reaction period.

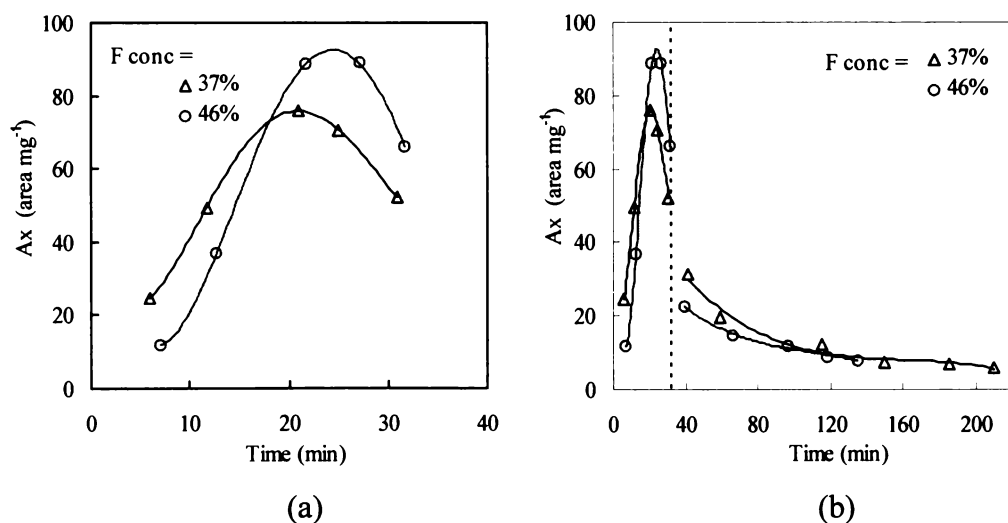


Figure 5.24. Plots of the effect of formaldehyde concentration (F conc) on the concentrations of DMUs vs reaction time during (a) the addition stage and (b) the entire reaction period.

#### 5.4.4 Initial Addition pH

Conditions common for all reactions in this sub-section are: F/U molar ratio = 2.0, formaldehyde concentration = 46%, condensation pH = 5.0, addition time = 32 min and reaction temperature = 88°C.

Similar free urea levels were observed for all the reactions performed using different initial addition pH (3.0-8.7) (see Figure 5.25).

The effect of the initial pH on MMU and DMU levels are shown in Figures 5.26 and 5.27. Initial pH had only a minor effect on MMU and DMU levels during the addition stage and no effect during the condensation stage.

MMU and DMU levels were slightly higher in the reaction with an initial pH of 8.7, compared to those of reactions with initial pHs of 3.0 to 7.3. No significant differences in MMU and DMU levels were observed in pH of 3.0, 5.0 and 7.3 reactions.

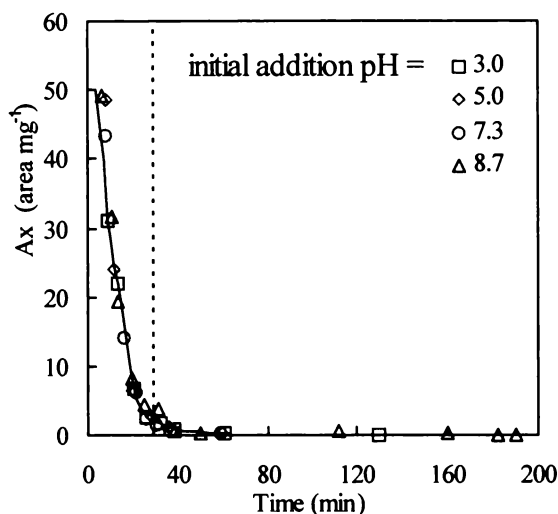


Figure 5.25. Plot of the effect of initial addition pH on free urea levels vs time.

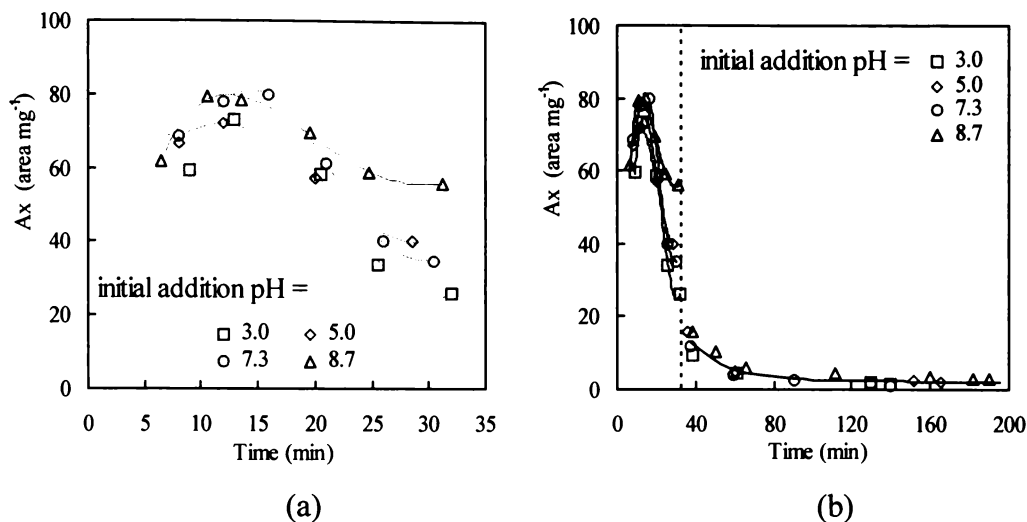


Figure 5.26. Plots of the effect of initial addition pH on the concentrations of MMUs vs reaction time during (a) the addition stage and (b) the entire reaction period.

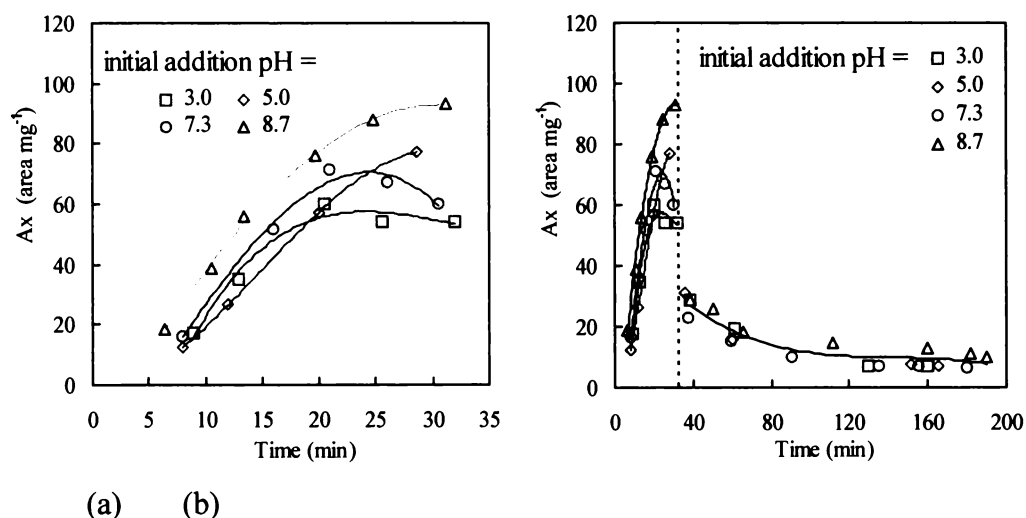


Figure 5.27. Plots of the effect of initial addition pH on the concentrations of DMUs vs reaction time during (a) the addition stage and (b) the entire reaction period.

### 5.4.5 Condensation pH

Conditions common for all reactions in this sub-section are: F/U molar ratio = 2.0, formaldehyde concentration = 46%, initial addition pH = 8.7, addition time = 32 min and reaction temperature = 88°C.

Since all the reaction conditions during the addition stage were identical, it was expected that similar results would be obtained (see Figures 5.28, 5.29 and 5.30). No significant differences in free urea levels were observed for reaction performed using condensation pHs of 4.3, 5.0 and 5.5 (see Figure 5.28).

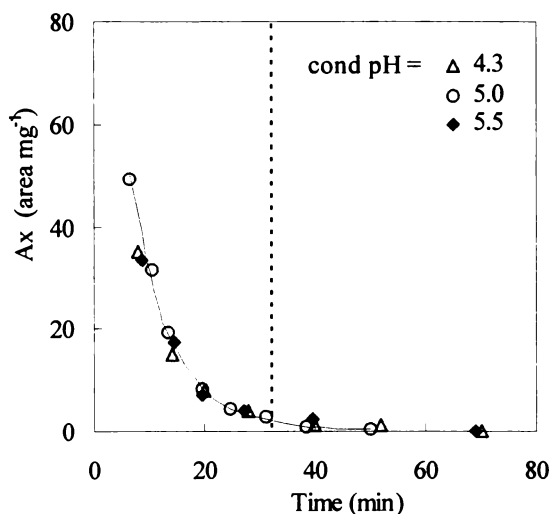


Figure 5.28. Plot of the effect of condensation pH on the free urea levels vs reaction time.

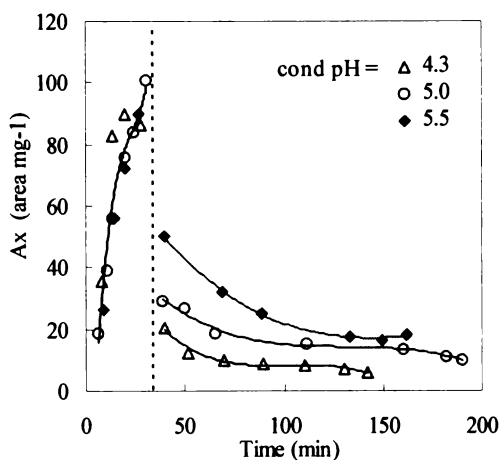


Figure 5.29. Plots of the effect of condensation pH on MMU levels vs reaction time.

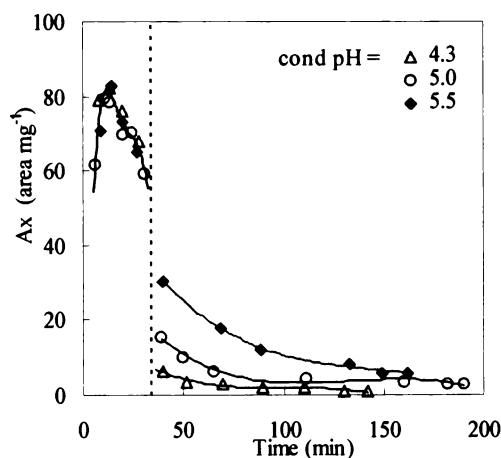


Figure 5.30. Plots of the effect of condensation pH on DMU levels vs reaction time.

The lower the condensation pH, the lower the MMU and DMU levels during the early condensation stage. However, differences were smaller during the late

condensation stage. This result is in agreement with dynamic NMR data (see Section 4.3.6).

#### 5.4.6 pH Control Methods

Conditions common for all the reactions in this sub-section are: F/U molar ratio = 2.0, formaldehyde concentration = 46%, initial addition pH = 8.7, condensation pH = 5.0, addition time = 32 min and reaction temperature = 88°C.

In conventional two-stage UF resin production, an initial alkaline addition stage (up to *c* pH 9), favouring the formation of methylol groups, is employed (see Section 4.3.5). During the addition stage, pH decreases with time (see Figure 4.36). Lower pH reduces the methylol formation rate and increases the ether formation rate.

Szesztay *et al.* (1994) has investigated the use of a buffer system to keep the pH relatively constant during the addition stage. The use of low concentrations (eg < 0.5%) of buffer systems comprised of organic acids, and their salts, did not stabilise the pH during the addition stage, while the use of higher concentrations of the buffer system afforded resins which had inferior wood panel bonding characteristics (Szesztay *et al.* 1994).

In this research addition of NaOH (5 mol L<sup>-1</sup>) solution was used to maintain the reaction stage between pH 8.3 and 8.6. In the absence of pH control, pH falls from 8.7 to 6.2.

Free urea levels did not show much difference using the ‘pH adjusted’ (or pH controlled) and ‘conventional’ methods (see Figure 5.31). However significant differences were apparent in MMU and DMU levels (see Figures 5.32 and 5.33). The pH adjusted reaction afforded lower MMU and higher DMU levels during both the addition stage and condensation stages. A greater level of DMU was produced, at an earlier stage (time), in the pH adjusted reaction. These observations are consistent with the base catalysed nature of methylol group formation. (Pizzi 1983 and Meyer 1979b).

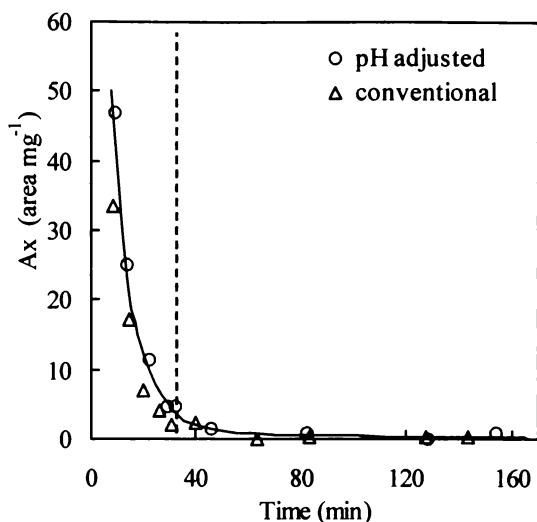


Figure 5.31. Plot of the effect of addition pH control on free urea levels vs reaction time.

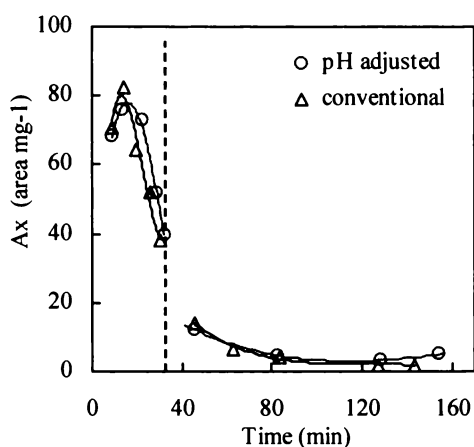


Figure 5.32. Plots of the effect of addition pH control on MMU levels vs reaction time.

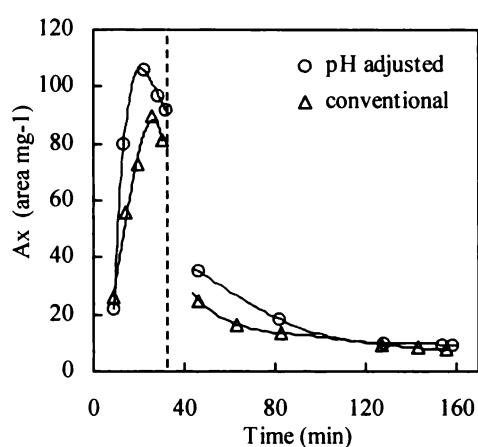


Figure 5.33. Plots of the effect of addition pH control on DMU levels vs reaction time.

#### 5.4.7 Summary

The HPLC columns and procedures utilised in the present investigation afforded useful information concerning low molecular species, especially free urea, MMU, DMU and TMU, present during the addition stage UF resin reactions. Generally, the HPLC data are consistent with dynamic (RAPID) NMR data.

Only limited information could be derived concerning higher molecular weight species present during the condensation stage.

## 5.5 IDENTIFICATION OF UF RESIN SPECIES BY ELECTROSPRAY MASS SPECTROMETRY

Since electrospray mass spectrometry (ESMS) uses a mild ionisation technique, electrospray mass spectra are generally less complex than conventional electron-impact (EI) mass spectra. ESMS ion intensities are dependent on acquisition conditions (especially cone voltage) and matrix effects and are more variable than is the case for conventional EI mass spectra.

Additionally, under ESMS conditions, solute (target) molecules may form cluster ions (eg  $M_2H^+$  ions), or adduct ions with metal cations (eg  $M+Na^+$  or  $M+K^+$  ions) or anions (eg  $M+Cl^-$  or  $M+COO^-$  ions) which are present in trace amounts in mobile phases (eg water), or absorbed on glassware or instrument surfaces. Because of the tendency to form cluster or adduct ions, it can be difficult to identify molecular ions.

A  $Da/e$  74.2 (background) ion observed during the acquisition of resin ESMS was always accompanied by a smaller  $Da/e$  75.3 ion, the intensity of which was *c* 3.6% that of the  $Da/e$  74.2 peak. The natural abundances of  $^{12}C$ ,  $^{13}C$ ,  $^{14}N$  and  $^{15}N$  (98.9, 1.1, 99.64 and 0.36% respectively) are consistent with the formulation of the  $Da/e$  74 ion as a  $CH_3CN+CH_3OH+H^+$  adduct ion, since the expected relative intensity of the  $Da/e$  75.3 ion is  $3 (^{13}C) \times 1.1\% + 1 (^{15}N) \times 0.36\% = 3.66\%$ .

Similarly, the medium intensity background  $Da/e$  96.3 ion was always accompanied by a  $Da/e$  97.2 ion, the intensity of which was *c* 3.6% that of the  $Da/e$  96.3 ion. This is consistent with the formulation of the  $Da/e$  96.3 ion as a  $CH_3CN+CH_3OH+Na^+$  adduct ion.

Since UF resin samples always contain traces of methanol, background  $CH_3CN+CH_3OH+H^+$  and  $CH_3CN+CH_3OH+Na^+$  adduct ions were generally observed when acetonitrile/water was used as the mobile phase.

Table 5.6. Proposed origin(s) of some background ESMS adduct ions observed when using acetonitrile/water (1:1) (v/v), or methanol, as the mobile phase (ES<sup>+</sup> mode).

ion ( <i>Da/e</i> )	proposed origin(s)	calculated mass (Dalton)
18.6 (m-w) <sup>a</sup>	H <sub>3</sub> O <sup>+</sup>	19.0
39.3 (w)	K <sup>+</sup>	39.1
46.6 (w)	CH <sub>3</sub> CH <sub>2</sub> OH+H <sup>+</sup>	47.1
50.2 (w)	HCN <sup>b</sup> +Na <sup>+</sup>	50.2
59.5 (s)	CH <sub>3</sub> CN+H <sub>3</sub> O <sup>+</sup> or (H <sub>2</sub> O) <sub>2</sub> +Na <sup>+</sup>	60.1, 59.0
64.5 (w)	CH <sub>3</sub> CN+Na <sup>+</sup>	64.0
71.2 (w)	CH <sub>3</sub> OH+K <sup>+</sup>	71.1
74.2 (s-w)	CH <sub>3</sub> CN+CH <sub>3</sub> OH+H <sup>+</sup>	74.1
78.2 (m-w)	CH <sub>3</sub> CN+(H <sub>2</sub> O) <sub>2</sub> +H <sup>+</sup>	78.1
80.2 (w)	CH <sub>3</sub> CN+K <sup>+</sup>	80.2
82.2 (m-w)	CH <sub>3</sub> CN+H <sub>2</sub> O+Na <sup>+</sup>	82.1
83.2 (m-w)	(CH <sub>3</sub> CN) <sub>2</sub> +H <sup>+</sup>	83.1
96.3 (s-m)	CH <sub>3</sub> CN+CH <sub>3</sub> OH+Na <sup>+</sup>	96.1
100.1 (m-w)	CH <sub>3</sub> CN+(H <sub>2</sub> O) <sub>2</sub> +Na <sup>+</sup>	100.1
105.1 (m)	(CH <sub>3</sub> CN) <sub>2</sub> +Na <sup>+</sup>	105.1

<sup>a</sup> typical ion intensities: s = strong, m = medium, w = weak; <sup>b</sup> HCN is a minor component of CH<sub>3</sub>CN.

Because of ‘memory effects’ arising from traces of solvent residues and cations, or anions, absorbed on glassware or surfaces in the instrument system, caution must be exercised in interpreting ESMS data, especially when the molecular weight is less than 200 Dalton and the sample concentration is low ( $c < 1 \times 10^{-3}$  mol L<sup>-1</sup>). In the present investigation, background spectra were routinely obtained immediately before sample spectra.

*ESMS of model compounds*

ESMS data for urea, biuret, MMU, DMU are given in Tables 5.7, 5.8 and 5.9. Background ions are not included in these tabulations. The positive ion ESMS of urea is presented in Table 5.7. The minimum acceptable urea concentration was found to be  $2 \times 10^{-4}$  mole L<sup>-1</sup>.

The ESMS of urea was dominated by *Da/e* 61.1 and 121.1 ions, attributable to MH<sup>+</sup> (NH<sub>2</sub>CONH<sub>2</sub>+H<sup>+</sup>) and M<sub>2</sub>H<sup>+</sup> ions respectively. A weak *Da/e* 133.1 ion was considered to arise from protonated MDU (H<sub>2</sub>NCONH-CH<sub>2</sub>-HNCONH<sub>2</sub>+H<sup>+</sup>). This conclusion was consistent with the detection of a small MDU peak in the HPLC trace of the urea sample (see Figure 5.6).

Table 5.7. Selected ions observed in the ESMS of urea (ES<sup>+</sup> mode).

ion ( <i>Da/e</i> )	proposed origin	calculated mass (Dalton)
61.3 (s) <sup>a</sup>	urea+H <sup>+</sup> (MH <sup>+</sup> )	61.1
79.0 (m)	urea+H <sub>3</sub> O <sup>+</sup>	79.1
83.4 (m)	urea+Na <sup>+</sup> (MNa <sup>+</sup> )	83.1
102.2 (m)	urea+CH <sub>3</sub> CN+H <sup>+</sup>	102.1
121.3 (s)	biurea+H <sup>+</sup> (M <sub>2</sub> H <sup>+</sup> )	121.1
133.1 (w)	MDU+H <sup>+</sup>	133.1

<sup>a</sup>typical ion intensities: s = strong, m = medium, w = weak.

The ESMS of MMU, DMU and biuret are shown in Tables 5.8, 5.9 and 5.10. The weak to medium intensity peaks were typically observed for protonated MMU and DMU. Depending on acquisition conditions, the corresponding M<sub>2</sub>H<sup>+</sup> or M+solvent+H<sup>+</sup> ions often had greater intensity. Biuret typically exhibited a medium to strong intensity MH<sup>+</sup> peak (Table 5.10).

Table 5.8. Selected ions observed in the ESMS of MMU (ES<sup>+</sup> mode).

ion ( <i>Da/e</i> )	proposed origin	calculated mass (Dalton)
91.2 (m)	MMU+H <sup>+</sup> (MH <sup>+</sup> )	91.1
121.2 (m)	DMU+H <sup>+</sup> (trace DMU in MMU) and/or diurea+H <sup>+</sup>	121.1
151.7 (w)	TMU+H <sup>+</sup>	151.1
162.2 (w)	DMU+CH <sub>3</sub> CNH <sup>+</sup> or biurea+CH <sub>3</sub> CN+H <sup>+</sup>	162.2
199.3 (w)	(MMU) <sub>2</sub> +H <sub>3</sub> O <sup>+</sup>	199.3

Table 5.9. Selected ions observed in the ESMS of DMU (ES<sup>+</sup> and ES<sup>-</sup> modes).

ion ( <i>Da/e</i> ) (ES <sup>+</sup> mode)	ion ( <i>Da/e</i> ) (ES <sup>-</sup> mode)	Proposed origin	calculated mass (Dalton)
121.2 (w)		DMU+H <sup>+</sup> (MH <sup>+</sup> )	121.2
	119.1 (m)	DMU-H <sup>-</sup>	119.1
240.7 (w)		(DMU) <sub>2</sub> +H <sup>+</sup> (M <sub>2</sub> H <sup>+</sup> )	241.2

Table 5.10. Selected ions observed in the ESMS of biuret (ES<sup>+</sup> and ES<sup>-</sup> modes).

ion ( <i>Da/e</i> ) (ES <sup>+</sup> mode)	ion ( <i>Da/e</i> ) (ES <sup>-</sup> mode)	proposed origin	calculated mass (Dalton)
104.2 (w)		biuret+H <sup>+</sup> (MH <sup>+</sup> )	104.1
	102.1 (m-w)	biuret-H <sup>-</sup>	102.1

### ESMS of UF resin samples

The ESMS spectra of UF resin samples were very complex and included ions with up to *Da/e* 3000. The strongest ions were low mass background adduct ions, with *Da/e* < 200. Only a limited number of ions, attributable to low mass components of

species present in the UF resin samples (urea, MMU, DMU, TMU, biuret and MDU and corresponding solvent and/or cation adducts), were recognisable amongst the more intense series of 'background' ions (peaks) (see Table 5.11).

Since more than 10 species are typically present in the HPLC trace of an UF resin sample (Figures 5.10 and 5.15) it was anticipated that ESMS of HPLC fractionated UF resin samples might be more informative than the ESMS of unfractionated UF resin samples. Attempts to obtain ESMS data for higher molecular weight species, using HPLC-ESMS, were not successful due to the low concentration of individual species and the high intensity of the background ions.

Table 5.11. Selected ions observed in the ESMS of UF resin samples (ES<sup>+</sup> mode).

ion ( <i>Da/e</i> )	proposed origin	calculated mass (Dalton)
61.3 (m-w)	urea+H <sup>+</sup>	61.1
91.2 (m)	MMU+H <sup>+</sup>	91.1
104.1 (m)	MMU-Me <sup>a</sup> +H <sup>+</sup> and/or biuret+H <sup>+</sup>	104.4
121.1 (m)	DMU+H <sup>+</sup>	121.1
150.4 (m-w)	TMU+H <sup>+</sup>	151.1
104.4 (w)	biuret+H <sup>+</sup>	104.1
133.1 (w)	MDU+H <sup>+</sup>	133.1
163.3 (m)	MMDU+H <sup>+</sup> <sup>b</sup>	163.2
193.6 (m)	MBMU+H <sup>+</sup> <sup>c</sup>	193.2

<sup>a</sup> MMU-Me = monomethylolurea methyl ether;

<sup>b</sup> MMDU = methylol methylene diurea: H<sub>2</sub>NCONHCH<sub>2</sub>NHCONHCH<sub>2</sub>OH;

<sup>c</sup> MBMU = methylene bismethylolurea: HOCH<sub>2</sub>NHCONHCH<sub>2</sub>NHCONHCH<sub>2</sub>OH.

## 5.6 CHARACTERISATION OF UF RESINS BY GPC

GPC is a useful technique for determining the molecular weight, and molecular weight distribution, of polymer molecules (Billmeyer 1984). It has been successfully

used in the investigation of UF resins (Pasch *et al.* 1990 & 1991, Hlaing 1986, Katuscak *et al.* 1981, Hope *et al.* 1973 and Tsuge 1974).

In this research, a triple-column GPC-triple detector system (see Section 2.3) was used to investigate the UF resin system. Each detector contributes different, but complementary information.

The most common chromatography detector, a differential refractometer, generates a differential refractive index (RI) signal which is proportional to the mass of the eluant in the solvent (ie the mobile phase solution). A viscometry detector yields a differential pressure (DP) signal, which is proportional to the viscosity of the eluant, while a laser light scattering detector produces a signal proportional to the weight average molecular weight ( $\bar{M}_w$ ) of the sample.

Conventional GPC analyses determine resin molecular weight relative to that of a reference material, based on a logarithmic relation between molecular weight ( $\log M$ ) and retention volume ( $V_r$ ). The reliability (precision) of the measurement depends on the molecular weight, molecular weight distribution and the molecular size (degree of branching, etc) of the reference material, compared to that of the sample material. Conventional GPC methods are principally used to identify the average molecular weight of a resin, relative to that of a standard material, rather than to define the absolute molecular weight of the resin.

The combination of an 'in-line' viscometer and a RI detector enables the continuous determination of the viscosity of the eluant (Elias 1977). A plot of  $\log([\eta]M)$  vs  $V_r$ , (where  $[\eta]M$  is a molecular size parameter (Billmeyer 1984) known as hydrodynamic volume) has universal validity and can be applied to a wide variety of both linear and branched polymers, provided the GPC separation is achieved mainly by a size exclusion mechanism (Viscotek Manual 1996).

The combination of all three detectors (RI, viscometer and LS) enables the continuous determination of absolute molecular weight and the derivation of

branching information, molecular size (the radius of gyration) and Mark-Houwink parameters ( $\alpha$  and  $k$ ) (Viscotek Manual 1996).

### 5.6.1 Calibration of the Triple Detector GPC System

A set of narrow molecular weight distribution polyethylene glycol (PEG) standards was used to calibrate the GPC system. The intrinsic viscosity ( $[\eta]$ ) of the PEG standards in the GPC solvent system (DMF + 0.1 mol L<sup>-1</sup> LiCl) was determined using an Ostwald-Fenske type capillary glass viscometer (Billmeyer 1984). Results are shown in Table 5.12 along with the retention volumes and nominal molecular weights. GPC traces of three of the PEG standard samples are shown in Figure 5.34.

Table 5.12. The nominal molecular weight ( $M$ ), intrinsic viscosity  $[\eta]$  and retention volume ( $V_r$ ) of the narrow molecular weight distribution PEG standard samples.

nominal $M$	106	200	415	630	998	1535	4820	9230	11 250	19 100
$[\eta]$ (dL g <sup>-1</sup> ) <sup>a</sup>	0.035	0.040	0.044	0.049	0.060	0.082	0.124	0.151	0.182	0.227
$V_r$ (mL)	35.5	34.9	33.3	32.1	30.8	29.2	26.0	23.9	23.2	21.8

<sup>a</sup> solvent: DMF + 0.1 mol L<sup>-1</sup> LiCl.

Since the molecular weight of the largest available PEG standard was 19 100 Dalton, a set of higher molecular weight ranges, narrow molecular weight distribution, polyethylene oxide (PEO) standards were also used. Their nominal molecular weight, intrinsic viscosity and the retention volumes are given in Table 5.13. The GPC trace of one of the PEO standard samples is shown in Figure 5.34.

Table 5.13. The nominal molecular weight ( $M$ ), intrinsic viscosity  $[\eta]$  and retention volume ( $V_r$ ) of the narrow molecular weight distribution PEO standard samples.

nominal $M$ (kDa)	18	39	86	145	252	594	996
$[\eta]$ (dL g <sup>-1</sup> ) <sup>a</sup>	0.36	0.56	0.92	1.18	1.77	1.80	2.62
$V_r$ (mL)	21.5	20.5	20.1	19.6	19.4	18.9	18.7

<sup>a</sup> solvent: DMF + 0.1 mol L<sup>-1</sup> LiCl.

The universal calibration curve, constructed using the data in Tables 5.12 and 5.13, is showed in Figure 5.35. The valid (linear) calibration range (exclusion limits) for the triple-column GPC system used in this research was between  $V_r = 21$  and 35 mL, corresponding to molecular weights in the range 200 to 20 kDa.

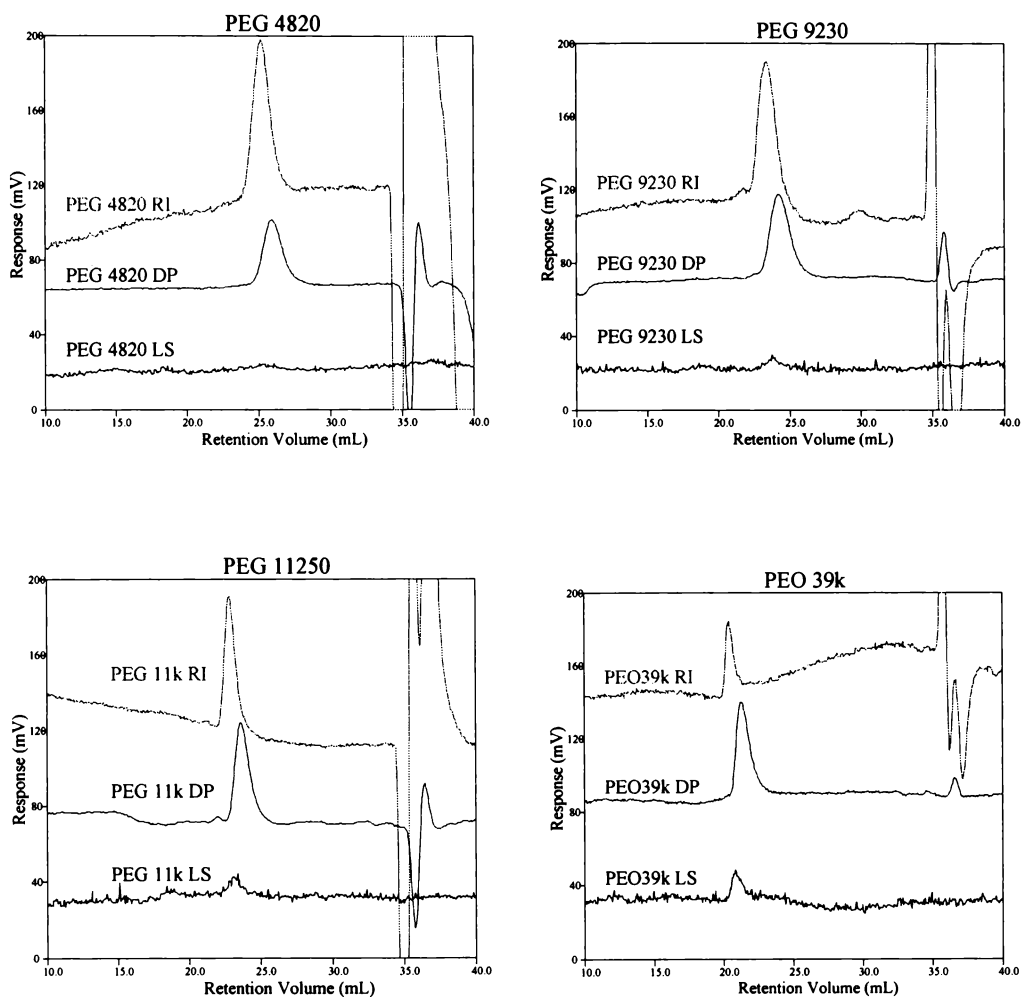


Figure 5.34. Triple-detector GPC traces of the PEG 4820, PEG 9230, PEG 11 250 and PEO 39 kDa standard samples.

RI = refractive index, DP = differential pressure, LS = light scattering

Because the DP response is proportional to the viscosity of the eluant, a greater DP response is observed for higher molecular weight species (see Figure 5.34). It is also apparent that the LS detector cannot detect PEG standard samples with the molecular weights less than *c* 10 kDa.

The triple-detector GPC traces determined for a typical UF resin are shown in Figure 5.36. The LS trace showed one strong peak (retention volume 20.5 mL) together with a tail along the higher  $V_r$  side (lower molecular weight side) until  $V_r \approx 25$  mL. It is apparent that the lower molecular weight species ( $M < 10$  kDa,  $V_r > 25$  mL) are not detected by the LS detector.

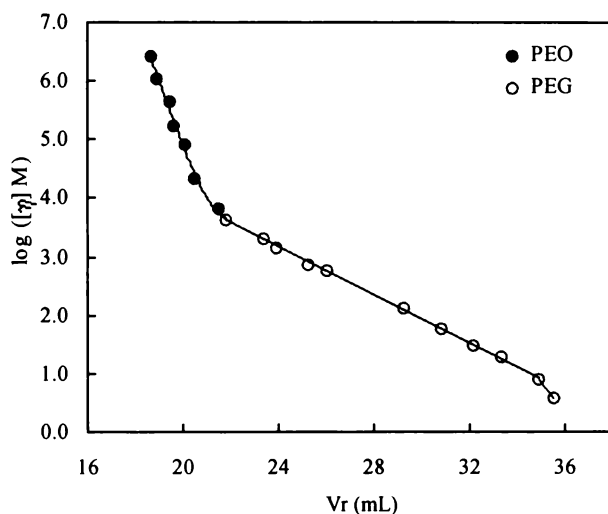


Figure 5.35. The universal calibration curve determined using the PEG and PEO standards.

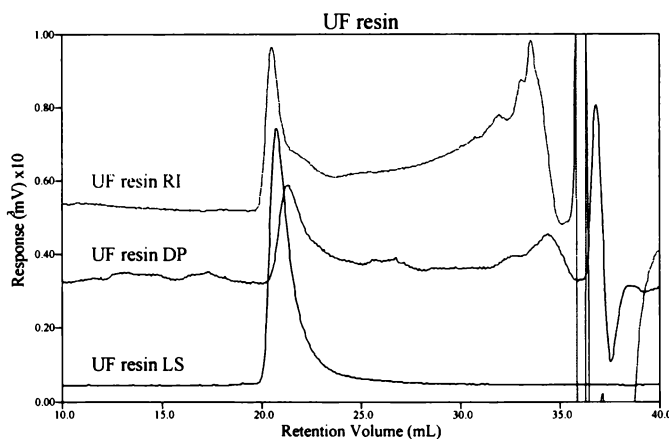


Figure 5.36. Triple detector GPC traces for a typical UF resin sample.

RI = refractive index, DP = differential pressure, LS = light scattering

A plot of intrinsic viscosity ( $\log[\eta]$ ) vs  $V_r$  is shown in Figure 5.37. Subtraction of the data depicted in Figure 5.37 from that depicted in Figure 5.35 (ie  $\log([\eta]M)$  vs  $V_r$ ) yields a plot of  $\log M$  vs  $V_r$  (see Figure 5.38). Thus, the average molecular weight can be calculated (Billmeyer 1984).

High levels of eluant species were observed at both end of the linear exclusion limits ( $V_r = 20$  to  $34.5$  mL), correspond to the molecular weight range of 270-68 kDa (see Figures 5.36 and 5.38). This shows that the molecular weight distribution of the UF resin is very broad, extending from less than the low molecular weight exclusion limit, to beyond high molecular weight exclusion limit.

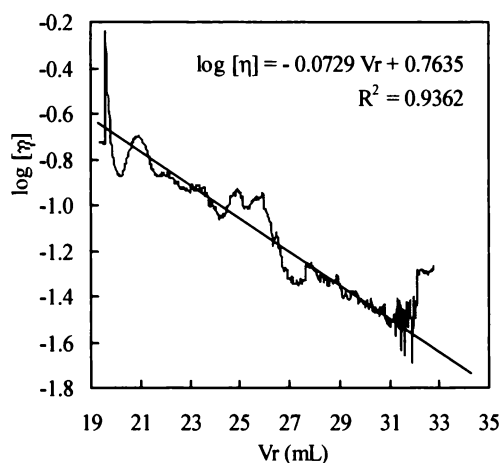


Figure 5.37. Plot of  $\log[\eta]$  vs  $V_r$  for a typical UF resin.

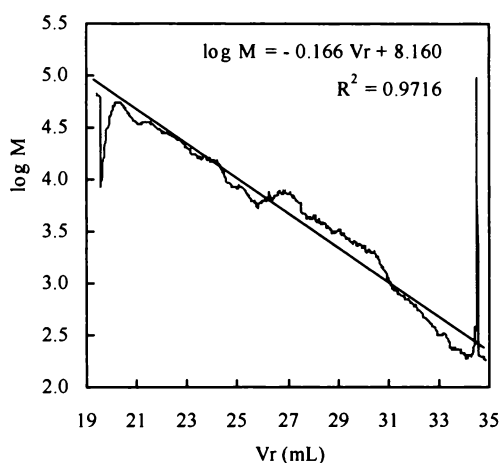


Figure 5.38. Plot of  $\log M$  vs  $V_r$  for a typical UF resin.

### 5.6.2 Effect of Reaction Time on the Molecular Weight and Molecular Weight Distribution

The effect of reaction time on the molecular weight and molecular weight distribution of typical UF resins was investigated. The resin preparation conditions, and the times at which sub-samples were collected for GPC analyses, are given in Table 5.14.

The RI traces of the series of sub-samples are shown in Figure 5.39. The number average molecular weight ( $\bar{M}_n$ ), weight average molecular weight ( $\bar{M}_w$ ) and the polydispersity coefficient ( $n$ ) determined for the sub-samples are given in Table 5.15. Average molecular weights and polydispersity coefficients increased with time.

After the addition of final urea,  $\bar{M}_n$  decreased and polydispersity coefficients increased significantly, while  $\bar{M}_w$  decreased slightly. This can be attributed to the formation of low molecular weight species (eg MMU). The  $\bar{M}_n$  and  $\bar{M}_w$  of the final resin are in the  $10^2$  (hundreds) and  $10^3$  (thousands) ranges respectively, which is agreement with the findings of other authors (Ludlam and King 1984, Katuscak *et al.* 1981).

Table 5.14. Properties of UF4 resin sub-samples examined using the GPC methodology.

code	time (min)	origin <sup>a</sup>	F/U ratio	viscosity (Pa·s)
UF4-1	26	alkaline addition	2.0	0.015
UF4-2	35	alkaline addition	2.0	0.025
UF4-3	50	alkaline addition	2.0	0.035
UF4-4	75	acidic condensation	2.0	0.054
UF4-5	100	acidic condensation	2.0	0.082
UF4-6	120	acidic condensation	2.0	0.14
UF4-7	140	acidic condensation	2.0	0.22
UF4-8	160	acidic condensation	2.0	0.31
UF4-9	165	final resin	1.3	0.16

<sup>a</sup> initial addition stage: pH 8.7 for 52 min; condensation stage: pH 5.0, at 88°C;

Table 5.15. Molecular weight characteristics determined for UF4 resin sub-samples.

sample	$\bar{M}_n$ (g mol <sup>-1</sup> )	$\bar{M}_w$ (g mol <sup>-1</sup> )	$n$ (= $\frac{\bar{M}_w}{\bar{M}_n}$ )
UF4-1	400	680	1.7
UF4-2	410	990	2.4
UF4-3	430	1330	3.1
UF4-4	500	1750	3.5
UF4-5	650	2310	3.6
UF4-6	900	5000	5.6
UF4-7	1000	6080	6.1
UF4-8	1200	8350	7.0
UF4-9	600	7000	11.7

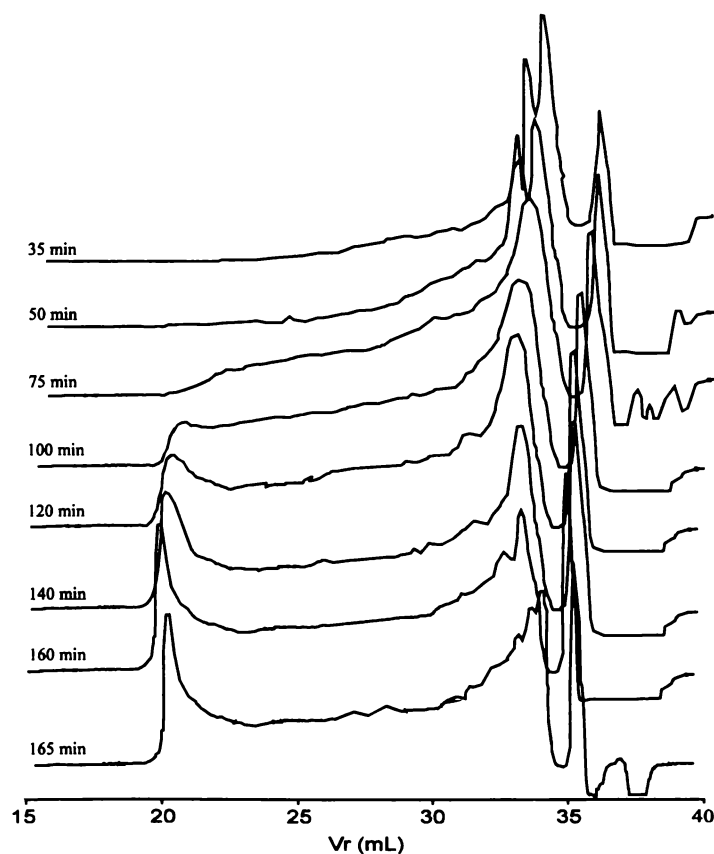


Figure 5.39. The effect of the reaction time on the GPC traces (RI responses).

### 5.6.3 Effect of Storage Time (Aging) on the Molecular Weight and Molecular Weight Distribution

The aging process was investigated for a resin sample prepared using the two-stage reaction system (initial F/U = 2.0, final F/U = 1.3, initial addition pH = 8.6, condensation pH = 5.0). Data determined over an 8-week period are given in Table 5.16.

The average molecular weight of the UF resin increased with time, while the polydispersity coefficient decreased slightly with time. This is consistent with the progressive conversion of some of the initially present lower molecular weight species into higher molecular weight species.

Table 5.16. The effect of storage time on the molecular weight of an UF resin.

storage time <sup>a</sup> (weeks)	$\bar{M}_n$ (g mol <sup>-1</sup> )	$\bar{M}_w$ (g mol <sup>-1</sup> )	$n$ (= $\frac{\bar{M}_w}{\bar{M}_n}$ )
0	750	10 100	13.5
2	870	11 400	13.1
5	960	12 300	12.8
8	1300	13 000	10.0

<sup>a</sup> storage temperature = 25°C.

### 5.6.4 Summary and Conclusions

The triple-column GPC system used in this research has the following exclusion limits for the UF resin:

upper limit:  $M = 68$  kDa (for  $V_r > 25$  mL)

lower limit:  $M = 270$  Dalton (for  $V_r = 34.5$  mL)

A LS detector cannot be used to determine UF resin molecular weights, since it does not reliably detect the low molecular weight species.

A typical UF resin contains a wide range of species with molecular weight from less than 270 Dalton to greater than 68 kDa. The  $\bar{M}_n$  and  $\bar{M}_w$  of the final UF resins are typically in the range of 600-750 Dalton and 8-10 kDa respectively.

The average molecular weight of an UF resin increases and its polydispersity coefficient decreases with storage time.

## **CHAPTER SIX**

# **RESIN DEVELOPMENT AND TESTING**

## 6.1 INTRODUCTION

The UF reaction process has been investigated by dynamic (RAPID) NMR (see Sections 4.2 and 4.3) and HPLC (see Section 5.4) techniques. The effects of different reaction conditions on the UF reaction system have been obtained and optimum or desirable reaction conditions have been predicted (see Section 4.3.7).

In addition, control of the addition stage pH between 8.3-8.6 throughout the addition reaction maximised methylol concentrations (see Section 5.4) and is expected to produce higher performance resins.

There are some differences in conditions in dynamic (RAPID) NMR experiments and laboratory scale resin preparations. For example, the temperature profile (heating rate) is likely to be different. Other reaction conditions that cannot be achieved in the dynamic (RAPID) NMR experiments include continuous pH adjustment and stirring.

A series of UF resins have been prepared using a range of reaction conditions encompassing the predicted optimum conditions. The properties of the resins and the wood panels bonded with these resins have been determined.

## 6.2 EXPERIMENTAL

The resins were prepared according to the preparation procedure described in Section 2.12 and the reaction conditions summarised in Table 6.1. The properties of the resins, including gel time (see Section 2.14) and enthalpy of curing ( $\Delta H_c$ ) were determined and are listed in Table 6.2. The properties of particleboard bonded with the corresponding resins including internal bond, formaldehyde emission and cold water swell have been determined. Results are listed in Table 6.2.

The performance of wood panels (eg internal bond and formaldehyde emission) depends not only on the bonding material (UF resin), but also on many other factors, eg the wood material and manufacture conditions (resin loading and panel thickness). Some preliminary investigations regarding the effect of these factors on the

properties of wood panels are reported in Appendix C. To avoid such variations, a standard procedure using the following conditions was used for all the property determination experiments:

- wood material: wood particles (*c* 20 mesh) (wood source: Carter-Holt-Harvey's Kopu site)
- board product: particleboard density 0.67-0.69 g cm<sup>-3</sup>
- resin loading: 8% of dried wood weight
- panel thickness: 8 mm (nominal)

The relative standard deviations of the experimental data (internal bond, formaldehyde emission and cold water swell) were normally less than 0.1 (in most cases < 0.07) (see Appendix C).

## **6.3 EFFECT OF REACTION CONDITIONS**

### **6.3.1 Effect of Formaldehyde Concentration**

Commercial formaldehyde solution is normally from 35% to 50% (w/w). From the dynamic (RAPID) NMR and HPLC investigations, it was found that the higher the formaldehyde concentration, the higher the reaction rate (see Sections 4.3.3 and 5.4.3). The effect of formaldehyde concentration on the resin properties and panel properties is summarised in Table 6.2 (resins R-01 to R-03).

Table 6.1. Resin preparation conditions.

resin	F conc (%)	F/U <sup>a</sup> ratio	temp (°C)	pH (a) <sup>b</sup>	pH (c) <sup>c</sup>	add t <sub>a</sub> (min)	total t (min)
R-01	30	2.0	88	8.7	5.0	32	359
R-02	37	2.0	88	8.7	5.0	32	273
R-03	46	2.0	88	8.7	5.0	32	162
R-04	46	1.8	88	8.7	5.0	32	150
R-05	46	2.2	88	8.7	5.0	32	220
R-06	46	2.0	70	8.7	5.0	32	240
R-07	46	2.0	80	8.7	5.0	32	180
R-08	46	2.0	88	8.7	5.0	32	150
R-09	46	2.0	97	8.7	5.0	32	125
R-10	46	2.0	88	3.0	5.0	32	157
R-11	46	2.0	88	5.0	5.0	32	167
R-12	46	2.0	88	7.3	5.0	32	155
R-13	46	2.0	88	8.6	5.0	32	200
R-14	46	2.0	88	9.1	5.0	32	185
R-15	46	2.0	88	8.7	4.3	32	59
R-16	46	2.0	88	8.7	4.7	32	92
R-17	46	2.0	88	8.7	5.0	32	152
R-18	46	2.0	88	8.7	5.5	32	252
R-19	46	2.0	88	8.7	5.0	7.2	130
R-20	46	2.0	88	8.7	5.0	13	170
R-21	46	2.0	88	8.7	5.0	24	150
R-22	46	2.0	88	8.7	5.0	31	167
R-23	46	2.0	88	8.7	5.0	40	190
R-24	46	2.0	88	8.7	5.0	72	200
R-25	46	2.0	88	8.7	5.0	123	270

<sup>a</sup> Initial F/U molar ratio. In all cases final F/U ratios were 1.10, <sup>b</sup> pH (a) = initial addition pH, <sup>c</sup> pH (c) = condensation pH.

Table 6.2. Resin properties.

resin	gel time <sup>a</sup> (sec)	T <sub>p</sub> <sup>b</sup> (°C)	ΔH <sub>c</sub> (J g <sup>-1</sup> )	IB <sup>c</sup> (MPa)	FE <sup>d</sup> (mg/100 g)	swell <sup>e</sup> (%)
R-01	88	82.5	76	1.6	6.7	21
R-02	85	79.9	86	1.7	7.0	20
R-03	74	81.0	98	1.9	8.5	20
R-04	73			1.95	8.0	20
R-05	75			1.90	8.3	20
R-06	82	80.5	85	1.6	8.4	20
R-07	78	82.5	96	1.7	7.5	19
R-08	74	80.9	99	1.9	7.2	20
R-09	70	81.0	96	1.9	7.0	18
R-10	70	80.7	85	1.7	8.7	19
R-11	69	80.9	89	1.8	8.4	20
R-12	67	80.8	100	1.8	7.5	19
R-13	74	81.0	101	1.9	7.2	19
R-14	75	82.9	96	1.9	7.3	19
R-15	76	82.0	100	1.9	8.1	20
R-16	72	81.5	102	1.8	8.0	20
R-17	74	81.2	105	1.9	7.7	20
R-18	74	81.5	95	1.8	7.8	19
R-19	85	81.5	81	1.8	8.1	19
R-20	82	82.0	86	1.8	7.0	17
R-21	75	82.2	96	2.1	7.5	17
R-22	72	80.5	99	2.1	7.2	19
R-23	70	80.9	96	2.1	8.4	19
R-24	75	81.6	98	2.1	7.5	21
R-25	74	82.6	96	2.0	8.3	18

<sup>a</sup> NH<sub>4</sub>Cl gel time; <sup>b</sup> T<sub>p</sub> = the maximum curing temperature; <sup>c</sup> IB = internal bond <sup>d</sup> FE = formaldehyde emission, mg HCHO/100 g wood panel; <sup>e</sup> swell = cold water swell.

Generally, resins made at lower formaldehyde concentrations show longer gel times (ie a lower curing rate) and lower  $\Delta H_c$ s, ie the reactivity of the resins was lower. The particleboards bonded with these resins have lower internal bonds and lower formaldehyde emissions (Table 6.2). The most significant effect of the formaldehyde concentration on the UF reaction is the reaction rate (see Table 6.1). For example, the reaction with the formaldehyde concentration of 30% has an excessively long reaction time of 359 min (c 6 h). These results suggest that a formaldehyde solution of less than 37% is not suitable for commercial production. Concentrations between 37-46% are appropriate for resin production. This result is consistent with the dynamic (RAPID) NMR data.

### 6.3.2 Effect of F/U Molar Ratio

The dynamic (RAPID) NMR data suggests an optimum F/U molar ratio range of 1.8-2.2 for the preparation of UF resins. The effect of F/U molar ratio on the properties of resins and wood panels is shown by the data for resins R-03 to R-05. The effect is mainly on the time required to reach the predetermined viscosity, ie the lower the F/U molar ratio the shorter the time required to finish the preparation.

### 6.3.3 Effect of Reaction Temperature

The effects of reaction temperature in the range 70°C to 97°C are shown by the properties of resins R-06 to R-09 of Table 6.2. The reaction temperature of 70°C resulted in a slightly longer gel time, lower  $\Delta H_c$ , lower internal bond and higher formaldehyde emission. Reaction temperatures over 80°C (80-97°C) had little effect on the internal bond, formaldehyde emission and cold water swell. The main effect of the reaction temperature was on the reaction rate. The higher the reaction temperature, the shorter the time required to reach the predetermined viscosity (see Table 6.2).

Higher reaction temperatures improve the efficiency of the preparation, whereas lower reaction temperatures allow better process control and the ability to condense at lower mole ratios without creating precipitate in the resin. The optimum

temperature of 88°C predicted by dynamic (RAPID) NMR experiment is consistent with results obtained.

### 6.3.4 Effect of Initial Addition pH

The dynamic (RAPID) NMR experiments indicated an optimum initial addition pH of 8-9. The effect of initial addition pH was investigated over the range of 3.0 to 9.1. It can be seen from the properties of resins R-10 to R-14 of Table 6.2 that the initial addition pH has little effect on the gel time of the final resins. The gel times were all very similar. An initial pH of 3 and 5 resulted in a slightly lower  $\Delta H_c$ . Some improvements in internal bond and formaldehyde emission were observed at higher pHs.

An initial addition pH higher than 9.0 is not recommended for the production of UF resins, because high pH (especially pH > 9.0) favours the Cannizzaro reaction. Also, to adjust the pH to over 9.0 will require more base and increase costs. Formaldehyde solutions are buffered by the formation of formate ions above pH 9 (see Figure 6.1).

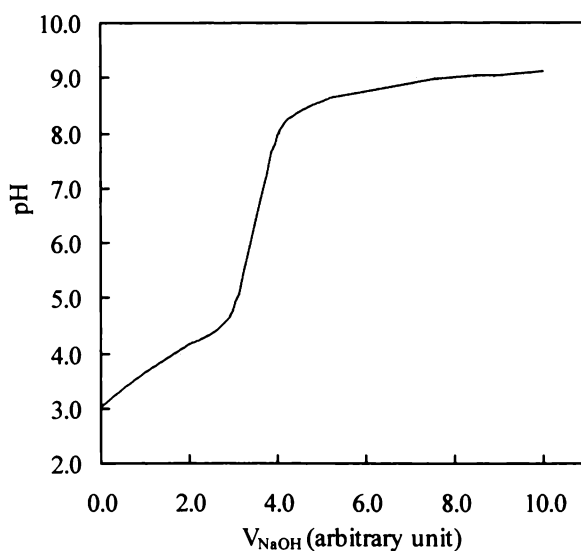


Figure 6.1. pH titration curve of a typical formaldehyde solution.

### 6.3.5 Effect of Condensation pH

The dynamic (RAPID) NMR studies indicated an optimum condensation pH of 4.5 to 5.0. The condensation pH affects the rate of the methylene formation. Effects of variation in condensation pH over the range 4.3 to 5.5 are illustrated by the resins R-15 to R-18 of Table 6.2.

The results show that condensation reaction pHs have no significant effects on either the properties of the resins or the wood panels produced. The effects of the condensation pHs on the total reaction time are given in Table 6.1. It can be seen that at pH 5.5 the total reaction time is over four hours, which is excessive. Appropriate reaction times of between 1 and 2.5 hours are obtained in the pH range of 4.3 to 5.0. This is consistent with the dynamic (RAPID) NMR data.

### 6.3.6 Effect of Addition Stage Reaction Time

The dynamic (RAPID) NMR experiments indicate an optimum addition time of between 25 and 30 min. The effect of the addition reaction time ( $t_a$ ) on the properties of wood panels is shown by the resins R-19 to R-25 of Table 6.2. Generally, if  $t_a$  is greater than 24 min, the addition reaction time has no effect on the properties of the wood panels. However, if shorter than 24 min (eg 7.2 and 12.5 min), the  $\Delta H_c$  of the resins and IB of the wood panels are slightly lower. The addition reaction time (from 7.2 to 123 min) has no obvious effect on formaldehyde emission and cold water swell.

These results are also consistent with the dynamic (RAPID) NMR experiments. Addition reaction times longer than the optimum ranges produce no advantage but increase costs.

### 6.3.7 Effect of pH Control During the Addition Reaction Stage

The pH adjusted method (pH control during the addition reaction stage) (see Section 5.4.6) and conventional method have been used to prepare UF resins. The pH

profiles along with the temperature profile during the reaction period are shown in Figure 6.2.

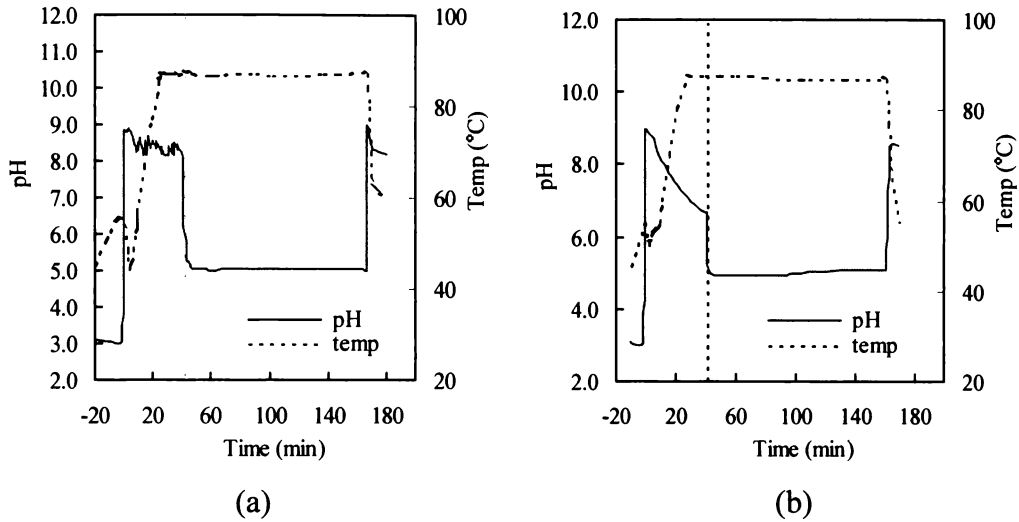


Figure 6.2. pH profiles for (a) the pH adjusted reaction and (b) conventional reaction during the UF resin preparation along with their corresponding temperature profiles.

The effects of the pH control during the addition reaction stage on the properties of resins and wood panels are shown in Table 6.3 and Figure 6.3. These two preparation methods have no obvious effect on the properties of the resins, except the appearance of the resins. It was observed that the pH adjusted reaction mixture became cloudy during the condensation stage, while the conventional reaction mixture remained clear. This suggests that more methylol species were formed in the pH adjusted method. Because the solubility of the methylol species in the aqueous reaction system is low, these species often precipitate out of solution when the methylol concentration is high or the temperature drops below 60°C.

The pH adjusted method does improve the properties of the wood panels as predicted. There is a marginal improvement in internal bond of about 7% (4-9% for different F/U molar ratio). Formaldehyde emission is reduced by up to 26% for resin R-26 (F/U molar ratio of 1.30). There is no improvement in formaldehyde emission for resin R-29 (low F/U molar ratio 0.95) (see Figure 6.4(b)). The results suggest that the pH adjusted preparation method has a greater effect on reducing the

formaldehyde emission, especially for the higher F/U molar ratio resin (F/U > 1.0), than on enhancing the internal bond. The most important finding is that this preparation method can achieve improvements in both internal bond and formaldehyde emission for resins with F/U > 1.0.

Table 6.3. Effect of pH controlling methods during the addition reaction stage on the properties of resins and wood panels.

method	pH adjusted				conventional			
	R-26	R-27	R-28	R-29	R-30	R31	R-32	R-33
resin								
F/U ratio	1.30	1.20	1.10	0.95	1.30	1.20	1.10	0.95
solid (%)	57.5	57.6	59.3	60.2	58.4	58.4	59.2	60.1
viscosity (Pa·s)	0.17	0.16	0.15	0.13	0.18	0.17	0.15	0.13
gel time (sec)	75	76	84	150	66	71	76	160
density (g cm <sup>-3</sup> )	0.69	0.67	0.70	0.68	0.68	0.68	0.69	0.67
IB <sup>a</sup> (MPa)	2.25	2.13	2.07	1.88	2.07	2.00	1.97	1.80
FE <sup>b</sup> (mg/100 g)	14.9	10.3	8.8	4.9	18.8	12.5	9.2	4.6
swell (%)	16.2	17.2	18.3	22.4	16.4	16.6	19.1	21.2

<sup>a</sup> IB = internal bond; <sup>b</sup> FE = formaldehyde emission.

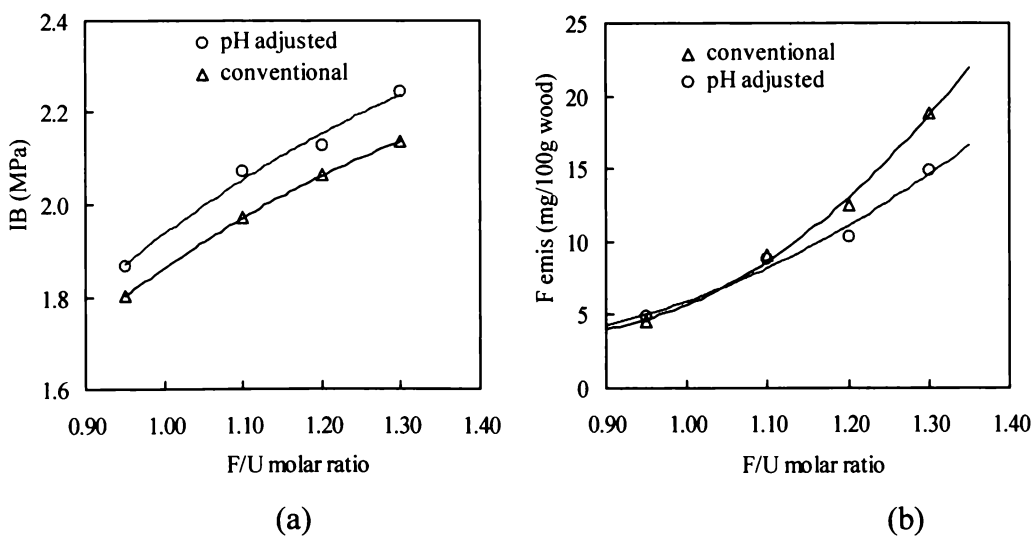


Figure 6.3. Effect of the pH controlling method on the (a) internal bond and (b) formaldehyde emission of the wood panel.

### 6.3.8 Other Important Variables

While no predictions could be made from NMR data, the effects of condensation reaction time and final F/U molar ratio were included in the study for completeness.

#### *Effect of condensation reaction time*

Condensation reaction times determine the extent of condensation of the UF resins. It was found that there was a linear relationship between the logarithm of viscosity and the reaction time of the condensation reaction stage (see Figure 6.4). The longer the condensation reaction time, the higher the viscosity and therefore the higher the average molecular weight of the resins (see Section 5.6.2).

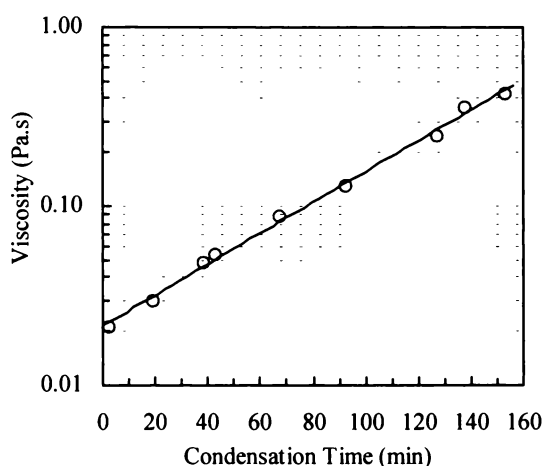


Figure 6.4. Plot of log viscosity vs condensation reaction time for a typical UF reaction.

The effects of the condensation reaction time on the properties of the resins and wood panels are summarised in Table 6.4. Generally, condensation times from 126 to 185 min have little effect on the properties of wood panels. The internal bonds and formaldehyde emissions decrease only slightly with the condensation time. Therefore, a reaction time to produce a viscosity of between 1.3 and 2.5 Pa·s can be considered appropriate. Low viscosity resins lack the tack required to form a pre-pressed mat. Also, low viscosity resins may have more free formaldehyde and higher

formaldehyde emission. However, high viscosity resins not only result in a lower internal bond wood panel, but also have shorter shelf (storage) lives.

Table 6.4. Effect of condensation reaction time (cond time) on resin performance.

cond time (min)	viscosity (Pa·s)		solid (%)	gel time (min)	IB <sup>b</sup> (MPa)	FE <sup>c</sup> (mg/100 g)	swell (%)
	(before) <sup>a</sup>	(after) <sup>a</sup>					
126	1.3	0.74	60.7	98	1.8	4.3	21
158	2.5	1.0	60.4	80	1.7	4.3	23
171	3.7	1.2	61.1	85	1.6	3.7	24
185	4.4	1.6	59.5	104	1.6	3.9	22

<sup>a</sup> the viscosity of before the addition of final urea (F/U = 2.0) and after the addition of final urea (F/U = 0.95); <sup>b</sup> IB = internal bond; <sup>c</sup> FE = formaldehyde emission.

#### *Effect of final F/U molar ratio*

A resin was prepared using the two stage (initial addition pH = 8.7, condensation pH = 5.0) method with an initial F/U molar ratio of 2.0. Final F/U molar ratios were adjusted by the addition of urea. The resin properties are shown in Table 6.5.

The results in Table 6.5 show that the lower the final F/U molar ratio, the higher the solid content, the lower the viscosity and the longer the gel time. The gel time increased with the lowering of the F/U molar ratio indicating decreased reactivity of the resins. The gel time increased abruptly when the F/U molar ratio decreased below 1.0.

The panel properties are shown in Table 6.6. Generally, higher internal bonds and higher formaldehyde emissions are obtained with higher final F/Us. By using a low F/U molar ratio (0.95) resin, a very low formaldehyde emission (4.5 mg/100 g wood panel) resin was achieved. Comparison with the F/U = 1.3 resin shows that the reduction (ie improvement) of formaldehyde emission is significant (76%), while the decrease (ie adverse effect) of internal bond is only 14%. This suggests that the final

F/U molar ratio has greater effect on the formaldehyde emissions than on internal bonds. It is well established that lowering the final F/U molar ratio is one of the most effective methods of reducing formaldehyde emissions.

Table 6.5. The relationship between final F/U molar ratio and resin properties<sup>a</sup>.

F/U ratio	solid content (%)	viscosity (Pa·s)	pH	gel time <sup>b</sup> (sec)
0.95	60.1	0.13	8.7	160
1.0	59.8	0.14	8.6	102
1.1	59.1	0.15	8.6	76
1.2	58.4	0.17	8.5	71
1.3	58.3	0.19	8.6	66

<sup>a</sup> formaldehyde concentration = 46%, reaction temperature = 88°C; <sup>b</sup> NH<sub>4</sub>Cl gel time.

Table 6.6. Effect of the final F/U molar ratio on the panel properties.

final F/U ratio	IB (MPa)	FE (mg/100 g)	swell (%)
0.95	1.8	4.5	21
1.0	1.9	7.0	20
1.1	2.0	9.1	19
1.2	2.1	12.5	17
1.3	2.1	18.8	16

## 6.4 COMPARISON OF EXPERIMENTAL RESINS WITH COMMERCIAL RESINS

### 6.4.1 Comparison with Literature Data

The F/U molar ratios of currently available commercial resins are lower than the F/U = 1.10 used in the studies described in the majority of this thesis. While not

ideal, a comparison can be made between the properties of the experimental resins summarised in Table 6.2 and those of some commercial resins or laboratory resins of similar F/U molar ratios recorded in the literature. The data are summarised in Table 6.7 below.

Table 6.7. Comparison of the experimental resin performance with literature data.

resin	density <sup>a</sup> (g cm <sup>-3</sup> )	IB (MPa)	FE (mg/100 g)	F/U ratio
conventional	0.67-0.69	1.97	9.2	1.10
pH adjusted	0.67-0.69	2.07	8.8	1.10
resin-1 <sup>b</sup>	0.63	0.45-0.55	8.0-16	1.17
	0.66-0.69	0.71-0.77	22-44	1.26
resin-2 <sup>c</sup>	0.67-0.69	0.6-0.1.3	6-13	1.10
resin-1 <sup>d</sup>	0.67-0.69	0.52-0.63	4.4-6.0 <sup>e</sup>	1.10

<sup>a</sup> particleboard density; <sup>b</sup> Pizzi *et al.* 1994. <sup>c</sup> Gumbley 1995b. <sup>d</sup> resin-1 of Ferg *et al.* 1993; <sup>e</sup> 24 h desiccator method.

It is clear that the experimental resins produced under the optimum conditions determined in this work generally show superior product properties, especially with respect to internal bond strength.

#### 6.4.2 Comparison of Experimental Resins with a Commercial Resin

Since the current project was initiated, the resin industry has moved towards lower F/U molar ratios. The only commercial unmodified UF resin available for comparison had a final F/U molar ratio of 0.95. Thus, in order to achieve a valid comparison, further experimental resins produced under previously determined optimum conditions but having a final F/U molar ratio of 0.95 were prepared. The reaction conditions for these resins are summarised in Table 6.8. The properties of the commercial resin and the experimental resins are summarised in Table 6.9.

Table 6.8. Resin preparation conditions.

resin (F/U ratio) <sup>a</sup>	F conc (%)	F/U <sup>b</sup>	temp (°C)	pH (a) <sup>c</sup>	pH (c) <sup>c</sup>	t <sub>a</sub> (min)
conventional						
UF1 (0.95)	46	2.0	88	8.7 <sup>e</sup>	5.0	32
UF4 (0.95)	46	2.0	88	8.7 <sup>e</sup>	5.0	40
pH adjusted						
UF3 (0.95)	46	2.0	88	8.5 <sup>f</sup>	5.0	40
UF15 (0.95)	46	2.0	88	8.5 <sup>f</sup>	5.0	32
UF20 (0.95)	46	2.0	88	8.5 <sup>f</sup>	5.0	32

<sup>a</sup> final F/U ratio; <sup>b</sup> initial F/U ratio (during the preparation); <sup>c</sup> pH (a) = initial addition pH; <sup>d</sup> pH (c) = condensation pH; <sup>e</sup> pH fell from 8.7 to 6.5 during the addition stage; <sup>f</sup> pH was maintained between 8.7 and 8.3 (average 8.5) during the addition stage (see Figure 6.2)

Table 6.9. Properties of resins and resins bonded particleboard.

resin	viscosity (Pa·s)		solid (%)	gel time (sec)	IB <sup>a</sup> (MPa)	FE <sup>b</sup> (mg/100 g)	swell (%)
	(before)	(after)					
commercial							
Sylvic 1004	--	1.52	67.1	90	1.68	4.5	23.0
conventional							
UF1 (0.95) <sup>c</sup>	0.33	0.14	60.5	130	1.80	4.1	24.0
UF4 (0.95) <sup>c</sup>	0.32	0.13	60.1	150	1.78	4.6	21.2
pH adjusted							
UF3 (0.95) <sup>c</sup>	0.31	0.13	60.2	160	1.89	4.5	22.4
UF15 (0.95) <sup>c</sup>	0.35	0.14	60.3	110	1.93	4.6	20.0
UF20 (0.95) <sup>c</sup>	0.25	0.14	60.7	92	1.83	4.3	22.5

<sup>a</sup> IB = internal bond; <sup>b</sup> FE = formaldehyde emission; <sup>c</sup> final F/U ratio is given in brackets.

The results of Table 6.9 indicate that by using the optimum reaction conditions (predicted by the dynamic (RAPID) NMR and HPLC experiments), UF resins of

lower F/U molar ratios having improved performance can be produced. The pH adjusted preparation produced resins with a 12% improvement in IB. With the conventional preparation the improvement of IB was about 6.5%. All of the resins had similar formaldehyde emissions and cold water swell.

The performance improvement by optimisation of the reaction conditions is about 12% in internal bond, which while marginal given experimental uncertainties, is considered significant. It appears that the commercial production conditions are already close to optimum. This is not surprising because commercial UF resins have been in production for at least 60 years.

## **6.5 CONCLUSIONS**

It has been shown that the predictions for optimum conditions based upon dynamic (RAPID) NMR and HPLC investigations are essentially correct. Over the range investigated, effects are generally not large.

The experimental resins prepared under optimum conditions, but at the same F/U molar ratio (0.95) as a commercial UF resin, gave a 12% higher internal bond in wood products. There was no improvement in formaldehyde emission.

## **CHAPTER SEVEN**

# **GENERAL CONCLUSIONS AND OVERVIEW**

## 7.1 DEVELOPMENT OF A DYNAMIC NMR METHOD

A dynamic (RAPID) NMR technique, whereby the UF reaction was performed and continuously monitored in a NMR tube, was developed to investigate the UF reaction. A  $\pi/2$  pulse ( $90^\circ$ ), a short interpulse delay time of 0.5 sec and continuous proton decoupling (with NOE enhancement) were used. A mixture of DMSO (0.20 mL) + DMSO- $d_6$  (0.40 mL) was used as internal integration reference.

Using the dynamic (RAPID) NMR method, a spectrum with reasonable signal to noise ratio ( $c$  100) could be obtained in a short time (typical 2.5 min, 100 scans). Normally about 20-30 spectra could be acquired for a typical UF reaction in 100 min.

The  $T_1$ s of different species present in the UF resin matrix were determined by the inversion-recovery method.  $T_1$ s decrease slightly with time during the UF reaction.

The NOE factors for different species in the UF resin matrix and the cross calibration factor between the signal intensity of a quantitative (STANDARD) NMR spectrum and a dynamic (RAPID) NMR spectrum have been estimated. NOE effects decrease slightly with time. Since both  $T_1$ s and NOE factors decrease slightly with time, the cross calibration factors also change slightly with the reaction time.

The integration methodology for the dynamic (RAPID) NMR spectra was evaluated. It was found that the signal intensities of species have both NOE and  $T_1$  dependence. Therefore, the signal intensity for any given species may have a systematic error in the range of 15%.

## 7.2 DYNAMIC NMR INVESTIGATION OF UF RESIN REACTION SYSTEMS

The dynamic (RAPID) NMR method was used to investigate the UF reaction process. The reaction profiles for the three main species, ie methylol, methylene and ether, were determined.

Using industrial experience it was concluded that optimum conditions for the production of UF resins would be those that maximised methylene species and minimised ether species at an industrially feasible reaction rate. The optimum reaction conditions predicted by the dynamic (RAPID) NMR data are:

Formaldehyde concentration:	35-46%
F/U molar ratio:	1.8-2.2
Initial addition pH:	8.0-9.0
Condensation pH:	4.5-5.0
Addition reaction time:	25-30 min
Reaction temperature:	88°C

During the addition stage, methylol species were the main species formed (accounting for about 70-80% of original urea). MMU and DMU increased rapidly with time during the early addition stage (*c* 20 min), reached a maximum and then decreased slightly. Most of the methylol species were present as MMU and DMU. TMU accounted for about 5% of total methylols.

Ether species were also formed during the addition stage. They accounted for about 20% of the original urea.

Only small amounts of methylene species were formed and they accounted for less than 5% of the original urea during the addition stage.

During the condensation stage, methylol species decreased with time and methylene species increased with time, while ether increased, reached a maximum and then decreased with time.

During the early condensation stage, the linear methylene species were dominant, while at the late condensation stage, the branched methylene species were dominant.

During the late condensation stage, methylol, methylene and ether species were relatively constant, however, the viscosity of the reaction system increased with time. This indicated that during the late condensation stage, the reaction was mainly the

conversion of the lower molecular weight methylene to higher molecular weight methylene species.

The ether species in the UF resins were mainly the simple ether form: -NH-CH<sub>2</sub>-O-CH<sub>2</sub>-NH-. There was no detectable polymeric form (-CH<sub>2</sub>O(CH<sub>2</sub>O)<sub>n</sub>-) of ether species (except a low level due to the free formaldehyde). It is postulated that the reaction of formaldehyde with urea or urea derivatives mainly involves monomeric formaldehyde (HCHO) or methylene glycol (HOCH<sub>2</sub>OH).

### **7.2.1 Standard NMR Monitoring of UF Reaction Systems**

A quantitative (STANDARD) NMR method was used to validate the results from the dynamic (RAPID) NMR method. The reaction profiles of methylol, methylene and ether groups determined by the quantitative (STANDARD) method were very similar to those obtained by dynamic (RAPID) NMR method.

The quantitative (STANDARD) NMR method and a GC-MS method were also used to investigate species present in formaldehyde solutions. Differences were found in the distribution of polyoxymethylene glycol species from batch to batch and with aging. Further investigation found that the formaldehyde solution aging had no significant effect on the properties of UF resins and resin bonded wood products.

### **7.2.2 Kinetic Studies**

The dynamic (RAPID) NMR data for a range of reaction temperatures were used to determine rate constants and activation energies for the formation of MMU and DMU. Values similar to those from earlier work using lower concentrations and temperatures (de Jong and de Jonge 1952) were obtained.

## **7.3 HPLC, ESMS AND GPC INVESTIGATIONS**

The HPLC procedures afforded useful information concerning low molecular weight species (eg free urea, MMU and DMU) present during the addition stage UF

resin reaction. Generally, the HPLC data are consistent with the dynamic (RAPID) NMR data.

Only limited information concerning the higher molecular weight species present during the condensation stage could be derived from HPLC. The method was useful in determining that a higher concentration of DMU species was formed during the addition stage when pH was controlled.

ESMS was used to identify some of the low molecular weight species present in the UF resins. They included free urea, MMU, DMU, TMU, biuret, MDU.

The triple-column GPC system was evaluated. The in-line LS detector could not be used to determine species present in typical UF resins, since it does not reliably detect species with molecular weight less than 10 kDa.

An in-line viscometer and a universal calibration were used to determine the molecular weight and molecular weight distribution parameters for the UF resins. A typical UF resin contains a wide range of species with molecular weight from less than 270 Dalton to greater than 68 kDa. The  $\bar{M}_n$  and  $\bar{M}_w$  of the final UF resins are typically in the range of 600-750 Dalton and 8 k-10 kDa respectively.

The average molecular weight increased and the polydispersity coefficient decreased, with storage time.

#### 7.4 TRIALS USING LABORATORY RESINS

To test the optimum reaction conditions predicted from dynamic (RAPID) NMR and HPLC data, a series of laboratory UF resins were prepared. Their performance in wood panel products was determined. Data for the laboratory resins were compared with literature data and data obtained for a commercial resin.

In general the resins prepared under the predicted optimum conditions gave the best performance data. However, the performance improvement was not large. The

resins prepared by the pH adjusted method gave a 4-9% improvement in internal bond and up to 26% improvement in formaldehyde emissions for final F/U molar ratio greater than 1.0. However for the low F/U molar ratio (0.95) resins, no formaldehyde emissions improvement was observed.

In comparison with the literature data, our experimental resins have significantly higher internal bonds, while the formaldehyde emissions are similar.

For the F/U = 0.95, the optimum conditions produced a resin having internal bond 12% higher than a commercial resin. The improvement while small is considered significant. However, it appears that commercial production conditions are already close to optimum. This is not surprising because unmodified UF resins have been in production for at least 60 years.

## **7.5 RECOMMENDATIONS FOR FUTURE RESEARCH**

Most present day commercial UF based resins have been modified by either structural (reactive) (eg melamine and phenol) or non-structural additives.

This is an area where further research is warranted. The techniques developed in the current work have provided new tools for such investigations.

### *Dynamic (RAPID) NMR analyses*

The dynamic (RAPID) NMR method can be applied to monitoring the reaction process. Some modification may be needed to improve quantification, eg the choice of an internal reference with a shorter  $T_1$  than DMSO.

One of the most important regions in the melamine modified UF resin is the 160-170 ppm range, where peaks for the very sensitive compounds containing the triazine carbons of melamine and their substituted derivatives are located (Panangama and Pizzi 1996). The other important regions (eg methylol, methylene and ether) will be similar to those observed in the unmodified UF system. By monitoring the peaks in

the 160-170 ppm region during the co-polymerisation, the reaction profiles for triazine species in melamine (eg 167.2, 166.5 and 166.2 ppm peaks) could be obtained. It is anticipated that these data could be correlated with the properties of the final resin and resin bonded wood panel products.

#### *HPLC methodology*

HPLC methodology was used to investigate the low molecular weight species formed during addition reaction stage. In chromatography to identify species separated, it is important to have model compounds available. The use of a preparative HPLC column to separate “model species” from a reaction mixture is suggested.

#### *GPC analyses*

GPC provides method to characterise resin molecular weight and molecular weight distribution and correlate these parameters with the resin performance. There remains much work to be done in this area.

#### *DSC Analyses*

The endothermic peak of UF resins arises from the dissociation of the ether groups. Therefore, the endotherms of uncured resins (no hardener added) should be proportional to the total ether groups in the resin and thus also to the formaldehyde emissions determined by perforator method. This has been demonstrated by the preliminary DSC experiments. The endotherms of cured resins (with hardener added) should be proportional to the total ether groups in the cured resins and thus also to the long term formaldehyde emissions. Further work needs to be done to develop the DSC method to allow prediction of formaldehyde emissions.

**APPENDIX A EUROPEAN AND JAPANESE STANDARDS FOR  
FORMALDEHYDE EMISSION**

*European standard (perforator test method EN 120)*

Class E1: average  $\leq 7$  mg/100 g dried wood,  
in any test, no a single value  $> 8$  mg/100 g dried wood.

Class E2:  $\leq 10$  mg/100 g dried wood, for particleboard  
 $\leq 15$  mg/100 g dried wood, for medium density fibreboard

*Japanese standard (desiccator method) (Meyer 1979a)*

Class E0:  $\leq 0.5$  mg/L

Class E1:  $\leq 0.5 - 1.5$  mg/L

Class E2:  $> 1.5$  mg/L

The formaldehyde emission (FE) value is greatly dependent on the testing method and many other factors (eg wood materials, resin properties and panel properties), however, based on experimental data, there is an approximate relationship between FE values determined by the two test methods, which may be expressed as:

$$FE (\text{perforator method}) \approx 30 \times FE (\text{desiccator method})$$

For example, a formaldehyde emission of 0.25 mg/L determined by the desiccator method is approximately equivalent to an emission level of 7.5 mg/100 g dried wood panel determined by the perforator method.

## APPENDIX B EFFECT OF FORMALDEHYDE AND RESIN AGING ON RESIN AND RESIN BONDED PARTICLEBOARD PROPERTIES

### *Ageing of formaldehyde solutions*

The effects of formaldehyde ageing on formaldehyde concentrations and acidity are shown in Figures B.1 and B.2.

The concentration of species present in aqueous formaldehyde solutions stored at 55°C increased with time. Because the plastic containers used in this research were not completely airtight and the vapor pressure of water is higher than that of formaldehyde species (Meyer 1979c), more water evaporated during storage at 55°C than was the case for formaldehyde.

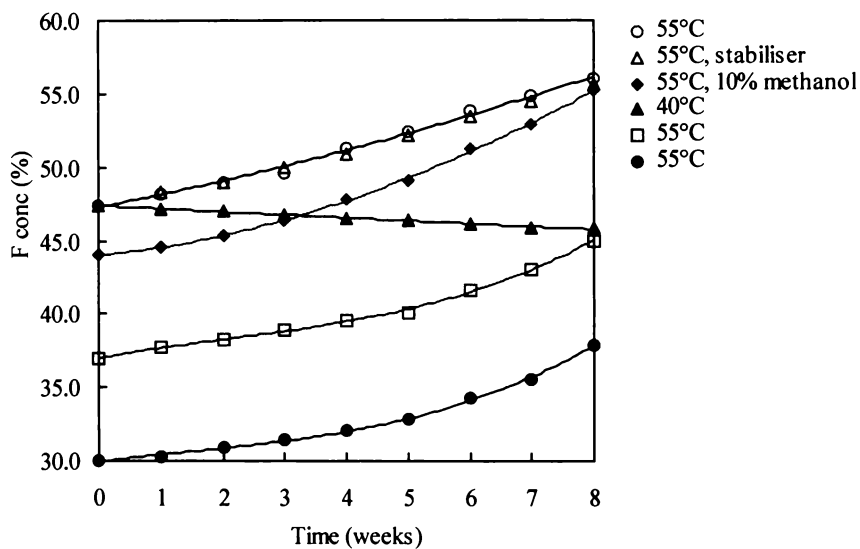
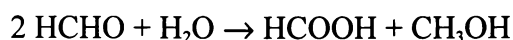


Figure B.1. The effect of formaldehyde ageing on the formaldehyde concentrations (total of aqueous formaldehyde species).

*c* 2% methanol was present in all of the formaldehyde solutions. 0.02% of “Brucelyzer” (a commercial formaldehyde stabiliser) and an additional 8% of methanol (total 10%), respectively, were added to one each of the solutions.

The acidity of the formaldehyde solutions increased with time. The addition of 0.02% of "Brucelyser" a commercial formaldehyde stabiliser had no effect on acidity. Addition of 10% methanol reduced the rate at which acidity increased during storage.

The increase in acidity during storage can be attributed to the production of formic acid via the well known Cannizzaro reaction:



The rate constant (k) for this process (assuming it is a first order process) can be estimated from data presented in Figure B.2 to be  $2.0 \times 10^{-5} \text{ week}^{-1}$  (ie  $k = 1.2 \times 10^{-7} \text{ h}^{-1}$ ) at 55°C, and the activation energy (E) to be  $134 \text{ kJ mol}^{-1}$  (ie  $E = 32 \text{ kcal mol}^{-1}$ ).

Less paraformaldehyde precipitation was observed for the formaldehyde solutions which contained stabiliser, or 10% methanol.

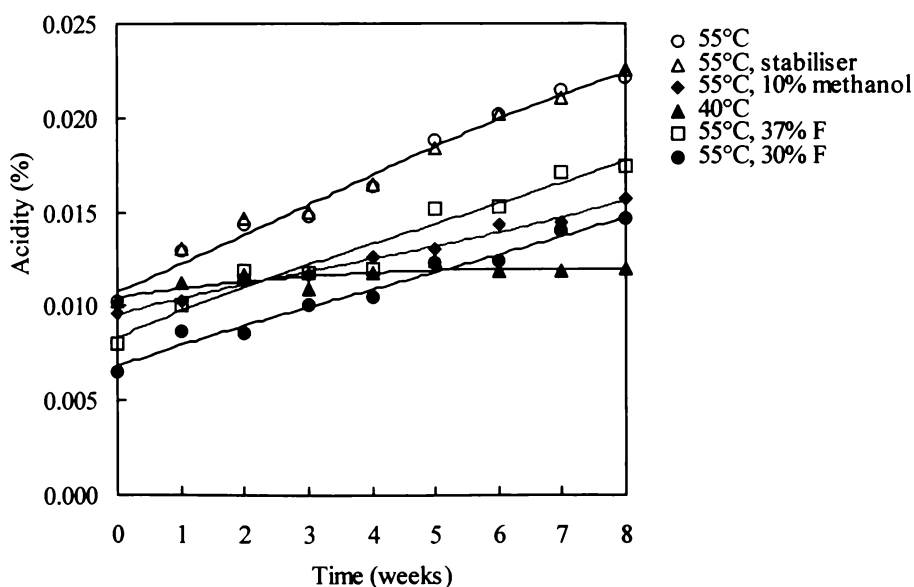


Figure B.2. The effect of formaldehyde aging on the acidity of formaldehyde solutions.

Unless otherwise indicated the initial formaldehyde concentration was 47%

*Effect of formaldehyde ageing on resin and resin bonded particleboard properties*

A series of UF resins were prepared using formaldehyde solutions which had been stored for varying times. The effects of formaldehyde ageing on the properties of the UF resins and wood panels are shown in Table B.1.

The use of formaldehyde solutions which had been stored at 40-55°C for up to 7 weeks had no significant effect on the properties of the UF resins and particleboard.

Table B.1. The effect of formaldehyde aging on the properties of resins<sup>a</sup> and resin bonded particleboard.

F ageing (weeks)	viscosity (Pa·s)	gel time (s)	IB (MPa) <sup>b</sup>	FE (mg/100 g)	swell (%)
fresh	0.15	78	2.0	8.3	21
4 w at 55°C	0.16	75	1.9	8.7	20
4 w at 40°C	0.14	76	1.9	8.5	22
7 w at 40°C	0.15	80	2.1	8.3	23

<sup>a</sup> resin preparation conditions: formaldehyde concentration = 46%, initial addition pH = 8.8, condensation pH = 5.0, addition reaction time = 32 min, final F/U molar ratio = 1.1.

<sup>b</sup> panel making conditions: particleboard, thickness = 8 mm, resin loading 8% on dried wood.

*Effect of resin ageing on resin and resin bonded particleboard properties*

It is well known that UF resins are reactive systems. Even at alkaline storage conditions (pH 7-9), condensation stages reactions continue to occur (though at very slow rate). Consequently the viscosity and molecular weight of a resin increases with time.

The effects of the storage time on the properties of resins and resin bonded particleboards are summarised in Table B.2 and B.3.

It is apparent that:

- the viscosity of a resin increases with storage time.
- the higher the final F/U molar ratio of a resin, the longer the storage life.
- conventional resins have a longer storage life than pH adjusted resins.
- internal bond strength and formaldehyde emission decrease with storage time.

Table B.2. The effect of resin aging on the viscosity of the resins and the shelf life of the resin.

resins-F/U ratio	viscosity (Pa·s)							shelf life <sup>b</sup> (months)
	(fresh)	(3 w) <sup>a</sup>	(6 w)	(10 w)	(15 w)	(20 w)	(26 w)	
<b>pH adjusted</b>								
UF3-1.30	0.17		0.22	0.25	0.27			4.5
UF3-1.20	0.16		0.20	0.24	0.29			4.0
UF3-1.10	0.15		0.21	0.27	0.35			3.5
UF3-0.95	0.13	0.15	0.20	0.30				3.0
<b>conventional</b>								
UF4-1.30	0.19	0.21	0.23	0.25	0.27	0.35	0.42	6.0
UF4-1.20	0.17	0.18	0.20		0.28	0.36		5.5
UF4-1.10	0.15	0.16	0.17	0.22	0.29	0.35		4.5
UF3-0.95	0.13	0.15	0.19	0.25	0.32			3.5

<sup>a</sup> storage time (at 20°C) in weeks (w). <sup>b</sup> shelf life is the storage life (months) until the resin lost its mobility (gelled to a thick white paste).

Table B.3. The effect of resin aging on the properties of the resin bonded particleboard.

storage time	fresh (1 week)	6 weeks	10 weeks
<u>resin UF3-1.10</u>			
IB (MPa)	2.10	1.99	1.80
FE (mg/100 g)	8.8	8.5	7.7
swell (%)	18	19	18
density (g/cm <sup>3</sup> )	0.70	0.68	0.68
<u>resin UF4-1.10</u>			
IB (MPa)	1.95	1.92	1.70
FE (mg/100 g)	9.2	8.7	8.0
swell (%)	19	20	20
density (g/cm <sup>3</sup> )	0.69	0.67	0.68

## **APPENDIX C EFFECT OF WOOD MATERIALS, RESIN LOADING AND PANEL THICKNESS ON WOOD PANEL PROPERTIES**

### *Effect of wood materials*

Particleboard and medium density fibreboard (MDF) are the two most common commercial wood panels which are bonded using UF resins.

Wood chips are normally produced simply by cutting or grinding the wood material into a wood particle, usually about 20 - 40 meshes. However, wood fibres are normally generated in a pressurised refiner using steam to help to break down wood lignins. Under refiner conditions (high pressure and temperatures) significant amounts of weak or strong organic acids are produced. The pH of product material is  $\approx$  4-5 (Suchsland and Woodson 1991, Maloney 1977, Moslemi 1974). It is not necessary to add hardener when manufacturing MDF since the acidity of the wood fibre material is sufficient to cure an UF resin at high temperature (*c* 160-180°C). However, it is necessary to use a hardener (eg NH<sub>4</sub>Cl or acetic acid) to cure the resin when manufacturing particleboard, the acidity of the wood chips is too low to cure the resin even at high temperature.

In order to choose an appropriate material to evaluate the resin performance, preliminary investigations using wood particles (chips) and fibre were undertaken.

An UF resin produced using the conventional two-pH stage reaction procedure was used to make four 28 by 38 cm<sup>2</sup> particleboard (PB) panels and four MDF panels (28 by 38 cm<sup>2</sup>). The resin preparation conditions and specification are given in Table C.1. Four sub-samples of the four trial panels (total 16 test panels) were used to determine the internal bond strength, formaldehyde emission, cold water swell and absorption properties of the panels (see Table C.2).

Table C.1. Resin preparation conditions and specifications.

F/U		pH		t <sub>a</sub>	temp	solid	viscosity	gel time
initial	final	init	add	(min)	(°C)	(%)	(Pa·s)	(sec)
2.0	1.3	8.9	5.0	40	88	57.1	0.20	74

Table C.2. Properties determined for trial panels (mean of 16 results).

wood panel	density	IB	water swell <sup>b</sup>	water abs <sup>b</sup>	FE <sup>c</sup>
	(g cm <sup>-3</sup> )	(MPa)	(%)	(%)	(mg/100 g)
PB <sup>a</sup>	0.70	2.1	15	77	26
MDF	0.73	1.4	5.6	19	41
RSD <sup>d</sup>	< 0.07	< 0.10	< 0.10	< 0.15	< 0.10

<sup>a</sup> Thickness of the wood panel was nominally 15 mm (actually *c* 14.6 mm); <sup>b</sup> cold water swell and absorption; <sup>c</sup> FE = formaldehyde emission in mg formaldehyde per 100 g dried wood panel; <sup>d</sup> RSD = relative standard deviation of the data (normally 16 data points), PB and MDF panels exhibited similar RSDs.

The data presented in Table C.2 show that:

- 1) the internal bond strength of particleboard is higher than that of MDF (2.0 and 1.4 MPa respectively).
- 2) the formaldehyde emission of particleboard is lower than that of MDF (26 and 41 mg/100g wood respectively).
- 3) the cold water swell and absorption characteristics of particleboard were much higher than those of MDF. Cold water swell showed less variation (*c* 10%) than cold water absorption (*c* 15%).

Since the wood panel properties were greatly dependent on wood materials, the performance determination must be based on one material. Particleboard panels were used for routine resin performance tests.

*Effect of panel thickness*

The effect of the panel thickness on the properties of the particleboard was shown in Table C.4. Generally, the thicker the panel the lower the internal bond and water swell, and the higher the formaldehyde emission. Since wood panel properties are dependent on panel thickness, performance tests were routinely performed using 8 mm thick panels.

Table C.4. The effect of board thickness on the resin performance<sup>a</sup>.

nominal thickness (mm)	IB (MPa)	FE (mg/100 g)	water swell (%)
3.0	2.2	5.6	21
8.0	2.0	6.9	19
12	1.9	8.3	18
15	1.7	9.4	16

<sup>a</sup> resin loading = 8.0 % on dried wood; 16 test samples for each thickness.

*Effect of resin loading*

The effects of the resin loading on the properties of the trial particleboard samples are shown in Table C.3. The higher the resin loading, the higher the internal bond strength, and the lower the formaldehyde emission, water swell and water absorption. A resin loading of 8% was used for all resin performance determinations.

Table C.3. The effect of resin loading on the properties of particleboard<sup>a</sup>.

resin loading (%)	IB (MPa)	FE (mg/100 g)	swell (%)	absorption (%)
4	1.5	9.2	29	105
8	2.0	8.8	19	83
12	2.5	7.0	14	78
16	2.8	6.3	12	71

<sup>a</sup> Panel thickness = 8 mm (nominal).

## **APPENDIX D PRELIMINARY INVESTIGATION OF UF RESINS USING DSC**

Temperature programmed DSC was used to investigate the resin curing process. The thermal characteristics observed in this investigation were consistent with experimental data reported by Szesztay (1993).

Features of the thermograms depicted in Figures D.1 are summarised below

- 1) The exothermic peak at 80-85°C (the first peak from the left in Figure D.1 (a) in the thermogram of a typical UF resin, to which hardener had been added, is attributable to crosslinking (curing) reactions. All of the resins to which hardener had been added exhibited similar curing profiles (over the range 80-85°C).
- 2) The thermogram of an UF resin, without added hardener, did not include an exothermic crosslinking peak at 80-85°C (see Figure D.1 (b)).
- 3) The large, and more variable, endothermic peak which occurred at 110-160°C, arises from the decomposition of ether groups ( $-\text{CH}_2\text{OCH}_2-$ ) (Szesztay *et al.* 1993).
- 4) The DSC thermograms of paraformaldehyde ( $\text{H}(\text{OCH}_2)_n\text{OH}$ ) showed similar endothermic peaks, ie ether ( $-\text{CH}_2\text{OCH}_2-$  decomposition) (see Figure D.1(c)). A plot of the area of the endothermic peak ( $= \Delta H_e$ ) vs the amount of paraformaldehyde (Q) showed a linear relationship up to  $Q = 3.0$  mg. This plot can be used as a calibration curve to estimate ether group content in the UF resins.
- 5) The multiple exothermic and endothermic peaks which appear over 200°C arise from resin decomposition. The degradation of the resin was visible over 200°C. Above 200°C the appearance of resin samples changed from yellowish liquids to dark coloured, crumbly, materials.

The enthalpy of the curing process ( $\Delta H_c$ ) is related to the reactivity of the resin, so it may relate to the properties of the resins and the wood panels bonded with these resins.

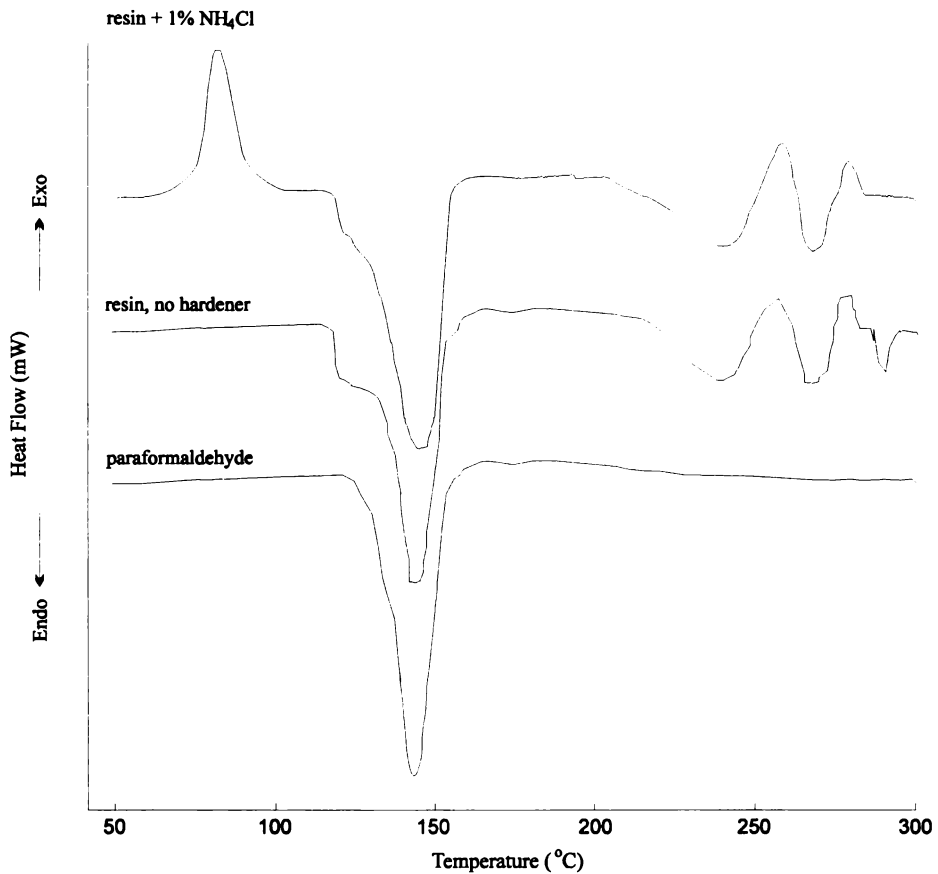


Figure D.1. DSC thermograms of a typical UF resin with (a) upper profile: 1 % hardener ( $\text{NH}_4\text{Cl}$ ) added; (b) middle profile: the same resin without hardener; (c) lower profile: paraformaldehyde.

Data are for resin sample: R-08 (see Section 6.2)

The peak area of the endothermic peak ( $\Delta H_e$ ), attributable to ether group decomposition, should be proportional to the concentration of ether groups in the resin. Therefore,  $\Delta H_e$ s should be proportional to the formaldehyde emissions (see Table D.1).

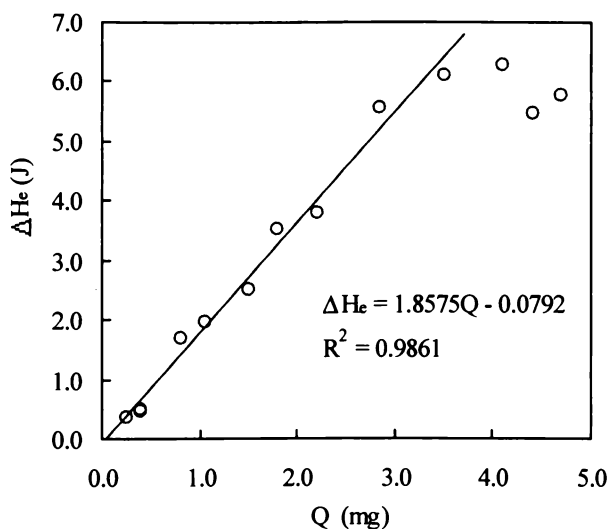


Figure D.2. The plot of  $\Delta H_e$  vs weight (Q) of paraformaldehyde

Data are for resin sample: R-08 (see Section 6.2).

Table D.1. Relationship between  $\Delta H_e$ s and formaldehyde emissions (FE).

$\Delta H_e$ (without hardener) ( $J g^{-1}$ )	600	485	455	385
$\Delta H_e$ (with hardener) <sup>a</sup> ( $J g^{-1}$ )	725	692	561	516
FE (mg/100 g wood panel)	8.7	7.4	7.0	6.3

<sup>a</sup> hardener: 2 mL 8%  $NH_4Cl$  in 20 g resin.

The onset temperature of ether group decomposition is assumed to depend on the internal physical structure, therefore, it should be proportional to the thermal stability of the UF resin.

#### *Effect of hardener*

The effect of adding different amounts of the 8%  $NH_4Cl$  solution on  $\Delta H_c$ , peak temperature of crosslinking ( $T_p$ ) and the onset temperature of the ether group decomposition ( $T_e$ ) is shown in Figure D.3. 0.8–1.2%  $NH_4Cl$  (ie 2-3 mL of the 8%  $NH_4Cl$  solution per 20 g resin) is recommended for completely curing the resin.

The effect of the time after the addition of hardener on the  $\Delta H_c$  is shown in Figure D.4.  $\Delta H_c$  decreased slowly with time.

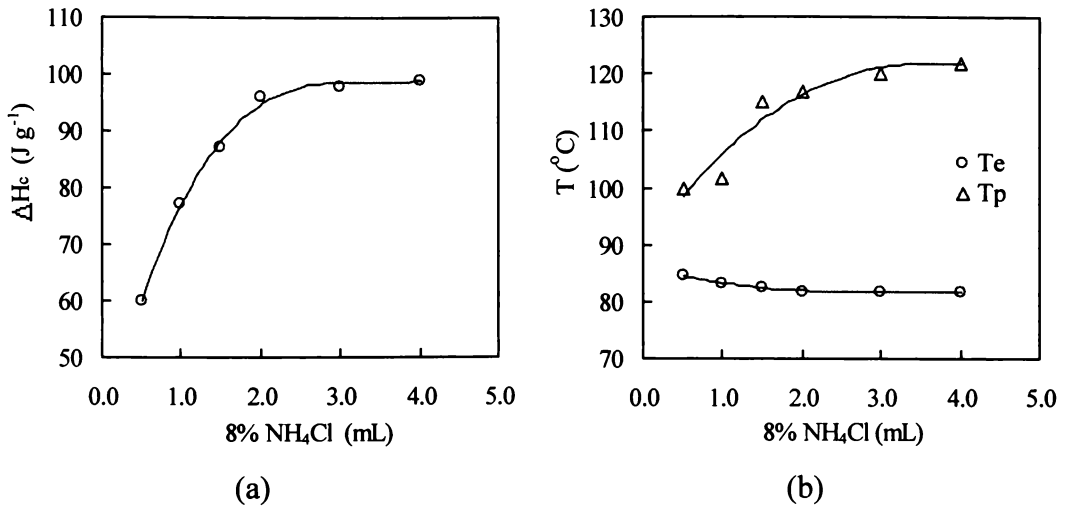


Figure D.3. The effects of the amount of the hardener (8% NH<sub>4</sub>Cl) added on the (a)  $\Delta H_c$  and (b) peak temperature of crosslinking ( $T_p$ ) and onset temperature of ether group decomposition ( $T_e$ ).

Data are for resin sample: R-08 (see Section 6.2) (F/U=1.10) 20 g.

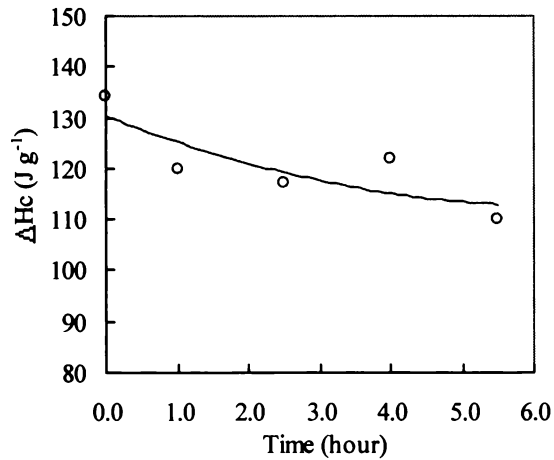


Figure D.4. The effect of the time after addition of NH<sub>4</sub>Cl on  $\Delta H_c$ .

## APPENDIX E CONVERSION OF DYNAMIC (RAPID) NMR DATA TO ABSOLUTE CONCENTRATIONS

Dynamic (RAPID) NMR data can be converted to absolute concentrations by the method described in Section 4.4.2. Results are summarised in Tables E.1 to E.5. Integrals are expressed in arbitrary unit (au). The initial integrals of urea and formaldehyde were  $I_{U_0} = 0.51$  au and  $I_{F_0} = 5.3$  au respectively. The corresponding urea and formaldehyde concentrations were  $[U]_0 = 6.4$  mol L<sup>-1</sup> and  $[F]_0 = 12.8$  mol L<sup>-1</sup>, respectively.

Reaction conditions common to all the experiments are: formaldehyde concentration = 46%, F/U molar = 2.0, initial addition pH = 8.7.

Table E.1. Conversion of dynamic (RAPID) NMR data to absolute concentrations for the reaction at 60°C.

time (sec)	<u>free urea</u>		<u>free F</u>		<u>MMU</u>		<u>DMU</u>	
	integral	mol L <sup>-1</sup>	integral	mol L <sup>-1</sup>	integral	mol L <sup>-1</sup>	integral	mol L <sup>-1</sup>
11.2	0.188	1.38	3.72	8.98	0.418	2.90	0.116	0.71
13.7	0.157	1.14	3.09	7.46	0.426	2.92	0.153	0.93
16.2	0.110	0.76	2.72	6.58	0.451	2.92	0.231	1.32
18.6	0.092	0.65	2.59	6.26	0.434	2.88	0.250	1.46
21.1	0.087	0.61	2.43	5.88	0.426	2.80	0.273	1.58
23.5	0.070	0.51	2.15	5.20	0.407	2.78	0.282	1.70
26.0	0.062	0.41	1.89	4.57	0.435	2.72	0.335	1.86
28.5	0.062	0.41	1.86	4.49	0.442	2.78	0.322	1.79

Table E.2. Conversion of dynamic (RAPID) NMR data to absolute concentrations for the reaction at 70°C.

time (min)	<u>free urea</u>		<u>free F</u>		<u>MMU</u>		<u>DMU</u>	
	integral	mol L <sup>-1</sup>	integral	mol L <sup>-1</sup>	integral	mol L <sup>-1</sup>	integral	mol L <sup>-1</sup>
9.1	0.192	1.549	3.40	8.22	0.368	2.79	0.097	0.65
11.6	0.110	0.831	2.57	6.20	0.386	2.75	0.225	1.41
14.0	0.058	0.455	2.08	5.03	0.381	2.81	0.266	1.73
16.5	0.061	0.439	1.77	4.28	0.394	2.67	0.314	1.88
19.0	0.042	0.298	1.54	3.72	0.343	2.29	0.406	2.40
21.4	0.053	0.382	1.29	3.12	0.352	2.39	0.370	2.22
23.9	0.025	0.172	1.24	3.00	0.358	2.32	0.435	2.50
26.3	0.041	0.262	1.25	3.01	0.369	2.22	0.471	2.51

Table E.3. Conversion of dynamic (RAPID) NMR data to absolute concentrations for the reaction at 80°C.

time (min)	<u>free urea</u>		<u>free F</u>		<u>MMU</u>		<u>DMU</u>	
	integral	mol L <sup>-1</sup>	integral	mol L <sup>-1</sup>	integral	mol L <sup>-1</sup>	integral	mol L <sup>-1</sup>
9.0	0.143	1.223	2.83	6.84	0.338	2.72	0.143	1.05
11.4	0.074	0.575	1.80	4.35	0.374	2.74	0.259	1.68
13.9	0.044	0.312	1.20	2.90	0.358	2.39	0.388	2.29
16.4	0.031	0.230	1.24	2.98	0.291	2.04	0.441	2.72
18.8	0.026	0.179	0.85	2.05	0.303	1.96	0.498	2.85
21.3	0.029	0.199	0.94	2.27	0.308	1.98	0.493	2.81
23.7	0.020	0.138	0.84	2.03	0.311	2.02	0.496	2.84
26.2	0.015	0.099	0.81	1.96	0.284	1.77	0.567	3.12

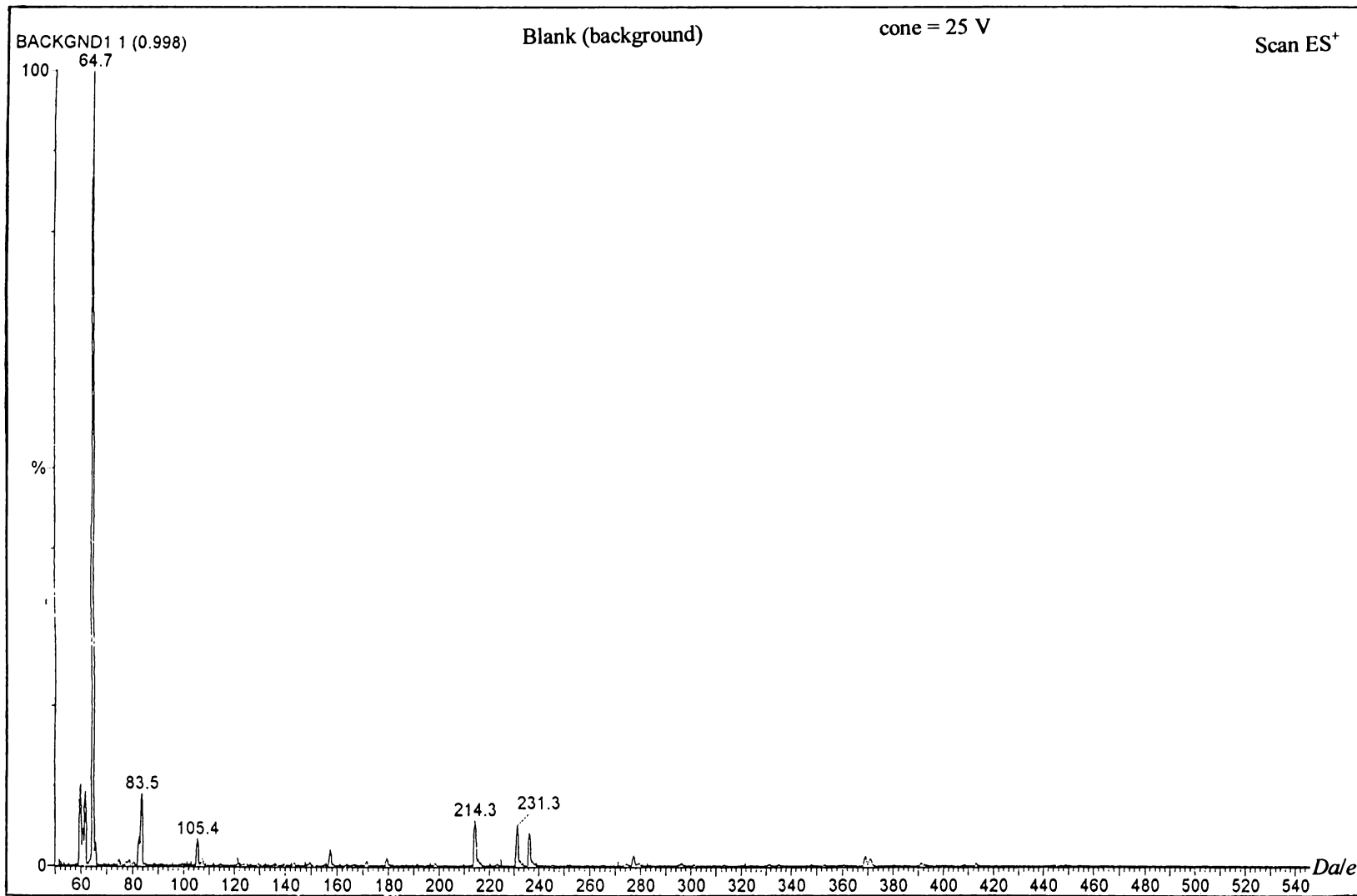
Table E.4. Conversion of dynamic (RAPID) NMR data to absolute concentrations for the reaction at 90°C.

time (min)	<u>free urea</u>		<u>free F</u>		<u>MMU</u>		<u>DMU</u>	
	integral	mol L <sup>-1</sup>	integral	mol L <sup>-1</sup>	integral	mol L <sup>-1</sup>	integral	mol L <sup>-1</sup>
9.07	0.115	0.894	2.19	5.30	0.367	2.69	0.218	1.41
11.5	0.065	0.458	1.05	2.53	0.334	2.22	0.395	2.32
14.0	0.056	0.362	0.83	2.05	0.307	1.87	0.512	2.76
16.5	0.033	0.206	0.67	1.62	0.303	1.79	0.578	3.00
18.9	0.040	0.261	0.69	1.66	0.313	1.93	0.515	2.80
21.4	0.022	0.132	0.57	1.37	0.282	1.60	0.651	3.26
23.9	0.031	0.178	0.62	1.50	0.283	1.53	0.685	3.28
26.4	0.025	0.144	0.55	1.33	0.255	1.38	0.726	3.47

Table E.5. Conversion of dynamic (RAPID) NMR data to absolute concentrations for the reaction at 97°C.

time (min)	<u>free urea</u>		<u>free F</u>		<u>MMU</u>		<u>DMU</u>	
	integral	mol L <sup>-1</sup>	integral	mol L <sup>-1</sup>	integral	mol L <sup>-1</sup>	integral	mol L <sup>-1</sup>
8.60	0.104	0.766	1.84	4.44	0.414	2.85	0.226	1.38
11.1	0.068	0.540	1.20	2.91	0.372	2.81	0.247	1.64
13.5	0.035	0.256	0.82	1.97	0.340	2.34	0.498	2.42
16.0	0.036	0.246	0.57	1.38	0.308	2.04	0.470	2.75
18.4	0.026	0.169	0.45	1.08	0.301	1.83	0.546	3.02

APPENDIX F ESMS SPECTRA OF MODEL COMPOUNDS  
AND UF RESINS

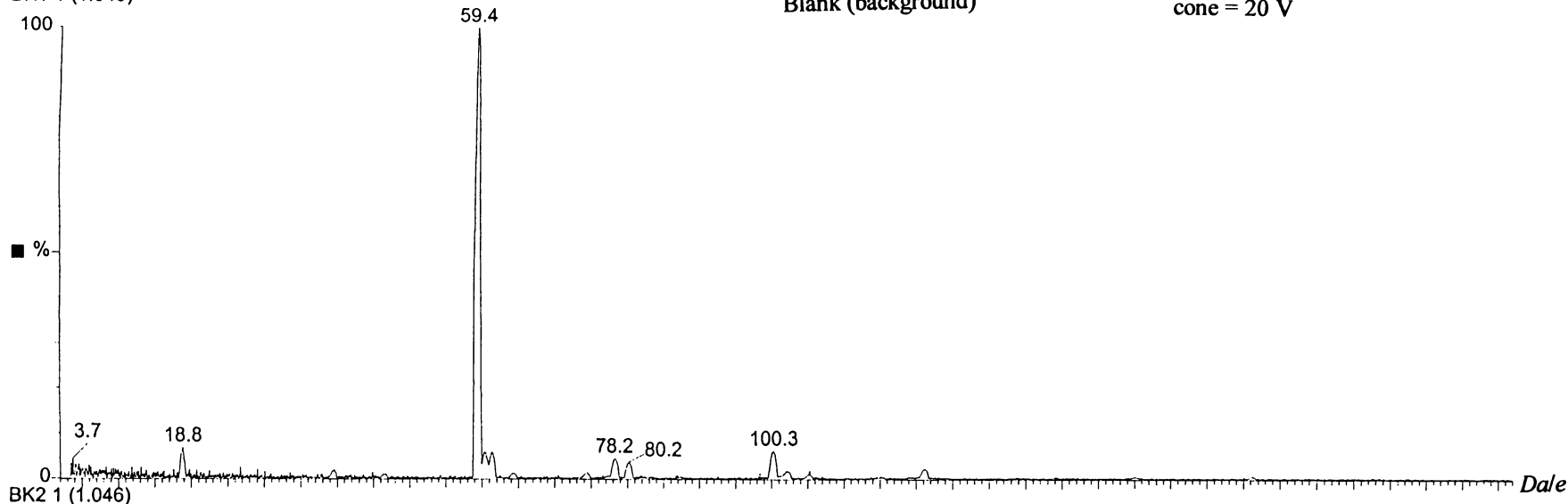


BK1 1 (1.045)

Blank (background)

cone = 20 V

Scan ES<sup>+</sup>

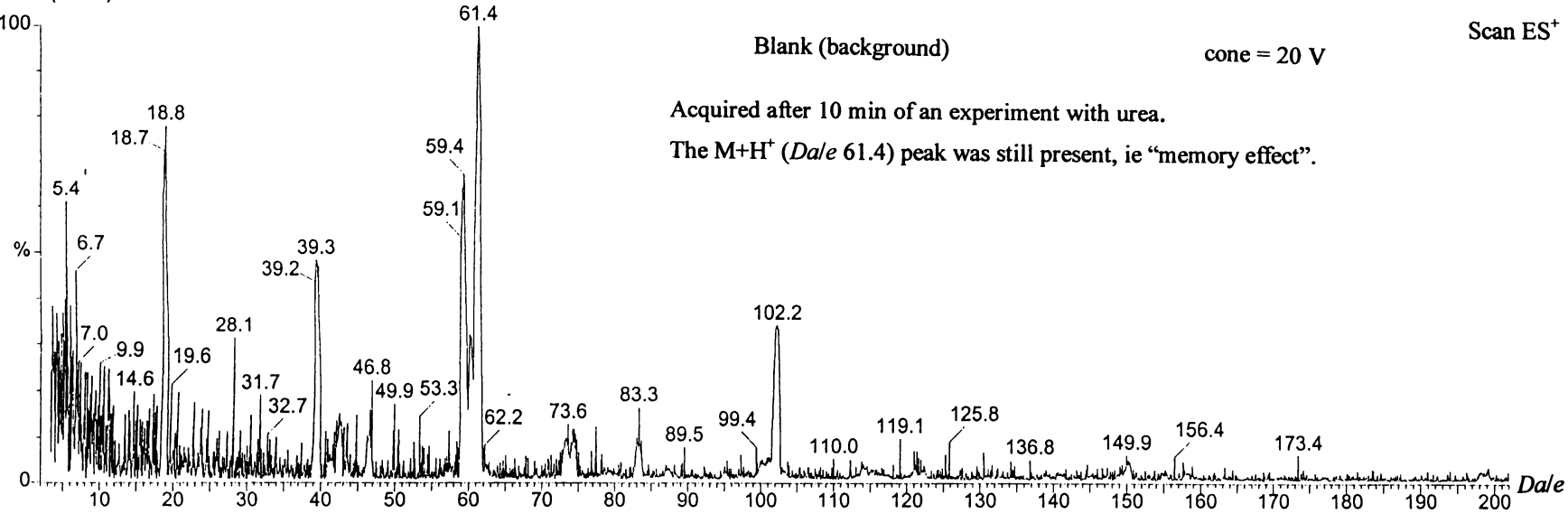


BK2 1 (1.046)

Blank (background)

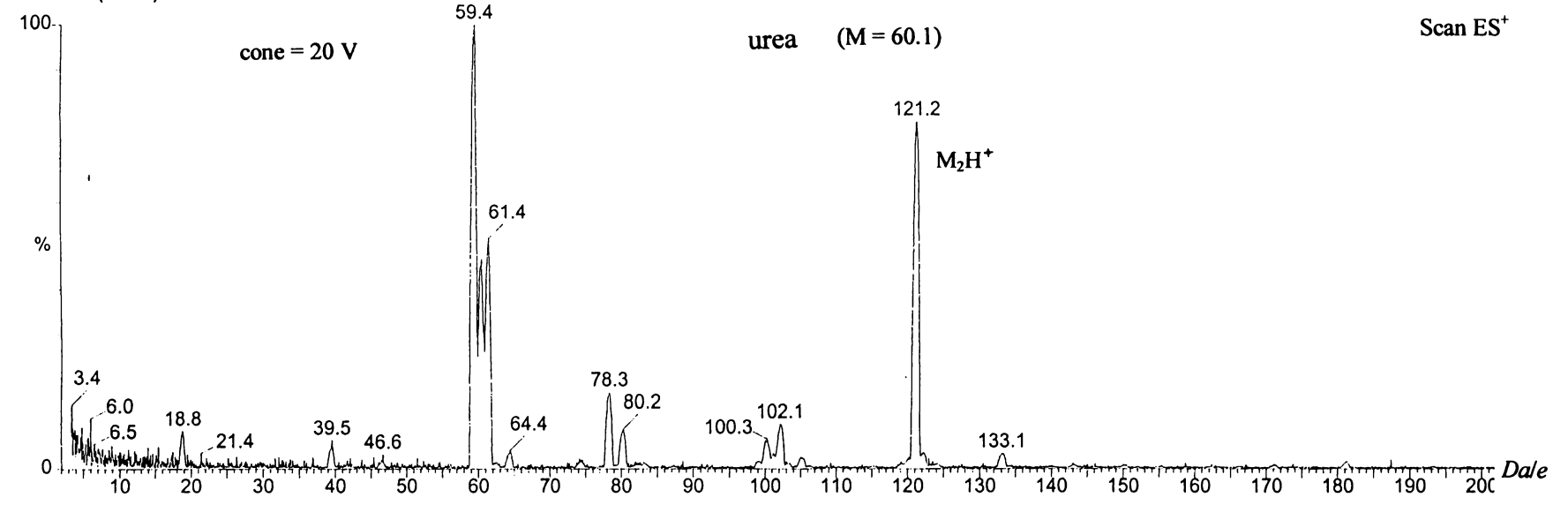
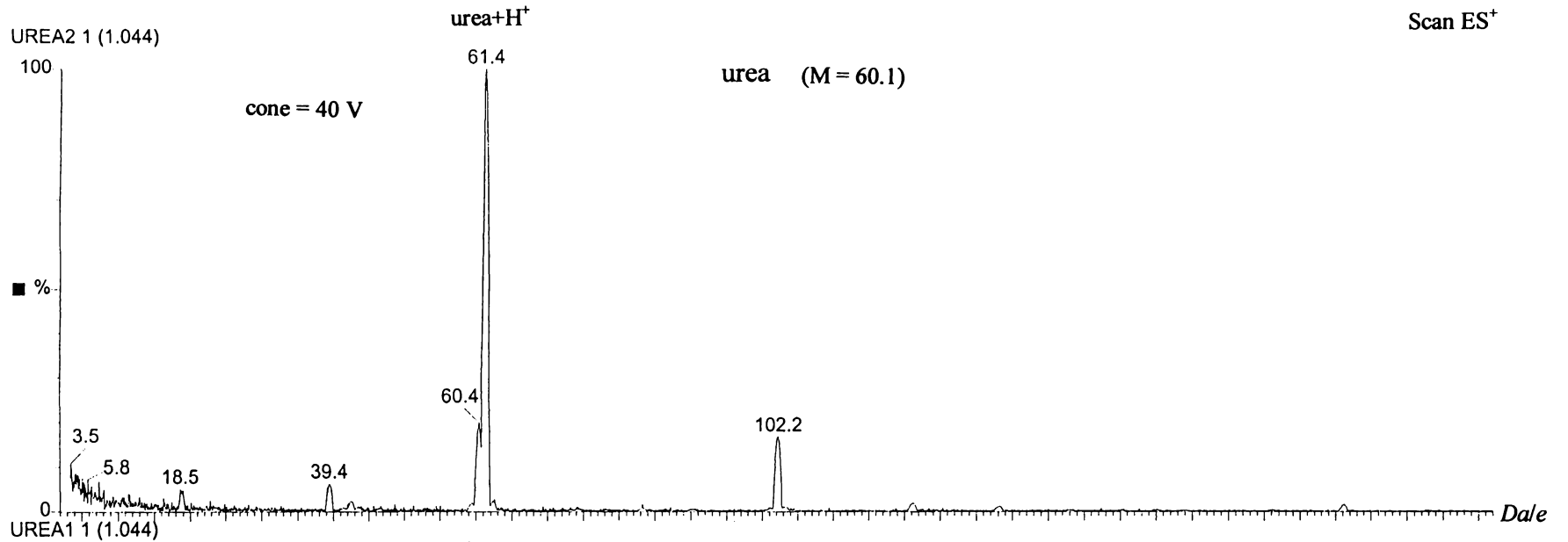
cone = 20 V

Scan ES<sup>+</sup>



Acquired after 10 min of an experiment with urea.

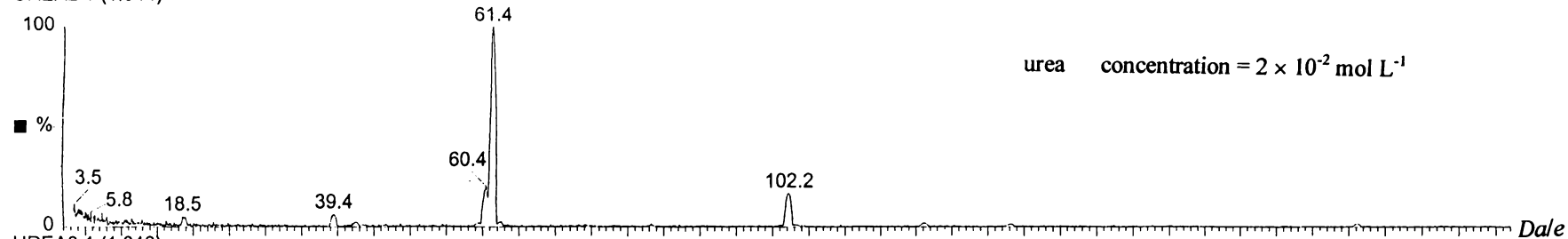
The M+H<sup>+</sup> (Dale 61.4) peak was still present, ie "memory effect".



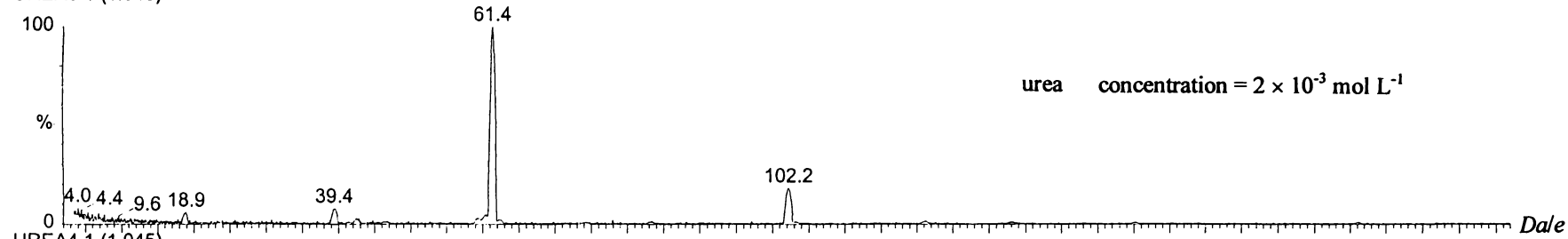
cone = 40 V

Scan ES<sup>+</sup>

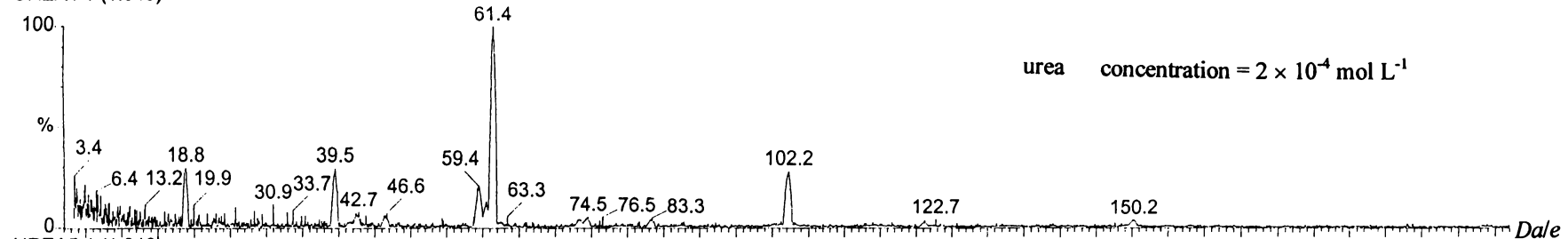
UREA2 1 (1.044)



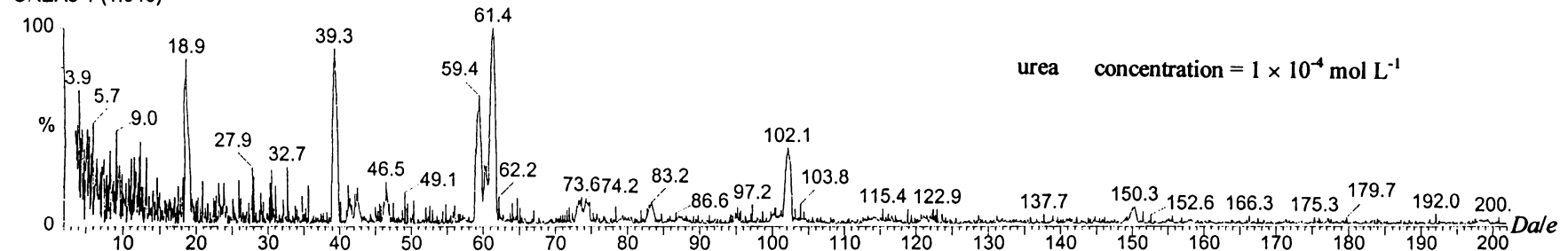
UREA3 1 (1.046)

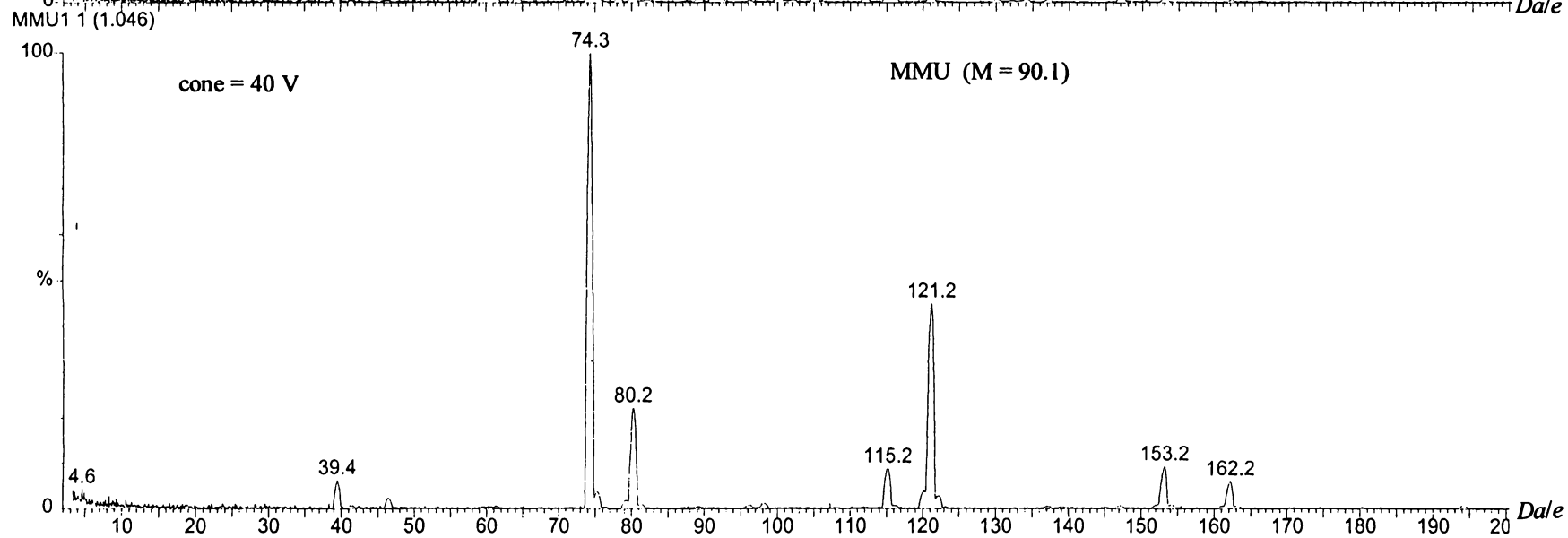
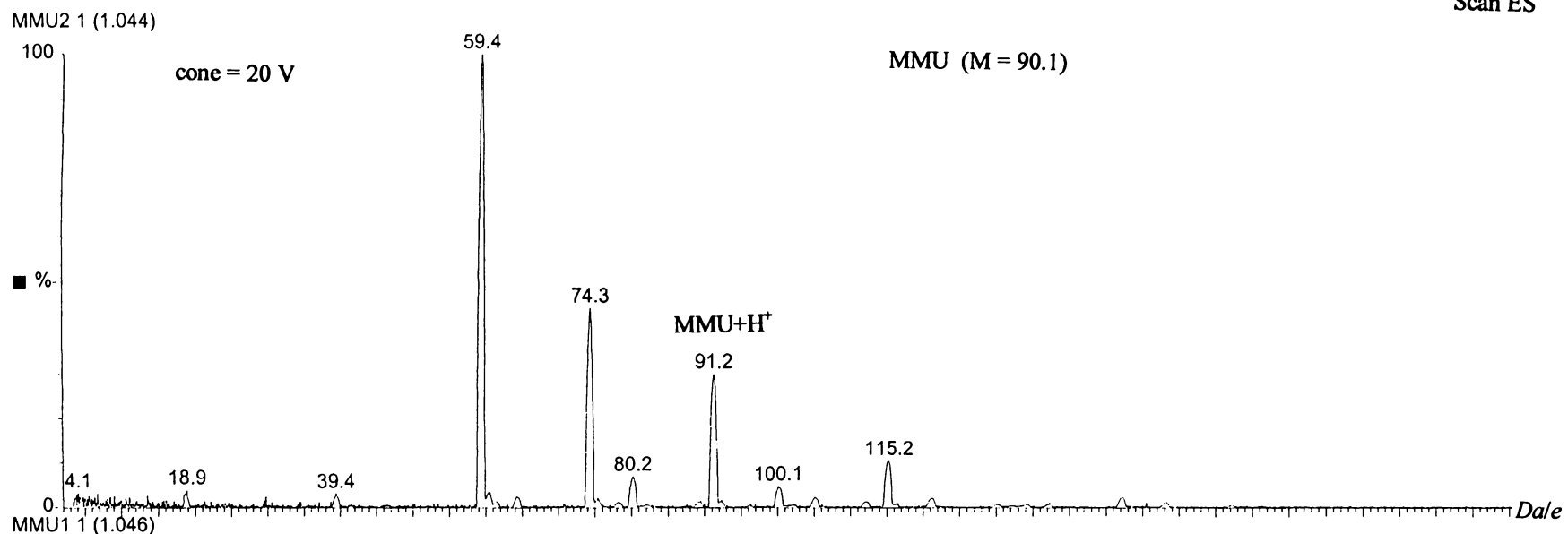


UREA4 1 (1.045)



UREA5 1 (1.046)



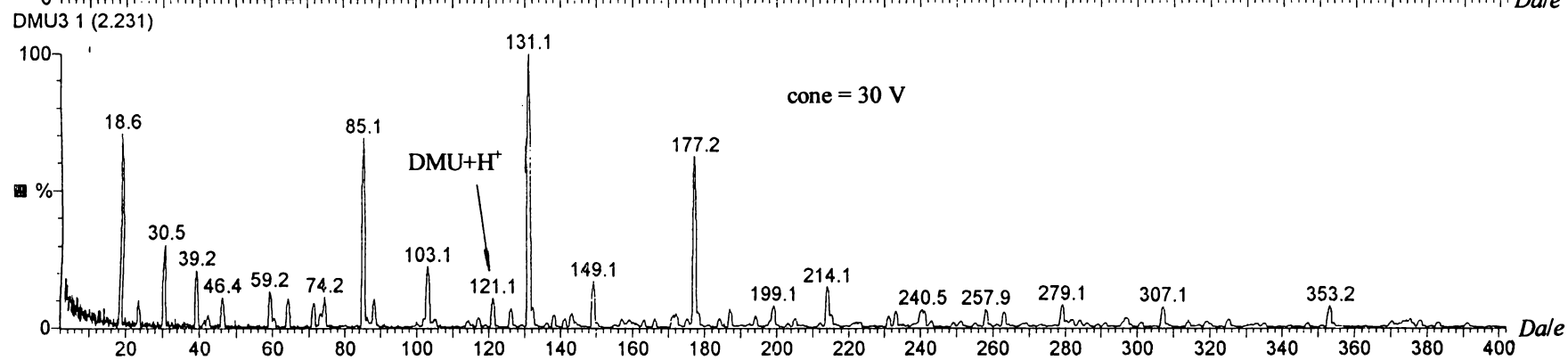
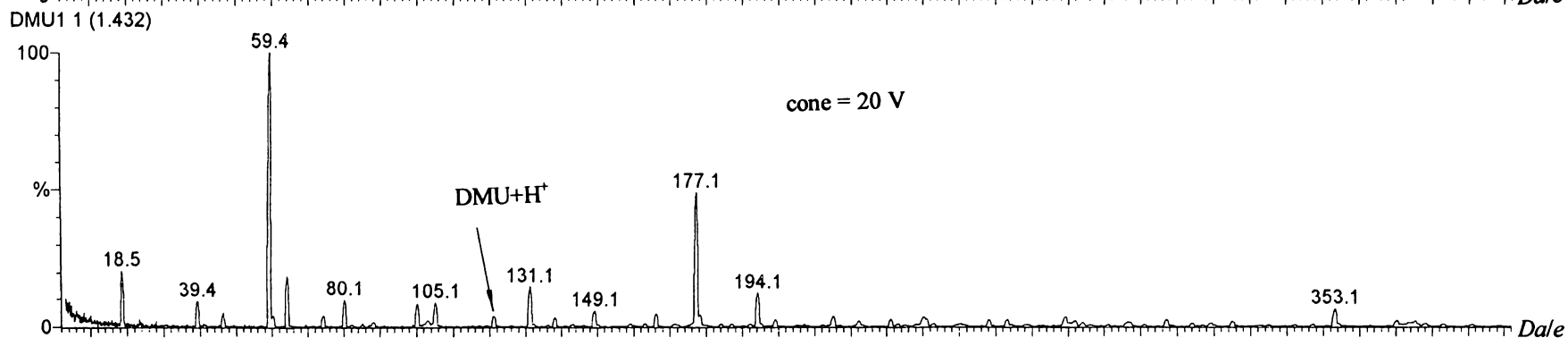
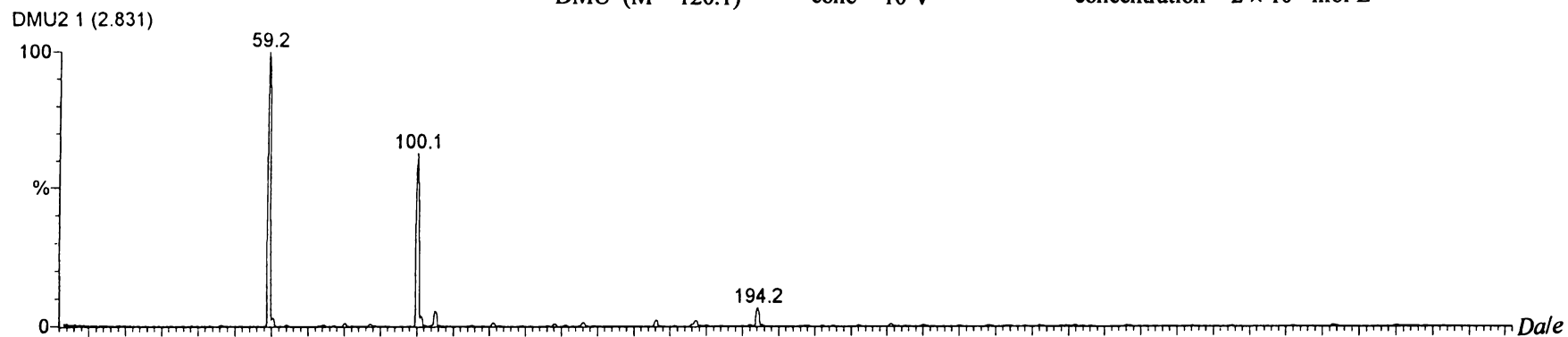


DMU (M = 120.1)

cone = 10 V

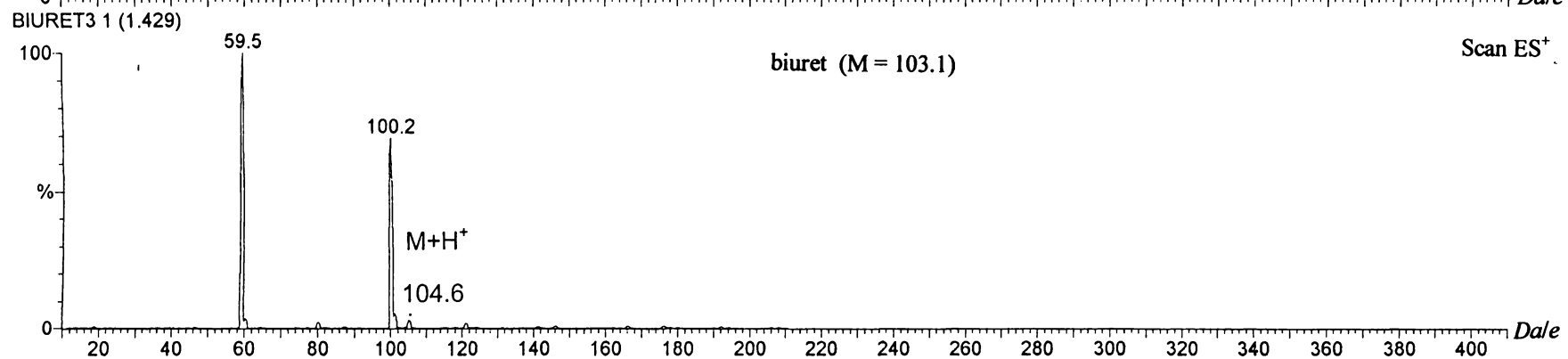
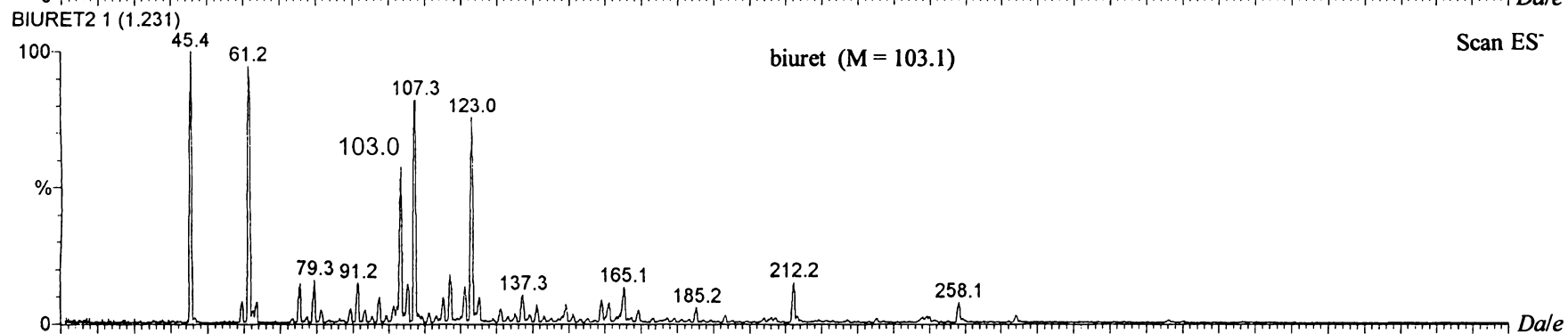
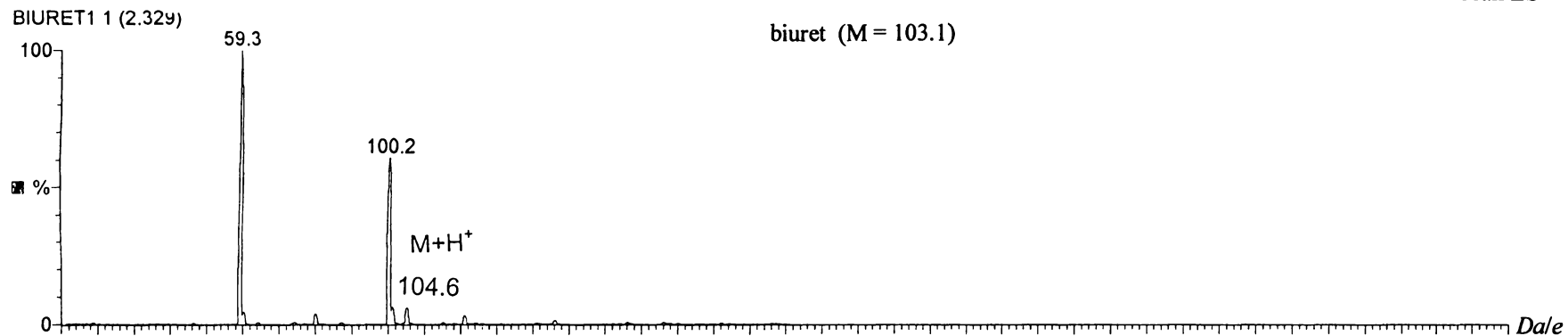
concentration =  $2 \times 10^{-3}$  mol L<sup>-1</sup>

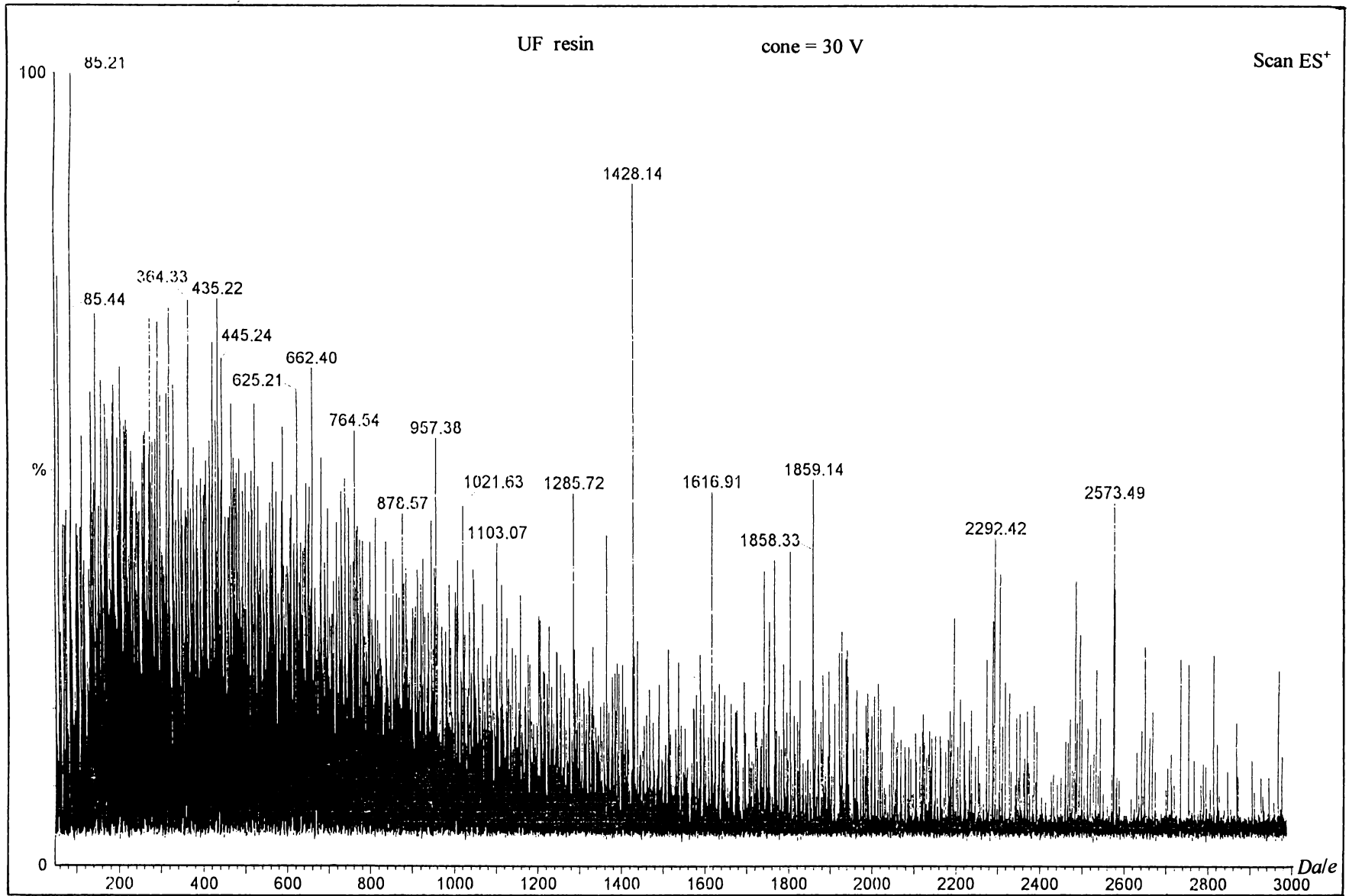
Scan ES<sup>+</sup>

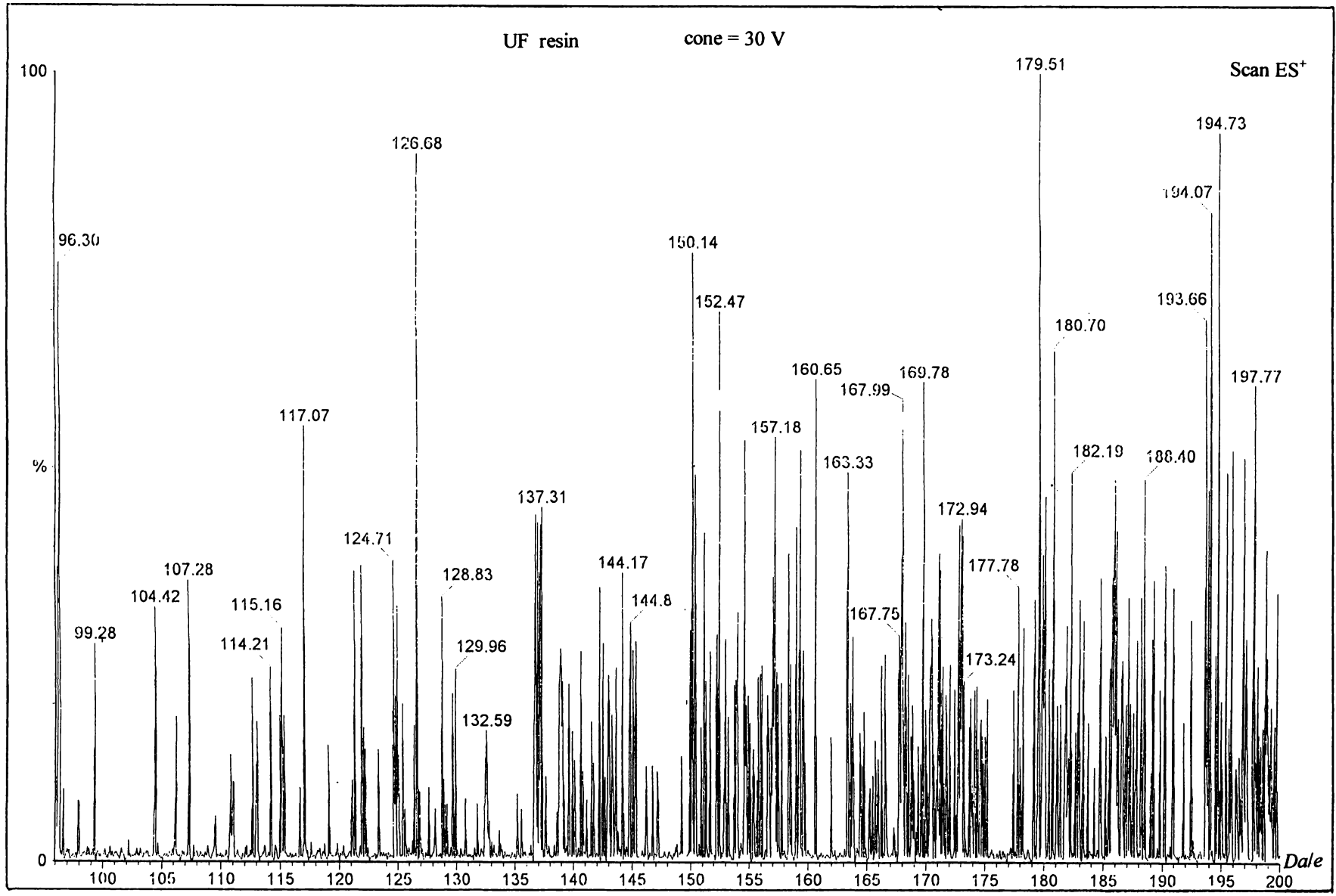


cone = 10 V

Scan ES<sup>+</sup>



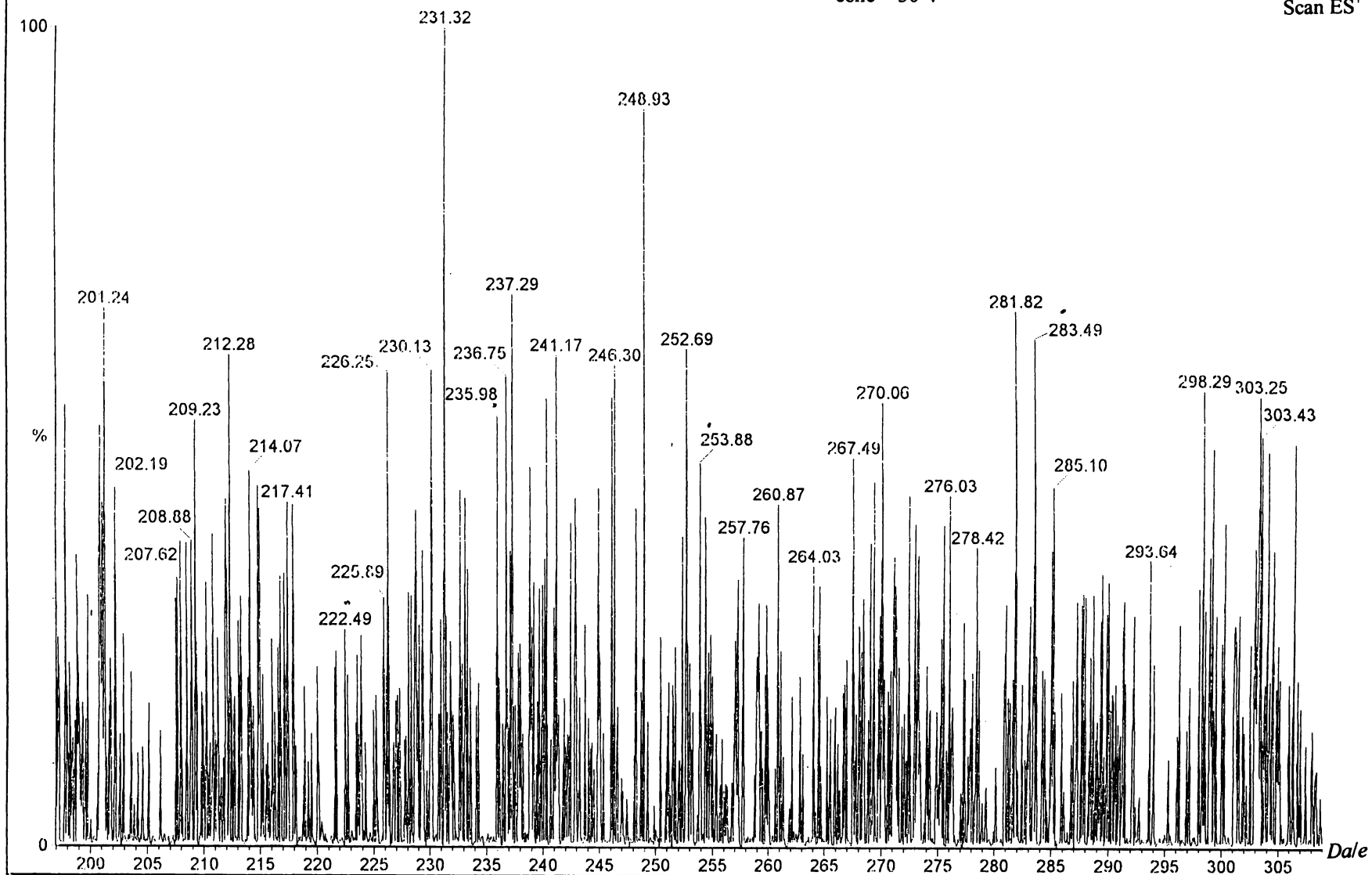




UF resin

cone = 30 V

Scan ES<sup>+</sup>



## BIBLIOGRAPHY

- Abraham, R. J., Fisher, J. and Loftus, P. 1988. *Introduction to NMR Spectroscopy*, John Willey & Sons Ltd., New York, U.S.A.
- Akitt, J. W. 1992. *NMR and Chemistry, An Introduction to Modern NMR Spectroscopy*, 3rd edition, Chapman & Hall, London, U.K.
- Alltech Associates Inc. 1995. *Chromatography Catalog 350*, Deerfield, Illinois, U.S.A.
- Andrews, B. A. K, Reinhardt, R. M, Frick, J. G, Jr. and Bertoniere, N. R. 1986. *ACS Symposium Series 316, Formaldehyde Release from Wood Products*, eds: Meyer, B., Andrews, B. A. K. and Reinhardt, R. M., American Chemical Society, Washington DC, U.S.A., 52-66.
- Armonas, J. E. 1970. *Forest Prod. J.*, **20**: 22-28.
- Bai, Y. 1981. *Hei Long Jiang Chem. Ind.*, **3**: 44-50.
- Baldwin, R. F. 1995. *Plywood and Veneer-Based Products: Manufacturing Practices*, Miller Freshman Inc., San Francisco, U.S.A.
- Becker, E. D. 1980. *High Resolution NMR -Theory and Chemical Applications*, 2nd edition, Academic Press Inc., New York, U.S.A.
- Bettelheim, L. and Cedwall, J. 1948. *Sven. Kem. Tidskr.*, **60**: 208.
- Billiani, J., Lederer, K. and Dunky, M. 1990. *Angew. Makromol. Chem.*, **180**: 199-208.
- Billmeyer, F. W. 1984. *Textbook of Polymer Science*, Wiley-Interscience, John Wiley & Sons, New York, U.S.A.
- Bolton, A. J. and Irle, M. A. 1987. *Holzforschung*, **41**: 155.
- Braun, D. and Bayersdorf, F. 1980. *Angew. Makromol. Chem.*, **89**: 183-200.
- Braun, D. and Bayersdorf, F. 1980. *Angew. Makromol. Chem.*, **85**: 1-13.
- Brzozowski, Z, Noniewicz, K, Mazur, J. and Pietrzak, B. 1996. Polish Patent 167,183.
- Calve, L. 1983. *J. Appl. Polym. Sci.*, **28**: 1969.
- Calve, L. 1984. *Adhesives Age*, **27**: 39.
- Camino, G, Luda, M. P., Costa, L. and Guaita, M. 1996. *Macromol. Chem. Phys.*, **197**: 41-60.
- Chang, T. T. 1994. *Anal. Chem.*, **66**: 3267-3273.

## Bibliography

- Chiavarini, M. and Bigatto, R. 1975. *Angew. Makromol. Chem.*, **46**: 151-162.
- Chow, S. and Troughton, G. E. 1975. *Forest Prod. J.*, **25**: 54.
- Christian, G. D. and O'Reilly, J. E. 1986. *Instrumental Analysis*, 2nd edition, Allyn and Bacon Inc., Boston, U.S.A.
- Christensen, G. 1980. *Prog. Org. Coatings*, **8**: 211-239.
- Christiansen, A. W., Gillespie, R. H., Myers, G. E. and River, B. H. 1985. *Wood Adhesives in 1985: Status and Needs*, Forest Products Research Society, Madison, Wisconsin, U.S.A. 27-33.
- Chuang, I.-S., Hawkins, B. L., Maciel, G. E. and Myers, G. E. 1985. *Macromol.*, **18**: 1482-1485.
- Chuang, I.-S. and Maciel, G. E. 1992. *Macromol.*, **25**: 3204-3226.
- Chuang, I.-S. and Maciel, G. E. 1994. *J. Appl. Polym. Sci.*, **52**: 1637-1651.
- Coakley, P. 1992. The Pacific Wood Composite Market - A New Zealand Perspective. In: *Proc. Pacific Rim Bio-Based Composites Symposium*, eds: Plackett, D. V. and Dunningham, E. A., Forest Research Institute, Rotorua, N.Z., 1-19.
- Cook, R. W. and Tod, D. A. 1993. *Int. J. Adhesion and Adhesives*, **13**: 157-162.
- Corwin, J. F. 1959. U.S. Patent 2,873,260.
- Crocombe, G. T., Enright, M. J. and Porter, M. E. 1991. *Upgrading New Zealand's Competitive Advantage*, Oxford University Press, London, U.K., 70-81 & 179-235.
- Crowe G. A. and Lynch, C. C. 1948. *J. Am. Chem. Soc.*, **70**, 3795-3797.
- Crowe G. A. and Lynch, C. C. 1949. *J. Am. Chem. Soc.*, **71**, 3731-3733
- Dalton, M. 1994. Total Extractable Formaldehyde: Perforator Method, In: *Orica (ICI) Test Methods Manual - Particleboard and MDF*, Section 9.1.W-21.
- Dankelman, W. and Daemen, J. M. H. 1976, *Anal. Chem.*, **48**: 401-404.
- Dankelman, W., Daemen, J. M. H., de Breet, A. J. J., Mulder, J. M., Huysmans, W. G. B. and Deanit, J. 1976. *Angew. Makromol. Chem.*, **54**: 187-201.
- de Breet, A. J. J., Dankelman, W., Huysmans, W. G. B. and de Wit, J., 1977. *Angew. Makromol. Chem.*, **62**: 7-31.
- de Jong, J. I. 1950. *Rec. Trav. Chim.*, **69**: 1566.
- de Jong, J. I. and de Jonge, J. 1952. *Rec. Trav. Chim.*, **71**: 643-667.
- de Jong, J. I. and de Jonge, J. 1953. *Rec. Trav. Chim.*, **72**: 88-156.

- de Rijk, P. 1994. Formaldehyde Solution, Formaldehyde Content by Sodium Sulphite Method, In: *Orica (ICI) Test Methods Manual - Formaldehyde and Methanol*, Section 9.1. C-1.
- Derome, A. E. 1989. *Org. Chem. Series, Vol. 6*, Pergamon Books Ltd., London, U.K.
- Dinwoodie, J. M. 1977. *Holzforschung*, **31**: 50.
- Dinwoodie, J. M. 1978. *J. Inst. Wood Sci.*, **8**: 59.
- Doi, K. 1994. *Proc. Adhesives & Bonded Wood Symposium*, eds: Hse, C.-Y., Tomita, B. and Branham, S. J., Forest Products Society, Madison, Wisconsin, U.S.A. 236-244.
- Doi, K., Ueda, K., Tanaka, K. and Koto, N. 1998. *Jpn. Kokai Tokkyo Koho* (Japanese Patent), JP 10109381 A2 19980428, 8 pp.
- Dunky, M., Lederer, K. and Zimmer, E. 1981. *Oesterr Kunstst. Z.*, **12**: 36-39.
- Dutkiewicz, J. 1983. *J. Polym. Sci.*, **28**: 3313.
- Dutkiewicz, J. 1984. *J. Appl. Polym. Sci.*, **29**: 45-55.
- Ebdon, J. R. and Heaton, P. E. 1977. *Polymer*, **18**: 971-974.
- Ebdon J. R., Heaton, P. E., Huckerby, T. N. and O'Rourke, W. T. S. 1984. *Polym.*, **25**: 821-825.
- Ebewele, R. O., River, B. H. and Myers, G. E. 1993. *Adhesives Age*, **12**: 23-30.
- Ebewele R. O., River, B. H. and Myers, G. E. 1994. *J. Appl. Polym. Sci.*, **52**: 689-700.
- Ebewele, R. O. 1995. *J. Appl. Polym. Sci.*, **58**: 1689-1700.
- Eisele W., Petersen, H. and Mayer, J. 1977. U.S. Patent 4,021,413.
- Elbert, A. A. 1984. *Prom-st.*, **4**: 6.
- Elias, H. G. 1977. *Macromolecules*, Plenum Press, New York, U.S.A.
- European Committee for Standardisation 1982. *Particleboards - Determination of Formaldehyde Content: Perforator Method. Standard EN-120*, European Committee for Standardisation, Brussels, Belgium.
- Ferg, E. E., Pizzi, A. and Levendis, D. C. 1993. *J. Appl. Polym. Sci.*, **50**: 907-915.
- Field, L. D. and Sternhell, S. 1989. *Analytical NMR*, John Wiley & Sons Ltd., New York, U.S.A.
- Fomicheva, O. V. and Semenenko, S. V. 1991. *Plast. Massy*, **9**: 7.
- Freeman, G. G. and Kreibich, S. Z. 1968. *Forest Prod. J.*, **18**: 39.

## Bibliography

- Fu, X. and Shuihua, C. 1981. *Physical Chemistry*, People's Education Press, Beijing, China.
- Gilbert, A. and Booth, C. 1986. *Br. Polym. J.*, **18**: 345-348.
- Gillet, S. and Delpuech, J. J. 1980. *J. Magn. Reson.*, **38**: 433.
- Gillham, J. K. and Lewis, A. F. 1963. *J. Appl. Polym. Sci.*, **7**: 2293-2306.
- Gillham, J. K. 1974. *Am. Ind. Chem. Eng. J.* **20**: 1066-1079.
- Ginzel, W. 1973. *Holz. Roh. Werkst.*, **31**: 18.
- Glazkov, S. S. and Boldyrev, V. S. 1997. *Derevookbrab. Prom-st.*, **4**: 15-18.
- Grisson, J. T. 1920. *Ind. Eng. Chem.*, **12**: 172.
- Groah, W. J., Gramp, G. D., Heroux, G. L. and Haavik, D. W. 1998. *Forest Prod. J.*, **48**: 75-80.
- Gross, M. L. 1986. Mass Spectrometry, In: *Instrumental Analysis*, 2nd edition, eds: Christian, G. D. and O'Reilly, J. E., Allyn & Bacon Inc., Boston, U.S.A.
- Gumbley, S. J. 1995a. Identification of Species in UF/MUF Resin HPLC by Electrospray MS, *Internal Research Report*, Orica N.Z. Ltd., Mt. Maunganui, N.Z.
- Gumbley, S. J. 1995b. UF Resin Developments Series, *Internal Research Report*, Orica N.Z. Ltd., Mt. Maunganui, N.Z.
- Hahnenstein, I., Hasse, H., Kreiter, C. G. and Maurer, G. 1994. *Ind. Eng. Chem. Res.*, **33**: 1022-1029.
- Hahmemstein, I., Albert, M., Hasse, H., Kreiter, C. G. and Maurer, G. 1995. *Ind. Eng. Chem. Res.*, **34**: 440-450.
- Hamada, M. J. 1955. *Chem. Soc. Japan, Ind. Chem. Sect.*, **58**: 286.
- He, Z. D., Zhang, X. C. and Cheng, R. S. 1982. *J. Liq. Chromatogr.*, **5**: 1209.
- Heftmann, E. 1983. *Chromatography, - Fundamentals and Applications of Chromatographic and Electrophoretic Methods, Part A: Fundamentals and Techniques*, Elsevier Scientific Publishing Co., New York, U.S.A.
- Higuchi, M. and Akata S. I. 1979. *Mokuzai Gakkaishi*, **25**: 496.
- Higuchi, K. 1998. *Jpn. Kokai Tokkyo Koho* (Japanese Patent), Application: JP 97-113545 19970415, 4pp.
- Hill, C. G., Hedren, A. M., Myers, G. E. and Koutsky, J. A. 1984. *J. Appl. Polym. Sci.*, **29**: 2749-2762.
- Hlaing, T., Gilbert, A. and Booth, C. 1986. *Br. Polym. J.*, **18**: 345-348.

## Bibliography

- Ho, C. K. 1985. Br. Patent, GB 2,150,939 A.
- Hope, P., Stark, P. and Zahir, S. A. 1973. *Br. Polym. J.*, **5**: 363-378.
- Horioka, K., Noguchi, M., Moriya, K. and Oguro, A. 1959. *Bull. Gov. For. Exp. Sta.* Tokyo, Japan, **113**: 20.
- Howald, M. S. 1928. Br. Patent 312,343.
- Hse, C.-Y. 1974a. *Mokuzai Gakkaishi*, **20**: 483-490.
- Hse, C.-Y. 1974b. *Mokuzai Gakkaishi*, **20**: 491-493.
- Hse, C.-Y. 1974c. *Mokuzai Gakkaishi*, **20**: 538-540.
- Hse, C.-Y. and Zhineng, H. 1990. Melamine Modified Urea-Formaldehyde Resin for Bonding Flakeboards, in: *Wood Adhesives Symposium*, eds: Conner, A. H., Christiansen, A. W., Myers, G. E., River, B. H., Vick C. B. and Spelter, H. N., U.S.D.A. Forest Products Laboratory and Forest Products Research Society, Madison, Wisconsin, U.S.A.
- Hse, C.-Y., Xia, Z.-Y. and Tomita, B. 1994. *Holzforschung*, **48**: 527-532.
- Huang, Z. and Guang, C. C. 1988. *Synthesis of Adhesives Series, - Wood Adhesive (Vol. 4)*, Academic Press, Beijing, China.
- Huber, H. A. 1958. *Forest Prod. J.*, **8**, 357.
- Inoue, M. K. and Itow, G. 1956. *Wood Ind. Jap.*, **11**: 85.
- Inoue, M. K. and Kawai, M. 1957. *Research Report*, Nagoya Municipal Industrial Research Institute, Japan, **17**: 1-5.
- Iosifov, G. G. and Refsemin, Z. 1985. *Pokroky vyrobe pouziti lepidiel drevopriem*, **7**: 83.
- Irle, M. A. and Bolton, A. J. 1988. *Holzforschung*, **42**: 53.
- Ito, Y. 1959. *Kogyo Kagaku Zasshi*, **62**: 1918.
- Ito, Y. 1961. *Kogyo Kagaku Zasshi*, **64**: 385-742.
- Iwatsuka, S. and Tanaka, H. 1956. *Wood Ind. Jap.*, **11**: 549.
- Jada, S. S. 1988. *J. Appl. Polym. Sci.*, **35**: 1573.
- Jada, S. S. 1990. *J. Macromol. Sci., Chem.*, **A27**: 361-375.
- John, H. 1920. U.S. Patent 1,355, 843.
- Jordan, R. C. 1980. *J. Liq. Chromatogr*, **3**: 439.
- Jorshak, V. V. 1984. *Viniti*, **398**: 12.
- Katuscak, S., Tomas, M. and Schiessi, O. 1981. *J. Appl. Polym. Sci.*, **26**: 381-394.

- Kearns, H. A. 1988. Gel Time at 100°C, In: *Orica (ICI) Test Methods Manual - Resin Testing*, Section 9.1.R-21.
- Kearns, H. A. 1990. Resin Analysis: Free Formaldehyde - Cold Sodium Sulphite Method, In: *Orica (ICI) Test Methods Manual - Resin Testing*, Section 9.1.R-7.
- Kelly, T. J., Smith, D. L. and Satola, J. 1999. *Environ. Sci. Technol.*, **33**: 81-88.
- Kim, M. G. 1999. *J. Polym. Sci., Part A: Polym. Chem.*, **37**: 995-1007.
- Kim, M. G. and Amos, L. W. 1990. *Ind. Eng. Chem. Res.*, **29**: 208-212.
- Kozlova, G. I., Dubikovskaya, L. V., Shvets, D. P. and Sereda, N. I. 1976. *Poluch., Svoistva Primen. Fenoplastov Ionoobmen. Smol.*, 73.
- Kumar, A. and Sood, A. 1990. *J Appl. Polym. Sci.*, **40**: 1473-1486.
- Kumlin, K. and Simonson, R. 1978a. *Angew. Makromol. Chem.*, **68**: 175-184.
- Kumlin, K. and Simonson, R. 1978b. *Angew. Makromol. Chem.*, **72**: 67-74.
- Kumlin, K. and Simonson, R. 1980. *Angew. Makromol. Chem.*, **86**: 143-156.
- Kumlin, K. and Simonson, R. 1981. *Angew. Makromol. Chem.*, **93**: 43-54.
- Lecka, J., Morze, Z. and Dziurka, D. 1999. *Zb. Ref.-Symp. Pokroky Vyroby Pouziti Lepodiel Drevopriem.*, **14**: 155-159.
- Lee, W. Y. 1972. *Anal. Chem.*, **44**: 1284.
- Levy, G. C. and Craik, D. J. 1984. *Topics in Carbon-13 NMR Spectroscopy*, ed: Levy, G. C., Wiley-Interscience, New York, U.S.A. **4**.
- Lewis, A. F. and Gillham, J. K. 1962. *J. Appl. Polym. Sci.*, **6**: 422.
- Lewis, A. F. and Gillham, J. K. 1963. *J. Appl. Polym. Sci.*, **7**: 685.
- Ludbrook, B. D. and Whitwood, R. J. 1992. *Int. J. Adhesion and Adhesives*, **12**: 138-144.
- Ludlam, P. R. 1973. *Analyst*, **98**: 107-115.
- Ludlam, P. R. and King, J. G. 1984. *J. Appl. Polym. Sci.*, **29**: 3863-3872.
- Maloney, T. M. 1977. *Modern Particleboard & Dry-Process Fibreboard Manufacturing*, Miller Freeman, San Francisco, California, U.S.A.
- Mansson, B., Sundin, B. and Sirenins, K. 1984. Swedish Patent 434,931.
- Maplesden, F. and Horgan, G. 1992. *Proc. Pacific Rim Bio-Based Composites Symposium*, eds: Plackett, D.V. and Dunningham, E. A., Forest Research Institute, Rotorua, N.Z., 32-41.

## Bibliography

- Margosian, R. 1995. *Proc. Wood Adhesives 1995 Symposium*, eds: Christiansen, A. W. and Conner, A. H., U.S.D.A. Forest Service, Forest Products Laboratory and Forest Products Research Society, Madison, Wisconsin, U.S.A., 14-20.
- Matsuzaki, T., Inoue, Y. and Ookubo, T. 1980. *J. Liq. Chromatogr.*, **3**: 353-365.
- Mayer, J. 1978. *Spanplatten-Heute und Morgen*, Weinbrenner DRW-Verlag GmbH, Stuttgart, Germany, 102.
- McGuire, M. L., Seluga, D. M. and Blum, M. R. 1985. U.S. Patent 4,501,628.
- Meyer, B. 1979a. *Urea-Formaldehyde Resins*, Addison-Wesley Publishing Inc., Reading, Massachusetts, U.S.A., 123-184.
- Meyer, B. 1979b. *Urea-Formaldehyde Resins*, Addison-Wesley Publishing Inc., Reading, Massachusetts, U.S.A., 79-103.
- Meyer, B. 1979c. *Urea-Formaldehyde Resins*, Addison-Wesley Publishing Inc., Reading, Massachusetts, U.S.A., 4-96.
- Meyer, B. 1979d. Formaldehyde Release from UF-Systems, In: *Proc. 13th Int. Particleboard Symposium, Washington State University*, American Chemical Society, Washington DC, U.S.A.
- Meyer, B. 1979e. *Urea-Formaldehyde Resins*, Addison-Wesley Publishing Inc., Reading, Massachusetts, U.S.A., 250-267.
- Meyer, B. 1984. *J Appl. Polym. Sci., Appl. Polym. Symp.*, **40**: 49.
- Meyer, B. and Numlist, R. 1981. *Polym. Prepr.*, **22**: 130-131.
- Meyer, B. and George, E. 1985a. *Forest Prod. J.*, **35**: 20.
- Meyer, B. 1985b. *Adv. Chem. Ser.*, **210**: 101.
- Meyer, B. and Hermanns, K. 1984. *J. Appl. Polym. Sci., Appl. Polym. Symp.*, **40**: 27-39.
- Meyer, B. and Hermanns, K. 1986. Formaldehyde Release from Wood Products: An Overview, In: *ACS Symposium Series 316 – Formaldehyde Release from Wood Products*, eds: Meyer, B., Andrews, B. A. K. and Reinhardt, R. M., American Chemical Society, Washington DC, U.S.A., 1-16.
- Meyer, B., Hermanns, K. and Baker, V. 1986. Cellulose Models for Formaldehyde Storage in Wood: Carbon-13 Nuclear Magnetic Resonance Studies, In: *ACS Symposium Series 316 – Formaldehyde Release from Wood Products*, eds: Meyer, B., Andrews, B. A. K. and Reinhardt, R. M., American Chemical Society, Washington DC, 67-75.

## Bibliography

- Mlynar, M. 1997. *Nonwovens Conf.*, TAPPI Press, Atlanta, U.S.A., 191-201.
- Morze, Z. N. 1983. *Drevo*, **38**: 131.
- Moslemi, A. A. 1974. *Particleboard*, Southern Illinois University Press, Feffer & Simons Inc., Amsterdam, The Netherlands.
- Mottola, A. H. and Mark, H. B., Jr. 1986. *Instrumental Analysis*, 2nd edition, eds: Christian, G. D. and O'Reilly, J. E., Allyn and Bacon Inc., Boston, U.S.A., 560-580.
- Myers, G. E. 1981. *J. Appl. Polym. Sci.*, **26**: 747.
- Myers, G. E. 1985. *Proc. Symposium on Wood Adhesives in 1985, Status and Needs*, U.S.D.A. Forest Service, Forest Product Laboratory and Forest Products Research Society, Madison, Wisconsin, U.S.A.
- Myers, G. E. 1986. *ACS Symposium Series 316 - Formaldehyde Release from Wood Products*, eds: Meyer, B., Andrews, B. A. K. and Reinhardt, R. M., American Chemical Society, Washington DC, U.S.A. 87-106.
- Myers, G. E. and Nagaoka, M. 1981. *Wood Sci.*, **13**: 140-150.
- Nair, B. B. and Francis, D. J. 1983. *Polym.*, **24**: 626-630.
- Nakarai, Y. and Watanabe, T. 1961. *Wood Ind. Jap.*, **16**: 577.
- Nakarai, Y. and Watanabe, T. 1962. *Wood Ind. Jap.*, **17**: 464.
- Neusser, H. and Schall, W. 1970. *Holzforsch. Holzerverwertung*, **22**: 116
- Nomayr, H., Rothbacher, H. and Korn, A. 1983. *Farbe Lack*, **89**: 351-353.
- Northeast Forestry College 1981. *Adhesives and Coatings*, China Forestry Press, Beijing, China, 33-46.
- Ohyama, M., Bunichiro and Hse, C.-Y. 1995. *Holzforschung*, **49**: 87-91.
- Osugi, E. and Tone, K. 2000. *Jpn. Kokai Tokkyo Koho* (Japanese Patent), Application: JP 98-290940 19981013, 5 pp.
- Panangama, L. A. and Pizzi, A. 1996. *J. Appl. Polym. Sci.*, **59**: 2055-2068.
- Pasch, H., Dairanieh, I. S. and Khan, Z. H. 1990. *J. Polym. Sci., Part A: Polym. Chem.*, **28**: 2063-2074.
- Pasch, H., Hovakeemian, G., Khan, Z. H. and Lahalih, S. 1991. *Polym. Commun.*, **32**: 54-57.
- Paul, R. L. and Hendra, P. J. 1976. *Miner. Sci. Eng.*, **8**: 171.
- Petrov, K. G. 1984. *Plast. Massy*, **11**: 27.

## Bibliography

- Pizzi, A. 1983. *Wood Adhesives, Chemistry and Technology*, Marcel Dekker Inc., New York, U.S.A., 59-104.
- Pizzi, A., Lipschitz, L. and Valenzuela, J. 1994. *Holzforschung*, **48**: 254-261.
- Price, A. F., Cooper, A. R. and Meskin, A. S. 1980. *J. Appl. Polym. Sci.*, **25**: 2597-2611.
- Pshenitsyna, V. P., Molotkova, N. N., Frenkel, M. D., Tikhomirova, Y. Y., Gurman, I. M., Aksel'rod, B. Y., Potekhina, Y. S., Maizel, N. S., Lagucheva, Y. S., Kochnov, I. M. 1980. *Polym. Sci. U.S.S.R.*, **21**: 2145.
- Rice, J. T. 1965. *Forest Prod. J.*, **15**: 107.
- Robitschek, P. and Christensen, R. L. 1976. *Forest Prod. J.*, **26**: 43.
- Roffael, E. 1973. *Holz.-Zentralblatt*, **99**: 845.
- Roffael, E., Dix, B. and Kehr, E. 1995. *Holz. Roh. Werkst.*, **53**: 315-320.
- Schäffler, L. 1997. *N. Z. Pine*, **18**: 32-35.
- Schildknecht, C. E. 1961. *Polymer Processes*, Interscience Publishers Inc., New York, U.S.A., 313-321.
- Schindlbauer, H. and Schuster, J. 1983. *Kunststoffe*, **73**: 325-328.
- Schoolery, J. N. 1977. *Prog. Nuc. Magn. Reson. Spectrosc.*, **11**: 79.
- Sebenik, A., Osredkar, U., Zigon, M. and Vizovisek, I. 1982. *Angew. Makromol. Chem.*, **102**: 81-85.
- Sedliacik, M. H., Ref-Semin., Z., Pouziti, P. V. 1985. *Lepidiel Drevopriem*, **7**: 13.
- Shiau, D. W. and Smith, E. 1985. U.S. Patent 4,536,245.
- Silcock, N. A. 1991. Particleboard and Fiberboard: Water Absorption and Thickness Swelling, In: *Orica (ICI) Test Methods Manual - Particleboard and MDF*, Section 9.1.W-13.
- Silcock, N. A. 1994. Resin Analysis: Gel Time - Acetic Acid Method, In: *Orica (ICI) Test Methods Manual - Resin Testing*, Section 9.1.R-29.
- Silcock, N. A. 1995. Particleboard and Fiberboard: Tensile Strength Perpendicular to the Plane of the Panel - Internal Bond, In: *Orica (ICI) Test Methods Manual - Particleboard and MDF*, Section 9.1.W-10.
- Silcock, N. A. 1996. Formaldehyde Solution: Acidity, In: *Orica (ICI) Test Methods Manual - Formaldehyde and Methanol*, Section 9.1.C-3.
- Silcock, N. A. 1996. Formaldehyde Solution Methanol Content, In: *Orica (ICI) Test Methods Manual - Formaldehyde and Methanol*, Section 9.1.C-2.

## Bibliography

- Simons, W. G. 1950. U.S. Patent 2,518,388.
- Skeist, I. 1965. *Handbook of Adhesives*, Reinhold Publishing Inc., Chapman & Hall, Ltd., London, U.K., 310-322.
- Skeist, I. 1977. *Handbook of Adhesives*, 2nd edition, Van Nostrand Reinhold Co., New York, U.S.A., 424-433.
- Slonim, I. Y. 1979. *J. Polym. Sci.*, U.S.S.R. (Engl. Transl.), **20**: 2569-76
- Slonim, I. Y., Alekseyeva, S. G., Urman, Y. G., Arshava, B. M., Aksel'rod, B. Y. and Smirnova, L. N. 1977. *Polym. Sci.*, U.S.S.R., **19**: 920-936.
- Smets, G. and Brozee, A. 1952. *J. Polym. Sci.*, **8**: 371-394.
- Smythe, L. E. 1947. *J. Phys. Colloid Chem.*, **51**: 369.
- Smythe, L. E. 1952. *J. Am. Chem. Soc.*, **74**: 2713-2715.
- Snyder, L. R. and Kirkland, J. J. 1974. *Introduction to Modern Liquid Chromatography*, John Wiley & Sons Inc., New York, U.S.A.
- Sotak, C. H., Dumoulin, C. L. and Levy, G. C. 1984. *Topics in Carbon-13 NMR Spectroscopy*, ed: Levy, G. C., Wiley-Interscience Inc., New York, U.S.A., **4**: 91.
- Spurlock, H. N. 1983. U.S. Patent 4,381,368.
- Steele, R. and Giddens, L. E. 1956. *Ind. Eng. Chem.*, **48**: 110.
- Steiner, P. R. 1974. *Wood Sci.*, **7**: 99.
- Steiner, P. R. 1973. *Forest Prod. J.*, **23**: 32.
- Steiner, P. R. and Warren, S. R. 1981. *Holzforschung*, **35**: 273-278.
- Sturgeon, M. G. 1992. *Proc. Pacific Rim Bio-Based Composites Symposium*, eds: Plackett, D. V. and Dunningham, E. A., Forest Research Institute, Rotoura, N.Z., 42-50.
- Suchsland, O. and Woodson, G. E. 1990. *Fibreboard Manufacturing Practices in the United States*, Forest Products Research Society, Washington DC, U.S.A.
- Sundin, B. 1978. *Proc. FESYP Int. Particleboard Symp.*, Hamburg, Germany, 112.
- Symthe, L. E. 1947. *J. Phys. Colloid Chem.*, **51**: 369.
- Szesztay, M., Laszlo-Hedvig, Z., Kovacsovics, E. and Tudos, F. 1993. *Holz. Roh. Werkstoff*, **51**: 297-300.
- Szesztay, M., Laszlo-Hedvig, Z., Takacs, C., Gacs-Baitz, E., Nagy, P. and Tudos, F. 1994. *Angew. Makromol. Chem.*, **215**: 79-91.
- Takahashi, A. 1952. *Chem. High Polym.* (Jap.) **9**: 173.
- Tamura, Y. 1985. *Mokuzai Gakkaishi*, **31**: 521.

## Bibliography

- Tamura, Y., Yamauchi, H. and Itoh, T. 1998. *Koen Yoshishu - Nippon Setchaku Gakkai Nenji Taikai*, **36**, 75-78.
- Tanaka, A. and Takashima, K. 1966. *J. Jap. Wood Res. Soc.*, **12**: 272.
- Tanaka, A. and Kamitani, M. 1967. *J. Jap. Wood Res. Soc.*, **13**: 285.
- Taylor, R., Pragnell, R. J. and McLaren, J. V. 1980. *J. Chromatogr.*, **195**: 154-157.
- Taylor, R., Pragnell, R. J., McLaren, J. V. and Snape, C. E. 1982. *Talanta*, **29**: 489-494.
- Tohmura, S.-I., Inoue, A. and Guo, L. 1998. *Mokuzai Gakaishi*, **44**: 433-440.
- Tokarova, L. and Juhas, S. 1995. Chemko, Strazske, Slovakia, *Zb. Ref. Symp.*, **12**, 173-177.
- Tomito, B. and Hatono, S. 1978. *J. Polym. Sci., Poly. Chem. Ed.*, **16**: 2509-2525.
- Tomita, B. and Hirose, Y. 1976. *J. Polym. Sci. Part A: Polym. Chem.*, **14**: 387.
- Tomita, B. and Hse, C.-Y. 1992. *J. Polym. Sci.: Part A: Polym. Chem.*, **30**: 1615-1624.
- Tomita, B. and Hse, C.-Y. 1993. *Mokuzai Gakkaishi*, **39**: 1276-1284.
- Torrey, S. 1978. *Adhesives Technology - Development Since 1977*, Noyes Data Co., 162-169.
- Troughton, G. E. 1969. *J. Inst. Wood Sci.*, **4**: 51.
- Troughton, G. E. and Chow, S. Z. 1968. *J. Inst. Wood Sci.*, **21**: 29.
- Troughton, G. E. and Chow, S. Z. 1969a. *J. Inst. Wood Sci.*, **23**: 51.
- Troughton, G. E. and Chow, S. Z. 1969b. *J. Inst. Wood Sci.*, **1**: 172.
- Trub, E. P., Boytsov, E. N. and Koryakin, A. G. 1989. *Pripisnova. Khim. Promst. Moscow, U.S.S.R.*, 22.
- Tsuge, M., Miyabayashi, T. and Tanaka, S. 1974. *Bunseki Kagaku (Jpn. Analyst)*, **23**: 1141-1150.
- Tsuge, M. 1976. *J. Adhes. Sci. Jpn.*, **12**: 257.
- Tsuge, M. 1981. *Prog. Org. Coatings*, **9**: 107-133.
- Tsuge, M. and Senba, T. 1981. *Netsu Kokasei Jushi*, **2**: 192-195.
- Utterback, F., Millington, D. S. and Gold, A. 1984. *Anal. Chem.*, **56**: 470-473.
- Valdez, D. 1995. *Proc. Wood Adhesives 1995 Symposium*, eds: Christiansen, A. W. and Conner, A. H., U.S.D.A. Forest Service, Forest Products Laboratory and the Forest Products Society, U.S.A., 193-200.

## Bibliography

- Vale, C. P. and Taylor, W. G. K. 1964. *Aminoplastics*, Iliffe Books Ltd., London, U.K., 20-43.
- Varghu, V. 1998. *Acta Biol. Hung.* **49**: 463-475.
- Vargiu, S., Giovanni, S. S. and Mazzoleni, G. and Nistri, U. 1974. U.S. Patent 3,842,039.
- Viscotek Manual 1996. *TriSEC GPC Software Version 3 Reference Manual*, Viscotek Co., Houston, U.S.A., A1-A22.
- Walker, J. F. 1967. *Formaldehyde*, 3rd edition., Reinhold Publishing Co., New York, U.S.A., 83-105, 483-510.
- Walker, N. and Anderson, I. 1992. *Proc. Pacific Rim Bio-Based Composites Symposium*, eds: Plackett, D. V. and Dunningham, E. A., Forest Research Institute, Rotorua, N.Z., 154-162.
- Waters Associates Inc. 1976. *Series R-400 Instruction Manual*, Waters Associates Inc., Milford, U.S.A.
- Weast, R. C. and Astle, M. J. 1978-1979. *CRC Handbook of Chemistry and Physics*, CRC Press Inc., Boca Raton, Florida, U.S.A, A-31 - A-121.
- White, J. T. 1990. *Proc. Wood Adhesives 1990 Symposium*, eds: Conner, A. H., Christiansen, A. W., Myers, G. E., Vick, C. B. and Spelter, H. N., U.S.D.A. Forest Service, Forest Products Laboratory and Forest Products Research Society, Madison, Wisconsin, U.S.A., 13-19.
- White, J. T. 1995. *Proc. Wood Adhesives 1995 Symposium*, eds: Christiansen, A. W. and Conner, A. H., U.S.D.A. Forest Service, Forest Products Laboratory and Forest Products Research Society, Madison, Wisconsin, U.S.A., 3-8.
- Whiteside, I. R. 1987. U.K. Patent GB 2,192,005 A.
- Williams, J. H. 1983a. U.S. Patent 4,409,293.
- Williams, J. H. 1983b. U.S. Patent 4,410,685.
- Williams, J. H. 1984. U.S. Patent 4,482,699.
- Word, M. A. 1984. *Adhesion*, **28**: 10-17.
- Yin, S., Deglise, X. and Masson, D. 1995. *Holzforschung*, **49**: 575-580.
- Yossifov, N., Glavchev, I. and Mihailova, J. 1999. *Zb. Ref.-Symp. Pokroky Vyrobe Pouziti Lepodiel Drevopriem*, **14**, 83-86.
- Zeman, S. and Tokarova, L. A. 1992. *Thermochimica Acta*, **202**: 181-189.
- Zigeuner, G. 1954. *Fette Seifen Austrichem.*, **56**: 973.

Bibliography

Zigeuner, G. 1955. *Fette Seifen Austrichem.*, 57: 14-100.

Zolochevski, V. A. and Zaved., L. V. U. 1983. *Lesn. Zh.*, 1: 101.